Temperature as a driver of phage community ecology and evolution

Samuel Terrence Edwards Greenrod

Department of Biology

University of Oxford

A thesis submitted for the degree of

Doctor of Philosophy

Trinity 2025

Declaration

I declare that I wrote this thesis and that the work is my own except where explicitly stated in the text. This work has not been submitted for any degree or professional qualification except as specified.

Samuel T.E Greenrod

Trinity 2025

Acknowledgements

I would like to thank both of my wonderful supervisors, Kayla King and Craig MacLean, for their support, guidance, and encouragement during my DPhil. I would like to pay special thanks to Kayla whose mentorship over the past four years has helped me to grow both as a scientist and as a person.

I would like to thank all past and present members of the King lab for the coffee chats and words of support that helped me to get through tough times: Emily Stevens, Toby Hector, Georgia Drew, Judy Li, Ian Will, Kieran Bates, Serena Johnson, Cameron Smith, Mike Blazanin, Dominik Vinopal, Luis Silva, Thomas Travers-Cook, Chelsea Higgins, and Sarzana Hossain. I'd also like to thank former lab member Alex Betts whose advice early in my DPhil continues to motivate me today.

My thanks equally extend to all the past and present members of the MacLean lab: Rachel Wheatley, Divjot Kaur, Lois Ogunlana, Cedric Lood, Michelle Yin, Eliza Rayner, Piotr Jedryszek, Weronika Slesak, Jordan Shutt-McCabe, William Matlock, Maria Stavraki, Adam Mulkern, and Daniel Cazares. I would like to make a special mention of Daniel Cazares who tirelessly supported my work throughout my DPhil and always stepped in to help with lab work, talk through ideas, or simply provide coffee and biscuits when times were tough.

I would like to thank the past and present members of the Oxford University Squash Racquets Club, and in particular the Men's Blues team who formed a fundamental part of my Oxford experience. Special thanks go to Tim Delport and James McCouat for their support and advice both on and off the court.

I am eternally grateful to my wonderful partner, Amy Stanford, who has always been there to celebrate with me during the highs and console me during the lows of DPhil life. She has been my number one supporter, and I couldn't have gotten through the last four years without her.

Finally, I would like to thank my family, especially my parents, Robyn and Mike, who have always been there to talk to when I needed it. I'm also deeply grateful to my late grandmother, Barbara Greenrod, who put so much into my academics growing up and who would've been thrilled to one day see me go to Oxford. This thesis is dedicated to her.

Publications and contributions

The following published and archived papers have arisen from this thesis, and are presented in the Introduction and Chapters 2, 3, and 4.

Introduction

Greenrod, STE., Hector, TE., Blazanin, M., Cazares D., King KC. (2025) Temperature as a Driver of Phage Ecology and Evolution. *Annual Review of Microbiology* (in press)

S.T.E.G. and K.C.K conceived the review. S.T.E.G. and K.C.K wrote the initial draft, with input from all the other authors.

Chapter 2

Greenrod, STE., Cazares, D., Johnson, S., Hector, TE., Stevens, EJ., MacLean, RC., King, KC. (2025) Warming alters life-history traits and competition in a phage community. *Applied and Environmental Microbiology*. 90:e00286-24.

S.T.E.G. and K.C.K conceived the project. S.T.E.G., C.M., T.H., E.J.S., and K.C.K. designed the experiment. S.T.E.G., D.C.L., and S.J. conducted the experiment and collected the data, with guidance from C.M. and K.C.K. S.T.E.G. analysed the data. S.T.E.G., C.M. and K.C.K. wrote the initial draft, with input from all other authors.

Chapter 3

Greenrod, STE., Cazares D, Slesak, W., Hector, TE., MacLean, RC., King KC. (2025) Evolutionary rescue accelerates competitive exclusion in a parasite community (In prep). bioRxv 2025.09.25.678511; doi: https://doi.org/10.1101/2025.09.25.678511

S.T.E.G. and K.C.K conceived the project. S.T.E.G., C.M., T.H., and K.C.K. designed the experiment. S.T.E.G., D.C.L., and W.S. conducted the experiment and collected the data, with guidance from C.M. and K.C.K. S.T.E.G. analysed the data. S.T.E.G. and K.C.K. wrote the initial draft, with input from all other authors.

Chapter 4

Greenrod, STE., Cazares D, Slesak, W., Hector, TE., MacLean, RC., King KC. Competition constrains parasite adaptation to thermal heterogeneity (In prep). bioRxv 2025.09.28.679032; doi: https://doi.org/10.1101/2025.09.28.679032

S.T.E.G. and K.C.K conceived the project. S.T.E.G., C.M., T.H., and K.C.K. designed the experiment. S.T.E.G., D.C.L., and W.S. conducted the experiment and collected the data, with guidance from C.M. and K.C.K. S.T.E.G. analysed the data. S.T.E.G. and K.C.K. wrote the initial draft, with input from all other authors.

Abstract

Thermal change has a profound impact on species fitness, ecological interactions, and evolutionary dynamics. Parasite communities are particularly sensitive to thermal change due to their complex life cycles, strong competition for host resources, and dependence on host thermal responses. Previous literature assessing the effects of thermal change on parasites has primarily focused on the relationship between parasites and their hosts. However, hosts in natural populations are frequently co-infected by a diversity of parasites which interact to reduce host fitness and increase host mortality rates. Despite the importance of parasite communities in animal and plant health, the extent to which thermal change alters parasite community dynamics, composition, and diversity remains unclear. In this thesis, I assessed the impact of temperature on parasite community ecology and evolution using a microbial host-parasite system consisting of the bacterium *Pseudomonas aeruginosa* (host) and three lytic bacteriophages (parasite). Firstly, I conducted an experimental study looking at the impact of temperature on growth rates, life-history traits, and competition in a phage community. Phages were found to vary in their responses to temperature and so thermal change altered competition outcomes and drove phage community composition shifts. I then used experimental evolution and follow-on genomic and phenotypic analyses to assess the interaction between thermal adaptation and phage community dynamics. I discovered that phages can avoid thermal extinction through evolutionary rescue. Rescue, however, results in changes to competition outcomes and promotes the exclusion and evolutionary constraint of phage competitors. This body of work demonstrates that thermal change is a major driver of parasite community ecology and evolution. The findings have implications for understanding the role of temperature in the structure and dynamics of phage communities associated with eukaryotic hosts, as well as the efficacy of phage therapies. More broadly, they show that thermal change can alter community dynamics and drive eco-evolutionary feedbacks, with consequences for species coexistence amidst global climate change.

Contents

1

Introduction

Section 1.3 has been published in *Annual Review of Microbiology*

1.1 Parasite thermal biology

Thermal change has a profound impact in biological systems through effects ranging from gene expression regulation, changes to growth rates, and alteration of community composition and diversity [1–3]. Changes in organismal fitness with thermal change are typified by thermal performance curves which show how phenotypes vary across temperatures. Thermal performance curves are characterised by three defining features; upper and lower thermal limits and a thermal optimum in which fitness is highest. Thermal performance curves across biological systems generally follow the same pattern: fitness increases gradually with temperature up to a thermal optimum, after which fitness rapidly decreases [4] (Figure 1). Variation in the effects of thermal change on species fitness depends on the bounds of thermal tolerance limits, and the position and breadth of the thermal optimum.

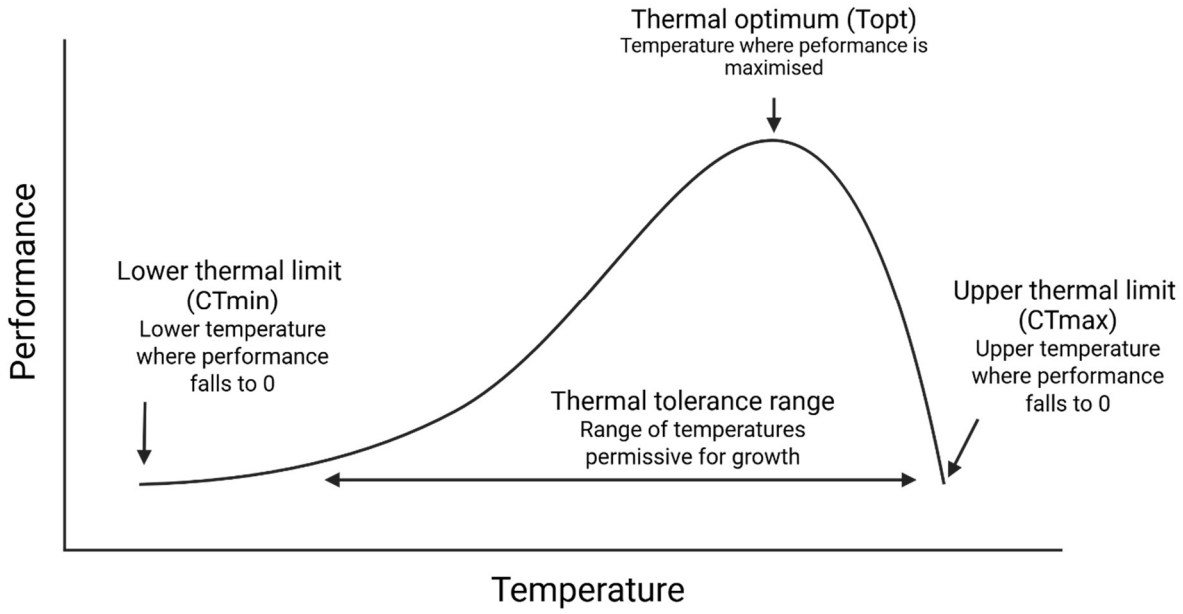

Figure 1. A typical thermal performance curve with critical features highlighted. Performance increases gradually with temperature from the lower thermal limit to the thermal optimum. After the thermal optimum, performance rapidly decreases. The thermal tolerance range is the range of temperatures between upper and lower thermal limits.

Parasite systems are particularly sensitive to thermal change due to their dependence on both parasite and host thermal responses. Hosts and parasites often differ in the shape and positioning of their thermal performance curves, called a mismatch [5]. Generally, parasites are thought to have broader thermal tolerance limits than do their hosts; parasite burden is highest either side of the host thermal optimum [5]. However, experimental studies frequently highlight cases where parasites have narrower thermal tolerance limits than their hosts [6,7]. Depending on the extent and position of host-parasite thermal performance mismatches, changes in temperature can either disrupt or exacerbate parasite infections. The effects of thermal change vary across host-parasite systems due to the additional dependence of some parasites on a vector for disease transmission [8].

1.2 Parasite community ecology

Thermal responses often vary between parasite species [9,10]. Therefore, thermal change has the potential to alter ecological interactions in parasite communities. Host populations and individuals are often infected by multiple parasites simultaneously [11,12]. Such co-infections can occur between multiple parasites from either the same or different species. By targeting the same host resource, co-infecting parasites are often in competition with each other [11,13,14]. Competition between parasites can be broadly divided into three types: exploitation competition, immune-mediated competition, and interference competition [15]. Exploitation competition occurs through parasites depleting the host population, thereby reducing the availability of hosts for competitors. Immune-mediated competition occurs when parasites activate host immune responses which then restrict co-infections by competitors. While immune activation can also be detrimental to all infecting parasites, immune priming can be specific and may allow parasites to maintain growth in the absence of competition [16]. Finally, interference competition occurs when parasites block competitor entry into host individuals [17] or directly restrict competitor growth [18].

Competition between parasites is a major driver of parasite evolution. Co-infections of host individuals and populations can select for increased virulence by elevating host mortality rates and reducing the benefits of high transmissibility [13]. Selection for increased virulence by competition is particularly strong in obligate killing parasites where transmission is directly linked to host mortality [19]. However, high virulence places parasite communities at risk of a "tragedy of the commons" where excessive host mortality then limits future infection potential [20]. At limiting host densities, selection can start to favour low virulence [21].

While inter-parasite competition contributes to parasite evolution, it can also lead to competitive exclusion and loss of parasite diversity [22]. Modern co-existence theory states that competition between species will lead to competitive exclusion unless: i) species have very similar levels of competitiveness (and so acquire equal proportions of resources) or ii) species have niche differences which reduce competition [23]. Parasite species may co-exist due to heterogeneity in host susceptibility to infection [24] or by evolving to expand their host ranges [25]. Parasite species can also co-exist with each other by specialising at either within-host or between-host competitiveness [26].

1.3 Temperature as a driver of phage ecology and evolution

Bacteriophages (phages), viral parasites of bacteria, are the most abundant biological entity on the planet (reviewed in [27,28]). Phages can be found in nearly all habitats permissive to life, with their abundance and diversity typically tracking those of their bacterial hosts. A primary impact of phages in microbial communities is through their lysis (killing) of bacterial cells. Phage lysis significantly impacts the abundance of bacterial genotypes and species and, thus, microbial community composition and structure. Importantly, phages disproportionately target the most abundant bacterial taxa and genotypes, and this targeting leads to negative, frequency-dependent selection [29]. These antagonistic interactions can be reciprocal driving rapid co-evolution [30].

In natural populations, phages are often exposed to extremes of salinity, pH, and temperature (reviewed in [31]). Temperature is a particularly important environmental factor that affects processes at all biological levels from enzyme kinetics [2] to ecological and evolutionary dynamics [32–34]. Phages are highly vulnerable to temperature due to their dependence on the activity of replicative and lytic enzymes and the growth rates of their bacterial hosts [35]. Given that phages also rapidly deplete their host populations and so exist predominantly in the environment as non-infecting particles [36], phages are susceptible to thermal or UV degradation [37,38]. Temperature changes can drive shifts in phage persistence [39] and growth rates [40].

By altering the mode of phage behaviour upon infection, environmental temperatures determine whether phages act as bacterial parasites or as mutualists. Lytic phages replicate immediately, and then they kill their bacterial hosts upon infection; conversely, some phages follow a lysogenic life cycle, and they integrate their genetic material into the bacterial chromosome and replicate in synchrony without inducing cell death [41]. Integrative (also known as "temperate") phage transmission among cells can facilitate bacterial horizontal gene transfer [42] through the carriage of genes involved in bacterial symbiont mutualism [43] as well as in pathogen virulence, metabolism, and competitiveness (reviewed in [44]). Finally, phages can follow "pseudolysogenic" life cycles, where they exist in a dormant, non-integrative state post-infection [45]. The three phage life cycle strategies are not mutually exclusive; many phages can swap between lytic and lysogenic/pseudolysogenic life cycles in response to changes in temperatures [46,47].

1.3.1 Phage thermal environments

1.3.1.1 Extreme thermal environments

Phages have been identified across many environments that have unique thermal distributions (Figure 2). At the thermal extremes, phages have been identified in polar ocean water and in both glacial and arctic sea ice where temperatures are stably maintained below 0°C [48–50]

(Figure 2a). Genomic signatures of phage infection and bacterial resistance evolution have also been found in Antarctic soils [51,52] where temperatures can fall to ~-25°C [53]. Extreme low temperatures generally increase phage stability and are used to preserve phages in experimental studies [54]. However, phage infection rates are limited by low metabolic potential [55] and low host availability as decreasing temperatures reduce the rates of bacterial growth [3,56].

Phages have also been isolated from extreme heat environments including hydrothermal vent plumes [57–59] and hot springs [60] (Figure 2g). Temperatures in vent plumes and hot springs increase with depth and, due to rising water pressures, can range from ~60°C up to > 400°C [61]. Vent plume and hot spring phages are generally associated with bacterial thermophiles which reach high densities through metabolism of dissolved organic carbon released during geological activity [62]. In order to persist under extreme heat and pressure, phages have evolved high particle and enzyme stability [60,63].

Phages in hot deserts [64,65] experience less extreme temperatures than those in polar ice or hydrothermal plumes (Figure 2d). Instead, they experience some of the highest temporal thermal variation. Average diurnal temperature ranges in deserts often exceed 40°C but temperatures can reach heights of 60°C during the day and lows of -10°C at night [66]. In addition to large thermal variation, hot deserts are characterised by long periods of desiccation which restrict bacterial growth rates [67]. Desert phages must contend with pressures found in opposite thermal extremes: thermal stress (found in hot environments) and limited host availability (found in cold environments).

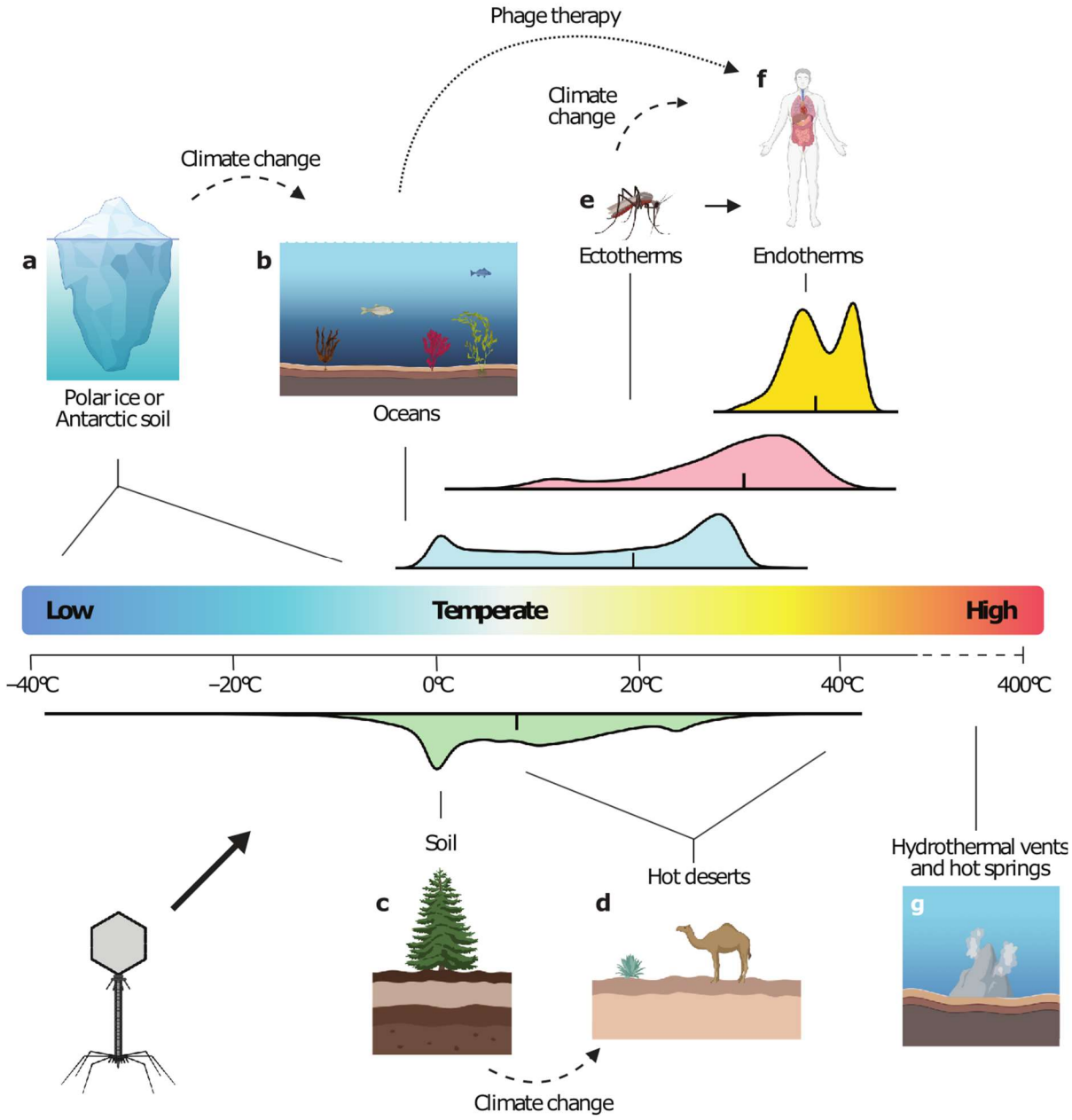

Figure 2. Examples of phage thermal environments spanning a thermal gradient. **a)** Extreme cold phage environments such as polar ice or Antarctic soil span a range of sub-zero temperatures [48]. **b)** Ocean phages [27] inhabit a more temperate environment, although temperatures are bimodal, with prevalence peaks at 0°C and 30°C. Global sea surface temperature data for the year 2023 were obtained from reference [68]**. c)** Soil phages [69] have similar general thermal ranges to those of ocean phages, with temperatures largely

occurring at or above 0°C. Thermal data were obtained from reference [70]. **d)** Desert phages [65] experience the highest daily thermal variation, with diurnal temperatures ranging from high heat to those of low cold [66]. **e)** Phages associated with ectotherms [71] experience higher temperatures and less thermal variation than free-living phages due to behavioural thermoregulation. **f)** Endotherms also carry phages [72] and have higher but more stable body temperatures than do ectotherms. Endotherm body temperatures are bimodal within a small range because of diel and nocturnal lifestyle differences. Ectotherm and endotherm body temperature data were obtained from reference [73]. **g)** Phages have been found in hydrothermal vents and hot springs [57], which often have temperatures above 90°C [61]. The blue-red bar shows the thermal gradient. Environmental temperatures for soil, oceans, ectotherms, and endotherms are presented as smoothed density plots. Plots were generated using R [74] and RStudio [75]. The vertical lines within plots show median values. The thermal ranges that are shown for extreme cold and desert environments reflect values reported in the literature. The dashed arrows show expected thermal environment changes with climate change such as polar ice melting, soil desertification, and ectotherm vector range expansion [76]. The block arrow between ectotherms and endotherms highlights potential ectotherm-endotherm phage transmission [77]. The dotted arrow shows the thermal shift of marine phages deployed as therapeutics [78]. Temperature information for phage thermal environments is shown in **Table 1**. Figure adapted from images created in BioRender.

1.3.1.2 Temperate thermal environments

1.3.1.2.1 Oceans and soil

In temperate environments, phages and their bacterial hosts often experience more hospitable temperatures where selection for thermal tolerance is weaker [79]. In 2023, year-long average ocean surface temperatures varied globally between -3.9°C and 37°C [68]. While the median ocean surface temperature was 19.7°C, temperatures had a bimodal distribution with peaks at ~0.5°C near to the poles and ~28°C near to the equator (Figure 2b). Soil surface temperatures

have a broader geospatial thermal range than ocean temperatures ranging between -38.2°C to 41.9°C [70]. However, extreme soil temperatures are rare; between the years 2017-2019 the median soil temperature was ~8°C with peaks at ~0.5°C nearer to the poles, ~10.2C between the poles and equator, and ~23.7°C near to the equator [70] (Figure 2c). As temperatures increase closer to the equator, there is a corresponding increase in ocean bacterial and phage abundance [80]. However, similar analyses have not been conducted on soils due to a lack of available data [28].

Phages in temperate environments experience regular temporal thermal variation. Oceans and soils exhibit diel (across day) and diurnal (day/night) thermal variation ranging from a few °C up to > 10°C, respectively [81,82]. In addition, ocean and soil temperatures vary seasonally [70,83] and can change with climate phenomena such as El Niño and La Niña events [84,85]. Ocean and soil viral abundances are generally higher in the summer months than the winter [86,87]. Ocean phage activity also varies daily although it can be difficult to separate temperature effects from light effects which increase bacterial growth through bacterial photosynthesis and carbon sequestration [88]. While it is unclear how El Niño and La Niña events affect phage growth, El Niño events can drive shifts in ocean bacterial composition [89] and so alter phage host availability.

1.3.1.2.2 Animal and plant host-associations

Many phages are associated with animal and plant hosts, most notably when they comprise part of the host gut or rhizosphere microbiome, respectively [72,90]. Rhizosphere phages are expected to experience similar spatial and temporal temperature variations as the surrounding topsoil (see above). In contrast, phages associated with land-based ectotherm animal hosts, such as insects [71,91], generally experience higher average temperatures than the surrounding environment. Land ectotherm body temperatures vary between 6°C and 40.8°C with a median temperature of 30.7°C [73] (Figure 2e). Land and oceanic ectotherm-associated phages experience lower thermal variation than do their surrounding environments due to

buffering by behavioural thermo-regulation [92,93], although this depends on the presence of local thermal refuges [93].

Phages are also associated with endothermic animals [72,94] that regulate their body temperatures internally. Endotherm body temperatures are generally higher than ectotherms with a range between 28.2°C and 42.6°C and a median temperature of 38.4°C [73] (Figure 2f). Notably, endotherms have bimodal body temperature distributions with prevalence peaks at ~37.1°C and at 42°C. This is thought to reflect endotherms having either nocturnal or diel lifestyles, respectively [73]. Endotherm internal environments also experience less thermal variation than ectotherms and so can be considered a relatively stable thermal environment for phages. Nonetheless, endotherm temperatures vary spatially throughout the body [95–97] and can experience spikes through the onset of fevers [98].

1.3.1.3 Transitions between thermal environments

Phages can move between environments potentially leading to considerable shifts in temperature. For example, phages can move from marine or soil environments to animal hosts via drinking water and by consuming soil [99] or plants and other animals [100,101]. Endotherm-associated phages can also be acquired through parasitism by ectotherm disease vectors. For example, mosquito and sand fly microbiota are transferred to mammalian hosts during feeding [77,102]. The movement of microbes from ectothermic to endothermic hosts is expected to coincide with a thermal increase [73]. Finally, phages isolated from soil, wastewater, and marine sources [78] are increasingly being deployed as therapeutics to treat both animal and plant bacterial infections [103,104]. Phage therapeutic candidates isolated from oceans or soil may experience similar temperatures when deployed in plant hosts due to the overlap in soil and plant root/rhizosphere temperatures. However, phages used in animal hosts likely experience large thermal upshifts as they move from an ambient external environment to a warm internal environment. By moving between thermal environments, phages may either act as invasive parasites targeting local bacterial populations [105] or be restricted through thermal inactivation [38].

Table 1. Estimated thermal profiles of phage environments

Thermal environment	Thermal range (°C)	Upper and lower quartiles (°C)	Median temperature (°C)	Phage reference	Temperature reference
Antarctic soil	ND	ND	~ -24.9	[51]	[53]
Glacial ice	-50 to -9	ND	ND	[106]	[50]
Soil	-36.3 to 39.9	1.00 to 15.5	8.04	[69]	[70]
Ocean	-1.85 to 35.0	7.76 to 26.8	19.7	[27]	[68]
Ectotherm	6.00 to 40.8	25.4 to 34.5	30.7	[107]	[73]
Endotherm	30.2 to 44.6	36.5 to 41.5	38.4	[72]	[73]
Desert	-10 to 60	ND	ND	[64]	[66]
Hot spring	0 (or 36.7*) to 108	28.7 to 55.0	~ 40	[108]	[109]
Hydrothermal vent	2 to 400	ND	ND	[57]	[61]

Abbreviation: ND, not determined.

* The defined temperature range of hot springs is not unanimously agreed [110].

1.3.2 Temperature and phage infection

1.3.2.1 Phage infectivity on bacteria

Phage thermal sensitivity is illustrated by the observed temperature-dependence of the sequential phage infection steps that are essential for replication (reviewed in [111]): phage adsorption to the bacterial cell, injection of phage genetic material, production of new phage particles (lytic life cycle) or integration of genetic material (lysogeny), and release of phage progeny through lytic enzyme activity. Phage infection steps can be grouped into life-history traits which contribute to phage fitness (Figure 3). Phage life-history traits include particle stability, adsorption rate, life cycle preference (lytic versus lysogenic), burst size (number of phage progeny per infected cell), latent period (time from infection to cell lysis), and host range. Temperature can affect each of these traits independently (Table 2) and can help shape phage life-history strategies across thermal environments.

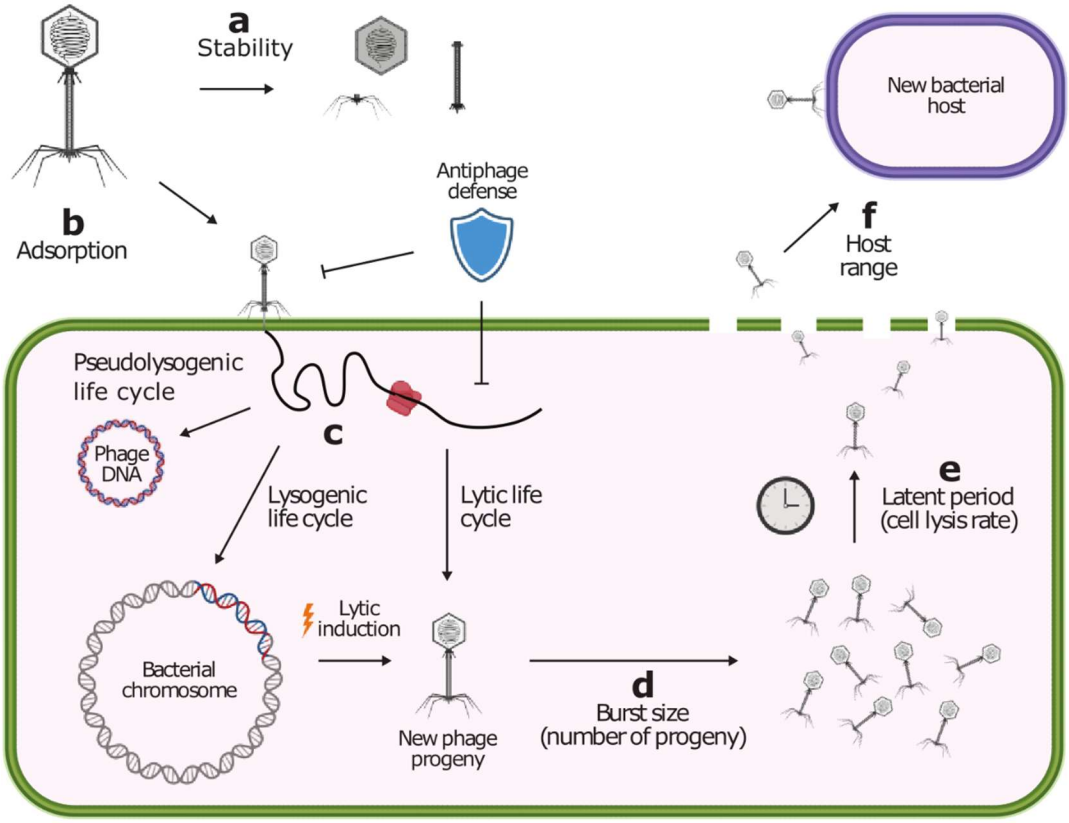

Figure 3. Phage life-history traits. Phage life-history traits, with those that contribute to phage fitness labelled with letters. **a)** Phage stability is a combination of the phage's intrinsic and extrinsic death rates (i.e., particle decay). **b)** Phage adsorption reflects the rate of attachment to bacterial cells. **c)** The lytic and lysogenic life cycles refer to the ability of phages to either start replicating immediately upon infection or integrate into the bacterial chromosome. The pseudolysogenic life cycle refers to the ability of phages to adopt a dormant, nonintegrative state postinfection. **d)** Burst size is the number of phage progeny (particles) released from a single cellular infection. **e)** Latent period is the time that passes from the point of infection to the point of cellular lysis. Burst size and latent period are coupled, as short latent periods restrict the time available to produce phage progeny. **f)** Host range represents the diversity and number of bacterial hosts that the phage can infect. Finally, antiphage defence is the ability of the bacterial host to resist phage infections. While antiphage defence is a bacterial trait rather than a phage trait, it was included because of its importance in the success of phage infection. The labels correspond to those in **Table 2**. Figure adapted from images created in BioRender.

1.3.2.2 Particle stability

Reviews that explore phages and temperature have primarily focused on phage inactivation through thermal effects on phage stability [31,112,113], likely because phage persistence in the environment is crucial for population survival during periods when bacterial densities are limiting. Additionally, there is growing interest in the use of phages as biocontrols and therapeutics which must remain stable during storage and may be used for products that will experience thermal extremes, such as foods undergoing pasteurisation [114,115].

Phage thermal stability is largely determined by the physical capsid structure of free phage particles. For example, as shown by Bull et al. [116], the evolution of phage thermal tolerance can occur through mutations in genes involved in capsid formation, likely because thermal destabilisation of phage proteins may disrupt their folding and assembly into phage particles.

High temperatures can also select for mutations in structural genes [117,118] or in their promoters [119]. These studies are supported by findings that natural phages isolated from hot springs exhibit preferences for GNA (glycine-*N*-alanine) sequences that promote the formation of thermostable disulfide bridges [60]. In some phages, thermal decay is determined by the stability of capsid-tail connector proteins that degrade at high temperatures; this degradation results in DNA expulsion [114,120]. Phage stability can be enhanced by the presence of "decoration" proteins which stabilise phage capsids and support particle assembly [121].

1.3.2.3 Adsorption

The first stage of phage infection involves adsorption to the bacterial cell (reviewed in [122]). Briefly, phages initially collide with bacterial cells through Brownian motion and then bind reversibly to common cell surface components. Through periodic adsorption and desorption, phages conduct a "random walk" across the bacterial surface until they find preferred receptors. Once target receptors are identified, phages bind irreversibly before injecting their genetic material into the cell. Bacterial surface receptors targeted by phages are diverse and often have roles in bacterial metabolism [122].

Rising temperatures reduce phage adsorption efficiencies [123–125]. However, the mechanisms behind reduced adsorption can vary. Thermal increases may alter the ability of phages to bind to their target receptor - for example, because of reduced phage binding affinities [126–128]. Consistent with this possibility, thermal adaptation in some phages has been linked to mutations in tail fiber genes that support phage attachment to bacterial surface receptors [129]. Theoretically, reduced binding may also reflect changes in the conformation of bacterial structures that are used as surface receptors, although studies demonstrating this hypothesis are lacking. Alternatively, warming may alter the expression of bacterial surface receptors [130] and so change the availability of attachment areas. Receptor access may be further affected by biofilm production [131], which can increase [132–134] or decrease [135] in response to temperature. Notably, the adsorption of some phage taxa appears to be resilient

to warming and so thermal effects may be taxon dependent [125,136]. Whether such effects are primarily driven by changes in phage binding ability or bacterial susceptibility to phage attachment is unclear.

1.3.3.4 Infection and genome stability

While phages may be able to attach to hosts at high temperatures, the injection of phage genetic material into the target bacterium can depend on temperature. For instance, during injection phage λ DNA undergoes a density transition that facilitates successful infection at 37°C, a process that can be hindered at higher or lower temperatures [137]. Similarly, under elevated temperatures phage Qβ rapidly evolves mutations in a protein involved in DNA transfer, suggesting strong temperature-dependency of genome injection [138,139]. Phages must be able to both adsorb to bacterial cells and transfer their genetic material at different temperatures to successfully establish infections.

Theoretically, injection and persistence of phage genetic material inside the bacterial cell may depend on the phage genome type: DNA vs RNA and double-stranded (ds) vs single-stranded (ss). For example, dsRNA is considered more thermo-stable than dsDNA [140] and so dsRNA phage genomes are expected to be at lower risk of thermal decay than dsDNA phage genomes. Similarly, dsDNA is thought to be more thermo-stable than ssDNA [141] suggesting ssDNA and potentially ssRNA phage genomes may be at higher risk of thermal decay. Notably, RNA and ssDNA phages have higher mutation rates than dsDNA phages [142]. Rising temperatures may increase RNA or dsDNA phage prevalence if genome stability is under selection. However, if thermal change selects on different phage traits, RNA or ssDNA phages may become more prevalent given their greater access to mutational diversity.

Table 2. Examples of studies reporting the impact of temperature increase on phage life-history traits[a]

Phage life-history trait	Bacteria used	Phage used	Phage family	Genome length (kB)	Genome type	Temperatures used (°C)	Effect of warming on trait	Reference
Stability	*Escherichia coli*	ΦX174	Microviridae	~ 5.4	ssDNA	37 to 44	Restricted particle formation	[116]
	Pseudomonas aeruginosa	ΦOMKO1	Myoviridae	~ 281.8	dsDNA	55 to 75	Increased particle decay	[38]
Adsorption rate	*Listeria monocytogenes*	ΦLP-026 (P70-like)	Siphoviridae	~67.1	dsDNA	6.5 to 37	Reduced phage binding affinity	[123]
		ΦLP-037 (P70-like)	Siphoviridae	~64.8	dsDNA			
		ΦLP-048 (P100-like)	Herelleviridae	~133	dsDNA			
		ΦLP-0125 (P100-like)	Herelleviridae	~135	dsDNA			
		ΦA511 (P100-like)	Herelleviridae	~134	dsDNA			
	Yersinia pestis	ΦvB_YpM_3 (Mu-like)	Myoviridae*	~ 39.4	dsDNA	26 and 37	Reduced phage receptor expression	[143]
		ΦvB_YpM_5 (Mu-like)	Myoviridae*	~ 37.2	dsDNA			
		ΦvB_YpM_6 (Mu-like)	Myoviridae*	~ 37.2	dsDNA			

		ΦvB_YpM_23 (Mu-like)	Myoviridae*	~ 38.7	dsDNA			
	Pseudomonas aeruginosa; Vibrio cholerae	Not tested	NA	NA	NA	23 and 37; 22 to 37	Altered receptor access through biofilm production	[131,132,135]
Life-cycle strategy	*Lactococcus lactis*	ΦLC3 (P335-like)	Siphoviridae*	~ 32.1	dsDNA	30 to 34.5	Lytic induction (thermal stress)	[144]
	Burkholderia pseudomallei	ΦBp-AMP1	Autographiviridae	~ 45	ND	25 to 37	Selection for lytic infection (virulence-transmission trade-off)	[145,146]
Burst size	*Lactobacillus paracasei*	ΦiLp84 (P22-like)	Siphoviridae	~39.4	dsDNA	30 to 37	Reduced burst size	[147]
		ΦiLp1308 (P22-like)	Siphoviridae	~34.1	dsDNA			
	Lactobacillus paracasei	ΦiLp84 (P22-like)	Siphoviridae	~39.4	dsDNA	20 to 37	Increased burst size	[148]
		ΦiLp1308 (P22-like)	Siphoviridae	~34.1	dsDNA			
		ΦB1	Siphoviridae	~ 38	dsDNA			
		ΦLDG	Siphoviridae	~ 26.6	dsDNA			
Latent period	*Lactobacillus paracasei*	ΦiLp84	Siphoviridae	~39.4	dsDNA	30 to 37	Reduced latent period	[147]

		ΦiLp1308	Siphoviridae	~34.1	dsDNA			
Host range	*Escherichia coli*	ΦWG01	Straboviridae	~170	dsDNA	28 to 42	Expanded host range	[149]
		ΦQL01	Straboviridae	~171	dsDNA			

Abbreviations: NA, not applicable; ND, not determined.

Asterisk indicates families that were inferred from similar phages.

[a]The National Center for Biotechnology Information database or discovery publications were used to determine phage families.

1.3.3.5 Life-cycle strategy

Phage life cycle strategies (lytic, lysogenic, or pseudolysogenic; see Figure 3) are not mutually exclusive and phages can move among them depending on environmental conditions [46,47]. While phages following a lysogenic life cycle are often under selection to preserve and even to protect host cells [150], high temperatures can induce integrated phages into a lytic cycle through the threat of cell death [144,151]. Temperature modulates lysis/lysogeny decisions during phage infections with higher temperatures generally encouraging phages to follow a lytic life cycle [47,143,146]. Phage preference for lysis at high temperatures may follow the same mechanism as lytic induction, with phages attempting to "jump ship" before the death of their hosts.

Lysis/lysogeny decisions are also affected by temperature-mediated changes to bacterial growth rates and population densities [152]. At high temperatures, bacterial growth rates are high, and so an abundance of bacterial hosts are available for phage infection [3]. High host densities select for virulent, lytic phages which rapidly replicate through host killing [153]. In contrast, poor bacterial growth at low temperatures selects for low phage virulence through long latent periods or lysogeny, in which phages replicate in tandem with their hosts [153]. Phage life cycle decisions vary in response to host densities; phages following lysogenic life cycles often possess quorum-sensing systems which allow them to become induced into a lytic cycle when susceptible bacterial host densities increase [154].

1.3.3.5.1 Extreme environments: phage shifts from parasitism to mutualism

Phage life-history strategies are largely determined by their thermal environments. In polar environments where bacterial densities are low, phages minimise virulence by adopting a lysogenic life cycle, integrating into the host genome rather than causing cell lysis [48]. Lysogeny in cold environments allows phages to maintain replication without depleting valuable host cells. Lysogeny also promotes the horizontal transfer of bacterial genes allowing phages to contribute to bacterial fitness and polar microbial genetic diversity [48]. Polar

phages exhibit seasonal variation in lysogeny-to-lytic conversions; while lysogeny is prevalent in the winter and spring months, lytic replication is favoured in the summer months [48]. Climate forecasts indicate that rising global temperatures will accelerate the melting of polar ice [76] leading to more frequent cold-to-temperate shifts that occur earlier in the year. In polar environments, phages largely exist as mutualists which benefit from host associations and facilitate the growth of their hosts. However, thermal upshifts may reduce polar lysogeny rates and push phages across the mutualism-parasitism continuum from lysogenic mutualists towards lytic parasites [155].

In contrast to polar regions, extreme heat environments have high extra-cellular phage densities indicating phages largely follow a lytic life cycle [108]. Heat stress is a well-known inducer of phage lysis as phages seek to avoid the thermal death of their host cell [144]. However, consistently high phage densities suggest that bacterial hosts are abundant and are likely able to resist high temperatures. Given phage maximum growth increases with thermal adaptation [156], high temperature environments may exhibit the highest levels of phage lysis. Yet, high temperature environments are not necessarily hotspots of phage parasitism. Lytic phages in hydrothermal vents [59] and hot springs [157] have been shown to carry genes involved in bacterial metabolic processes. It was suggested that phage infections may support bacterial growth in high temperature environments by compensating for poor bacterial metabolic activity. Lytic phage-encoded genes have also been linked to the stabilisation of bacterial heat shock proteins [158] although the presence of these genes in high temperature environments is unclear. By supporting the growth rates of their bacterial hosts, phages appear to favour parasitism in temperate environments but move towards mutualism at the thermal extremes.

Desert environments represent a unique extreme thermal environment due to large daily thermal fluctuations and low soil moisture content. The combined effects of thermal variation and low soil moisture restricts bacterial growth [159] and is expected to select for phage lysogeny. In agreement, it is difficult to isolate phages from desert samples without using

protocols that induce phages out of a lysogenic life cycle ([64,160], see [65] for more examples). Desert phages act as mutualists by carrying genes involved in bacterial extremotolerance [161]. A notable exception is Antarctic desert soil which, despite being a low temperature environment, often has high levels of extracellular phage [69]. This may reflect high levels of biofilm in Antarctic soil communities which create high local bacterial densities [65]. Extracellular phages may also be more detectable at low temperatures due to lower phage decay rates [54].

1.3.3.6 Latent period and burst size

Following successful adsorption and DNA injection, the phage lytic life cycle involves the production of phage particles, the replication and packaging of phage genetic material, and lysis of the bacterial cell. The success of these steps can be exemplified by two correlated, temperature-dependent phage traits: latent period and burst size. The latent period represents the time taken from cell infection to cell lysis and is determined by the expression and activity of lytic enzymes [162]. The burst size represents the number of viral particles produced from a single infection cycle and is determined by the replicative period length (latent period) and the reaction rates of phage replication proteins [163]. Given more rapid cell lysis shortens the time available to replicate, a longer latent period allows for a larger burst size.

Theory suggests that, by altering lytic enzyme activity, thermal change will either increase or reduce latent periods and burst sizes. High temperatures have indeed been found to shorten latent periods and reduce burst sizes; these findings indicate higher lytic enzyme activity [147]. Warming temperatures can also reduce latent periods and burst sizes through host density effects that increase bacterial growth rates and densities [152]. High host densities select for phages with shorter latent periods [153], as the benefit of ongoing transmission outweighs the cost of a smaller burst size.

Some studies have found that thermal change disrupts the coupling between latent period and burst size, with higher temperatures generally shortening the latent period but increasing the

burst size [35,148,164]. One explanation for this de-coupling is that lytic enzymes and replicative/packaging proteins may have different responses to temperature. If replicative proteins have steeper thermal performance curves than do lytic enzymes, rising temperatures may cause phage particle production rates to rise more rapidly than do lysis rates. Given that latent period and burst size determine phage virulence and transmission potential [153], further investigation of the tripartite relationship between temperature, burst size, and latent period is needed to better understand how phage fitness varies in natural environments.

1.3.3.7 Host range

Changes in phage host ranges across temperatures can alter phage population dynamics and competition outcomes [165]. In microbial communities, phages are often surrounded by diverse bacteria including many they are unable to infect. The presence of unavailable hosts creates a strong selection pressure for host range expansion as phage host range generalists have higher host encounter rates [166]. Accordingly, some phages have broad host ranges and can infect multiple unrelated bacterial species [167]. Yet, broad host ranges come with fitness trade-offs [168], and so most phages have species- or even strain-specific associations with bacterial hosts [169]. By expanding or narrowing phage host ranges, temperature change could either increase bacterial host availability or reduce phage competitive fitness.

Phage host range expansion typically occurs through mutations in tail fiber genes, which are responsible for phage adsorption to the bacterial cell surface [166,170]. Interestingly, tail fiber mutations are also frequent mutational targets when phages adapt to thermal stress [129]; this observation raises the possibility that thermal adaptation may have pleiotropic effects on host range. For example, Chen et al. [149] found that tail fiber mutations that widen phage thermal tolerance ranges also expand phage host range. Yehl et al. [170] provided further details and found that changes in phage host range and thermal tolerance range depend on thermally adaptive mutations occurring in the “host-range-determining region” of the tail fiber gene. However, thermal adaptation in other traits, such as phage particle stability, can restrict phage

host range evolvability [171]. Different modes of thermal adaptation may exert opposing pressures on phage host range.

High host diversity selects for phage host range expansion [166]. Given that bacterial diversity often increases with temperature [172], co-selection for host range expansion and thermal tolerance may be frequent under warming conditions. Selection for host range shifts is exacerbated by temperature-mediated changes in bacterial community composition [173]. While overall species richness may increase with warming, some bacterial taxa may be excluded, with this exclusion forcing phages to change their focal host to avoid extinction.

1.3.3.8 Life-history trade-offs

Life-history theory posits that life-history traits must have fitness trade-offs to explain the absence of "Darwinian demons", which are hypothetical organisms capable of achieving maximal fitness for all traits [174]. Such trade-offs are frequently found in phage systems [175–178], and some have been shown to be temperature-dependent [179]. For example, rising temperatures can reduce phage stability but increase replication rates, thereby modulating phage population dynamics [180]. Similarly, selection for increased phage thermal stability can lead to a reduction in replication rates [181]. Thermal trade-offs and trade-ups have also been found among phage stability and adsorption rate, latent period, and burst size [182,183]. The evolution of trade-offs is restricted by thermal variation; fluctuating temperatures that alternately select for thermal stability and replication rate can remove the stability/replication trade-off [184].

1.3.3.9 Bacterial resistance to phage

Virulent phage infections create a strong selection pressure for phage resistance evolution in bacterial hosts, although the mechanisms and costs of phage resistance vary across temperatures. In single species experiments, phage resistance typically arises through mutations in surface receptors [185,186]. These mutations prevent phages from adsorbing to the bacterial membrane but generally come with high fitness costs through pleiotropic effects

on growth rates, virulence, and antibiotic susceptibility [187]. Padfield et al. [7] showed that the costs of receptor mutation-based phage resistance on bacterial growth rates were highest at the bacterial thermal optimum. These findings likely reflect the fact that mutated receptors generally have functions in bacterial metabolism [122]; receptor mutations restrict growth at the thermal optimum by reducing metabolic rates.

Resistance can alternatively arise through the evolution or horizontal acquisition of phage defence systems [188,189], which also have temperature-dependent costs [190]. However, Aframian et al. [190] found that the costs of certain phage defense systems, in contrast to those of receptor-based mutations, decrease closer to the bacterial thermal optimum. These findings suggest that phage defence systems may be preferred at the thermal optimum, while receptor mutations are favoured away from the optimum. The best route for phage resistance may depend on the level of warming experienced and phage defence system availability.

The relative benefits of receptor mutations and phage defence systems can be further affected by the effects of temperature on bacterial growth rates. At low temperatures, longer bacterial generation times increase the probability of multiple phage infections within a single bacterial reproductive cycle. As a result, selection at low temperatures favours phage defence systems which respond to ongoing infections, such as CRISPR-Cas, over receptor mutations [191]. In addition, temperature can alter the expression of phage defence systems [192], although such temperature-dependent expression is not universal across all bacterial taxa [193].

1.3.4 Mismatches in bacteria and phage thermal responses

1.3.4.1 Mismatches in ecological time

Phages are obligate parasites and so tend to have narrower thermal limits than do their bacterial hosts (Figure 4a). In addition, studies generally find that phage thermal optima are either the same [7], or lower than bacterial thermal optima [156]. The mismatch among bacterial and phage thermal optima and upper thermal limits represents a thermal refuge in

which bacteria can grow in the absence of phage infection [7]. Using a panel of 15 G4-like *Escherichia coli* phages, Knies et al. [156] found that phages infecting the same bacterial strain exhibit considerable thermal optimum and tolerance limit variation. As observed in bacteria [194], rising temperatures are expected to lead to the extinction of thermally sensitive phages and in turn a decrease in phage diversity. Reduced phage infection will increase the relative abundance of dominant bacterial genotypes [29], although resource availability will decrease because of reduced nutrient cycling [195]. Phage infection can be maintained at high temperatures by the presence of thermally tolerant phage community members [9].

Phages generally follow a "hotter-is-better" thermal strategy whereby higher thermal optima tend to coincide with higher maximum population growth rates [156] (Figure 4b). The "hotter-is-better" strategy stems from the fact that rising temperatures increase reaction rates and allow for faster growth. The relationship between maximum growth and thermal optima exacerbates bacteria-phage thermal mismatches as phages adapted to low temperatures will have lower fitness relative to their bacterial hosts. While a "hotter-is-better" strategy is also observed in insects [196], a recent meta-analysis found only limited support for the strategy across species [197]. One reason that evidence from phages may show stronger support for the strategy could be because phage thermal responses depend on the reaction norms of individual proteins involved in phage infection and replication [9]. More complex organisms may also be able to maintain high fitness at low temperatures through thermal acclimation, behavioural modifications, or internal thermoregulation. In addition to "hotter-is-better", phages also follow a "hotter-is-broader" strategy whereby phages with higher thermal optima tend to have broader thermal tolerance limits [156]. A correlation between thermal optimum, thermal tolerance range, and maximum fitness contradicts specialist-generalist theory, which states that an increase in thermal tolerance range should lead to a trade-off with maximum performance [198]. However, the strategy means that cold-adapted phages will rapidly lose activity as temperatures increase, with this loss leading to phage community shifts and a decrease in phage diversity.

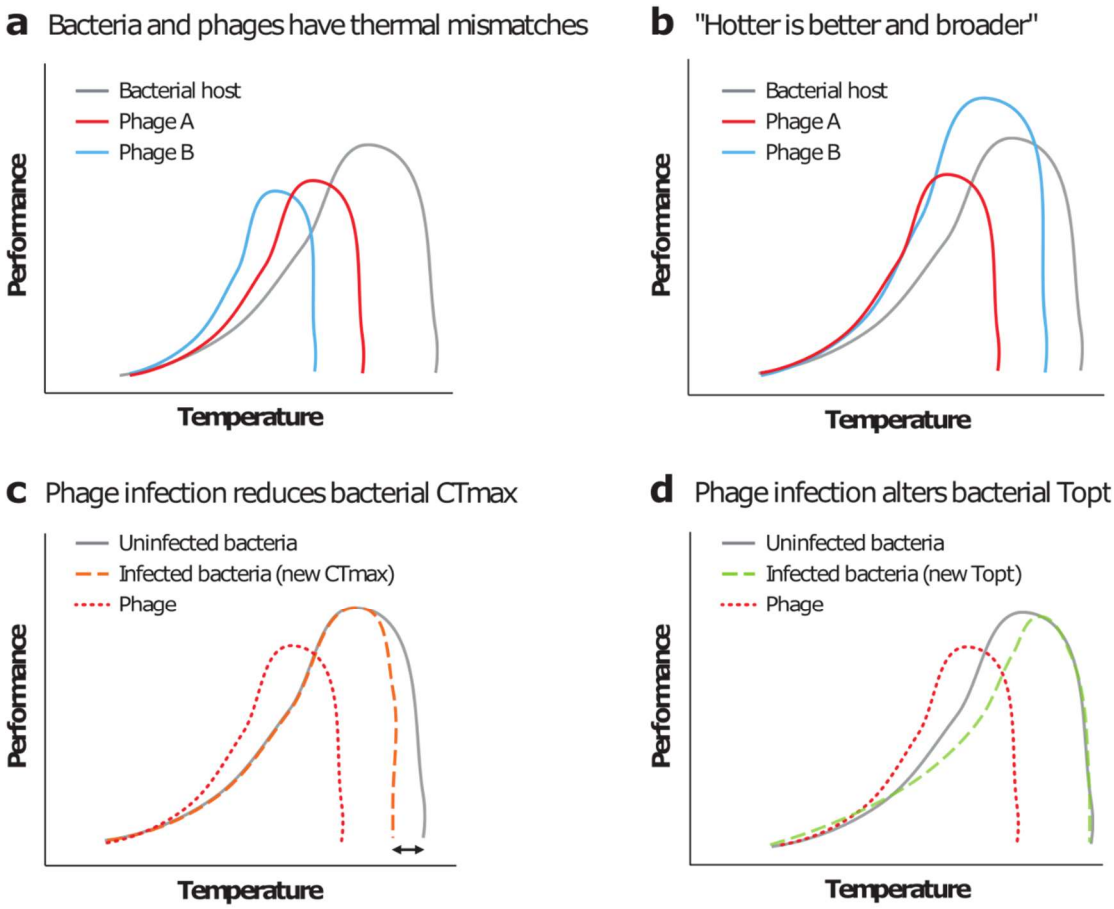

Figure 4. Examples of bacteria and phage thermal performance curves. a) Bacteria and phages have thermal mismatches. Phages generally have lower thermal optima and thermal maxima than do their bacterial hosts [7]. However, thermal responses vary among phages [156]. **b)** Phages generally follow "hotter-is-better" and "hotter-is-broader" thermal strategies whereby phages with higher thermal optima tend to have higher maximum performance and higher upper thermal limits [156]. **c)** Phage infection may reduce bacterial upper thermal limits (CTmax) through the metabolic costs associated with antiphage defence [199,200]. The two-sided arrow shows the shift in the bacterial upper thermal limit. **d**) Phage infection can lead to shifts in the bacterial thermal optimum (Topt) through higher growth at phage non-permissive temperatures and temperature-dependent fitness costs of phage resistance [7]. Figure adapted from images created in BioRender.

Host-parasite thermal performance mismatches are not fixed. For example, Hector et al. [199] found that parasite infection can reduce host upper thermal limits through exploitation of host resources and costly activation of immune responses. Additionally, parasites, being smaller than their hosts, are expected to rapidly acclimate to thermal change, with this rapid acclimation potentially reducing mismatches [201,202]. In bacteria-phage systems, the activation of phage defence systems has temperature-dependent fitness costs linked to autoimmunity [190]. To what extent phages are capable of plastic responses to thermal change is unclear. However, one mechanism for phage acclimation could include temperature-dependent expression of decoration or structural proteins to stabilise phage particles [119,203]. Through the activation of bacterial immune responses and phage thermal acclimation, bacterial and phage upper thermal limits may become increasingly aligned (Figure 4c). Alignment of bacterial and phage thermal responses will remove the high temperature bacterial thermal refuge and could increase the probability of bacterial population collapses during warming events.

1.3.4.2 Mismatches in evolutionary time

Bacteria-phage thermal mismatches can change over time as thermal performance evolves. Phage infection has been shown to select for upshifts in bacterial host thermal optima [7,204]. In some bacteria-phage systems, the evolution of phage resistance results in temperature-dependent fitness costs, and these costs are highest at the bacterial thermal optimum [7]. As bacterial fitness at the thermal optimum decreases following resistance evolution, relative bacterial fitness above the thermal optimum increases, creating a new, higher thermal optimum [7]. An upshift in bacterial thermal optima is expected to exacerbate bacteria-phage thermal mismatches as bacteria start to specialise at high temperatures (Figure 4d).

Phage thermal adaptation can reduce thermal mismatches by aligning both thermal optima and thermal tolerance limits to their bacterial hosts. By re-analysing the evolved populations from Holder and Bull [117], Knies et al. [9] showed that the “hotter-is-better” and “hotter-is-broader” strategies are evolvable; selection for extended upper thermal limits resulted in an

increase in phage thermal optima and maximum performance (Figure 4b). A correlation between phage thermal optima and upper thermal limits may be expected when thermal stress affects proteins directly involved in phage replication. For example, fitness-reducing phage polymerase mutations have been shown to simultaneously reduce phage replication at both the thermal optimum and upper thermal limit [205]. The evolvability of phage thermal optima and upper thermal limits means that thermal adaptation may reduce the size of bacterial thermal refuges. In addition, heat stress that reduces bacterial growth may still permit phage infections leading to reduced phage infectious periods and low bacterial host availability. We might predict that reduced phage virulence will evolve under extreme warming [153,206].

The evolution of thermal performance curves depends on thermal variability. Static temperatures are expected to select for specialists with narrow thermal ranges, in which performance is highest at the evolved temperature. In contrast, fluctuating temperatures favour thermal generalists with wider thermal tolerance limits but lower maximum fitness [207]. Studies in phages suggest that selection under fluctuating temperatures is primarily driven by the most extreme temperature [208]. However, other studies have found that fluctuations can reduce the strength of selection for phage high-temperature adaptation [209] and restrict co-evolutionary dynamics with bacterial hosts [210]. The lack of consensus among studies on the relationship between fluctuating temperatures and thermal adaptation likely reflects the different fluctuation conditions and phages used. While slow fluctuations facilitate the fixation of thermally adapted genotypes, rapid fluctuations increase the impact of genetic drift relative to selection and thereby reduce fixation rates and slow adaptation [211]. In addition, some phages can rapidly adapt to high temperatures, although evolution for other phages is impeded because of inhibited growth [117].

1.3.5 Phage communities and thermal sensitivity

1.3.5.1 Phageome composition and dynamics

Phages exist in diverse communities, termed phageomes (reviewed in [212]), whose compositions are expected to change with temperature because of phage-specific thermal responses [156]. Theoretically, a change in temperature should select for phages whose thermal optima most closely match the new environmental temperature [173,213]. Thermal selection should also favour phages that are able to rapidly adapt to thermal change through altered thermal optima or extended thermal tolerance limits [117]. In agreement, rising temperatures alter relative phage growth rates and allow weaker phage competitors to become more dominant [9]. Thermal increases also cause some phage species to decay more rapidly than others and potentially lead to the exclusion of these phages from the community [114,214].

Phageome composition is also expected to change with temperature because of thermal sensitivity in the bacterial host community. In bacterial communities, species vary in their thermal tolerance ranges and thermal optima [173]. Accordingly, thermal change generally leads to changes in bacterial community composition [213,215], including in animal microbiomes [1]. Bacteria and phages have modular interaction networks where each phage generally targets a small subset of bacterial community members [169]. Changes to bacterial relative abundances - for example through dysbiosis of gut microbiota with warming - are expected to lead to phageome composition shifts [216]. The effects of temperature on phage community composition likely depends on the thermal regime. Static thermal shifts generally reduce genotypic and species diversity by selecting for a few thermal specialists [173]. In both bacterial and phage communities, thermal fluctuations may promote the maintenance of species and genetic diversity through selection for a range of thermal optima [217].

1.3.5.2 Inter-phage competition

Phage competition outcomes depend on both relative phage growth rates and the rate of host population depletion (virulence) [13,218,219]. When host densities are high, phages maximise

their host share by rapidly depleting the host population. Rapid host depletion benefits fast-growing phages by reducing the availability of hosts for slow growing competitors. In contrast, when host densities are low, high-virulence phages rapidly run out of available hosts, and so selection favours low-virulence phages which maximise within-host replication and transmission potential [153].

The rate of bacterial clearance by phages is determined by temperature-dependent life-history traits including adsorption rate, latent period, and burst size. Rapid adsorption and short latent periods mean host cells are lysed quickly at the cost of a reduced burst size. High temperatures have been shown to reduce latent periods in some phages [147], with this reduction potentially making the phages more virulent [153]. In addition, phage virulence may increase with temperature through pleiotropy with thermal adaptation. For example, Kashiwagi et al. [183] found that mutations arising from thermal selection resulted in more rapid adsorption, reduced latent periods, and extended burst sizes. Given that thermal adaptation occurs more rapidly in some phages than others [117], pleiotropy may allow phages to improve competition outcomes as host availability rises during warming events.

The interaction between thermal adaptation and competition is bi-directional. While thermal adaptation can alter competitiveness, competition has the potential to restrict species' thermal adaptation [220]. Competition restricts thermal adaptation by reducing population growth rates and restricting the generation of adaptive mutations [221]. Competition can also reduce the time available for thermal adaptation by promoting the exclusion of thermally maladapted taxa [222]. The presence of competitors is expected to restrict phage thermal adaptation. However, some studies have suggested that competition can promote thermal adaptation when both selection pressures are acting in the same direction [197,214]. For instance, in some phage systems, both competition and high temperatures select for shorter latent periods [153,183]. Synergistic selection between competition and thermal adaptation may help to stabilise phageomes during thermal perturbations.

1.4 *Pseudomonas aeruginosa* as a model host

The focal host used in this thesis is the bacterium *Pseudomonas aeruginosa*. *P. aeruginosa* is an opportunistic, gram-negative bacterium commonly associated with infections of plants, nematodes, insects, and mammals. In humans, *P. aeruginosa* can cause infections in patients with cystic fibrosis where it establishes early in life and persists as part of the sputal microbiome [223]. Yet, *P. aeruginosa* is also associated with infections of burn wounds and urinary tract infections, and individual strains are capable of translocating between body sites [224]. The ability of this bacterium to grow across diverse environments reflects a broad metabolic capacity; *P. aeruginosa* is a facultative aerobe being able to respire both aerobically and anaerobically in the presence of nitrate. *P. aeruginosa* is also highly resilient to environmental stresses with a thermal tolerance range of ~4°C to ~42°C+ [225] and has high resistance to common antibiotics [226].

P. aeruginosa strains have a set of distinctive, shared traits. Firstly, *P. aeruginosa* strains produce a series of pigments, including pyoverdine and pyocyanin, which contribute to nutrient acquisition and biofilm formation. The production of these pigments led to the first descriptions of the species in 1882 in a report on causes of bandage colouration in patients [225]. In addition to pigments, *P. aeruginosa* produces large quantities of biofilm, an extra-cellular matrix comprised of bacterial cells and exopolysaccharides, assembled by adhesins [227]. Biofilm production plays an important role in *P. aeruginosa* pathogenesis and resistance to antibiotics and phages. Finally, *P. aeruginosa* cells are coated by an array of type IV pili and flagella involved in surface adhesion, DNA uptake, and motility [228].

A focal *P. aeruginosa* strain used in experimental research is PAO1. Obtained from a patient wound in Australia in 1954, *P. aeruginosa* PAO1 was the first strain to undergo full genome sequencing [229]. It has a genome size of 6.3 Mbp (66.6% G + C content) and ~5,700 genes. In contrast to most *P. aeruginosa* strains, PAO1 does not carry any prophages [225]. This lack of prophages makes *P. aeruginosa* PAO1 a powerful system for phage research without the risk of phage contaminants. However, as a result of its widespread use for general bacterial

research, *P. aeruginosa* PAO1 has undergone its own evolution over the last 70 years leading to wide genetic and phenotypic heterogeneity [230].

1.5 Pseudomonas phages as model parasites

The focal parasites used in this thesis are three lytic bacteriophages of *P. aeruginosa* PAO1 named φPEV2, φLUZ19, and φ14-1. These phages were first characterised around 2010 and have since been used in studies to determine phage infection mechanisms [231], assess phage ecological and evolutionary dynamics [232,233], and characterise the evolution of bacterial antiphage resistance [22,185].

φPEV2 is an "N4-like" phage belonging to the Podoviridae family, characterised by an icosahedral capsid and a short, non-contractile tail [234]. The life-history traits of φPEV2 are presented in detail in Ceyssens et al. [234] and include a short latent period of ~18-25 minutes at 37°C (also see [235]) and an intermediate burst size of ~100-150 particles/cell. φPEV2 can infect under both aerobic and anaerobic conditions although infection length is extended under the latter. The genome of PEV2 is 72,697 bp in length encoding 92 proteins and has a GC content of 54.9% [234]. The phage encodes transcriptional machinery for all stages of phage replication and carries a viral RNA polymerase in its capsid which is translocated into the cell during infection. φPEV2 is thought to infect cells by adsorbing to LPS on the cell surface but potentially uses the outer-membrane protein NrfA as a target receptor for DNA transfer [235,236].

φLUZ19 is a "φKMV-like" phage belonging to the Autographiviridae family [237]. This family is characterised by phages encoding a single sub-unit RNA polymerase and relying on host transcriptional machinery for the expression of early and middle stage genes. φLUZ19 has a latent period of ~20 minutes and a smaller burst size of ~100 particles/cell [238]. The phage genome length is 43,548 bp and has a GC content of 62.3%, encoding for 54 proteins. φLUZ19

is thought to infect cells by adsorbing to type IV pili [239]. Infection by φLUZ19 can suppress superinfections through the downregulation of type IV pilus expression [237,238].

Finally, φ14-1 is a "PB1-like" phage belonging to the Myoviridae family [240], characterised by an icosahedral capsid and a long, contractile tail. While the life-history traits of φ14-1 have not been characterised, PB1-like phages generally have latent periods of ~50 minutes and large burst sizes of ~180 particles/cell [241]. φ14-1 has a genome size of 66,238 bp and GC content of 55.6%, encoding for 90 proteins. In contrast to φPEV2 and φLUZ19, φ14-1 does not encode its own transcriptional machinery and so depends on that of its host. φ14-1 is thought to infect cells through adsorption to LPS although a specific target receptor has not yet been identified [241].

φPEV2, φLUZ19, and φ14-1 differ in their competitive abilities such that, in direct competition, φPEV2 is the most competitive and excludes the other two [22]. This outcome is consistent with theory that suggests that selection favours phages with short latent periods and large burst sizes [153]. Competition outcomes between φLUZ19 and φ14-1 are less clear with phage dominance varying over time, possibly reflecting co-evolutionary dynamics [22].

Serial passaging of all three phages in *P. aeruginosa* populations has revealed that these viruses can rapidly adapt to their hosts [22,232]. The phages have also been shown to select for the evolution of bacterial anti-phage resistance [185,232]. The bacterial mutations that are under selection confirm the phage bacterial surface targets; φPEV2 and φ14-1 resistance arises from mutations in LPS production genes while φLUZ19 resistance arises from type IV pili mutations [185]. While both phages and bacterial hosts display reciprocal co-evolution, co-evolutionary dynamics vary between phages [233]. φ14-1 and φPEV2 both exhibit arms-race co-evolutionary dynamics whereby directional selection occurs for both phage infectivity and host resistance [233]. In contrast, co-evolution with φLUZ19 occurs via fluctuating selection dynamics where there is negative frequency dependent selection for bacterial and phage genotypes [233].

1.6 Thesis outline

In this thesis I will develop on the above themes. Specifically:

In **Chapter 2**, I investigate the impact of temperature on phage infection, life-history traits, and competition dynamics in a three-phage community. I show that temperature has variable effects on phage infection whereby some phages have high thermal sensitivity while others are thermally tolerant. I further show that phage thermal sensitivity is driven by temperature effects on different life-history traits including adsorption and replication. Finally, I demonstrate that, by changing life-history traits, temperature can alter inter-phage competition dynamics and drive shifts in community composition.

In **Chapter 3**, I investigate the interaction between thermal adaptation and phage community ecology. I show that phages can avoid thermal extinctions via rapid evolutionary rescue. However, rescue can alter competition dynamics leading to exclusion and constrained evolution rates in a phage competitor. Phage co-existence can recover through stabilising mechanisms. The results highlight that adaptation to thermal stress can de-stabilise community interactions by altering the competitive hierarchy.

In **Chapter 4**, I extend the work of Chapter 3 to consider the impact of community interactions on phage adaptation to thermal heterogeneity. I show that, in monoculture, fluctuating temperatures select for intermediate thermal phenotypes in one phage and more variable evolutionary trajectories compared to static temperatures. However, the presence of competition constrains thermal adaptation and evolution rates. The results highlight that community interactions may constrain adaptation in response to thermal heterogeneity.

Finally, in **Chapter 5**, I summarise the main findings from Chapters 2-4 and discuss the wider implications of thermal stress and variability for parasite communities.

1.7 References

1. Li J, Bates KA, Hoang KL, Hector TE, Knowles SCL, King KC. Experimental temperatures shape host microbiome diversity and composition. Global Change Biology. 2023;29(1):41–56.

2. Peterson ME, Daniel RM, Danson MJ, Eisenthal R. The dependence of enzyme activity on temperature: determination and validation of parameters. Biochem J. 2007 Mar 1;402(Pt 2):331–7.

3. Ratkowsky DA, Olley J, McMeekin TA, Ball A. Relationship between temperature and growth rate of bacterial cultures. J Bacteriol. 1982 Jan;149(1):1–5.

4. Schulte PM, Healy TM, Fangue NA. Thermal Performance Curves, Phenotypic Plasticity, and the Time Scales of Temperature Exposure. Integrative and Comparative Biology. 2011 Nov 1;51(5):691–702.

5. Cohen JM, Venesky MD, Sauer EL, Civitello DJ, McMahon TA, Roznik EA, et al. The thermal mismatch hypothesis explains host susceptibility to an emerging infectious disease. Ecology Letters. 2017;20(2):184–93.

6. Gehman ALM, Hall RJ, Byers JE. Host and parasite thermal ecology jointly determine the effect of climate warming on epidemic dynamics. Proceedings of the National Academy of Sciences. 2018 Jan 23;115(4):744–9.

7. Padfield D, Castledine M, Buckling A. Temperature-dependent changes to host–parasite interactions alter the thermal performance of a bacterial host. ISME J. 2020 Feb;14(2):389–98.

8. Kirk D, O'Connor MI, Mordecai EA. Scaling effects of temperature on parasitism from individuals to populations. Journal of Animal Ecology. 2022;91(10):2087–102.

9. Knies JL, Izem R, Supler KL, Kingsolver JG, Burch CL. The Genetic Basis of Thermal Reaction Norm Evolution in Lab and Natural Phage Populations. PLOS Biology. 2006 Jun 6;4(7):e201.

10. Ismail S, Farner J, Couper L, Mordecai E, Lyberger K. Temperature and intraspecific variation affect host-parasite interactions. Oecologia. 2024 Feb;204(2):389–99.

11. Viney ME, Graham AL. Patterns and processes in parasite co-infection. Adv Parasitol. 2013;82:321–69.

12. Read AF, Taylor LH. The ecology of genetically diverse infections. Science. 2001 May 11;292(5519):1099–102.

13. Hasik AZ, King KC, Hawlena H. Interspecific host competition and parasite virulence evolution. Biology Letters. 2023 May 3;19(5):20220553.

14. Nabity PD, Barron-Gafford GA, Whiteman NK. Intraspecific competition for host resources in a parasite. Current Biology. 2021 Mar 22;31(6):1344-1350.e3.

15. Mideo N. Parasite adaptations to within-host competition. Trends in Parasitology. 2009 Jun 1;25(6):261–8.

16. Hoang KL, King KC. Symbiont-mediated immune priming in animals through an evolutionary lens. Microbiology. 2022;168(4):001181.

17. Nguyen TVP, Wu Y, Yao T, Trinh JT, Zeng L, Chemla YR, et al. Coinfecting phages impede each other's entry into the cell. Current Biology. 2024 Jul 8;34(13):2841-2853.e18.

18. Selva L, Viana D, Regev-Yochay G, Trzcinski K, Corpa JM, Lasa íñigo, et al. Killing niche competitors by remote-control bacteriophage induction. Proceedings of the National Academy of Sciences. 2009 Jan 27;106(4):1234–8.

19. Ebert D, Weisser WW. Optimal killing for obligate killers: the evolution of life histories and virulence of semelparous parasites. Proceedings of the Royal Society of London Series B: Biological Sciences. 1997 Jul 22;264(1384):985–91.

20. Rankin DJ, Bargum K, Kokko H. The tragedy of the commons in evolutionary biology. Trends in Ecology & Evolution. 2007 Dec 1;22(12):643–51.

21. Gandon S, Jansen VAA, Baalen M van. Host life history and the evolution of parasite virulence. Evolution. 2001 May 1;55(5):1056-1062.

22. Betts A, Gray C, Zelek M, MacLean RC, King KC. High parasite diversity accelerates host adaptation and diversification. Science. 2018 May 25;360(6391):907–11.

23. Chesson P. Mechanisms of Maintenance of Species Diversity. Annual Review of Ecology, Evolution, and Systematics. 2000 Nov 1;31(Volume 31, 2000):343–66.

24. Pyenson NC, Leeks A, Nweke O, Goldford JE, Schluter J, Turner PE, et al. Diverse phage communities are maintained stably on a clonal bacterial host. Science. 2024 Dec 13;386(6727):1294–300.

25. Best A, White A, Kisdi É, Antonovics J, Brockhurst MA, Boots M. The Evolution of Host-Parasite Range. The American Naturalist. 2010 Jul;176(1):63–71.

26. Hochberg ME, Holt RD. The Coexistence of Competing Parasites. I. The Role of Cross-Species Infection. The American Naturalist. 1990 Oct;136(4):517–41.

27. Suttle CA. Marine viruses — major players in the global ecosystem. Nat Rev Microbiol. 2007 Oct;5(10):801–12.

28. Williamson KE, Fuhrmann JJ, Wommack KE, Radosevich M. Viruses in Soil Ecosystems: An Unknown Quantity Within an Unexplored Territory. Annu Rev Virol. 2017 Sep 29;4(1):201–19.

29. Maslov S, Sneppen K. Population cycles and species diversity in dynamic Kill-the-Winner model of microbial ecosystems. Sci Rep. 2017 Jan 4;7(1):39642.

30. Koskella B, Brockhurst MA. Bacteria–phage coevolution as a driver of ecological and evolutionary processes in microbial communities. FEMS Microbiology Reviews. 2014 Sep 1;38(5):916–31.

31. Jończyk E, Kłak M, Międzybrodzki R, Górski A. The influence of external factors on bacteriophages--review. Folia Microbiol (Praha). 2011 May;56(3):191–200.

32. Kordas RL, Harley CDG, O'Connor MI. Community ecology in a warming world: The influence of temperature on interspecific interactions in marine systems. Journal of Experimental Marine Biology and Ecology. 2011 Apr 30;400(1):218–26.

33. Gillooly JF, Allen AP, West GB, Brown JH. The rate of DNA evolution: Effects of body size and temperature on the molecular clock. Proceedings of the National Academy of Sciences. 2005 Jan 4;102(1):140–5.

34. Bennett AF, Lenski RE. An experimental test of evolutionary trade-offs during temperature adaptation. Proceedings of the National Academy of Sciences. 2007 May 15;104(suppl_1):8649–54.

35. Nabergoj D, Modic P, Podgornik A. Effect of bacterial growth rate on bacteriophage population growth rate. Microbiologyopen. 2017 Dec 1;7(2):e00558.

36. Wiggins BA, Alexander M. Minimum bacterial density for bacteriophage replication: implications for significance of bacteriophages in natural ecosystems. Applied and Environmental Microbiology. 1985 Jan;49(1):19–23.

37. Wommack KE, Hill RT, Muller TA, Colwell RR. Effects of sunlight on bacteriophage viability and structure. Appl Environ Microbiol. 1996 Apr;62(4):1336–41.

38. Blazanin M, Lam WT, Vasen E, Chan BK, Turner PE. Decay and damage of therapeutic phage OMKO1 by environmental stressors. PLOS ONE. 2022 Feb 23;17(2):e0263887.

39. Bettarel Y, Bouvier T, Bouvy M. Viral persistence in water as evaluated from a tropical/temperate cross-incubation. Journal of Plankton Research. 2009 Aug 1;31(8):909–16.

40. Danovaro R, Corinaldesi C, Dell'Anno A, Fuhrman JA, Middelburg JJ, Noble RT, et al. Marine viruses and global climate change. FEMS Microbiology Reviews. 2011 Nov 1;35(6):993–1034.

41. Howard-Varona C, Hargreaves KR, Abedon ST, Sullivan MB. Lysogeny in nature: mechanisms, impact and ecology of temperate phages. ISME J. 2017 Jul;11(7):1511–20.

42. Touchon M, Moura de Sousa JA, Rocha EP. Embracing the enemy: the diversification of microbial gene repertoires by phage-mediated horizontal gene transfer. Current Opinion in Microbiology. 2017 Aug 1;38:66–73.

43. Oliver KM, Degnan PH, Hunter MS, Moran NA. Bacteriophages Encode Factors Required for Protection in a Symbiotic Mutualism. Science. 2009 Aug 21;325(5943):992–4.

44. Taylor VL, Fitzpatrick AD, Islam Z, Maxwell KL. Chapter One - The Diverse Impacts of Phage Morons on Bacterial Fitness and Virulence. In: Kielian M, Mettenleiter TC, Roossinck MJ, editors. Advances in Virus Research. Academic Press; 2019. p. 1–31.

45. Ripp S, Miller RV. The role of pseudolysogeny in bacteriophage-host interactions in a natural freshwater environment. Microbiology (Reading). 1997 Jun;143(6):2065–70.

46. Oppenheim AB, Kobiler O, Stavans J, Court DL, Adhya S. Switches in bacteriophage lambda development. Annu Rev Genet. 2005;39:409–29.

47. Yang L, Wang J, Lu S, Zhong Y, Xiong K, Liu X, et al. Temperature-dependent carrier state mediated by H-NS promotes the long-term coexistence of Y. pestis and a phage in soil. PLOS Pathogens. 2023 Jun 22;19(6):e1011470.

48. Anesio AM, Bellas CM. Are low temperature habitats hot spots of microbial evolution driven by viruses? Trends in Microbiology. 2011 Feb 1;19(2):52–7.

49. Heinrichs ME, Piedade GJ, Popa O, Sommers P, Trubl G, Weissenbach J, et al. Breaking the Ice: A Review of Phages in Polar Ecosystems. Methods Mol Biol. 2024;2738:31–71.

50. Price PB, Nagornov OV, Bay R, Chirkin D, He Y, Miocinovic P, et al. Temperature profile for glacial ice at the South Pole: Implications for life in a nearby subglacial lake. Proceedings of the National Academy of Sciences. 2002 Jun 11;99(12):7844–7.

51. Bezuidt OKI, Lebre PH, Pierneef R, León-Sobrino C, Adriaenssens EM, Cowan DA, et al. Phages Actively Challenge Niche Communities in Antarctic Soils. mSystems. 2020 May 5;5(3):10.1128/msystems.00234-20.

52. Adriaenssens EM, Kramer R, Van Goethem MW, Makhalanyane TP, Hogg I, Cowan DA. Environmental drivers of viral community composition in Antarctic soils identified by viromics. Microbiome. 2017 Jul 19;5(1):83.

53. McKay C, Mellon MT, Friedmann EI. Soil temperatures and stability of ice-cemented ground in the McMurdo Dry Valleys, Antarctica. Antarct Sci. 1998 Mar;10(1):31–8.

54. Selcuk E, Dokuz S, Ozbek T. Evaluating the Stability of Lytic and Lysogenic Bacteriophages in Various Protectants. Journal of Pharmaceutical Sciences. 2024 Jun 1;113(6):1488–97.

55. Brown JH, Gillooly JF, Allen AP, Savage VM, West GB. Toward a Metabolic Theory of Ecology. Ecology. 2004;85(7):1771–89.

56. D'Amico S, Collins T, Marx J, Feller G, Gerday C, Gerday C. Psychrophilic microorganisms: challenges for life. EMBO reports. 2006 Mar;7(4):385–9.

57. Cheng R, Li X, Jiang L, Gong L, Geslin C, Shao Z. Virus diversity and interactions with hosts in deep-sea hydrothermal vents. Microbiome. 2022 Dec 24;10(1):235.

58. Wei D, Zhang X. Proteomic Analysis of Interactions between a Deep-Sea Thermophilic Bacteriophage and Its Host at High Temperature. J Virol. 2010 Mar;84(5):2365–73.

59. He T, Li H, Zhang X. Deep-Sea Hydrothermal Vent Viruses Compensate for Microbial Metabolism in Virus-Host Interactions. mBio. 2017 Jul 11;8(4):e00893-17.

60. Marks TJ, Rowland IR. The Diversity of Bacteriophages in Hot Springs. In: Tumban E, editor. Bacteriophages: Methods and Protocols. New York, NY: Springer US; 2024. p. 73–88.

61. Zierenberg RA, Adams MWW, Arp AJ. Life in extreme environments: Hydrothermal vents. Proceedings of the National Academy of Sciences. 2000 Nov 21;97(24):12961–2.

62. Cathalot C, Roussel EG, Perhirin A, Creff V, Donval JP, Guyader V, et al. Hydrothermal plumes as hotspots for deep-ocean heterotrophic microbial biomass production. Nat Commun. 2021 Nov 25;12(1):6861.

63. Kering KK, Zhang X, Nyaruaba R, Yu J, Wei H. Application of Adaptive Evolution to Improve the Stability of Bacteriophages during Storage. Viruses. 2020 Apr 9;12(4):423.

64. Prestel E, Salamitou S, DuBow MS. An examination of the bacteriophages and bacteria of the Namib desert. J Microbiol. 2008 Aug;46(4):364–72.

65. Zablocki O, Adriaenssens EM, Cowan D. Diversity and Ecology of Viruses in Hyperarid Desert Soils. Appl Environ Microbiol. 2016 Feb 1;82(3):770–7.

66. Zhao Y, Norouzi H, Azarderakhsh M, AghaKouchak A. Global Patterns of Hottest, Coldest and Extreme Diurnal Variability on Earth. Bulletin of the American Meteorological Society. 2021 May 10;102:1–23.

67. Makhalanyane TP, Valverde A, Gunnigle E, Frossard A, Ramond JB, Cowan DA. Microbial ecology of hot desert edaphic systems. FEMS Microbiology Reviews. 2015 Mar 1;39(2):203–21.

68. Sea Surface Temperature (1 month - Aqua/MODIS) | NASA [Internet]. Sea Surface Temperature (1 month - Aqua/MODIS) | NASA. NASA Earth Observations (NEO); 2024 [cited 2024 Jun 11]. Available from: https://neo.gsfc.nasa.gov/view.php?datasetId=MYD28M

69. Williamson KE. Soil Phage Ecology: Abundance, Distribution, and Interactions with Bacterial Hosts. In: Witzany G, editor. Biocommunication in Soil Microorganisms. Berlin, Heidelberg: Springer; 2011. p. 113–36.

70. Lembrechts JJ, van den Hoogen J, Aalto J, Ashcroft MB, De Frenne P, Kemppinen J, et al. Global maps of soil temperature. Global Change Biology. 2022;28(9):3110–44.

71. Vallino M, Rossi M, Ottati S, Martino G, Galetto L, Marzachì C, et al. Bacteriophage-Host Association in the Phytoplasma Insect Vector Euscelidius variegatus. Pathogens. 2021 May 17;10(5):612.

72. Manrique P, Bolduc B, Walk ST, van der Oost J, de Vos WM, Young MJ. Healthy human gut phageome. Proceedings of the National Academy of Sciences. 2016 Sep 13;113(37):10400–5.

73. Moreira MO, Qu YF, Wiens JJ. Large-scale evolution of body temperatures in land vertebrates. Evolution Letters. 2021 Oct 1;5(5):484–94.

74. R Core Team. R: A language and environment for statistical computing. [Internet]. Foundation for Statistical Computing, Vienna, Austria.; 2021. Available from: https://www.R-project.org/

75. RStudio Team. RStudio: Integrated Development for R. [Internet]. RStudio, PBC, Boston, M; 2020. Available from: http://www.rstudio.com/

76. AR6 Synthesis Report: Climate Change 2023. Available from: https://www.ipcc.ch/report/ar6/syr/

77. Accoti A, Damiani C, Nunzi E, Cappelli A, Iacomelli G, Monacchia G, et al. Anopheline mosquito saliva contains bacteria that are transferred to a mammalian host through blood feeding. Front Microbiol. 2023 Jul 18;14.

78. Hyman P. Phages for Phage Therapy: Isolation, Characterization, and Host Range Breadth. Pharmaceuticals (Basel). 2019 Mar 11;12(1):35.

79. Clarke A. The thermal limits to life on Earth. International Journal of Astrobiology. 2014 Apr;13(2):141–54.

80. Clasen JL, Brigden SM, Payet JP, Suttle CA. Evidence that viral abundance across oceans and lakes is driven by different biological factors. Freshwater Biology. 2008;53(6):1090–100.

81. Kawai Y, Wada A. Diurnal sea surface temperature variation and its impact on the atmosphere and ocean: A review. J Oceanogr. 2007 Oct 1;63(5):721–44.

82. Liu B, Zhou W, Henderson M, Sun Y, Shen X. Climatology of the Soil Surface Diurnal Temperature Range in a Warming World: Annual Cycles, Regional Patterns, and Trends in China. Earth's Future. 2022;10(1):e2021EF002220.

83. Shaltout M. Recent sea surface temperature trends and future scenarios for the Red Sea. Oceanologia. 2019 Oct 1;61(4):484–504.

84. Cai W, Ng B, Geng T, Jia F, Wu L, Wang G, et al. Anthropogenic impacts on twentieth-century ENSO variability changes. Nat Rev Earth Environ. 2023 Jun;4(6):407–18.

85. Cai W, Borlace S, Lengaigne M, van Rensch P, Collins M, Vecchi G, et al. Increasing frequency of extreme El Niño events due to greenhouse warming. Nature Clim Change. 2014 Feb;4(2):111–6.

86. Payet J, Suttle C. Physical and biological correlates of virus dynamics in the southern Beaufort Sea and Amundsen Gulf. J Mar Syst. 2007 Jan 1;74.

87. Cornell CR, Zhang Y, Van Nostrand JD, Wagle P, Xiao X, Zhou J. Temporal Changes of Virus-Like Particle Abundance and Metagenomic Comparison of Viral Communities in Cropland and Prairie Soils. mSphere. 2021 Jun 2;6(3):10.1128/msphere.01160-20.

88. Hevroni G, Philosof A. Daily and Seasonal Rhythms of Marine Phages of Cyanobacteria. In: Johnson CH, Rust MJ, editors. Circadian Rhythms in Bacteria and Microbiomes. Cham: Springer International Publishing; 2021. p. 387–415.

89. Larkin AA, Moreno AR, Fagan AJ, Fowlds A, Ruiz A, Martiny AC. Persistent El Niño driven shifts in marine cyanobacteria populations. PLoS One. 2020 Sep 16;15(9):e0238405.

90. Ashy RA, Jalal RS, Sonbol HS, Alqahtani MD, Sefrji FO, Alshareef SA, et al. Functional annotation of rhizospheric phageome of the wild plant species Moringa oleifera. Frontiers in Microbiology. 2023;14.

91. López-Cuevas O, González-Gómez JP, Aguirre-Sánchez JR, Gomez-Gil B, Torres-Montoya EH, Medrano-Félix JA, et al. Genomic Characterization of Twelve Lytic Bacteriophages Infecting Midgut Bacteria of Aedes aegypti. Curr Microbiol. 2022 Nov 3;79(12):385.

92. Haesemeyer M. Thermoregulation in fish. Mol Cell Endocrinol. 2020 Dec 1;518:110986.

93. Kearney M, Shine R, Porter WP. The potential for behavioral thermoregulation to buffer "cold-blooded" animals against climate warming. Proceedings of the National Academy of Sciences. 2009 Mar 10;106(10):3835–40.

94. Wang H, Ling Y, Shan T, Yang S, Xu H, Deng X, et al. Gut virome of mammals and birds reveals high genetic diversity of the family Microviridae. Virus Evolution. 2019 Jan 1;5(1):vez013.

95. Godyń D, Herbut P, Angrecka S. Measurements of peripheral and deep body temperature in cattle – A review. Journal of Thermal Biology. 2019 Jan 1;79:42–9.

96. McFadden ER, Pichurko BM, Bowman HF, Ingenito E, Burns S, Dowling N, et al. Thermal mapping of the airways in humans. J Appl Physiol (1985). 1985 Feb;58(2):564–70.

97. Sund-Levander M, Forsberg C, Wahren LK. Normal oral, rectal, tympanic and axillary body temperature in adult men and women: a systematic literature review. Scandinavian Journal of Caring Sciences. 2002;16(2):122–8.

98. Leggett JE. Approach to fever or suspected infection in the normal host. In: Goldman-Cecil Medicine. 26th ed. Philadelphia, PA: Elsevier; 2020. p. 1809–15.

99. Abrahams PW. Involuntary soil ingestion and geophagia: A source and sink of mineral nutrients and potentially harmful elements to consumers of earth materials. Applied Geochemistry. 2012 May 1;27(5):954–68.

100. Zhang T, Breitbart M, Lee WH, Run JQ, Wei CL, Soh SWL, et al. RNA Viral Community in Human Feces: Prevalence of Plant Pathogenic Viruses. PLoS Biol. 2006 Jan;4(1):e3.

101. Carlino N, Blanco-Míguez A, Punčochář M, Mengoni C, Pinto F, Tatti A, et al. Unexplored microbial diversity from 2,500 food metagenomes and links with the human microbiome. Cell. 2024 Oct 3; pp. 5775-5795.e5715.

102. Dey R, Joshi AB, Oliveira F, Pereira L, Guimarães-Costa AB, Serafim TD, et al. Gut Microbes Egested during Bites of Infected Sand Flies Augment Severity of Leishmaniasis via Inflammasome-Derived IL-1β. Cell Host Microbe. 2018 Jan 10;23(1):134-143.e6.

103. Pirnay JP, Djebara S, Steurs G, Griselain J, Cochez C, De Soir S, et al. Personalized bacteriophage therapy outcomes for 100 consecutive cases: a multicentre, multinational, retrospective observational study. Nat Microbiol. 2024 Jun;9(6):1434–53.

104. Wang X, Wei Z, Yang K, Wang J, Jousset A, Xu Y, et al. Phage combination therapies for bacterial wilt disease in tomato. Nature Biotechnology. 2019 Dec;37(12):1513–20.

105. Lim ES, Zhou Y, Zhao G, Bauer IK, Droit L, Ndao IM, et al. Early life dynamics of the human gut virome and bacterial microbiome in infants. Nat Med. 2015 Oct;21(10):1228–34.

106. Zhong ZP, Tian F, Roux S, Gazitúa MC, Solonenko NE, Li YF, et al. Glacier ice archives nearly 15,000-year-old microbes and phages. Microbiome. 2021 Jul 20;9(1):160.

107. Leigh BA, Bordenstein SR, Brooks AW, Mikaelyan A, Bordenstein SR. Finer-Scale Phylosymbiosis: Insights from Insect Viromes. mSystems. 2018 Dec 18;3(6):e00131-18.

108. Breitbart M, Wegley L, Leeds S, Schoenfeld T, Rohwer F. Phage Community Dynamics in Hot Springs. Appl Environ Microbiol. 2004 Mar;70(3):1633–40.

109. Tamburello G, Chiodini G, Ciotoli G, Procesi M, Rouwet D, Sandri L, et al. Global thermal spring distribution and relationship to endogenous and exogenous factors. Nat Commun. 2022 Oct 26;13(1):6378.

110. Pentecost A, Jones B, Renaut RW. What is a hot spring? Can J Earth Sci. 2003 Nov;40(11):1443–6.

111. Campbell A. The future of bacteriophage biology. Nat Rev Genet. 2003 Jun;4(6):471–7.

112. Mojica KDA, Brussaard CPD. Factors affecting virus dynamics and microbial host–virus interactions in marine environments. FEMS Microbiology Ecology. 2014 Sep 1;89(3):495–515.

113. Bertrand I, Schijven JF, Sánchez G, Wyn-Jones P, Ottoson J, Morin T, et al. The impact of temperature on the inactivation of enteric viruses in food and water: a review. Journal of Applied Microbiology. 2012 Jun 1;112(6):1059–74.

114. Ahmadi H, Radford D, Kropinski AM, Lim LT, Balamurugan S. Thermal-Stability and Reconstitution Ability of Listeria Phages P100 and A511. Frontiers in Microbiology. 2017;8.

115. Marcó MB, Suárez VB, Quiberoni A, Pujato SA. Inactivation of Dairy Bacteriophages by Thermal and Chemical Treatments. Viruses. 2019 May;11(5):480.

116. Bull JJ, Badgett MR, Wichman HA. Big-Benefit Mutations in a Bacteriophage Inhibited with Heat. Molecular Biology and Evolution. 2000 Jun 1;17(6):942–50.

117. Holder KK, Bull JJ. Profiles of adaptation in two similar viruses. Genetics. 2001 Dec;159(4):1393–404.

118. Cox J, Schubert AM, Travisano M, Putonti C. Adaptive evolution and inherent tolerance to extreme thermal environments. BMC Evolutionary Biology. 2010 Mar 12;10(1):75.

119. Brown CJ, Zhao L, Evans KJ, Ally D, Stancik AD. Positive selection at high temperature reduces gene transcription in the bacteriophage ϕX174. BMC Evolutionary Biology. 2010 Dec 3;10(1):378.

120. Vörös Z, Csík G, Herényi L, Kellermayer M. Temperature-Dependent Nanomechanics and Topography of Bacteriophage T7. J Virol. 2018 Sep 26;92(20):e01236-18.

121. Dedeo CL, Teschke CM, Alexandrescu AT. Keeping It Together: Structures, Functions, and Applications of Viral Decoration Proteins. Viruses. 2020 Oct;12(10):1163.

122. Bertozzi Silva J, Storms Z, Sauvageau D. Host receptors for bacteriophage adsorption. FEMS Microbiology Letters. 2016 Feb 1;363(4):fnw002.

123. Tokman JI, Kent DJ, Wiedmann M, Denes T. Temperature Significantly Affects the Plaquing and Adsorption Efficiencies of Listeria Phages. Frontiers in Microbiology. 2016;7.

124. Seeley ND, Primrose SB. The Effect of Temperature on the Ecology of Aquatic Bacteriophages. Journal of General Virology. 1980;46(1):87–95.

125. Tomat D, Aquili V, Casabonne C, Quiberoni A. Influence of Physicochemical Factors on Adsorption of Ten Shigella flexneri Phages. Viruses. 2022 Dec;14(12):2815.

126. Conley MP, Wood WB. Bacteriophage T4 whiskers: a rudimentary environment-sensing device. Proceedings of the National Academy of Sciences. 1975 Sep;72(9):3701–5.

127. Pope WH, Haase-Pettingell C, King J. Protein folding failure sets high-temperature limit on growth of phage P22 in Salmonella enterica serovar Typhimurium. Appl Environ Microbiol. 2004 Aug;70(8):4840–7.

128. Sae-Ueng U, Bhunchoth A, Phironrit N, Treetong A, Sapcharoenkun C, Chatchawankanphanich O, et al. Thermoresponsive C22 phage stiffness modulates the phage infectivity. Sci Rep. 2022 Jul 29;12(1):13001.

129. Cole AW, Tran SD, Ellington AD. Heat adaptation of phage T7 under an extended genetic code. Virus Evol. 2021 Dec 1;7(2):veab100.

130. Leon-Velarde CG, Happonen L, Pajunen M, Leskinen K, Kropinski AM, Mattinen L, et al. Yersinia enterocolitica-Specific Infection by Bacteriophages TG1 and ϕR1-RT Is Dependent on Temperature-Regulated Expression of the Phage Host Receptor OmpF. Appl Environ Microbiol. 2016 Sep 1;82(17):5340–53.

131. Visnapuu A, Van der Gucht M, Wagemans J, Lavigne R. Deconstructing the Phage–Bacterial Biofilm Interaction as a Basis to Establish New Antibiofilm Strategies. Viruses. 2022 May 16;14(5):1057.

132. Bisht K, Moore JL, Caprioli RM, Skaar EP, Wakeman CA. Impact of temperature-dependent phage expression on Pseudomonas aeruginosa biofilm formation. npj Biofilms Microbiomes. 2021 Mar 16;7(1):1–9.

133. Buck LD, Paladino MM, Nagashima K, Brezel ER, Holtzman JS, Urso SJ, et al. Temperature-Dependent Influence of FliA Overexpression on PHL628 E. coli Biofilm Growth and Composition. Front Cell Infect Microbiol. 2021 Dec 17;11.

134. Bisht K, Luecke AR, Wakeman CA. Temperature-specific adaptations and genetic requirements in a biofilm formed by Pseudomonas aeruginosa. Frontiers in Microbiology. 2023;13.

135. del Peso Santos T, Alvarez L, Sit B, Irazoki O, Blake J, Warner BR, et al. BipA exerts temperature-dependent translational control of biofilm-associated colony morphology in Vibrio cholerae. Garrett WS, Mignot T, Zhu J, editors. eLife. 2021 Feb 16;10:e60607.

136. Binetti AG, Quiberoni A, Reinheimer JA. Phage adsorption to Streptococcus thermophilus. Influence of environmental factors and characterization of cell-receptors. Food Research International. 2002 Jan 1;35(1):73–83.

137. Villanueva Valencia JR, Tsimtsirakis E, Krueger S, Evilevitch A. Temperature-induced DNA density transition in phage λ capsid revealed with contrast-matching SANS. Proceedings of the National Academy of Sciences. 2023 Nov 7;120(45):e2220518120.

138. Laguna-Castro M, Rodríguez-Moreno A, Llorente E, Lázaro E. The balance between fitness advantages and costs drives adaptation of bacteriophage Qβ to changes in host density at different temperatures. Front Microbiol. 2023;14:1197085.

139. Hossain MdT, Yokono T, Kashiwagi A. The Single-Stranded RNA Bacteriophage Qβ Adapts Rapidly to High Temperatures: An Evolution Experiment. Viruses. 2020 Jun 12;12(6):638.

140. Kankia BI, Marky LA. DNA, RNA, and DNA/RNA Oligomer Duplexes: A Comparative Study of Their Stability, Heat, Hydration, and Mg2+ Binding Properties. J Phys Chem B. 1999 Oct 1;103(41):8759–67.

141. Pal A, Levy Y. Structure, stability and specificity of the binding of ssDNA and ssRNA with proteins. PLoS Comput Biol. 2019 Apr 1;15(4):e1006768.

142. Duffy S, Shackelton LA, Holmes EC. Rates of evolutionary change in viruses: patterns and determinants. Nat Rev Genet. 2008 Apr;9(4):267–76.

143. Meng B, Qi Z, Li X, Peng H, Bi S, Wei X, et al. Characterization of Mu-Like Yersinia Phages Exhibiting Temperature Dependent Infection. Microbiology Spectrum. 2023 Jul 19;11(4):e00203-23.

144. Lunde M, Aastveit AH, Blatny JM, Nes IF. Effects of Diverse Environmental Conditions on φLC3 Prophage Stability in Lactococcus lactis. Appl Environ Microbiol. 2005 Feb;71(2):721–7.

145. Alizon S, Hurford A, Mideo N, Van Baalen M. Virulence evolution and the trade-off hypothesis: history, current state of affairs and the future. Journal of Evolutionary Biology. 2009;22(2):245–59.

146. Shan J, Korbsrisate S, Withatanung P, Adler NL, Clokie MRJ, Galyov EE. Temperature dependent bacteriophages of a tropical bacterial pathogen. Frontiers in Microbiology. 2014;5.

147. Mercanti DJ, Ackermann HW, Quiberoni A. Characterization of Two Temperate Lactobacillus paracasei Bacteriophages: Morphology, Kinetics and Adsorption. Intervirology. 2015 Feb 24;58(1):49–56.

148. Zaburlin D, Quiberoni A, Mercanti D. Changes in Environmental Conditions Modify Infection Kinetics of Dairy Phages. Food Environ Virol. 2017 Sep 1;9(3):270–6.

149. Chen M, Zhang L, Abdelgader SA, Yu L, Xu J, Yao H, et al. Alterations in gp37 Expand the Host Range of a T4-Like Phage. Applied and Environmental Microbiology. 2017 Nov 16;83(23):e01576-17.

150. Bondy-Denomy J, Qian J, Westra ER, Buckling A, Guttman DS, Davidson AR, et al. Prophages mediate defense against phage infection through diverse mechanisms. ISME J. 2016 Dec;10(12):2854–66.

151. Li D, Liang W, Hu Q, Ren J, Xue F, Liu Q, et al. The effect of a spontaneous induction prophage, phi458, on biofilm formation and virulence in avian pathogenic Escherichia coli. Front Microbiol. 2022 Nov 14;13.

152. Pietikäinen J, Pettersson M, Bååth E. Comparison of temperature effects on soil respiration and bacterial and fungal growth rates. FEMS Microbiology Ecology. 2005 Mar 1;52(1):49–58.

153. Abedon ST, Hyman P, Thomas C. Experimental Examination of Bacteriophage Latent-Period Evolution as a Response to Bacterial Availability. Appl Environ Microbiol. 2003 Dec;69(12):7499–506.

154. Aframian N, Omer Bendori S, Kabel S, Guler P, Stokar-Avihail A, Manor E, et al. Dormant phages communicate via arbitrium to control exit from lysogeny. Nat Microbiol. 2022 Jan;7(1):145–53.

155. Drew GC, Stevens EJ, King KC. Microbial evolution and transitions along the parasite–mutualist continuum. Nat Rev Microbiol. 2021 Oct;19(10):623–38.

156. Knies JL, Kingsolver JG, Burch CL. Hotter is better and broader: thermal sensitivity of fitness in a population of bacteriophages. Am Nat. 2009 Apr;173(4):419–30.

157. McKay LJ, Nigro OD, Dlakić M, Luttrell KM, Rusch DB, Fields MW, et al. Sulfur cycling and host-virus interactions in Aquificales-dominated biofilms from Yellowstone's hottest ecosystems. ISME J. 2022 Mar;16(3):842–55.

158. Perrody E, Cirinesi AM, Desplats C, Keppel F, Schwager F, Tranier S, et al. A bacteriophage-encoded J-domain protein interacts with the DnaK/Hsp70 chaperone and stabilizes the heat-shock factor σ32 of Escherichia coli. PLoS Genet. 2012;8(11):e1003037.

159. Bian H, Li C, Zhu J, Xu L, Li M, Zheng S, et al. Soil Moisture Affects the Rapid Response of Microbes to Labile Organic C Addition. Front Ecol Evol. 2022 Jun 22;10.

160. Prigent M, Leroy M, Confalonieri F, Dutertre M, DuBow MS. A diversity of bacteriophage forms and genomes can be isolated from the surface sands of the Sahara Desert. Extremophiles. 2005 Aug 1;9(4):289–96.

161. Hwang Y, Rahlff J, Schulze-Makuch D, Schloter M, Probst AJ. Diverse Viruses Carrying Genes for Microbial Extremotolerance in the Atacama Desert Hyperarid Soil. mSystems. 2021 May 18;6(3):10.1128/msystems.00385-21.

162. Young I, Wang I, Roof WD. Phages will out: strategies of host cell lysis. Trends Microbiol. 2000 Mar;8(3):120–8.

163. Kannoly S, Oken G, Shadan J, Musheyev D, Singh K, Singh A, et al. Single-Cell Approach Reveals Intercellular Heterogeneity in Phage-Producing Capacities. Microbiol Spectr. 11(1):e02663-21.

164. Müller-Merbach M, Kohler K, Hinrichs J. Environmental factors for phage-induced fermentation problems: Replication and adsorption of the Lactococcus lactis phage P008 as influenced by temperature and pH. Food Microbiology. 2007 Oct 1;24(7):695–702.

165. Koskella B, Meaden S. Understanding Bacteriophage Specificity in Natural Microbial Communities. Viruses. 2013 Mar 11;5(3):806–23.

166. Sant DG, Woods LC, Barr JJ, McDonald MJ. Host diversity slows bacteriophage adaptation by selecting generalists over specialists. Nat Ecol Evol. 2021 Mar;5(3):350–9.

167. Cazares D, Cazares A, Figueroa W, Guarneros G, Edwards RA, Vinuesa P. A Novel Group of Promiscuous Podophages Infecting Diverse Gammaproteobacteria from River Communities Exhibits Dynamic Intergenus Host Adaptation. mSystems. 2021 Feb 2;6(1):e00773-20.

168. Poullain V, Gandon S, Brockhurst MA, Buckling A, Hochberg ME. The evolution of specificity in evolving and coevolving antagonistic interactions between a bacteria and its phage. Evolution. 2008 Jan;62(1):1–11.

169. Piel D, Bruto M, Labreuche Y, Blanquart F, Goudenège D, Barcia-Cruz R, et al. Phage–host coevolution in natural populations. Nat Microbiol. 2022 Jul;7(7):1075–86.

170. Yehl K, Lemire S, Yang AC, Ando H, Mimee M, Torres MDT, et al. Engineering Phage Host-Range and Suppressing Bacterial Resistance through Phage Tail Fiber Mutagenesis. Cell. 2019 Oct 3;179(2):459-469.e9.

171. Strobel HM, Horwitz EK, Meyer JR. Viral protein instability enhances host-range evolvability. PLOS Genetics. 2022 Feb 17;18(2):e1010030.

172. Zhou J, Deng Y, Shen L, Wen C, Yan Q, Ning D, et al. Temperature mediates continental-scale diversity of microbes in forest soils. Nat Commun. 2016 Jul 5;7(1):12083.

173. Garcia FC, Warfield R, Yvon-Durocher G. Thermal traits govern the response of microbial community dynamics and ecosystem functioning to warming. Frontiers in Microbiology. 2022;13.

174. Law R. Optimal Life Histories Under Age-Specific Predation. The American Naturalist. 1979;114(3):399–417.

175. Gallet R, Shao Y, Wang IN. High adsorption rate is detrimental to bacteriophage fitness in a biofilm-like environment. BMC Evolutionary Biology. 2009 Oct 5;9(1):241.

176. Keen EC. Tradeoffs in bacteriophage life histories. Bacteriophage. 2014 Feb 27;4:e28365.

177. García-Villada L, Drake JW. Experimental selection reveals a trade-off between fecundity and lifespan in the coliphage Qß. Open Biology. 2013 Jun;3(6):130043.

178. Paepe MD, Taddei F. Viruses' Life History: Towards a Mechanistic Basis of a Trade-Off between Survival and Reproduction among Phages. PLOS Biology. 2006 Jun 13;4(7):e193.

179. Goldhill DH, Turner PE. The evolution of life history trade-offs in viruses. Current Opinion in Virology. 2014 Oct 1;8:79–84.

180. Demory D, Weitz JS, Baudoux AC, Touzeau S, Simon N, Rabouille S, et al. A thermal trade-off between viral production and degradation drives virus-phytoplankton population dynamics. Ecology Letters. 2021;24(6):1133–44.

181. Dessau M, Goldhill D, McBride RC, Turner PE, Modis Y. Selective pressure causes an RNA virus to trade reproductive fitness for increased structural and thermal stability of a viral enzyme. PLoS Genet. 2012;8(11):e1003102.

182. Kashiwagi A, Sugawara R, Sano Tsushima F, Kumagai T, Yomo T. Contribution of Silent Mutations to Thermal Adaptation of RNA Bacteriophage Qβ. J Virol. 2014 Oct;88(19):11459–68.

183. Kashiwagi A, Kadoya T, Kumasaka N, Kumagai T, Tsushima FS, Yomo T. Influence of adaptive mutations, from thermal adaptation experiments, on the infection cycle of RNA bacteriophage Qβ. Arch Virol. 2018 Oct 1;163(10):2655–62.

184. McGee LW, Aitchison EW, Caudle SB, Morrison AJ, Zheng L, Yang W, et al. Payoffs, Not Tradeoffs, in the Adaptation of a Virus to Ostensibly Conflicting Selective Pressures. PLOS Genetics. 2014 Oct 2;10(10):e1004611.

185. Betts A, Gifford DR, MacLean RC, King KC. Parasite diversity drives rapid host dynamics and evolution of resistance in a bacteria-phage system. Evolution. 2016;70(5):969–78.

186. Wright R, Friman VP, Smith M, Brockhurst M. Resistance Evolution against Phage Combinations Depends on the Timing and Order of Exposure. MBio. 2019 Aug 29;10.

187. Mangalea MR, Duerkop BA. Fitness Trade-Offs Resulting from Bacteriophage Resistance Potentiate Synergistic Antibacterial Strategies. Infect Immun. 2020 Jun 22;88(7):e00926-19.

188. Doron S, Melamed S, Ofir G, Leavitt A, Lopatina A, Keren M, et al. Systematic discovery of anti-phage defense systems in the microbial pan-genome. Science. 2018 Mar 2;359(6379):eaar4120.

189. Vale PF, Lafforgue G, Gatchitch F, Gardan R, Moineau S, Gandon S. Costs of CRISPR-Cas-mediated resistance in Streptococcus thermophilus. Proc Biol Sci. 2015 Aug 7;282(1812):20151270.

190. Aframian N, Bendori SO, Hen T, Guler P, Eldar A. High defense system expression broadens protection range at the cost of increased autoimmunity. bioRxiv; 2023. p. 2023.11.30.569366. Available from: https://www.biorxiv.org/content/10.1101/2023.11.30.569366v2

191. Høyland-Kroghsbo NM, Muñoz KA, Bassler BL. Temperature, by Controlling Growth Rate, Regulates CRISPR-Cas Activity in Pseudomonas aeruginosa. mBio. 2018 Nov 13;9(6):e02184-18.

192. Bidnenko E, Chopin A, Ehrlich SD, Chopin MC. Activation of mRNA translation by phage protein and low temperature: the case of Lactococcus lactis abortive infection system AbiD1. BMC Molecular Biology. 2009 Jan 27;10(1):4.

193. Wang J, Wang X, Yang K, Lu C, Fields B, Xu Y, et al. Phage selection drives resistance-virulence trade-offs in Ralstonia solanacearum plant-pathogenic bacterium irrespective of the growth temperature. Evol Lett. 2024 Apr;8(2):253–66.

194. Donhauser J, Niklaus PA, Rousk J, Larose C, Frey B. Temperatures beyond the community optimum promote the dominance of heat-adapted, fast growing and stress resistant bacteria in alpine soils. Soil Biology and Biochemistry. 2020 Sep 1;148:107873.

195. Wilhelm SW, Suttle CA. Viruses and Nutrient Cycles in the Sea: Viruses play critical roles in the structure and function of aquatic food webs. BioScience. 1999 Oct 1;49(10):781–8.

196. Frazier MR, Huey RB, Berrigan D. Thermodynamics constrains the evolution of insect population growth rates: 'warmer is better'. Am Nat. 2006 Oct;168(4):512–20.

197. Malusare SP, Zilio G, Fronhofer EA. Evolution of thermal performance curves: A meta-analysis of selection experiments. J Evol Biol. 2023 Jan;36(1):15–28.

198. Kassen R. The experimental evolution of specialists, generalists, and the maintenance of diversity. Journal of Evolutionary Biology. 2002;15(2):173–90.

199. Hector TE, Sgrò CM, Hall MD. Pathogen exposure disrupts an organism's ability to cope with thermal stress. Global Change Biology. 2019;25(11):3893–905.

200. Aframian N, Omer Bendori S, Hen T, Guler P, Eldar A. Expression level of anti-phage defence systems controls a trade-off between protection range and autoimmunity. Nat Microbiol. 2025 Aug;10(8):1954–62.

201. Rohr JR, Civitello DJ, Cohen JM, Roznik EA, Sinervo B, Dell AI. The complex drivers of thermal acclimation and breadth in ectotherms. Ecology Letters. 2018;21(9):1425–39.

202. Paull SH, Raffel TR, LaFonte BE, Johnson PTJ. How temperature shifts affect parasite production: testing the roles of thermal stress and acclimation. Functional Ecology. 2015;29(7):941–50.

203. Zhao L, Stancik AD, Brown CJ. Differential Transcription of Bacteriophage φX174 Genes at 37°C and 42°C. PLoS One. 2012 Apr 23;7(4):e35909.

204. Quance MA, Travisano M. Effects of temperature on the fitness cost of resistance to bacteriophage T4 in Escherichia coli. Evolution. 2009 Jun;63(6):1406–16.

205. Kumar JK, Kremsdorf R, Tabor S, Richardson CC. A Mutation in the Gene-encoding Bacteriophage T7 DNA Polymerase That Renders the Phage Temperature-sensitive *. Journal of Biological Chemistry. 2001 Dec 7;276(49):46151–9.

206. Hector TE, Gehman ALM, King KC. Infection burdens and virulence under heat stress: ecological and evolutionary considerations. Philos Trans R Soc Lond B Biol Sci. 378(1873):20220018.

207. Gilchrist GW. Specialists and Generalists in Changing Environments. I. Fitness Landscapes of Thermal Sensitivity. The American Naturalist. 1995;146(2):252–70.

208. Arribas M, Kubota K, Cabanillas L, Lázaro E. Adaptation to Fluctuating Temperatures in an RNA Virus Is Driven by the Most Stringent Selective Pressure. PLOS ONE. 2014 Jun 25;9(6):e100940.

209. Hao YQ, Brockhurst MA, Petchey OL, Zhang QG. Evolutionary rescue can be impeded by temporary environmental amelioration. Ecology Letters. 2015;18(9):892–8.

210. Duncan AB, Dusi E, Jacob F, Ramsayer J, Hochberg ME, Kaltz O. Hot spots become cold spots: coevolution in variable temperature environments. Journal of Evolutionary Biology. 2017;30(1):55–65.

211. Cvijović I, Good BH, Jerison ER, Desai MM. Fate of a mutation in a fluctuating environment. Proc Natl Acad Sci U S A. 2015 Sep 8;112(36):E5021–8.

212. Chevallereau A, Pons BJ, van Houte S, Westra ER. Interactions between bacterial and phage communities in natural environments. Nat Rev Microbiol. 2022 Jan;20(1):49–62.

213. Smith TP, Mombrikotb S, Ransome E, Kontopoulos DG, Pawar S, Bell T. Latent functional diversity may accelerate microbial community responses to temperature fluctuations. Coleman ML, Schuman MC, editors. eLife. 2022 Nov 29;11:e80867.

214. Westley J, García FC, Warfield R, Yvon-Durocher G. The community background alters the evolution of thermal performance. Evolution Letters. 2024 Mar 16;qrae007.

215. Ruan Y, Ling N, Jiang S, Jing X, He JS, Shen Q, et al. Warming and altered precipitation independently and interactively suppress alpine soil microbial growth in a decadal-long experiment. eLife. 2024 Apr 2;12.

216. Wheatley RM, Holtappels D, Koskella B. Phage as signatures of healthy microbiomes [Internet]. bioRxiv; 2024. p. 2024.03.18.585470. Available from: https://www.biorxiv.org/content/10.1101/2024.03.18.585470v1

217. Zhao XF, Li BH, Shu WS, Hao YQ. The contrasting effects of fluctuating temperature on bacterial diversity and performances in temperate and subtropical soils. Molecular Ecology. 2023;32(13):3686–701.

218. Berngruber TW, Froissart R, Choisy M, Gandon S. Evolution of Virulence in Emerging Epidemics. PLoS Pathog. 2013 Mar 14;9(3):e1003209.

219. Griette Q, Raoul G, Gandon S. Virulence evolution at the front line of spreading epidemics. Evolution. 2015;69(11):2810–9.

220. Walberg PB. Competition Increases Risk of Species Extinction during Extreme Warming. The American Naturalist. 2024 Mar;203(3):323–34.

221. Johansson J. Evolutionary responses to environmental changes: how does competition affect adaptation? Evolution. 2008 Feb;62(2):421–35.

222. de Mazancourt C, Johnson E, Barraclough TG. Biodiversity inhibits species' evolutionary responses to changing environments. Ecol Lett. 2008 Apr;11(4):380–8.

223. Elborn JS. Cystic fibrosis. The Lancet. 2016 Nov 19;388(10059):2519–31.

224. Wheatley RM, Caballero JD, van der Schalk TE, De Winter FHR, Shaw LP, Kapel N, et al. Gut to lung translocation and antibiotic mediated selection shape the dynamics of Pseudomonas aeruginosa in an ICU patient. Nat Commun. 2022 Nov 22;13(1):6523.

225. Diggle SP, Whiteley M. Microbe Profile: Pseudomonas aeruginosa: opportunistic pathogen and lab rat. Microbiology (Reading). 2020 Jan;166(1):30–3.

226. Pang Z, Raudonis R, Glick BR, Lin TJ, Cheng Z. Antibiotic resistance in Pseudomonas aeruginosa: mechanisms and alternative therapeutic strategies. Biotechnol Adv. 2019;37(1):177–92.

227. Rather MA, Gupta K, Mandal M. Microbial biofilm: formation, architecture, antibiotic resistance, and control strategies. Braz J Microbiol. 2021 Sep 23;52(4):1701–18.

228. Burrows LL. Pseudomonas aeruginosa twitching motility: type IV pili in action. Annu Rev Microbiol. 2012;66:493–520.

229. Stover CK, Pham XQ, Erwin AL, Mizoguchi SD, Warrener P, Hickey MJ, et al. Complete genome sequence of Pseudomonas aeruginosa PAO1, an opportunistic pathogen. Nature. 2000 Aug;406(6799):959–64.

230. Chandler CE, Horspool AM, Hill PJ, Wozniak DJ, Schertzer JW, Rasko DA, et al. Genomic and Phenotypic Diversity among Ten Laboratory Isolates of Pseudomonas aeruginosa PAO1. J Bacteriol. 2019 Feb 11;201(5):e00595-18.

231. De Smet J, Zimmermann M, Kogadeeva M, Ceyssens PJ, Vermaelen W, Blasdel B, et al. High coverage metabolomics analysis reveals phage-specific alterations to Pseudomonas aeruginosa physiology during infection. ISME J. 2016 Aug;10(8):1823–35.

232. Betts A, Vasse M, Kaltz O, Hochberg ME. Back to the future: evolving bacteriophages to increase their effectiveness against the pathogen Pseudomonas aeruginosa PAO1. Evolutionary Applications. 2013;6(7):1054–63.

233. Betts A, Kaltz O, Hochberg ME. Contrasted coevolutionary dynamics between a bacterial pathogen and its bacteriophages. Proceedings of the National Academy of Sciences. 2014 Jul 29;111(30):11109–14.

234. Ceyssens PJ, Brabban A, Rogge L, Lewis MS, Pickard D, Goulding D, et al. Molecular and physiological analysis of three Pseudomonas aeruginosa phages belonging to the "N4-like viruses". Virology. 2010 Sep 15;405(1):26–30.

235. Danis-Wlodarczyk K, Cai A, Chen A, Gittrich M, Sullivan M, Wozniak D, et al. Friends or Foes? Rapid Determination of Dissimilar Colistin and Ciprofloxacin Antagonism of Pseudomonas aeruginosa Phages. Pharmaceuticals. 2021 Nov 15;14:1162.

236. Kiino DR, Rothman-Denes LB. Genetic analysis of bacteriophage N4 adsorption. J Bacteriol. 1989 Sep;171(9):4595–602.

237. Lavigne R, Lecoutere E, Wagemans J, Cenens W, Aertsen A, Schoofs L, et al. A multifaceted study of Pseudomonas aeruginosa shutdown by virulent podovirus LUZ19. mBio. 2013 Mar 19;4(2):e00061-00013.

238. Brandão A, Pires DP, Coppens L, Voet M, Lavigne R, Azeredo J. Differential transcription profiling of the phage LUZ19 infection process in different growth media. RNA Biology. 2021 Nov 2;18(11):1778–90.

239. Chibeu A, Ceyssens PJ, Hertveldt K, Volckaert G, Cornelis P, Matthijs S, et al. The adsorption of Pseudomonas aeruginosa bacteriophage phiKMV is dependent on expression regulation of type IV pili genes. FEMS Microbiol Lett. 2009 Jun;296(2):210–8.

240. Ceyssens PJ, Miroshnikov K, Mattheus W, Krylov V, Robben J, Noben JP, et al. Comparative analysis of the widespread and conserved PB1-like viruses infecting Pseudomonas aeruginosa. Environmental Microbiology. 2009;11(11):2874–83.

241. Garbe J, Wesche A, Bunk B, Kazmierczak M, Selezska K, Rohde C, et al. Characterization of JG024, a pseudomonas aeruginosa PB1-like broad host range phage under simulated infection conditions. BMC Microbiology. 2010 Nov 26;10(1):301.

2

Warming alters life-history traits and competition in a phage community

This Chapter has been published in *Applied and Environmental Microbiology*

2.1 Abstract

Host-parasite interactions are highly susceptible to changes in temperature due to mismatches in species thermal responses. In nature, parasites often exist in communities, and responses to temperature are expected to vary between host-parasite pairs. Temperature change thus has consequences for both host-parasite dynamics and parasite-parasite interactions. Here, we investigate the impact of warming (37°C, 40°C, 42°C) on parasite life-history traits and competition using the opportunistic bacterial pathogen *Pseudomonas aeruginosa* (host) and a panel of three genetically diverse lytic bacteriophages (parasites). We show that phages vary in their responses to temperature; while 37°C and 40°C did not have a major effect on phage infectivity, infection by two phages was restricted at 42°C. This outcome was attributed to disruption of different phage life-history traits including host attachment and replication inside hosts. Furthermore, we show that temperature mediates competition between phages by altering their competitiveness. These results highlight phage trait variation across thermal regimes with the potential to drive community dynamics. Our results have important implications for eukaryotic viromes and the design of phage cocktail therapies.

2.2 Introduction

Organism performance typically increases with temperature up to an optimum after which performance rapidly decreases (1). Host-parasite interactions are particularly susceptible to changes in temperature due to mismatches in thermal performance between hosts and parasites (2). While parasites and their hosts often share thermal optima, parasites are thought to acclimate rapidly to changing environmental conditions resulting in higher performance either side of the thermal optimum than their hosts during interactions (2–4). Warming beyond the thermal optimum may increase parasite performance relative to host performance and exacerbate parasite burden. Increased parasite burden with warming may also feed back into host thermal responses by reducing host thermal maxima (5,6). However, in some systems, primarily those containing obligate intracellular parasites, parasites have lower thermal maxima than hosts (7,8) creating a thermal niche where hosts can grow in the absence of parasites.

Temperature generally alters parasite infectivity by disrupting parasite life-history traits (9–11). Studies in mosquito populations have shown that higher temperatures can lead to shorter development times, smaller body sizes, and higher intrinsic mortality rates (12–14). Further studies have revealed temperature-dependence of other parasite traits including attachment to hosts (15), reproductive capacity (population growth rates) (7), and virulence (16). In line with the thermal mismatch hypothesis, the impact of temperature on life-history traits often varies between hosts and parasites. *Plasmodium falciparum*, a parasite of mosquitoes and vertebrates, exhibits more rapid development and population growth with warming despite a decrease in the survival of their mosquito hosts (14,17). Similar results are shown with bacteria and their viral parasites, bacteriophages (hereafter referred to as “phages”), albeit in the opposite direction. While warming generally increases bacterial growth rates (18), phages often experience concurrent reductions in host attachment (15), reproductive capacity (7), and stability (19).

Hosts are often attacked by a diversity of parasite genotypes (20–23) and species (24–26). Given parasite genotypes and species often vary in their upper thermal limits (27) and thermal optima (28), the effects of temperature may vary between host-parasite pairs thus shaping the host-parasite community. Temperature change may also alter the outcomes of inter-parasite competition in communities (29) as different parasites become more or less competitive. This phenomenon is not unique to parasites and has also been observed in free-living communities (30–32). Outcomes of parasite competition are additionally affected by variation in specific life-history traits, such as virulence, which can change with temperature (8). Parasite virulence – here defined as the rate at which parasite epidemics reduce host population densities – can play a key role in parasite competition (33,34). Highly virulent parasites, which rapidly reduce host population densities, restrict the availability of host resources for parasite competitors thereby reducing their reproductive capacities (35). By altering parasite virulence, warming may further affect competition outcomes.

Bacteria and phages are the most abundant host-parasite system on Earth (36,37). Phages play key roles in animal microbiomes and plant rhizospheres by maintaining microbiome diversity and providing protection from invasive pathogens (38–41). They are also increasingly viewed as potential therapeutic alternatives to antibiotics given growing levels of antimicrobial resistance (42–45). Bacteria and phages experience broad temperature variation as part of the microbiomes of eukaryotic hosts (39). Body temperatures vary between species (46–50) and individuals (51). Temperatures also vary within individuals across space (48) and over time (52) especially following the onset of fevers during pathogen infection (53). Additionally, phages typically exist in communities either as complex, often host-associated phageomes (39) or through therapeutic deployment in multi-phage cocktails (54). The effects of temperature on bacteria-phage and phage-phage interactions therefore have acute relevance for animal and plant health.

Here, we investigated parasite life-history traits and competition across three temperatures (37°C, 40°C, and 42°C) using the opportunistic bacterial pathogen *Pseudomonas aeruginosa*

and a panel of three genetically diverse lytic bacteriophages targeting different bacterial surface receptors (lipopolysaccharides (LPS) and type IV pili). These temperatures were intended to represent a gradient of warming during a human fever (53) or a diversity of animal resting body temperatures (48–50). Phage thermal responses were determined by measuring different life-history traits (stability, host attachment, reproductive capacity, and virulence) across temperatures. Additionally, the impact of temperature on phage-phage interactions was assessed by measuring population growth in the presence or absence of phage competitors.

We hypothesised the impact of warming on phage population growth would vary across phage types given differential effects on attachment to hosts (15,55), viral replication (56), and lytic ability (57). We further hypothesised that warming would alter phage competition outcomes by increasing the competitiveness of more thermo-tolerant phages (58). Our findings provide insight into how temperature variation may affect parasite life-history traits and interactions in communities. Further, they improve our understanding of how temperature affects parasite community dynamics with important implications for the functioning of eukaryotic host viromes and the design of phage therapies.

2.3 Methods and Materials

2.3.1 Strains, storage, and culture conditions

Pseudomonas aeruginosa PAO1 was used with a collection of three lytic bacteriophages: φPEV2, φLUZ19, and φ14-1. These phages, which have previously been used in ecological and evolutionary biology studies of *P. aeruginosa* at 37°C (59–62), were selected based on their genetic diversity (63) and the different bacterial receptors they target. φPEV2 (N4-like phage) (64) and φ14-1 (PB1-like phage) (65) are both thought to target bacterial LPS surface receptors (66,67) although N4 phage infection has also been linked to the outer-membrane protein NrfA (68). φLUZ19, a T7-like phage, adsorbs to type IV pili (55,69). The three phages also vary in

core phage replicative traits. While φPEV2 and φLUZ19 have latent periods (time from infection to burst) of ~18 minutes (67) and ~20 minutes (69) respectively, PB1-like phages (such as φ14-1) have latent periods up to ~50 minutes (66). φPEV2 and φLUZ19 also have similar burst sizes (number of progeny) (~100-130 virions) (67,70) whereas PB1-like phages can have burst sizes up to ~180 virions (66).

Bacteria were streaked for single colonies from -80°C frozen glycerol stocks (25% glycerol) onto LB (Lennox) agar. Single colonies were inoculated into 15ml LB broth in 50ml falcons and incubated at 37°C, 40°C, or 42°C in static incubators for 16h. After incubation, cultures were centrifuged at 4000 x g for 5 mins to pellet bacterial cells and the pellet was re-suspended in 15ml fresh LB to remove potential secondary metabolites.

Phage lysates were prepared by inoculating a 15ml *P. aeruginosa* PAO1 culture (at a density of ~10^8 CFU/ml) with a sample of -80°C frozen phage glycerol stocks. Samples were taken from frozen stocks with an inoculation loop. Phage-inoculated PAO1 cultures were incubated at 37°C for ~6 hours. Cultures were then centrifuged at 3,095 x g for 5 mins to pellet cell debris and the supernatants (phage lysates) were sterilised using 0.22μM filters.

Phage stocks were quantified using the standard double-layer overlay plaque method (71). Bottom-layer agar was prepared in sterile 12cm/12cm square-petri dishes with LB-agar and top-layer agar was prepared with LB-agarose (0.4% agarose) supplemented with $MgSO_4$ and $CaCl_2$ (10 mM). Briefly, bacterial lawns were prepared by mixing 10ml of melted top agar (~40°C) with 300μL of a *P. aeruginosa* PAO1 overnight culture (approximately 3 x 10^8 CFU/ml). Phage stocks were serially diluted and 10μL were spotted onto the bacterial lawns. After an incubation period of the plates of 6-8 h at 37°C, spots with the highest number of discernible plaques were counted and reported as an average of three technical replicates. Phage stocks were quantified one day before use in experiments and were stored at 4°C.

2.3.2 Experimental design of bacterial and phage growth across temperatures

Bacterial cultures grown at 37°C, 40°C, and 42°C were diluted with LB to a starting concentration of ~3 x 10^7 CFU/ml. Isogenic φPEV2, φLUZ19, and φ14-1 phage stocks were diluted to a concentration of ~3 x 10^7 PFU/ml. Pairwise and 3-phage combinations were prepared by mixing single-phage stocks in equal volumes. Single-phage (10µL), pairwise (20µL), and 3-phage (30µL) stocks were added to loose-lid 5ml falcon tubes and LB was added up to a final volume of 30µL. Diluted bacterial cultures (970µL) were then added to a final volume of 1ml. A no-phage control was included containing 30µL LB and 970µL bacterial culture. Starting concentrations of each phage in single and multi-phage combinations were ~3 x 10^5 PFU/ml resulting in a phage/host ratio (multiplicity of infection - MOI) = 0.01. Cultures were incubated statically at 37°C, 40°C, or 42°C for five hours to allow bacterial and phage growth. Each hour, tubes were destructively sampled for bacterial and phage quantification. Six biological replicates were carried out for each treatment at each temperature over three days with two replicates performed per day.

2.3.3 Measuring bacterial and phage population growth

Bacterial growth was measured using optical density and colony-forming units (CFU). Optical density (595nm) of bacterial cultures was measured over five hours in 96-well plates using a Synergy 2 plate reader (BioTek, Vermont, USA), normalised against LB blanks. Due to the high number of samples, two plates were measured per hour and all phage treatments and temperatures were represented on each plate. Bacterial CFUs in the no-phage control were measured at hours 0 and 5 using serial dilutions in LB, of which 20µL was immediately spotted onto LB-agar. Spots with the highest number of distinct colonies were counted and data represents the average of three technical replicates.

To measure bacterial CFUs in the presence of phage, 100μL aliquots were taken from single-phage treatments at hours 0, 2, and 5, and no-phage treatments at hours 0 and 5. Aliquots were ten-fold serially diluted in a solution of sodium citrate (50 mM) and phosphate-buffered saline (PBS) to reduce phage binding and killing after sampling (72,73). Dilutions were spotted (20uL) onto LB-agar supplemented with sodium citrate (5 mM). Plates were incubated at 37°C for ~16 hours and spots with the highest number of distinct colonies were counted. Data shown represents an average of three technical replicates.

Phage growth in single-phage samples was determined based on plaque-forming units (PFU) using plaque assays as previously described. Aliquots of each sample (100μL) were transferred to 1.5ml Eppendorf tubes and centrifuged at 10,000 x g for five minutes. Phage supernatants were then extracted and ten-fold serially diluted in SM buffer (NaCl 100 mM, $MgSO_4$ 10mM, Tris-HCl (pH 8) 50mM). Serial dilutions were spotted (10uL) onto *P. aeruginosa* PAO1-inoculated bacterial lawns. Plates were incubated at 37°C until visible plaques formed (6-8 hours), and spots with the highest number of distinct plaques were counted. Data shown represents an average of three technical replicates.

Phage growth in multi-phage samples was determined using quantitative PCR (qPCR). qPCR primers were designed based on φPEV2, φLUZ19, and φ14-1 genomes downloaded from NCBI (Table S1). Phage genomes were aligned using progressiveMauve (74) with Geneious (v. 2022.1.1) (https://www.geneious.com). Phage-specific regions with no observable sequence overlap were extracted from each genome and used to create qPCR primers (Table S2) with IDT PrimerQuest (https://eu.idtdna.com/pages/tools/primerquest). Primers were designed to have an annealing temperature of ~60°C with products ~80 bp in length. qPCR melt curves showed single peaks for each primer pair indicating high specificity.

Phage densities were determined based on standard curves. Phage DNA for standard curves was extracted from phage lysates (~10^9 PFU/ml) using the Norgen Biotek Phage DNA Isolation Kit (Norgen Biotek) with added DNase I to remove lysed bacterial DNA. Purified DNA was quantified using NanoDrop 2000c (Thermo Scientific). Duplicate standard curves

were generated from purified DNA dilutions with Luna Universal qPCR Master Mix (New England BioLabs) using a StepOnePlus Real-Time PCR System (Applied Biosystems).

Aliquots of phage lysates (100µL) were taken hourly for qPCR quantification. Phage aliquots were boiled at 100°C for 10 mins to denature bacterial cells and phage particles. Samples were then stored at -20°C. qPCR was carried out on boiled samples diluted in Ambion Nuclease-Free Water (Invitrogen) using phage-specific primers with Luna Universal qPCR Master Mix. Forward and reverse primers (10 µM) were added to final concentration of 0.25 µM. Amplification conditions included initial denaturation (95°C for 60 seconds) followed by 40 cycles of denaturation (95°C for 15 seconds) and annealing/extension (60°C for 30 seconds). One qPCR plate was used per primer pair. Due to space constraints, no technical replicates were performed, but all biological replicates were analysed. Phage DNA concentrations were determined through comparison with standard curves and fold change in DNA copies was calculated by dividing by the average phage DNA concentration at hour 0.

2.3.4 Phage decay and adsorption rates

To measure decay rate, phage stocks were diluted in LB to ~10^5 PFU/ml. Diluted phage stocks (1ml) were added to 1.5ml Eppendorf tubes and incubated statically at 37°C, 40°C, and 42°C for 24h. Samples were taken at 2.5h, 5h, 7.5h, and 24h, serially diluted in SM buffer, and spotted (10uL) onto PAO1-inoculated bacterial lawns. Three independent biological replicates were conducted per temperature for each phage. Plaque numbers for each biological replicate are averages of three technical replicates.

To measure phage adsorption rates, bacterial cultures were grown for ~16 hours at 37°C, 40°C, and 42°C, diluted into 15ml fresh LB in loose-lid 50ml falcon tubes, and grown to mid-exponential phase (~ 10^8 CFU/ml). Mid-exponential phase bacterial cultures (1.485ml) were aliquoted into 1.5ml Eppendorf tubes and placed into heat blocks set at 37°C, 40°C, and 42°C. Phage stocks were diluted to ~10^7 PFU/ml and 15µL were added to the Eppendorf tubes to a

final phage concentration of ~10^5 PFU/ml (MOI = ~0.001) and then mixed by inversion. At five-minute intervals, 100µL samples were taken and centrifuged at 17,000 x g for 1 min. To measure unadsorbed phage, supernatant was sampled, serially diluted in SM buffer, and spotted (10uL) onto PAO1-inoculated bacterial lawns. Three biological replicates were carried out per temperature for each phage. PFUs for each biological replicate are averages of three technical replicates.

2.3.5 Statistical analysis

Statistical analyses and data visualisation were carried out using Microsoft Excel (v.2102) (75), R (v.4.0.3) (76) and RStudio (v1.4.1103) (77). Line graphs and boxplots were generated using the "ggplot2" R package (78). Radar charts were generated using the "ggradar" R package.

The impact of phage on bacterial population densities was determined by comparing optical densities between phage and no-phage treatments at the end of the experiment between temperatures. This was conducted using separate linear mixed effects models for each temperature with the "nlme" R package where optical density was the response variable and phage was a fixed explanatory variable. Experimental batch (three batches as experiment performed across three days) was included as a random effect. Unequal variances between groups were accounted for using the "varIdent" function (79). Similar mixed effect models were used to compare phage PFU/ml and $\log_2$(DNA concentrations) at the start and end of the experiment at each temperature. Additionally, a similar model was used to determine the impact of temperature on bacterial densities where optical density was the response variable and explanatory variables included temperature, time, and a temperature-time interaction term. Post-hoc analyses were carried out using the R "emmeans" package. The relationship between optical density and colony-forming units were determined using a linear model. A square-root transformation was used on CFUs to meet model assumptions.

The impact of temperature on phage decay and host attachment was tested using a Poisson generalised linear model with PFU/ml as response variable and time, temperature, and the interaction between time and temperature as explanatory variables. As more than ~90% attachment occurred before the first measurement for φ14-1, an ANOVA between 0 and 5min was performed rather than GLM. The time required for 50% phage attachment/decay was determined by generating predicted PFU/ml over time with 95% confidence intervals from the GLM. A time range where PFU/ml confidence intervals overlapped with 50% starting densities was recorded.

The impact of temperature on bacterial doublings in the presence of phage (CFU) and phage doublings (PFU) was tested by calculating mean log2 ratios of T5 / T0 or T2 / T0 values. Standard errors of log ratios were calculated using the formula: $SE\left[\log_2\left(\frac{T_n}{T0}\right)\right] = \sqrt{\frac{SE[\overline{T0}]^2}{\overline{T0}^2} + \frac{SE[\overline{T_n}]^2}{\overline{Tn}^2}}$ where SE = standard error of mean, T_n = values at time point *n* (T2 or T5), T0 = values at initial time point (T0) (80). Statistical significance between ratios at each temperature was determined by calculating 95% confidence intervals of the difference between ratio means using the formula:

$CI_{95} = \bar{x}_1 - \bar{x}_2 \pm 1.96\sqrt{SE_{\bar{x}_1} + SE_{\bar{x}_2}}$. Comparisons were considered significant when confidence intervals did not overlap with 0.

The impact of competitors on phage growth was tested using linear mixed-effect models as previously described. We included phage DNA concentration of the focal phage as the response variable, and phage competitor, temperature, and their interaction as fixed explanatory variables.

Phage competitiveness across temperatures was determined by comparing phage resistance to competitors and phage suppression of competitors. For resistance to competitors, the ratio of phage densities (DNA concentrations) at hour 5 in the presence and absence of each competitor was calculated. An average of ratios for all competitors was used to determine the average impact of competitors on phage growth. For suppression of competitors, the ratio of

competitor densities (DNA concentrations) at hour 5 in the presence and absence of each phage was calculated. An average of ratios was determined to give the relative competitor growth compared to a single-phage control. The average of ratios was taken away from 1 to determine the average impact of focal phage on competitor growth.

R script and data files used to generate figures and carry out statistical tests are publicly available at: https://github.com/SamuelGreenrod/Warming_parasite_paper

2.4 Results

2.4.1 Temperature shapes infectivity across phages

We initially investigated the impact of temperature on bacteria-phage interactions by measuring bacterial population growth in the presence of three different phages at 37°C, 40°C, and 42°C (Figure 1A). At the end of the experiment, the presence of phage had significantly reduced bacterial densities relative to the no-phage control at 37°C and 40°C (ANOVA – 37°C: $F_{2,17} = 115.4$, $p < 0.001$; 40°C: $F_{2,17} = 41.7$, $p < 0.001$). All phages had a significant effect on bacterial growth (post-hoc contrasts, $p < 0.05$). While phage presence also significantly reduced bacterial densities at 42°C (ANOVA - $F_{2,17} = 578.7$, $p < 0.001$), this trend was significantly driven by φLUZ19 (post-hoc - $p < 0.001$). Neither φ14-1 nor φPEV2 had a significant impact on bacterial growth at 42°C (post-hoc - φ14-1: $p = 0.33$; φPEV2: $p = 0.15$).

An important assumption of this assay is that optical density (OD) is correlated with bacterial cell density. To test this assumption, we directly measured viable cell density by counting bacterial colony-forming units (CFUs) in a sub-set of our treatments. There was a significant relationship between OD and CFU (ANOVA: $F = 121$; d.f = 1, 96; $p < 0.001$) (Figure S1). Accordingly, the results of CFU counts recapitulated the two key features of our OD data (Figure S2). First, bacterial CFUs decreased over time at 37°C and 40°C for all phages. Second, bacterial densities decreased at 42°C with φLUZ19, but not φPEV2 or φ14-1. Notably, the relationship between OD and CFU was less clear at OD < 0.05 indicating bacterial densities

reached a lower detection OD threshold (Figure S1). Therefore, measurement of CFU counts may provide greater resolution than OD as bacterial densities start to collapse.

To better understand the decrease in phage lytic activity with temperature, we also measured phage densities using both plaque-forming units (PFUs) to quantify infectious phage particles and qPCR to quantify phage DNA concentrations. All phage particle densities increased over time at 37°C and 40°C (Figure 1B). While φPEV2 and φLUZ19 densities started to plateau after T2, φ14-1 densities plateaued at T3 (Figure 1B-C). At 42°C, φLUZ19 densities increased significantly ($F_{2,5}$ = 129.1, $p < 0.05$) but φPEV2 densities decreased ($F_{2,5}$ = 270.4, $p < 0.05$) possibly due to φPEV2 particles attaching to the bacterial surface but not replicating. φ14-1 densities did not change significantly ($F_{2,5}$ = 1.41, $p = 0.36$). However, φ14-1 densities were not static, initially decreasing and then increasing indicative of attachment followed by replication. These results were supported by measures of phage DNA concentrations (Figure 1C) which showed significant increases for all phage at 37°C and 40°C (37°C - φPEV2: $F_{2,5}$ = 1219; φLUZ19: $F_{2,5}$ = 2257; φ14-1: $F_{2,5}$ = 299.8; 40°C - PEV2: $F_{2,5}$ = 1260; φLUZ19: $F_{2,5}$ = 1355; φ14-1: $F_{2,5}$ = 1936; $p < 0.001$ for all phage). At 42°C, significant increases in DNA concentrations were observed with φLUZ19 ($F_{2,5}$ = 391.4, $p < 0.001$) and φ14-1 ($F_{2,5}$ = 44.2, $p = 0.001$), but not with φPEV2 ($F_{2,5}$ = 0.078, $p = 0.79$).

Phage replication rates are intrinsically linked to bacterial growth rates (81) which typically vary with temperature (18). We assessed the potential impact of bacterial growth rates on phage activity by measuring bacterial growth in the absence of phage using both optical densities and CFUs. There was no significant impact of temperature on bacterial densities ($F_{2,79}$ = 2.73, $p = 0.0713$), or interaction between temperature and time point ($F_{5,79}$ = 253.7, $p = 0.465$), in the no-phage control measured with optical density (Figure S3A). Further, no significant differences were observed between temperatures at the end of the experiment based on CFU counts ($F_{2,17}$ = 0.43, $p = 0.52$) (Figure S3B), despite bacteria being in mid-log phase. Temperature appears to have had a minimal impact on bacterial growth rates within the 5-hour period. However, a lack of temperature effects may reflect restricted overall

bacterial growth in our experimental system; bacteria spent the start of the 5-hour period in lag-phase and only underwent a total of 3.26 (37°C), 3.07 (40°C), and 2.84 (42°C) doublings.

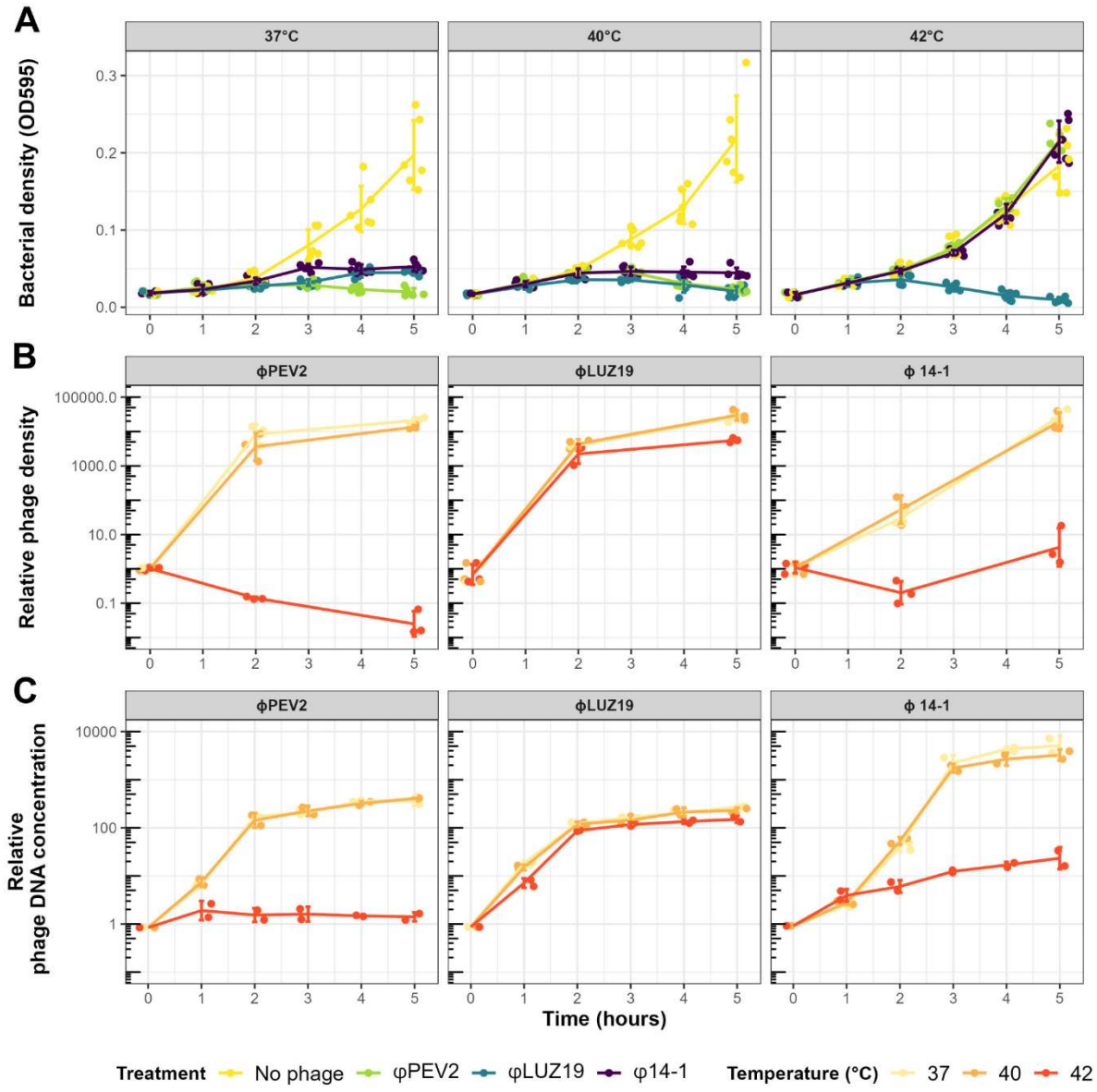

Figure 1. High temperatures can restrict phage infectivity. **A)** Bacterial growth curves over 5h in the presence of phage at 37°C, 40°C, and 42°C. Growth curves are split by temperature and coloured by phage treatment. Results shown represent six biological replicates. **B** & **C)** Phage growth curves over 5h at 37°C, 40°C, and 42°C measured using

plaque-forming units (**B**) or phage DNA concentrations (**C**). For (**C**), Y-axis shows the fold change in phage DNA determined based on the change in phage DNA concentration relative to T0. Plots are split by phage and coloured by temperature. For (**A**) and (**C**), populations were destructively sampled at one-hour intervals. Results shown represent six biological replicates. For (**B**), populations were destructively sampled at hours 0, 2, and 5. Results shown represent three biological replicates. Error bars show standard error of the mean.

2.4.2 Temperature alters phage infectivity via life-history traits

Phage population growth is dependent on different parasite life-history traits including stability (free-phage decay rates), host attachment (adsorption to bacterial cells), and virulence (impact on bacterial densities). We investigated whether disruption of these traits may explain reduced phage infectivity at high temperatures (Figure 2A).

Phage stability outside of cells can be temperature-sensitive (82). Using Poisson generalised linear models, we observed a significant interaction between temperature and time on phage stability for all phage (Poisson GLM. φPEV2: LR χ^2 = 30359, $p < 0.001$; φLUZ19: LR χ^2 = 17172, $p < 0.001$; φ14-1: LR χ^2 = 5986.5, $p < 0.001$) (Figure S4). φ14-1 stability was found to decrease significantly from 37°C to 40°C but no change was observed from 40°C to 42°C (post-hoc – 37-40°C: $p < 0.0001$; 40-42°C: $p = 0.50$). While φPEV2 stability also decreased significantly with temperature (post-hoc - $p < 0.0001$), φLUZ19 stability significantly increased (post-hoc – $p < 0.0001$). All phages were predicted to require a minimum of 18 hours before phage densities reduced by 50% at any temperature (Table S3). Stability thus likely played a minimal role in temperature effects on phage infectivity.

Similarly, the interaction between temperature and time on host attachment varied across phages. A temperature by time interaction was observed for φPEV2 and φLUZ19 attachment, but not for φ14-1 (Poisson GLM. φPEV2: LR χ^2 = 19489, $p < 0.001$; φLUZ19: LR χ^2 = 116.5, $p < 0.001$; ANOVA. φ14-1: $F_{2,5} = 0.029$, $p = 0.97$) (Figure S5). φLUZ19 attachment was found to

increase significantly with temperature (post-hoc - $p < 0.0001$). However, φPEV2 attachment significantly decreased (post-hoc – $p < 0.0001$) with no attachment observed at 42°C. Following attachment, phage reproduction is dependent on the ability to replicate and lyse bacterial host cells. The impact of temperature on phage virulence and population growth was determined by calculating the mean number of bacterial doublings in the presence of phage (CFU/ml) or phage doublings (PFU/ml), respectively, between the beginning and end of the experiment (Figure S2 & 1B; Table S3). Statistical significance between temperatures ($p < 0.05$) was determined by measuring the overlap in 95% confidence intervals of the difference between bacterial or phage doublings for each temperature.

The virulence of all phage varied significantly with temperature ($p < 0.05$), decreasing with warming for φPEV2 and φ14-1 ($p < 0.05$) and increasing with warming for φLUZ19 ($p < 0.05$). In line with this, population growth of φPEV2 and φ14-1 also decreased significantly with warming ($p < 0.05$) although differences were greater between 40°C and 42°C than between 37°C and 40°C. The relationship between virulence and population growth was less clear with φLUZ19; while φLUZ19 population growth significantly decreased with warming ($p < 0.05$), virulence significantly increased.

Variation in phage virulence and population growth across temperatures may be masked as phages reached maximum densities with all available hosts lysed. Virulence and population growth were re-analysed within the first two hours (Figure 2B). The virulence and population growth of all phages significantly varied between temperatures ($p < 0.05$). However, the magnitude of virulence changes were greater for φPEV2 than for other phages, particularly between 37°C and 40°C.

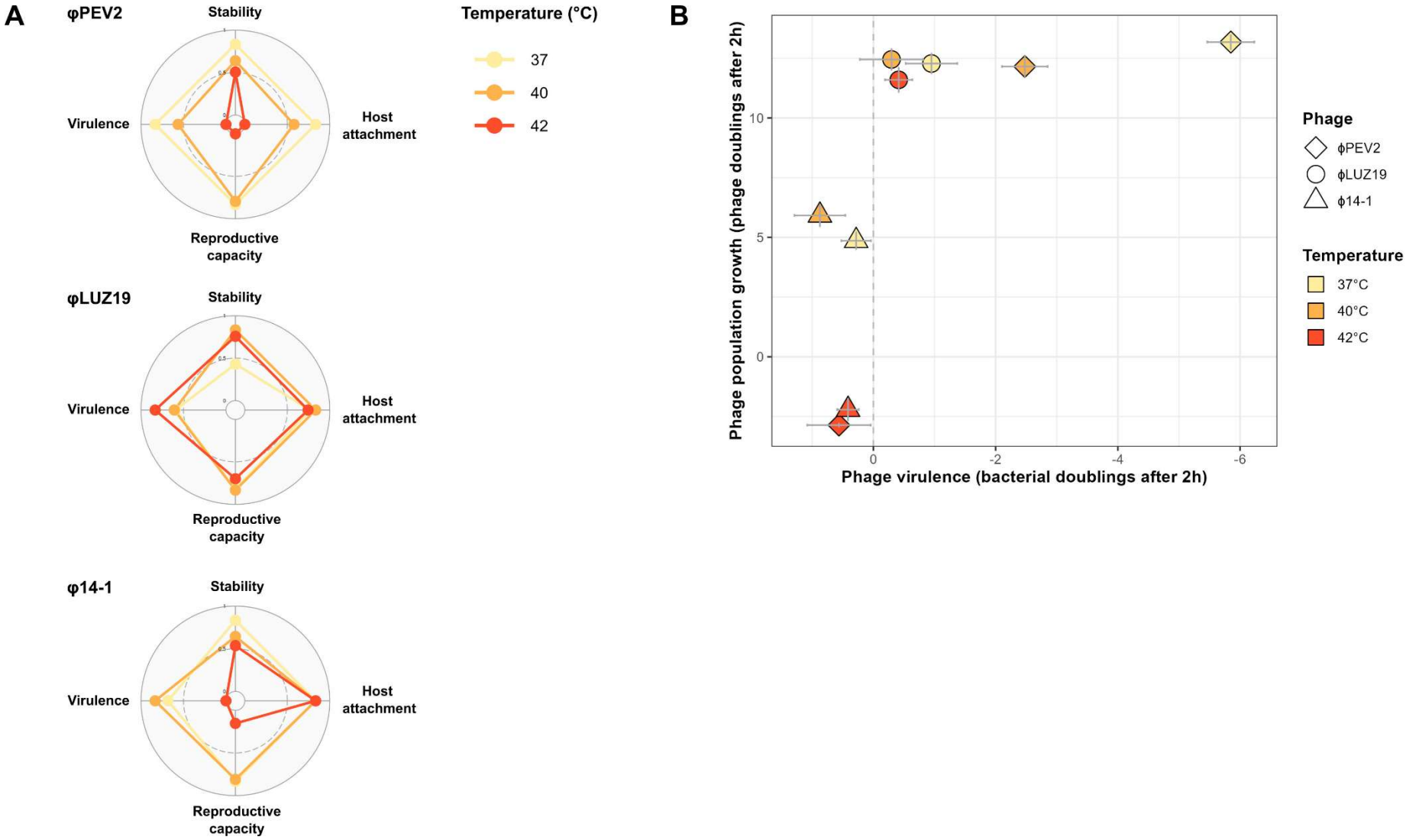
A
φPEV2
Stability
Virulence
Host attachment
Reproductive capacity
φLUZ19
Stability
Virulence
Host attachment
Reproductive capacity
φ14-1
Stability
Virulence
Host attachment
Reproductive capacity
Temperature (°C)
37
40
42
B
Phage population growth (phage doublings after 2h)
10
5
0
0
-2
-4
-6
Phage virulence (bacterial doublings after 2h)
Phage
ϕPEV2
ϕLUZ19
ϕ14-1
Temperature
37°C
40°C
42°C

Figure 2. Temperature drives variation in phage life-history traits. A) Radar charts showing relative change in phage life-history traits and population growth at 37°C, 40°C, and 42°C. Stability and host attachment reflect average time for 50% of phage particles to decay or adsorb to bacterial cells, respectively. Virulence and population growth reflect the number of bacterial doublings (in presence of phage) or phage doublings, respectively during the five-hour experiment. Data points show relative values across temperatures by dividing values at each temperature by 1.2 x highest value. All life-history trait values including 95% confidence interval ranges and standard errors are shown in **Table S3**. **B)** Scatter plot shows relationship between phage virulence and population growth measured within the first two hours. Data points are shaped by phage and coloured by temperature. Error bars (inside data points) show standard errors of the $\log_2(T2/T0)$ ratios. Grey dotted line shows starting bacterial density where > 0 reflects an increase in bacterial densities and < 0 reflects a decrease in bacterial densities (due to phage lysis).

2.4.3 Competition is temperature-dependent in phage communities

Parasites often exist in communities where they compete to acquire host resources (29,83). To determine whether temperature variation affects competition between phages, we measured the impact of competitors on phage population growth in pairwise and 3-phage combinations across temperatures.

At 37°C, the presence of competitors significantly reduced phage population growth by hour 5 for all phages (ANOVA. φPEV2: $F_{2,17} = 9.16$, $p < 0.001$; φLUZ19: $F_{2,17} = 18.1$, $p < 0.001$; φ14-1: $F_{2,17} = 23.8$, $p < 0.001$) (Figure 3A). Competition was less clear at hour 2 compared to the hour 5 endpoint with no significant impact of competitors on population growth observed for φPEV2 or φLUZ19 (ANOVA. φPEV2: $F_{2,17} = 0.88$, $p = 0.47$; φLUZ19: $F_{2,17} = 1.11$, $p = 0.37$) (Figure S6). Competitors were found to have a significant impact on φ14-1 population growth after 2h ($F_{2,17} = 8.16$, $p = 0.001$), although post-hoc contrasts showed this was only with the 3-phage combination ($p < 0.05$).

Phages varied in competitiveness at 37°C (Figure 3A). φPEV2 was the most resistant to competitors with only φLUZ19 significantly reducing φPEV2 population growth (post-hoc contrasts, $p < 0.01$). φPEV2 also had a significantly greater impact on competitor growth than φLUZ19 or φ14-1 (post-hoc contrasts, PEV2 vs. φLUZ19: $p < 0.001$; φPEV2 vs φ14-1: $p < 0.01$). Competition with φLUZ19 and φ14-1 was weaker and more varied. While 14-1 population growth was unaffected by the presence of φLUZ19 (post-hoc contrasts, $p = 0.15$), φ14-1 significantly reduced φLUZ19 population growth. φLUZ19 was significantly more restrictive than φ14-1 against φPEV2 growth (post-hoc contrasts, $p < 0.05$).

Phage competition was found to be temperature-dependent, with significant interactions detected between competitor and temperature for all phages (ANOVA. φPEV2: $F_{2,47} = 4.28$, $p = 0.001$; φLUZ19: $F_{2,47} = 4.15$, $p = 0.001$; φ14-1: $F_{2,47} = 16.5$, $p < 0.001$) (Figure 3A). Between 37°C and 40°C, φ14-1 restriction of φPEV2 growth increased significantly (post-hoc contrasts, $p < 0.05$) and φPEV2 and 3-phage restriction of φ14-1 both significantly decreased (post-hoc contrasts, PEV2: $p < 0.001$; 3-phage: $p < 0.001$). In contrast, there was no change in φLUZ19 restriction of φPEV2 (post-hoc contrasts, $p = 1.0$) or φ14-1 (post-hoc contrasts, $p = 0.93$) between 37°C and 40°C. No significant difference in phage growth, with or without competitors, was detected at 42°C (Figure S7; post-hoc contrasts, $p > 0.05$) indicating competition was removed.

The change in phage competitiveness across temperatures was analysed further by comparing phage growth in the presence of competitors (Resistance to competitors) with the reduction in competitor growth caused by each phage (Suppression of competitors) (see methods for more detailed description) (Figure 3B). This showed that between 37°C and 40°C, φPEV2 became less competitive and φ14-1 became more competitive. As φLUZ19 competitiveness was unchanged, the competitiveness of all phages appeared to converge. Phage competition was removed between 40°C and 42°C with all phages growing equally with and without competitors.

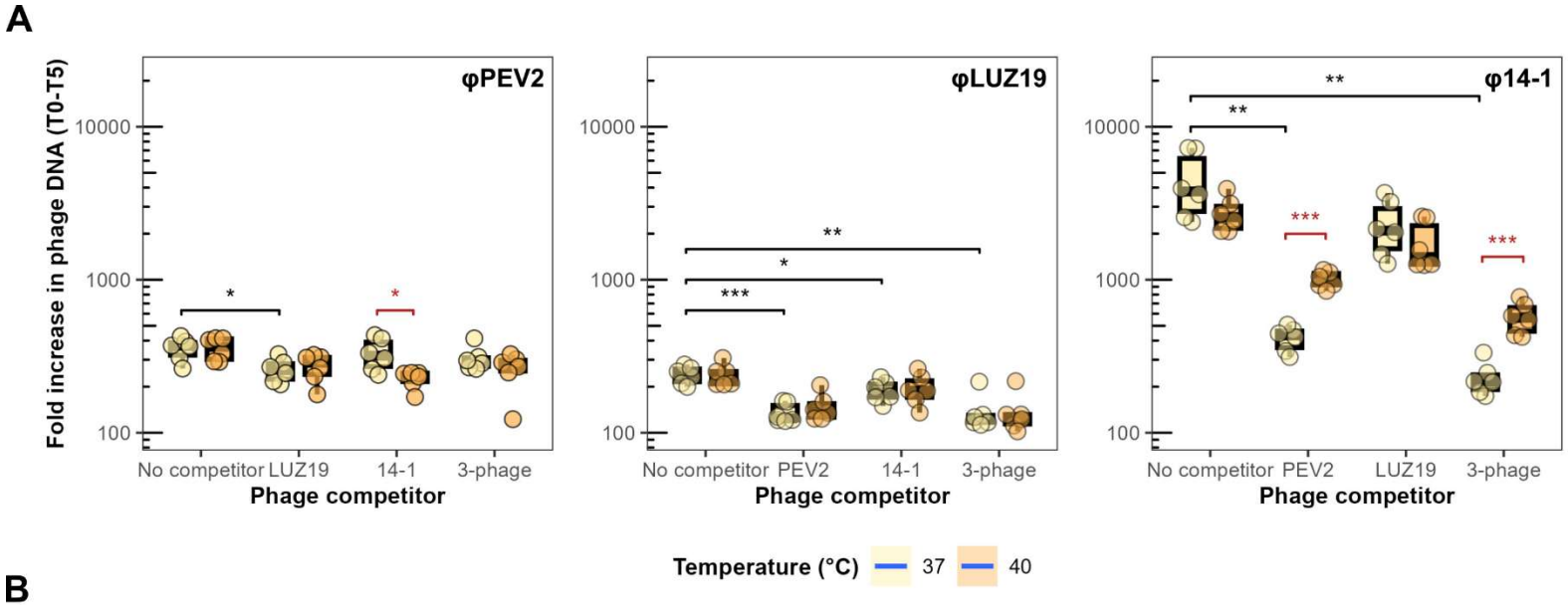
A
φPEV2
φLUZ19
φ14-1
Fold increase in phage DNA (T0-T5)
10000
1000
100
No competitor
LUZ19
PEV2
14-1
3-phage
Phage competitor
Temperature (°C)
37
40

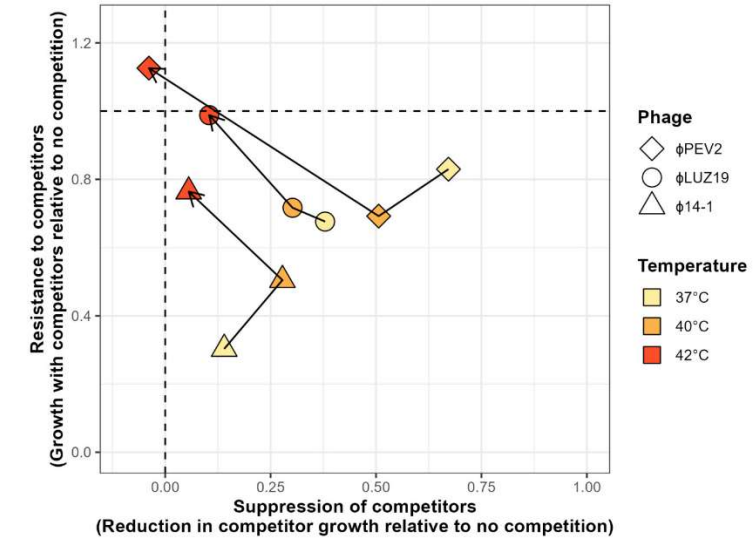
B
Resistance to competitors
(Growth with competitors relative to no competition)
1.2
0.8
0.4
0.0
0.00
0.25
0.50
0.75
1.00
Suppression of competitors
(Reduction in competitor growth relative to no competition)
Phage
ϕPEV2
ϕLUZ19
ϕ14-1
Temperature
37°C
40°C
42°C

Figure 3. Phage competition is temperature-dependent. A) Fold change in phage DNA concentration in the presence and absence of competitors between T0 and T5. Data is divided into 37°C and 40°C treatments. Asterisks show significant differences between competitor and no-competitor treatments based on a mixed effect model, with phage DNA concentration as the response variable and competitor as the explanatory variable. Significant differences within temperatures are shown with a black asterisk whereas differences between temperatures are shown with a red asterisk. * = $p < 0.05$, ** = $p < 0.005$, *** = $p < 0.0001$). Boxes and points are coloured by temperature. Results shown represent six biological replicates. **B)** Change in phage competitiveness across temperatures (see materials and methods for more information). Y-axis shows the resistance of focal phage to competitors (average focal phage DNA in the presence of competitors relative to no-competitor control). X-axis shows suppression of competitors by focal phage (average competitor DNA in the presence of focal phage relative to no-competitor control). Black arrows show change in phage competitiveness with warming. Phage are distinguished by point shape with temperatures by point colour.

2.5 Discussion

The effects of temperature on host-parasite interactions depend on mismatches in host and parasite thermal responses (7,84,85). Using a bacteria-phage system, we show that thermal response mismatches are not only present between parasites and their hosts, but also between different parasites. This finding supports previous studies which identified thermal performance variation in malaria parasites and their mosquito vectors (27,86,87), midges (88,89), and honeybee parasites (90). However, our study made several additional contributions. Firstly, we found that the temperature range between phage thermal optima and phage inactivation can be as small as 2°C. Secondly, we found that phage upper thermal limits may sit within feasible human fever/animal resting temperatures. These findings indicate that even small increases in body temperature may have significant effects on the

functioning of animal gut viromes. Further, they suggest that body temperature variation may limit the functional diversity, and ultimately efficacy, of phage therapy treatments. The notion that thermal regulation is used by eukaryotes to restrict the growth of parasites is not a new one (91). However, our results highlight that temperature change can affect hyperparasites, as well as parasites, possibly to the detriment of their eukaryotic hosts.

The effects of temperature on parasite performance are typically attributed to changes in parasite life-history traits (9,12,15). We found that temperature change affected different life-history traits in different parasites (also found in (91)). For one phage, high temperatures reduced attachment to the bacterial cell thereby restricting the phage's ability to infect host cells. In *P. aeruginosa*, variable phage attachment has been attributed to the production of bacterial surface exopolysaccharides (EPS) which block phage adsorption (92,93). However, while *P. aeruginosa* EPS production generally increases with temperature from 25°C to 37°C, it decreases between 37°C and 42°C (94) and so cannot explain the decrease in adsorption with warming. Disruption of host attachment by temperature has previously been reported in other bacteria-phage pairs (15,91) and in more complex host-parasite systems (95,96). Host attachment therefore appears to be particularly sensitive to temperature change, perhaps due to its dependence on the parasite's binding ability (97) and host's attachment susceptibility (8,96,98). In a different phage, high temperatures restricted phage population growth while having no impact on phage attachment ability. Phage replication inside host cells, like other viruses (99), depends on multiple reproductive stages possibly disrupted by high temperatures. For example, temperature change may affect phage ability to replicate their DNA (100,101), form phage particles, or lyse the bacterial cell (57). Further work is needed to characterise the mechanisms underlying temperature disruption on life-history traits and would improve our understanding of both parasite thermal ecology and the evolutionary hurdles parasites must overcome to adapt to temperature variation.

Similar to other parasite systems (102–104), phages typically exist in communities and compete to infect hosts. Phages are also increasingly deployed in multi-phage cocktails for the

therapeutic treatment of bacterial infections (43,105). We show that while phages compete in combinations, they vary in their competitiveness; some phages were more restrictive of and resistant to competitors than others. Parasite competitive success during epidemics has previously been linked to virulence as highly virulent parasites can rapidly transmit and deplete host resources thereby reducing the availability of hosts for other parasite competitors (33–35). We found that the most competitive phage, φPEV2, was also the most virulent and caused the earliest collapse in host population densities. The least competitive phage, φ14-1, was the least virulent. Phage virulence depends on two correlated life-history traits: latent period (time between infection and burst) and burst size (number of viral progeny). Specifically, at high bacterial densities, phage virulence and competitiveness both increase when latent periods are shorter despite a reduced burst size (106). Supporting this, φPEV2 is known to have the shortest latent period (~18 mins) out of the phages tested (67) while PB1-like phages, such as φ14-1, have longer latent periods (~50 mins) (66). Notably, the relationship between virulence and competitiveness depends on host availability; at low bacterial densities selection favours longer latent periods with larger bursts (106). Our results highlight that viromes and phage cocktails may be less functionally diverse than previously thought as relative phage densities are skewed towards the most competitive phage genotypes/species (62).

Phage virulence varied with temperature. Therefore, we hypothesised that a change in temperature may also result in a change in phage competition outcomes. We found that temperature-mediated reductions in phage virulence corresponded with reductions in phage competitiveness. Temperature has previously been shown to affect competition outcomes in parasites of mosquitoes (10) and fruit flies (11). However, in these studies competition was tested in the absence of hosts and so changes were attributed to non-host related parasite traits such as larval survivorship and development times (10). Our results highlight that temperature can also affect competition for access to hosts and therefore may drive parasite community dynamics during epidemics. Surprisingly, temperature primarily affected interactions between two phages (φPEV2 and φ14-1). This could be explained by the co-occurrence of

competition for host resources and phage-phage synergy in specific phage pairs (reviewed in (107)). However, variation between phages could reflect parasite-specific temperature effects given both φPEV2 and φ14-1 are thought to target LPS-associated bacterial surface receptors (59,67). Alternatively, a reduction in φPEV2 virulence may have a greater impact on competition with low virulence competitors whose growth rate depends on the increase in host availability.

In conclusion, our study demonstrates that variation in temperature, particularly within a human fever range, can have a significant impact on phage population and community dynamics. Specifically, rising temperatures may alter the composition and functioning of phage communities and restrict the efficacy of phages to treat bacterial infections. Our findings also highlight the complex effects of temperature within tri-partite host-parasite-hyperparasite systems. Fevers often push both mammalian hosts and their parasites above their thermal optima, with parasites incurring greater costs. However, high temperatures may also restrict the growth of hyperparasites which target higher-level parasites thereby reducing their benefit to the mammalian host.

2.6 References

1. Schulte PM, Healy TM, Fangue NA. Thermal Performance Curves, Phenotypic Plasticity, and the Time Scales of Temperature Exposure. Integrative and Comparative Biology. 2011 Nov 1;51(5):691–702.

2. Cohen JM, Venesky MD, Sauer EL, Civitello DJ, McMahon TA, Roznik EA, et al. The thermal mismatch hypothesis explains host susceptibility to an emerging infectious disease. Ecology Letters. 2017;20(2):184–93.

3. Mojica KDA, Brussaard CPD. Factors affecting virus dynamics and microbial host–virus interactions in marine environments. FEMS Microbiology Ecology. 2014 Sep 1;89(3):495–515.

4. Brown JH, Gillooly JF, Allen AP, Savage VM, West GB. Toward a Metabolic Theory of Ecology. Ecology. 2004;85(7):1771–89.

5. Hector TE, Gehman ALM, King KC. Infection burdens and virulence under heat stress: ecological and evolutionary considerations. Philos Trans R Soc Lond B Biol Sci. 378(1873):20220018.

6. Hector TE, Sgrò CM, Hall MD. Pathogen exposure disrupts an organism's ability to cope with thermal stress. Global Change Biology. 2019;25(11):3893–905.

7. Padfield D, Castledine M, Buckling A. Temperature-dependent changes to host–parasite interactions alter the thermal performance of a bacterial host. ISME J. 2020 Feb;14(2):389–98.

8. Sillankorva S, Oliveira R, Vieira MJ, Sutherland I, Azeredo J. Pseudomonas fluorescens infection by bacteriophage ΦS1: the influence of temperature, host growth phase and media. FEMS Microbiology Letters. 2004 Dec 1;241(1):13–20.

9. Singh R, Prathibha P, Jain M. Effect of temperature on life-history traits and mating calls of a field cricket, Acanthogryllus asiaticus. Journal of Thermal Biology. 2020 Oct 1;93:102740.

10. Evans MV, Drake JM, Jones L, Murdock CC. Assessing temperature-dependent competition between two invasive mosquito species. Ecological Applications. 2021;31(5):e02334.

11. Comeault AA, Matute DR. Temperature-Dependent Competitive Outcomes between the Fruit Flies Drosophila santomea and Drosophila yakuba. The American Naturalist. 2021 Mar;197(3):312–23.

12. Ciota AT, Matacchiero AC, Kilpatrick AM, Kramer LD. The effect of temperature on life history traits of Culex mosquitoes. J Med Entomol. 2014 Jan;51(1):55–62.

13. Christiansen-Jucht C, Parham PE, Saddler A, Koella JC, Basáñez MG. Temperature during larval development and adult maintenance influences the survival of Anopheles gambiae s.s. Parasites & Vectors. 2014 Nov 5;7(1):489.

14. Shapiro LLM, Whitehead SA, Thomas MB. Quantifying the effects of temperature on mosquito and parasite traits that determine the transmission potential of human malaria. PLOS Biology. 2017 Oct 16;15(10):e2003489.

15. Tokman JI, Kent DJ, Wiedmann M, Denes T. Temperature Significantly Affects the Plaquing and Adsorption Efficiencies of Listeria Phages. Frontiers in Microbiology. 2016;7.

16. Kimes NE, Grim CJ, Johnson WR, Hasan NA, Tall BD, Kothary MH, et al. Temperature regulation of virulence factors in the pathogen Vibrio coralliilyticus. ISME J. 2012 Apr;6(4):835–46.

17. Waite JL, Suh E, Lynch PA, Thomas MB. Exploring the lower thermal limits for development of the human malaria parasite, Plasmodium falciparum. Biol Lett. 2019 Jun;15(6):20190275.

18. Ratkowsky DA, Olley J, McMeekin TA, Ball A. Relationship between temperature and growth rate of bacterial cultures. J Bacteriol. 1982 Jan;149(1):1–5.

19. Blazanin M, Lam WT, Vasen E, Chan BK, Turner PE. Decay and damage of therapeutic phage OMKO1 by environmental stressors. PLOS ONE. 2022 Feb 23;17(2):e0263887.

20. Orsucci M, Navajas M, Fellous S. Genotype-specific interactions between parasitic arthropods. Heredity. 2017 Mar;118(3):260–5.

21. Lambrechts L, Halbert J, Durand P, Gouagna LC, Koella JC. Host genotype by parasite genotype interactions underlying the resistance of anopheline mosquitoes to Plasmodium falciparum. Malar J. 2005 Jan 11;4:3.

22. Klemme I, Louhi KR, Karvonen A. Host infection history modifies co-infection success of multiple parasite genotypes. Journal of Animal Ecology. 2016;85(2):591–7.

23. Read AF, Taylor LH. The ecology of genetically diverse infections. Science. 2001 May 11;292(5519):1099–102.

24. Eswarappa SM, Estrela S, Brown SP. Within-Host Dynamics of Multi-Species Infections: Facilitation, Competition and Virulence. PLoS One. 2012 Jun 21;7(6):e38730.

25. Tang J, Templeton TJ, Cao J, Culleton R. The Consequences of Mixed-Species Malaria Parasite Co-Infections in Mice and Mosquitoes for Disease Severity, Parasite Fitness, and Transmission Success. Frontiers in Immunology. 2020;10.

26. Pedersen AB, Fenton A. Emphasizing the ecology in parasite community ecology. Trends in Ecology & Evolution. 2007 Mar 1;22(3):133–9.

27. Mozaffer F, Menon GI, Ishtiaq F. Exploring the thermal limits of malaria transmission in the western Himalaya. Ecology and Evolution. 2022;12(9):e9278.

28. Mordecai EA, Caldwell JM, Grossman MK, Lippi CA, Johnson LR, Neira M, et al. Thermal biology of mosquito-borne disease. Ecol Lett. 2019 Oct;22(10):1690–708.

29. Mideo N. Parasite adaptations to within-host competition. Trends in Parasitology. 2009 Jun 1;25(6):261–8.

30. Mei X, Gao S, Liu Y, Hu J, Razlustkij V, Rudstam LG, et al. Effects of Elevated Temperature on Resources Competition of Nutrient and Light Between Benthic and Planktonic Algae. Frontiers in Environmental Science. 2022;10.

31. Kordas RL, Harley CDG, O'Connor MI. Community ecology in a warming world: The influence of temperature on interspecific interactions in marine systems. Journal of Experimental Marine Biology and Ecology. 2011 Apr 30;400(1):218–26.

32. Seth H, Gräns A, Sandblom E, Olsson C, Wiklander K, Johnsson JI, et al. Metabolic Scope and Interspecific Competition in Sculpins of Greenland Are Influenced by Increased Temperatures Due to Climate Change. PLOS ONE. 2013 May 14;8(5):e62859.

33. Berngruber TW, Froissart R, Choisy M, Gandon S. Evolution of Virulence in Emerging Epidemics. PLoS Pathog. 2013 Mar 14;9(3):e1003209.

34. Griette Q, Raoul G, Gandon S. Virulence evolution at the front line of spreading epidemics. Evolution. 2015;69(11):2810–9.

35. Hasik AZ, King KC, Hawlena H. Interspecific host competition and parasite virulence evolution. Biology Letters. 2023 May 3;19(5):20220553.

36. Breitbart M, Bonnain C, Malki K, Sawaya NA. Phage puppet masters of the marine microbial realm. Nat Microbiol. 2018 Jul;3(7):754–66.

37. Williamson KE. Soil Phage Ecology: Abundance, Distribution, and Interactions with Bacterial Hosts. In: Witzany G, editor. Biocommunication in Soil Microorganisms. Berlin, Heidelberg: Springer; 2011. p. 113–36.

38. Marantos A, Mitarai N, Sneppen K. From kill the winner to eliminate the winner in open phage-bacteria systems. PLoS Comput Biol. 2022 Aug 8;18(8):e1010400.

39. Manrique P, Bolduc B, Walk ST, van der Oost J, de Vos WM, Young MJ. Healthy human gut phageome. Proceedings of the National Academy of Sciences. 2016 Sep 13;113(37):10400–5.

40. Ashy RA, Jalal RS, Sonbol HS, Alqahtani MD, Sefrji FO, Alshareef SA, et al. Functional annotation of rhizospheric phageome of the wild plant species Moringa oleifera. Frontiers in Microbiology. 2023;14.

41. Pratama AA, Terpstra J, de Oliveria ALM, Salles JF. The Role of Rhizosphere Bacteriophages in Plant Health. Trends in Microbiology. 2020 Sep 1;28(9):709–18.

42. Murray CJ, Ikuta KS, Sharara F, Swetschinski L, Aguilar GR, Gray A, et al. Global burden of bacterial antimicrobial resistance in 2019: a systematic analysis. The Lancet. 2022 Feb 12;399(10325):629–55.

43. Van Nieuwenhuyse B, Van der Linden D, Chatzis O, Lood C, Wagemans J, Lavigne R, et al. Bacteriophage-antibiotic combination therapy against extensively drug-resistant Pseudomonas aeruginosa infection to allow liver transplantation in a toddler. Nat Commun. 2022 Sep 29;13(1):5725.

44. Gigante A, Atterbury RJ. Veterinary use of bacteriophage therapy in intensively-reared livestock. Virology Journal. 2019 Dec 12;16(1):155.

45. Eskenazi A, Lood C, Wubbolts J, Hites M, Balarjishvili N, Leshkasheli L, et al. Combination of pre-adapted bacteriophage therapy and antibiotics for treatment of fracture-related infection due to pandrug-resistant Klebsiella pneumoniae. Nat Commun. 2022 Jan 18;13(1):302.

46. Gariepy C, Amiot J, Nadai S. Ante-mortem detection of PSE and DFD by infrared thermography of pigs before stunning. Meat Science. 1989 Jan 1;25(1):37–41.

47. Hannon JP, Bossone CA, Wade CE. Normal physiological values for conscious pigs used in biomedical research. Lab Anim Sci. 1990 May;40(3):293–8.

48. Godyń D, Herbut P, Angrecka S. Measurements of peripheral and deep body temperature in cattle – A review. Journal of Thermal Biology. 2019 Jan 1;79:42–9.

49. Protsiv M, Ley C, Lankester J, Hastie T, Parsonnet J. Decreasing human body temperature in the United States since the Industrial Revolution. Jit M, Franco E, Waalen J, Rühli F, editors. eLife. 2020 Jan 7;9:e49555.

50. Prinzinger R, Preßmar A, Schleucher E. Body temperature in birds. Comparative Biochemistry and Physiology Part A: Physiology. 1991 Jan 1;99(4):499–506.

51. Obermeyer Z, Samra JK, Mullainathan S. Individual differences in normal body temperature: longitudinal big data analysis of patient records. BMJ. 2017 Dec 13;359:j5468.

52. Harding C, Pompei F, Bordonaro SF, McGillicuddy DC, Burmistrov D, Sanchez LD. The daily, weekly, and seasonal cycles of body temperature analyzed at large scale. Chronobiol Int. 2019 Dec;36(12):1646–57.

53. Leggett JE. Approach to fever or suspected infection in the normal host. In: Goldman-Cecil Medicine. 26th ed. Philadelphia, PA: Elsevier; 2020. p. 1809–15.

54. Abedon ST, Danis-Wlodarczyk KM, Wozniak DJ. Phage Cocktail Development for Bacteriophage Therapy: Toward Improving Spectrum of Activity Breadth and Depth. Pharmaceuticals (Basel). 2021 Oct 3;14(10):1019.

55. Chibeu A, Ceyssens PJ, Hertveldt K, Volckaert G, Cornelis P, Matthijs S, et al. The adsorption of Pseudomonas aeruginosa bacteriophage phiKMV is dependent on expression regulation of type IV pili genes. FEMS Microbiol Lett. 2009 Jun;296(2):210–8.

56. Pollard E, Woodyatt S. The Effect of Temperature on the Formation of T1 and T2r Bacteriophage. Biophys J. 1964 Sep;4(5):367–85.

57. Park J, Yun J, Lim JA, Kang DH, Ryu S. Characterization of an endolysin, LysBPS13, from a Bacillus cereus bacteriophage. FEMS Microbiology Letters. 2012 Jul 1;332(1):76–83.

58. Costaz TPM, de Jong PW, Harvey JA, van Loon JJA, Dicke M, Gols R. Temperature affects the outcome of competition between two sympatric endoparasitoids. Animal Behaviour. 2023 Sep 1;203:11–20.

59. Betts A, Gifford DR, MacLean RC, King KC. Parasite diversity drives rapid host dynamics and evolution of resistance in a bacteria-phage system. Evolution. 2016;70(5):969–78.

60. Betts A, Vasse M, Kaltz O, Hochberg ME. Back to the future: evolving bacteriophages to increase their effectiveness against the pathogen Pseudomonas aeruginosa PAO1. Evolutionary Applications. 2013;6(7):1054–63.

61. Betts A, Kaltz O, Hochberg ME. Contrasted coevolutionary dynamics between a bacterial pathogen and its bacteriophages. Proceedings of the National Academy of Sciences. 2014 Jul 29;111(30):11109–14.

62. Betts A, Gray C, Zelek M, MacLean RC, King KC. High parasite diversity accelerates host adaptation and diversification. Science. 2018 May 25;360(6391):907–11.

63. De Smet J, Zimmermann M, Kogadeeva M, Ceyssens PJ, Vermaelen W, Blasdel B, et al. High coverage metabolomics analysis reveals phage-specific alterations to Pseudomonas aeruginosa physiology during infection. ISME J. 2016 Aug;10(8):1823–35.

64. Ceyssens PJ, Brabban A, Rogge L, Lewis MS, Pickard D, Goulding D, et al. Molecular and physiological analysis of three Pseudomonas aeruginosa phages belonging to the "N4-like viruses". Virology. 2010 Sep 15;405(1):26–30.

65. Ceyssens PJ, Miroshnikov K, Mattheus W, Krylov V, Robben J, Noben JP, et al. Comparative analysis of the widespread and conserved PB1-like viruses infecting Pseudomonas aeruginosa. Environmental Microbiology. 2009;11(11):2874–83.

66. Garbe J, Wesche A, Bunk B, Kazmierczak M, Selezska K, Rohde C, et al. Characterization of JG024, a pseudomonas aeruginosa PB1-like broad host range phage under simulated infection conditions. BMC Microbiology. 2010 Nov 26;10(1):301.

67. Danis-Wlodarczyk K, Cai A, Chen A, Gittrich M, Sullivan M, Wozniak D, et al. Friends or Foes? Rapid Determination of Dissimilar Colistin and Ciprofloxacin Antagonism of Pseudomonas aeruginosa Phages. Pharmaceuticals. 2021 Nov 15;14:1162.

68. Kiino DR, Rothman-Denes LB. Genetic analysis of bacteriophage N4 adsorption. J Bacteriol. 1989 Sep;171(9):4595–602.

69. Lavigne R, Lecoutere E, Wagemans J, Cenens W, Aertsen A, Schoofs L, et al. A multifaceted study of Pseudomonas aeruginosa shutdown by virulent podovirus LUZ19. mBio. 2013 Mar 19;4(2):e00061-00013.

70. Brandão A, Pires DP, Coppens L, Voet M, Lavigne R, Azeredo J. Differential transcription profiling of the phage LUZ19 infection process in different growth media. RNA Biology. 2021 Nov 2;18(11):1778–90.

71. Kropinski AM, Mazzocco A, Waddell TE, Lingohr E, Johnson RP. Enumeration of Bacteriophages by Double Agar Overlay Plaque Assay. In: Clokie MRJ, Kropinski AM, editors. Bacteriophages: Methods and Protocols, Volume 1: Isolation, Characterization, and Interactions. Totowa, NJ: Humana Press; 2009. p. 69–76.

72. Kuo TT, Chow TY, Lin YT, Yang CM, Li HW. Specific Dissociation of Phage Xp12 by Sodium Citrate. Journal of General Virology. 1971;10(2):199–202.

73. Yamamoto N, Fraser D, Mahler HR. Chelating agent shock of bacteriophage T5. J Virol. 1968 Sep;2(9):944–50.

74. Darling AE, Mau B, Perna NT. progressiveMauve: Multiple Genome Alignment with Gene Gain, Loss and Rearrangement. PLoS One. 2010 Jun 25;5(6):e11147.

75. Microsoft Corporation. Microsoft Excel [Internet]. 2018. Available from: https://office.microsoft.com/excel

76. R Core Team. R: A language and environment for statistical computing. [Internet]. Foundation for Statistical Computing, Vienna, Austria.; 2021. Available from: https://www.R-project.org/

77. RStudio Team. RStudio: Integrated Development for R. [Internet]. RStudio, PBC, Boston, M; 2020. Available from: http://www.rstudio.com/

78. Wickham H. ggplot2. WIREs Computational Statistics. 2011;3(2):180–5.

79. Zuur AF, Ieno EN, Walker N, Saveliev AA, Smith GM. Mixed effects models and extensions in ecology with R. New York, NY: Springer; 2009. (Statistics for Biology and Health).

80. Hedges LV, Gurevitch J, Curtis PS. The Meta-Analysis of Response Ratios in Experimental Ecology. Ecology. 1999;80(4):1150–6.

81. Nabergoj D, Modic P, Podgornik A. Effect of bacterial growth rate on bacteriophage population growth rate. Microbiologyopen. 2017 Dec 1;7(2):e00558.

82. Mocé-Llivina L, Muniesa M, Pimenta-Vale H, Lucena F, Jofre J. Survival of Bacterial Indicator Species and Bacteriophages after Thermal Treatment of Sludge and Sewage. Applied and Environmental Microbiology. 2003 Mar;69(3):1452–6.

83. Refardt D. Within-host competition determines reproductive success of temperate bacteriophages. ISME J. 2011 Sep;5(9):1451–60.

84. Nowakowski AJ, Whitfield SM, Eskew EA, Thompson ME, Rose JP, Caraballo BL, et al. Infection risk decreases with increasing mismatch in host and pathogen environmental tolerances. Ecology Letters. 2016;19(9):1051–61.

85. Gehman ALM, Hall RJ, Byers JE. Host and parasite thermal ecology jointly determine the effect of climate warming on epidemic dynamics. Proceedings of the National Academy of Sciences. 2018 Jan 23;115(4):744–9.

86. Buxton M, Nyamukondiwa C, Dalu T, Cuthbert RN, Wasserman RJ. Implications of increasing temperature stress for predatory biocontrol of vector mosquitoes. Parasites & Vectors. 2020 Dec 1;13(1):604.

87. Villena OC, Ryan SJ, Murdock CC, Johnson LR. Temperature impacts the environmental suitability for malaria transmission by Anopheles gambiae and Anopheles stephensi. Ecology. 2022;103(8):e3685.

88. Verhoef FA, Venter GJ, Weldon CW. Thermal limits of two biting midges, Culicoides imicola Kieffer and C. bolitinos Meiswinkel (Diptera: Ceratopogonidae). Parasites & Vectors. 2014 Aug 20;7(1):384.

89. Tugwell LA, England ME, Gubbins S, Sanders CJ, Stokes JE, Stoner J, et al. Thermal limits for flight activity of field-collected Culicoides in the United Kingdom defined under laboratory conditions. Parasites & Vectors. 2021 Jan 18;14(1):55.

90. Palmer-Young EC, Raffel TR, Evans JD. Hot and sour: parasite adaptations to honeybee body temperature and pH. Proceedings of the Royal Society B: Biological Sciences. 2021 Dec;288(1964):20211517.

91. Seeley ND, Primrose SB. The Effect of Temperature on the Ecology of Aquatic Bacteriophages. Journal of General Virology. 1980;46(1):87–95.

92. Knecht LE, Veljkovic M, Fieseler L. Diversity and Function of Phage Encoded Depolymerases. Frontiers in Microbiology. 2020;10.

93. Chegini Z, Khoshbayan A, Taati Moghadam M, Farahani I, Jazireian P, Shariati A. Bacteriophage therapy against Pseudomonas aeruginosa biofilms: a review. Ann Clin Microbiol Antimicrob. 2020 Sep 30;19:45.

94. Chug R, Mathur S, Kothari SL, Harish, Gour VS. Maximizing EPS production from Pseudomonas aeruginosa and its application in Cr and Ni sequestration. Biochemistry and Biophysics Reports. 2021 Jul 1;26:100972.

95. Dalvin S, Are Hamre L, Skern-Mauritzen R, Vågseth T, Stien L, Oppedal F, et al. The effect of temperature on ability of Lepeophtheirus salmonis to infect and persist on Atlantic salmon. Journal of Fish Diseases. 2020;43(12):1519–29.

96. Sun SJ, Dziuba MK, Jaye RN, Duffy MA. Temperature modifies trait-mediated infection outcomes in a Daphnia–fungal parasite system. Philosophical Transactions of the Royal Society B: Biological Sciences. 2023 Feb 6;378(1873):20220009.

97. Conley MP, Wood WB. Bacteriophage T4 whiskers: a rudimentary environment-sensing device. Proceedings of the National Academy of Sciences. 1975 Sep;72(9):3701–5.

98. Leon-Velarde CG, Happonen L, Pajunen M, Leskinen K, Kropinski AM, Mattinen L, et al. Yersinia enterocolitica-Specific Infection by Bacteriophages TG1 and ϕR1-RT Is Dependent on Temperature-Regulated Expression of the Phage Host Receptor OmpF. Appl Environ Microbiol. 2016 Sep 1;82(17):5340–53.

99. Ryu WS. Virus Life Cycle. Molecular Virology of Human Pathogenic Viruses. 2017;31–45.

100. Bull JJ, Badgett MR, Wichman HA, Huelsenbeck JP, Hillis DM, Gulati A, et al. Exceptional Convergent Evolution in a Virus. Genetics. 1997 Dec;147(4):1497–507.

101. Brown CJ, Zhao L, Evans KJ, Ally D, Stancik AD. Positive selection at high temperature reduces gene transcription in the bacteriophage ϕX174. BMC Evolutionary Biology. 2010 Dec 3;10(1):378.

102. Bashey F. Within-host competitive interactions as a mechanism for the maintenance of parasite diversity. Philos Trans R Soc Lond B Biol Sci. 2015 Aug 19;370(1675):20140301.

103. Hudson P, Greenman J. Competition mediated by parasites: biological and theoretical progress. Trends in Ecology & Evolution. 1998 Oct 1;13(10):387–90.

104. Shen SS, Qu XY, Zhang WZ, Li J, Lv ZY. Infection against infection: parasite antagonism against parasites, viruses and bacteria. Infectious Diseases of Poverty. 2019 Jun 15;8(1):49.

105. Wang X, Wei Z, Yang K, Wang J, Jousset A, Xu Y, et al. Phage combination therapies for bacterial wilt disease in tomato. Nature Biotechnology. 2019 Dec;37(12):1513–20.

106. Abedon ST, Hyman P, Thomas C. Experimental Examination of Bacteriophage Latent-Period Evolution as a Response to Bacterial Availability. Appl Environ Microbiol. 2003 Dec;69(12):7499–506.

107. Sanjuán R. The Social Life of Viruses. Annu Rev Virol. 2021 Sep 29;8(1):183–99.

2.7 Supplementary figures

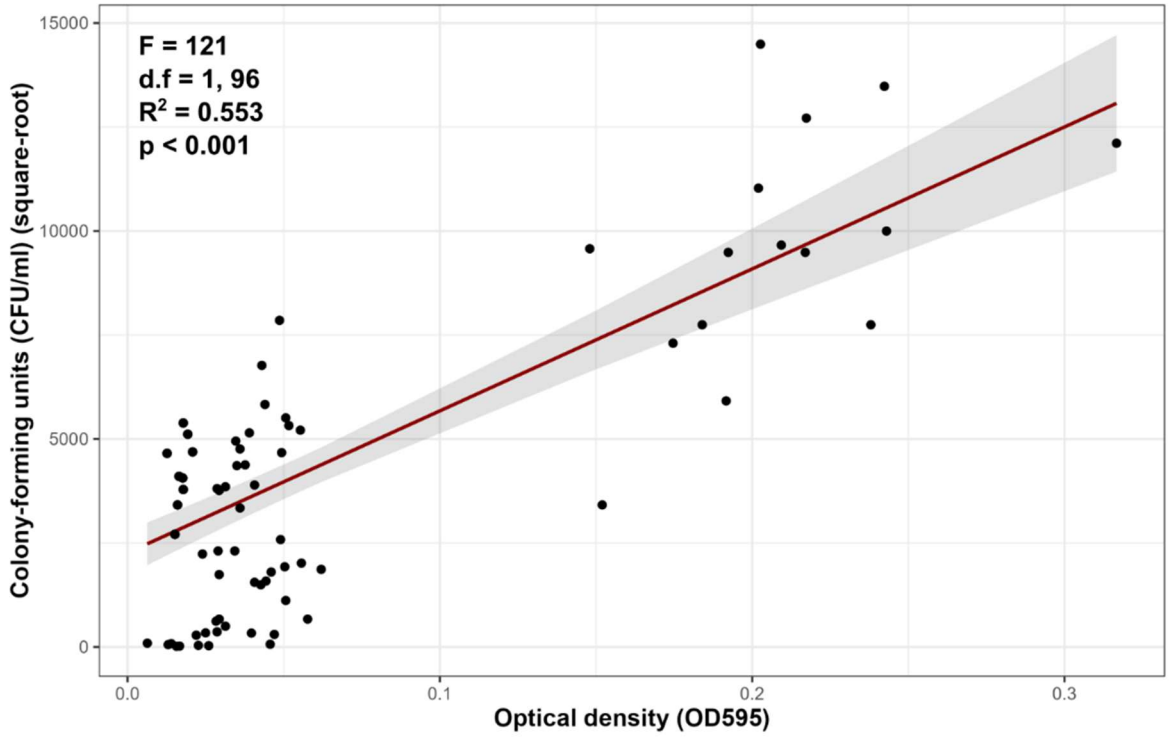

Figure S1. Optical density is correlated with colony-forming units. Regression analysis of optical density of bacterial samples and colony-forming units (CFU)/ml (square-rooted to meet model assumptions). Model line is plotted in red with shaded area showing model standard errors. Model parameters including F-statistic, degrees of freedom, adjusted R-squared, and p-value are shown in the top left.

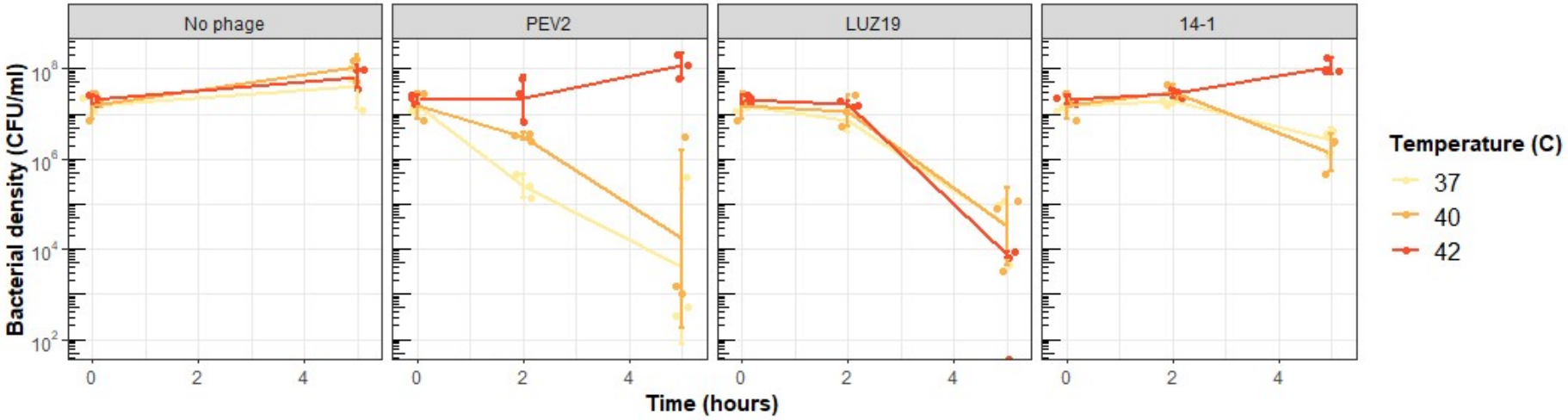

Figure S2. Temperature has a phage-specific impact on phage lytic activity. Change in bacterial densities over 5h shown in the presence of phage at 37°C, 40°C, and 42°C measured using colony-forming units. Plots are split by phage treatment and coloured by temperature. Results shown represent three biological replicates. For all graphs, error bars show standard error.

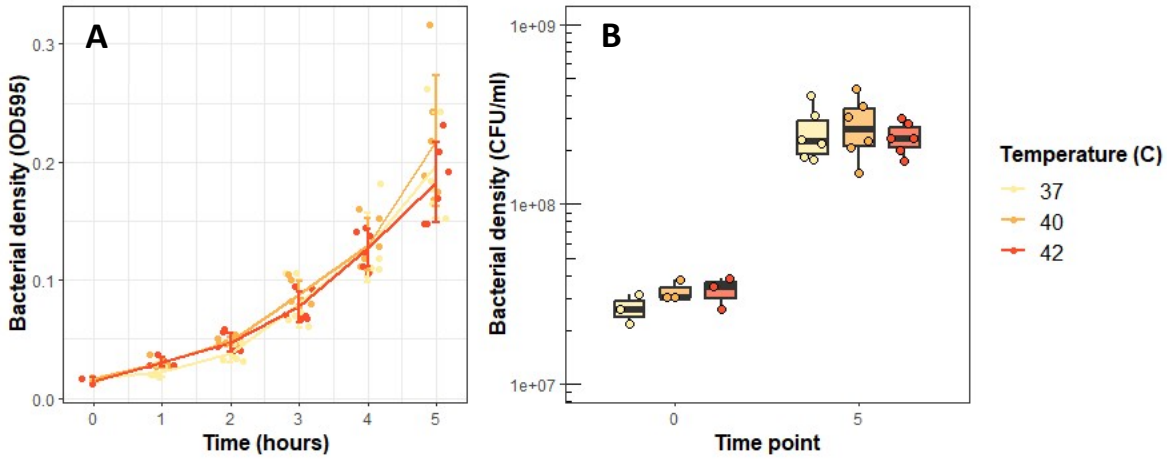

Figure S3. Bacterial growth in absence of phage is similar between temperatures. **A**) Bacterial growth in the absence of phage across 5h at 37°C, 40°C, and 42°C measured using optical densities. Results shown represent six biological replicates. Error bars show standard error. **B**) Bacterial densities (CFU/ml) at start and end-point of the experiment in the absence of phage at 37°C, 40°C, and 42°C. Results shown represent six biological replicates.

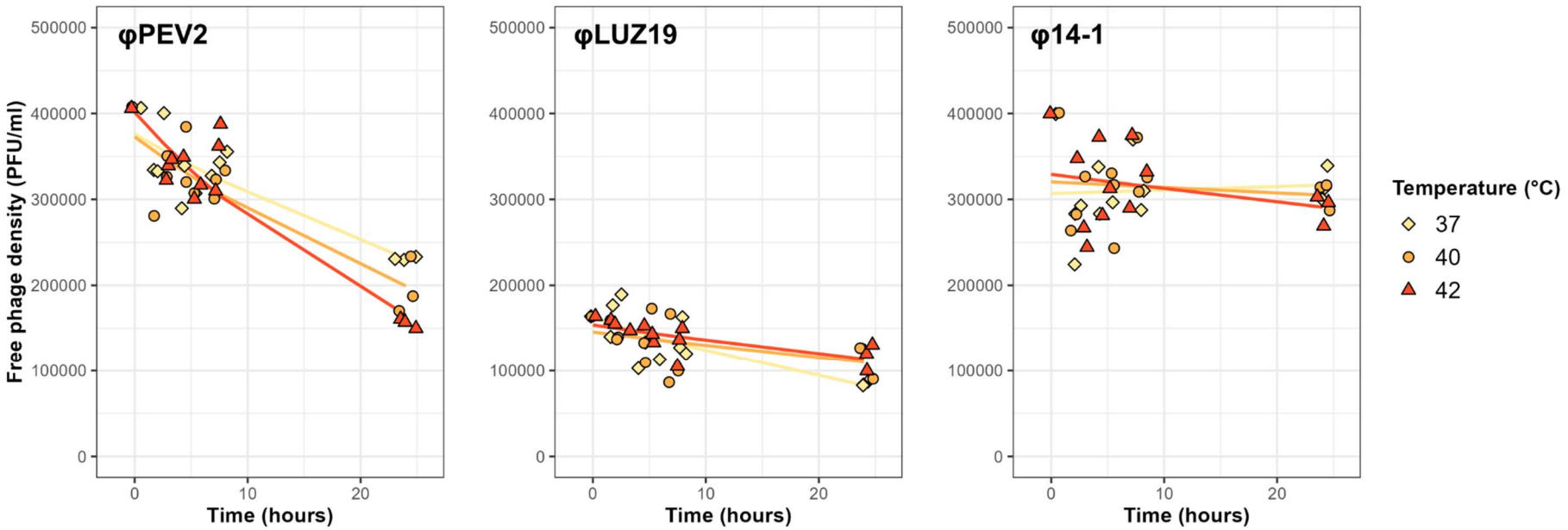

Figure S4. Phage survivorship varies with temperature. Change in free-phage density (PFU/ml) over time in the absence of bacterial hosts at 37°C, 40°C, and 42°C. Plots are split by phage and coloured and shaped by temperature. Lines show predicted values from generalised linear models where PFU/ml is response variable and time, temperature, and an interaction term between time and temperature are explanatory variables. 95% confidence intervals are shown as shaded region around model lines. Results shown represent three biological replicates.

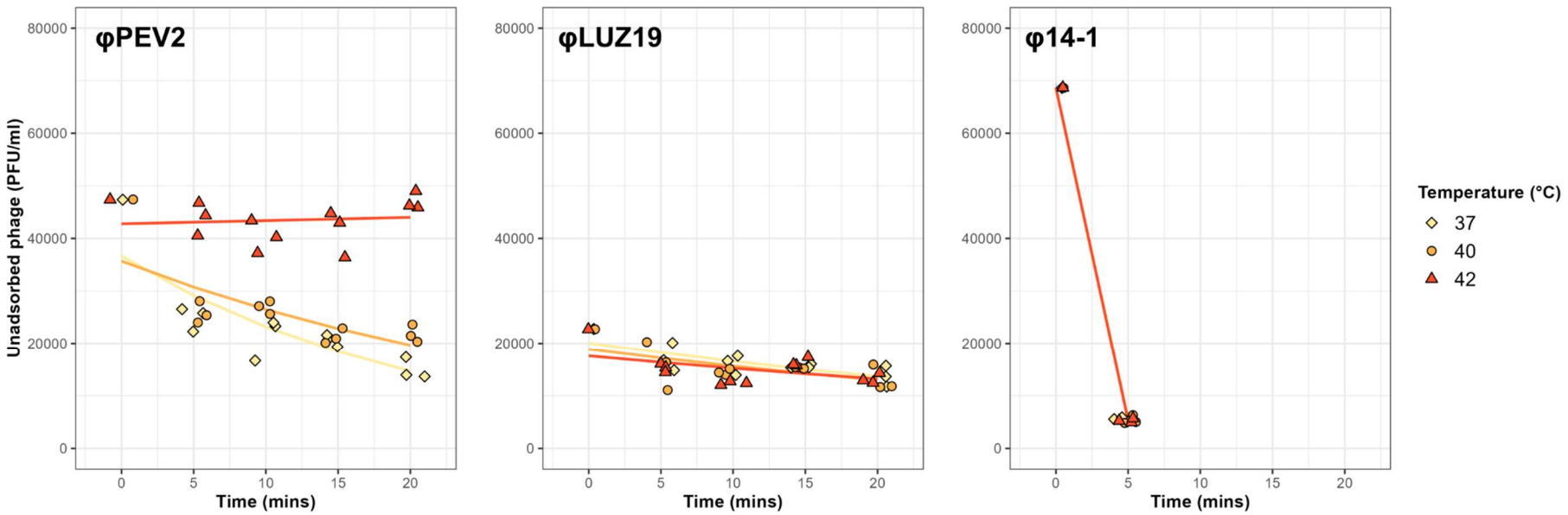

Figure S5. Phage adsorption rates are temperature-dependent. Plots showing the change in unadsorbed phage (PFU/ml) over time at 37°C, 40°C, and 42°C. Plots are split by phage and coloured and shaped by temperature. For φPEV2 and φLUZ19, lines show predicted values from generalised linear models where PFU/ml is response variable and time, temperature, and an interaction term between time and temperature are explanatory variables. For φ14-1, linear model of PFU/ml between 0 and 5 minutes is shown due to rapid phage attachment. Linear model has the same terms as the GLM. 95% confidence intervals are shown as shaded region around model lines. Results shown represent three biological replicates.

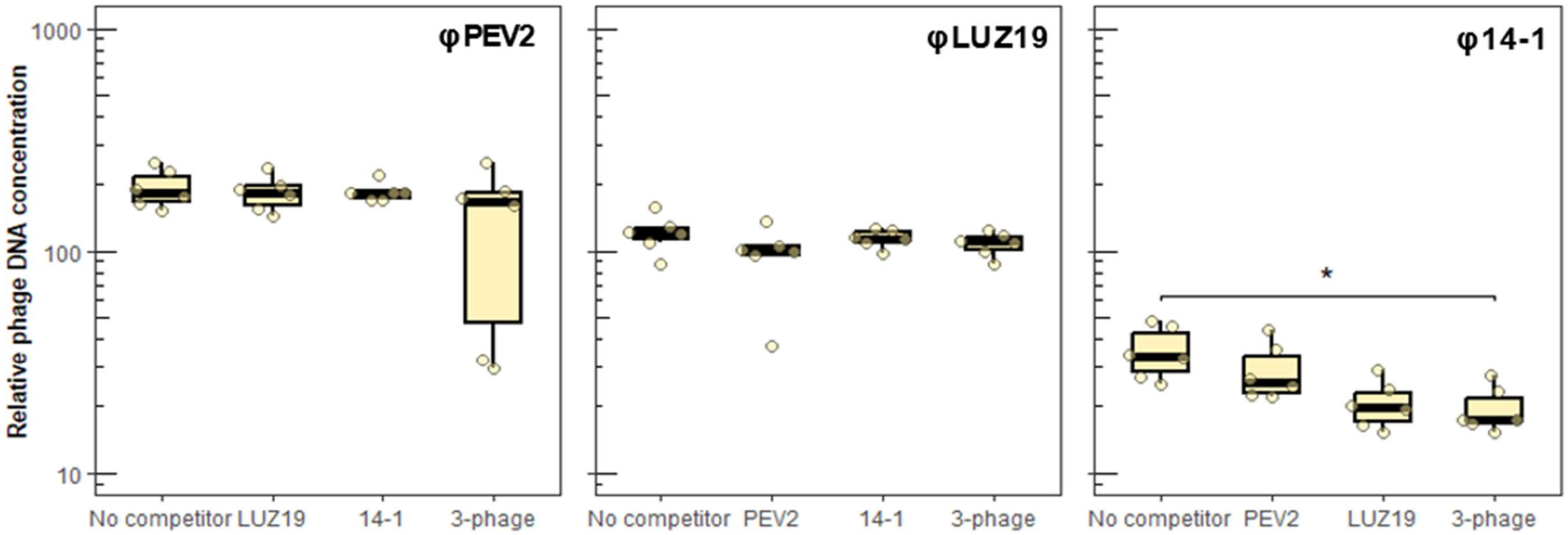

Figure S6. Phage competition is minimal at early stages of epidemic. Fold change in DNA copies after 2h for each phage at 37°C in the presence and absence of competitors. Asterisks show significant differences between competitor and no-competitor treatments based on a mixed effect model, with phage DNA concentration as the response variable and competitor as the explanatory variable (* = $p < 0.05$, ** = $p < 0.005$, *** = $p < 0.0001$). Results shown represent six biological replicates.

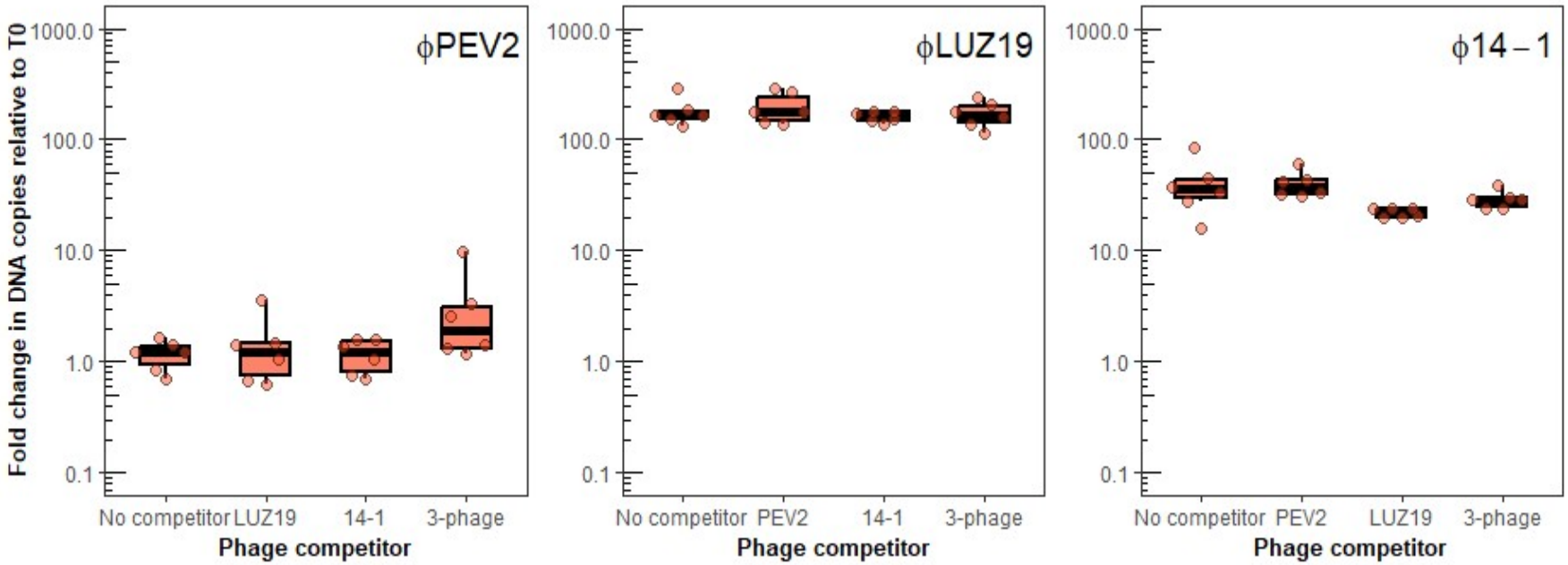

Figure S7. Phage competition is removed at high temperatures. Boxplots showing fold change in DNA concentration at T5 for each phage at 42°C in the presence and absence of competitors. Plots are split by phage. No significant differences were observed between competitor and no-competitor treatments based on a mixed effect model with phage DNA concentration as response variable and temperature, competitor, and their interaction as explanatory variables. Results shown represent six biological replicates.

2.8 Supplementary tables

Table S1. Phage genome accession numbers

Phage	NCBI accession
φPEV2	NC_031063
φLUZ19	NC_010326
φ14-1	NC_011703

Table S2. Phage qPCR primer sequences

Phage	Primer	Sequence
φPEV2	Forward Primer	CTAGTAACTACCGCCGACTCTA
φPEV2	Reverse Primer	GCCAGTTCCGCTATCTTCTT
φLUZ19	Forward Primer	TCGCAAGGCAACCATCAT
φLUZ19	Reverse Primer	ACGCGAGGTTCGTGTAAAG
φ14-1	Forward Primer	AGCGTGATCTTGTCCTTCATC
φ14-1	Reverse Primer	GCCATCGTAACTCTCACCATAC

Table S3. Phage life-history traits and population growth across temperature

		Host attachment	Survivorship	Virulence (T5)	Virulence (T2)	Population growth (T5)	Population growth (T2)
Phage	**Temp. (°C)**	**Time to 50% adsorption (mins)**	**Time to 50% decay (hours)**	**Log_2 ratio of T5 and To bacterial densities (CFU) (+- SE)**	**Log_2 ratio of T2 and To bacterial densities (CFU) (+- SE)**	**Log_2 ratio of T5 and To phage densities (PFU) (+- SE)**	**Log_2 ratio of T2 and To phage densities (+- SE)**
φPEV2	37	8.7-8.8	30.2-30.4	-6.9 +- 1.0	-5.85 +- 0.39	14.3 +- 0.14	13.2 +- 0.32
	40	12.5-12.7	23.2-23.3	-4.1 +- 1.1	-2.48 +- 0.37	13.7 +- 0.10	12.2 +- 0.45
	42	Inf (no adsorption)	18.4	2.60 +- 0.36	0.56 +- 0.52	-4.98 +- 0.53	-2.86 +- 0.08
φLUZ19	37	28.9-30.1	19.0-19.1	-7.86 +- 0.51	-0.955 +- 0.42	15.06 +- 0.46	12.3 +- 0.43
	40	26.6-27.8	36.5-37.3	-8.06 +- 0.61	-0.30 +- 0.52	15.2 +- 0.47	12.4 +- 0.46
	42	29.5-31.4	38.1-39.0	-12.1 +- 0.53	-0.42 +- 0.22	12.8 +- 0.44	11.6 +- 0.52
φ14-1	37	2.7	Inf (no decay)	-2.45 +- 0.35	0.28 +- 0.24	14.7 +- 0.33	4.86 +- 0.37
	40	2.7	217.2-241.8	-3.37 +- 0.51	0.87 +- 0.42	14.2 +- 0.43	5.9 +- 0.48
	42	2.7	95.1-99	2.48 +- 0.28	0.41 +- 0.18	2.71 +- 0.74	-2.21 +- 0.47

3

Evolutionary rescue accelerates competitive exclusion in a parasite community

This Chapter is in prep and has been released on BioRvx

3.1 Abstract

Environmental stress drives biodiversity loss by altering competitive hierarchies and pushing taxa towards extinction. Parasites and their communities are particularly vulnerable to stress due to environmental sensitivity of infection steps, variation in species tolerance during co-infections, and dependence on host fitness. Parasite populations might avoid extinction through evolutionary rescue – whereby rapid adaptation to stress enables persistence – but whether this process can preserve community diversity remains unclear. Here, we study the impact of evolutionary rescue in a simple parasite community by propagating populations of two viral parasites (bacteriophages φ14-1 and φLUZ19) of *Pseudomonas aeruginosa* in monoculture and co-culture under two thermal conditions, a control temperature (37°C) and a high temperature that restricts φ14-1 growth (42°C). We show that evolutionary rescue of φ14-1 prevented extinction in monoculture. Rescue of this phage in co-culture made it a superior competitor, and it replaced φLUZ19 as the dominant phage at high temperature. We determine that evolutionary rescue occurred through mutations in genes linked to attachment to bacterial hosts and within-host replication. We also show that competitive suppression by φ14-1 constrained φLUZ19 molecular evolution. Our findings suggest that evolutionary rescue can prevent the extinction of some parasites but may inadvertently destabilise the community and facilitate further biodiversity loss. This work underscores the need to take an eco-evolutionary approach to predict the responses of communities to global climate change.

3.2 Introduction

Environmental stress is a primary driver of biodiversity loss (1,2). On an ecological timescale, only those species with environmental optima and tolerance ranges best aligned with prevailing conditions can persist (3–5). As community composition shifts towards fewer species, the probability of extinction events (6) and ecological tipping points (7) is heightened. On an evolutionary timescale, however, biodiversity could be maintained via evolutionary rescue, whereby adaptation to environmental stress facilitates population recovery (7,8). Evolutionary rescue has been shown to prevent diversity loss in communities and increase the prevalence of rare taxa whose relative fitness increases following adaptation (9–11). Alternatively, evolutionary rescue can alter the competitive hierarchy in communities and drive competitor decline and exclusion (12,13). Whether evolutionary rescue can counteract the diversity-eroding impacts of environmental stress is unclear. Understanding how environmental stress affects biodiversity requires consideration of both ecological and evolutionary dynamics in communities (14).

Parasite communities are expected to be among those most disrupted by climate change, with consequences for global disease dynamics and ecosystem stability (15). Parasite diversity has been shown to decrease with thermal stress through widening inter-parasite fitness differences (16) and increasing host resistance (17). Diversity can also be lost through thermal alterations to parasite life-history strategies (18) or a reduction in niche differences (19,20). Microbial parasites offer a powerful model system to study evolutionary rescue in communities due to their rapid evolution rates and frequent competitive interactions with other parasites (21,22). Parasites can be highly sensitive to thermal extremes ((23–25), see Introduction, 1.3) and, in isolation, have been shown to avoid thermal extinction through evolutionary rescue (16,26). However, the evolutionary responses to thermal stress in communities are more complex. Inter-parasite competition can constrain evolutionary rescue by reducing population growth rates and mutational supply (5,18,27,28). Alternatively, rescue may be promoted with competition and thermal stress selecting on the same parasite life-

history traits ((29), see Introduction, 1.3). Evolutionary rescue may thus alter parasite competitiveness and increase the risk of competitor exclusion (13,30,31) in response to stressful temperatures.

Evolutionary rescue is predicted to increase the absolute fitness of a parasite species during warming and prevent extinction. While competition in parasite communities could constrain evolution through limiting mutational supply (28), adaptation could skew the competitive hierarchy towards the rescued, thereby accelerating competitive exclusion. To test these predictions, we passaged two lytic viral parasites (thermal generalist φLUZ19 and specialist φ14-1) through evolutionarily static populations of a bacterial host, *Pseudomonas aeruginosa* (Figure 1). These phages are obligate killers; following phage attachment and infection of host cells, they immediately initiate replication and host cell lysis (death). Phages were evolved under a control temperature (37°C) or high temperature that restricts the growth of the φ14-1 phage (42°C) (see Chapter 2) in monoculture or co-culture. We tested for effects on phage growth rates and competitiveness by conducting phenotypic assays of phage infectivity in the absence and presence of a phage competitor. We also used sequencing to measure changes in the genomic composition of phage populations through time.

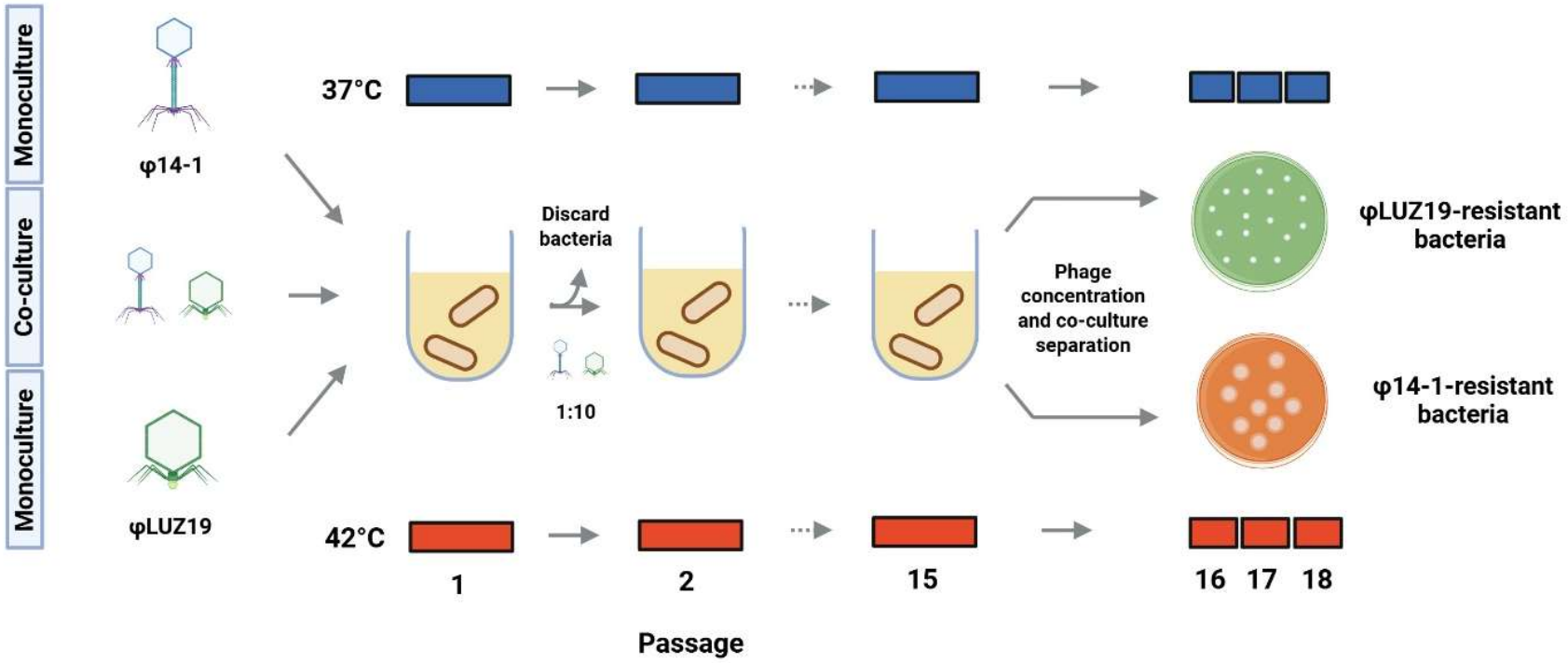

Figure 1. Overview of phage experimental evolution framework. Phages evolved in monoculture or co-culture at 37°C or 42°C for 15 passages. At the end of each passage, phages were isolated from lysates and used to infect fresh, evolutionarily static bacterial hosts (Passages 1-15). At the end of the selection experiment, phages were concentrated and co-cultures separated through three rounds of confluent lysis plating on phage-resistant bacteria (Passages 16-18) under the same thermal regime as earlier passages. Phage icons illustrate the two different phages used in the experiments (φ14-1, myovirus in blue; φLUZ19, autographivirus in green) (32) and are used hereafter to refer to phages in figures. Figure was created using BioRender.

3.3 Methods and Materials

3.3.1 Strains, storage, and culture conditions

Pseudomonas aeruginosa PAO1 (hereafter referred to as PAO1) was used with two lytic bacteriophages: φLUZ19 (33,34), and φ14-1 (35). These phages have been used to test several ecological and evolutionary hypotheses at 37°C ((36–39), also see Chapter 2). The phages were also selected based on their distinct responses to temperature: φLUZ19 has high growth rates at 37°C and 42°C, while φ14-1 has restricted growth at 42°C (see Chapter 2). Bacterial stocks and phage lysates were prepared as in Chapter 2.

3.3.2 Experimental evolution

A schematic of the experimental evolution framework is shown in Figure 1. Each of 15 evolutionary passages were made across three phage treatments (φLUZ19 and φ14-1 monocultures and co-culture) and two temperatures (37°C and 42°C). Each treatment consisted of six, independent replicate populations started from a single ancestral lysate.

Phage were propagated without shaking with a non-evolving ancestral PAO1 bacterial host. For the initial passage, ancestral phage lysates were diluted to 10^8 PFU/ml and 300µl were added to 2.7ml 10^8 CFU/ml bacterial culture in loose-lid 14ml falcon tubes. Phage co-culture populations were prepared by combining 150µl each of φLUZ19 and φ14-1 10^8 PFU/ml stocks prior to mixing with bacteria. Phages were added at a 1:1 ratio to mimic a phage community that is already stable and at the maximum level of biodiversity possible with a two species system. The initial passage phage densities were ~10^7 PFU/ml resulting in a phage/bacteria ratio (multiplicity of infection, MOI) = ~0.1. Bacterial culture densities were standardised using optical density (OD595) based on a CFU:OD standard curve (Figure S1). Following addition of bacterial cultures, tubes were incubated statically at 37°C or 42°C in circulating water baths for 8h.

After each passage, phage lysates were centrifuged at 3,095xg for 5 mins to pellet remaining bacterial cells. Phage lysates were then sterile-filtered using 0.2µm syringe filters into 2ml cryotubes and stored at 4°C. At the beginning of each passage, 2.7ml of fresh ancestral PAO1 was seeded with 300µl of the preceding passage's filtered phage lysate.

3.3.3 Phage quantification

Phage titres were determined via the double-layer overlay method (40) following the same protocol as in Chapter 2. Briefly, bacterial lawns were prepared by mixing 10mL of melted top agar with 300µL of a *P. aeruginosa* PAO1 overnight culture. Phage stocks were serially diluted, and 10µL was spotted onto bacterial lawns. After incubating plates for 6–8 h at 37°C, spots with the highest number of discernible plaques were counted. Top-agar bacterial lawns were seeded with φLUZ19-resistant and φ14-1-resistant PAO1 strains to quantify φ14-1 and φLUZ19 populations, respectively. Phage resistant PAO1 strains were generated by spotting high titre phage stocks (~ 10^{10} PFU/ml) onto wild-type PAO1 top-agar lawns. Plates were then incubated for ~48h or until colonies started to grow on top of phage clearance zones. Five colonies were picked for each phage and were re-streaked twice before being used to seed 10ml Luria-Bertani (LB) (Lennox) and grown statically at 37°C in 50ml falcon tubes. The absence of phage in resistant cultures was determined through sterile-filtration of the bacterial supernatant and spotting onto ancestral PAO1 bacterial lawns.

Phage resistance was confirmed through the absence of plaques when spotting high titre phage stocks onto lawns seeded with each resistant line. One resistant line was selected for each phage by spotting phage stocks of known concentration (based on wild-type PAO1 estimates) and selecting the line that had the closest plaque count, turbidity, and size. Phage-resistant PAO1 mutants underwent whole-genome hybrid (long- and short-read) sequencing and variant calling (see Phage population genomics, 3.3.6). While both PAO1 mutants had multiple mutations compared to wild-type (Table S1), we identified mutations that were previously linked to phage resistance. φLUZ19-resistant PAO1 had a mutation in a GspL type-II secretion

system protein (BlastP: 99.5% similarity and 100% query cover); Gsp gene mutations have previously shown to provide resistance to type-IV pilus dependent phages (41). φ14-1-resistant PAO1 had a mutation in a glycosyltransferase (BlastP: 100% similarity and query cover); glycosyltransferase mutations have been shown to provide resistance to LPS-dependent phages (42). To maintain comparability, both monoculture and co-culture populations were quantified using resistant PAO1 strains.

Changes in phage counts during the evolution experiment could reflect evolutionary changes in efficiency of plaque formation rather than changes in phage densities. The efficiencies of plaque formation of the passage 15 evolved and ancestral phage populations were found to be similar when tested on the ancestral and resistant PAO1 strains separately (Figure S2). This outcome confirmed that phage counts reflected changing phage densities.

3.3.4 Phage separation and concentration

Evolved phage populations needed to be concentrated and purified to separate co-cultures and create high titre stocks for phage population sequencing (Figure 1). High titre, pure phage stocks were made using a selective confluent lysis double-layer overlay method. Briefly, bacteria-phage lawns were prepared by mixing 180µl of either φLUZ19-resistant or φ14-1-resistant PAO1 overnight cultures (approximately 3 x 10^8 CFU/ml) with 30µl of phage lysate diluted to 10^8 PFU/ml. Initial bacterial culture densities were ~10^8 CFU/ml and phage densities were ~10^6 PFU/ml phage, MOI = ~0.01. Bacteria-phage mixtures were left at room temperature for ~10 mins to allow phage adsorption after which 5ml of molten top agar (~40°C) was added and agar was poured onto pre-filled LB-agar plates. Plates were incubated for ~20h at temperatures appropriate for each evolved population: 37°C for 37°C evolved phage populations, 42°C for 42°C evolved populations. After incubation, top-agar was scraped off plates into 15ml falcon tubes containing 5ml phage buffer (NaCl (100 mM), $MgSO_4$ (10 mM), $CaCl_2$ (5 mM), Tris-HCl (pH 8) (50 mM), Gelatin (0.01%)). Tubes were incubated at 4°C on a rotating carousel shaker at 10rpm for 24h to extract phage from top agar. Phages were

separated from bacteria and agar by centrifuging tubes at 6,000xg for 10 mins followed by sterile-filtering. The purification/concentration process was repeated three times to remove non-focal phages and purity was assessed based on the absence of competitor plaques following high-titre spotting. To ensure comparability, monoculture populations underwent the same purification and concentration process as co-culture populations.

3.3.5 Phage phenotypic assays

3.3.5.1 Growth rates

The thermal phenotypes of purified evolved phage populations relative to the ancestor were assessed by measuring phage and bacterial growth across an 8h window under static incubation at 37°C and 42°C. Phage stocks were diluted to 10^5 PFU/ml and 300uL was used to inoculate 2.7ml of 10^8 CFU/ml wild-type PAO1, with a resulting MOI = ~0.0001. This low MOI was chosen to extend phage growth curves to capture differences in phage growth rates as, at higher phage densities, both phages tend to reach carrying capacity within 2-3h (see Chapter 2). For φLUZ19, samples were taken for phage quantification at 2h, 4h, and 8h. For φ14-1, samples were taken at 4h and 8h as preliminary assays indicated that phage growth was minimal at the 2h timepoint. Phage quantification was performed by adding 200µl samples to 96-well filter plates (Agilent) followed by centrifugation at 2,230xg for 5 mins before spotting onto φ14-1 or φLUZ19 resistant PAO1 double-layer overlay plates. Each fitness assay included a single replicate of each evolved phage line and three replicates of the phage ancestor. Growth rate assays were repeated three times across a two-week period to produce three technical replicates.

3.3.5.2 Competitive ability

We assessed the competitiveness of evolved φ14-1 37°C and 42°C co-culture populations across time. Competitive ability was determined by growing phages under the same conditions as the fitness assay (37°C and 42°C) either alone or in the presence of an ancestral φLUZ19

competitor. For the monoculture treatment, 300µl of phage lysate was added to 2.7ml 10^8 CFU/ml wild-type PAO1 stock. For the co-culture treatment, 150µl of evolved phage stock and 150µl of ancestral phage competitor was added. A 1:1 phage ratio was used to replicate the experimental evolution selective environment. The competition assay was conducted with two phage starting densities, 10^5 PFU/ml (MOI = ~0.0001) and 5 x 10^8 PFU/ml (MOI = ~5).

Phages were grown for 8h after which samples were taken for phage quantification as previously described. Evolved φ14-1 competitiveness was determined by calculating ancestral φLUZ19 competitor growth in co-culture with evolved and ancestral φ14-1 populations against phage growth in monoculture (43). Competition assays were repeated three times across a four-week period to produce three technical replicates.

3.3.6 Phage population genomics

3.3.6.1 DNA extraction and sequencing

Phage DNA was extracted using a customised protocol. We used 500µl aliquots of post-purification evolved and ancestral phage lysates (~10^{10} PFU/ml). Firstly, we added DNase (5µl of 1000U/ml, 5U) to remove bacterial DNA and RNase (2µl of 100mg/ml, 0.2mg) to remove RNA. Lysates were then incubated at 37°C in a heat block for 1h and inverted every 15 mins. After incubation, 67.5µl lysis (AL) buffer and 4µl proteinase K was added to each tube before incubating at 56°C for 15 mins. After 15 mins, tubes were then incubated at 95°C for 10 minutes to denature the proteinase K. After denaturing, the tubes were placed on ice and 150µl of precipitation (N4) buffer was added. Tubes were immediately centrifuged at 13,000xg for 10 mins to pellet cell debris and the supernatant was transferred to a clean 2ml Eppendorf. Cold 100% isopropanol (1.5x tube volume, ~1.1ml) was then added and the tubes were placed in an orbital rotator set to 10rpm for 5 mins to precipitate DNA. The tubes were centrifuged at 13,000xg for 20 mins to pellet DNA after which the supernatant was discarded. The DNA pellet was then washed with 1ml 70% ethanol and mixed for a further 5 mins on the orbital rotator before being centrifuged again at 13,000xg for 20 mins. This wash step was repeated

twice and after the second centrifugation step the supernatant was discarded and the pellet dried in a heat block set to 37°C to evaporate any remaining ethanol. Finally, 30µl of nuclease-free water was added to re-suspend the pellet.

DNA purity and contamination were measured using NanoDrop 2000c (Thermo Scientific). The presence of phage DNA was confirmed using gel electrophoresis using a 100kb ladder and a phage lambda DNA control with bands observed at the expected phage genome size. DNA was quantified using Qubit 4 (Thermofisher). Samples were diluted to DNA concentration of 50ng/µl and sent for Illumina short-read sequencing with AZENTA/GENEWIZ using their Microbe-EZ pipeline. One extraction from each evolved population was sent for sequencing in addition to three extractions of each phage ancestor. For ancestral and phage-resistant PAO1 bacterial genome sequencing, bacterial samples were sent to MicrobesNG for DNA extraction and hybrid (long- and short-read) sequencing.

3.3.6.2 Sequence analysis

Phage sequence reads were pre-processed through read trimming using Trim Galore (v.0.5.0) (https://github.com/FelixKrueger/TrimGalore) with a fastqc step and 33 phred-score read cut off. Due to high and uneven read depth, reads were downsampled using bbnorm from the bbmap package (v.39.18) (https://sourceforge.net/projects/bbmap/) to a target read depth of 1500x and a minimum depth of 1000x. Ancestral phage genomes were assembled using shovill (v1.1.0) (https://github.com/tseemann/shovill) with default parameters and downsampled phage reads were mapped to the assemblies using Bowtie2 (v.2.3.4.2) (44) with default parameters. Read depth was checked for evenness using SAMtools (v.0.1.2) (45) view, sort, and depth functions. Ancestral phage assemblies were annotated using prokka (v.1.14.5) (46), guided by the NCBI GenBank file for each phage (φ14-1: NC_011703; φLUZ19: NC_010326). Genetic variants in phage populations were detected using breseq (v.0.36.1) (47) under default parameters, using the annotated ancestral genomes as a reference.

Wild-type PAO1 reads were processed using an in-house pipeline. We first quality-controlled the long-reads using Filtlong (v. 0.2.1) (https://github.com/rrwick/Filtlong) with parameters

--min_length 1000 --keep_percent 95. We then used Autocycler (v. 0.4.0) (48) to recover a consensus genome assembly, calling the assemblers Canu (v. 2.3) (49), Flye (v. 2.95), Miniasm (v. 0.3) (50), plassembler (v. 1.7.0) (51) and Raven (v. 1.8.3) (52). Next, we quality-controlled the short-reads using fastp (v. 0.24.2) (53), indexed the assembly with BWA (v. 0.7.19) (54), and polished with Polypolish (v. 0.6.0) (55). Lastly, we re-oriented the assembly with Dnaapler (v. 1.2.0) (56). The workflow was deployed using a Dockerised Nextflow pipeline (v. 1.0.2) available at https://doi.org/10.5281/zenodo.15706447. The wild-type PAO1 assembly was annotated using prokka (v.1.14.5) (46). φLUZ19 and φ14-1-resistant PAO1 mutations were detected by mapping long reads to the wild-type assembly with minimap2 (v.2.24) (57) and variant calling with medaka (v.2.1) (https://github.com/nanoporetech/medaka). SNPs were filtered so only those with quality scores >= 10 were kept.

3.3.7 Statistics and data visualisation

All statistical analyses and data visualisation were conducted using packages in R (v.4.3.2) and RStudio (58,59). Data wrangling was performed using "Tidyverse" (v.2.0.0) R packages (60). Phage growth and evolution rates were compared between evolution treatments using linear mixed effect models with the "lme4" (v.1.1-36) R package (61) where the response variable was phage density (pfu/ml) or genetic distance from ancestor, the explanatory variable was an interaction term between evolution treatment and temperature, and batch was a random effect. Genetic divergence between evolved populations was calculated using Principle Coordinate Analysis (PCoA) ANOSIM with 10,000 permutations using the "ape" (v.5.8) R package (62). Congruence between Euclidean genetic and phenotypic distance neighbour-joining trees was calculated using Procrustes Approach to Cophylogenetic Analysis (PACo) (v.0.4.2) R package with 10,000 permutations (63). Data and code used in analyses can be found at https://github.com/SamuelGreenrod/Phage_thermal_adaptation. Phage sequence reads are accessible on NCBI (https://www.ncbi.nlm.nih.gov/) under BioProject ID:

PRJNA1332698. Bacterial sequence reads are available on NCBI under BioProject ID: PRJNA1332799.

3.4 Results

3.4.1 Evolutionary rescue prevents phage extinctions in monoculture

While the ancestral φLUZ19 grows equally at 37°C and 42°C, ancestral φ14-1 populations show no signs of growth at 42°C at a starting density of 10^4 PFU/ml (Figure 2A). Passaging at this density would have thus resulted in dilution to extinction. We hypothesised that the thermally sensitive phage φ14-1 would avoid extinction by rapidly adapting to tolerate thermal stress. While φ14-1 growth was initially restricted at 42°C, it rapidly reached and maintained high densities (>10^9 PFU/ml) across temperatures (Figure 2B). High densities were also reached by the thermal generalist φLUZ19. Across both phages, no replicate populations went extinct.

We measured bacterial growth using optical densities at 37°C and 42°C (Figure S3) to account for any host-mediated variation in phage densities. Without phage, *P. aeruginosa* had significantly higher growth rates at 42°C compared to 37°C ($F_{3,62} = 78.9$, $p < 0.001$). Based on a standard curve of optical density to colony forming units (Figure S1), average bacterial densities at 42°C were found to be approximately double those at 37°C across an 8h passage. Yet, phage densities at each passage were the same or lower at 42°C than 37°C indicating that variation in phage densities could not be explained by differences in bacterial growth rates.

To determine whether φ14-1 densities were maintained at 42°C through evolutionary rescue, we conducted population growth assays for the end-point evolved phage populations at 37°C and 42°C (Figure 2E). Phage population growth rates depended on an interaction between evolution treatment (37°C or 42°C) and assay temperature (φ14-1: $F_{2, 19.1} = 199$, $p < 0.0001$; φLUZ19: $F_{2,19.1} = 100.0$, $p < 0.0001$). φ14-1 populations evolved at 42°C showed a significant increase in growth at 42°C compared to ancestor ($t(20.9) = -18.1$, $p < 0.0001$). However, 37°C evolved populations showed no change in growth at 37°C ($t(20.9) = 0.64$, $p = 0.987$), likely

due to phages reaching close to carrying capacity at the point of measurement (Figure S4). φLUZ19 populations also had significantly higher growth rates at their evolved temperatures compared to the ancestor (37°C: $t(20.9) = -7.68$, $p < 0.0001$; 42°C: $t(20.9) = -7.04$, $p < 0.0001$).

Higher growth rates under evolved conditions may reflect merely adaptation to the host rather than temperature-specific fitness changes. We assessed phage growth at allopatric (e.g., mismatched) temperatures (Figure 2E). φ14-1 evolved populations showed no improvement in growth at allopatric temperatures (37°C evolved populations: $t(20.9) = 2.37$, $p = 0.212$, 42°C evolved populations: $t(20.9) = 1.00$, $p = 0.912$). In addition, φLUZ19 populations evolved at 37°C exhibited a significant growth rate decrease at 42°C ($t(20.9) = 5.13$, $p < 0.001$). However, φLUZ19 populations evolved at 42°C were found to also have significantly higher growth rates at 37°C than ancestor ($t(20.9) = -4.79$, $p < 0.01$) indicative of adaptation to the host as opposed to the thermal regime in this instance.

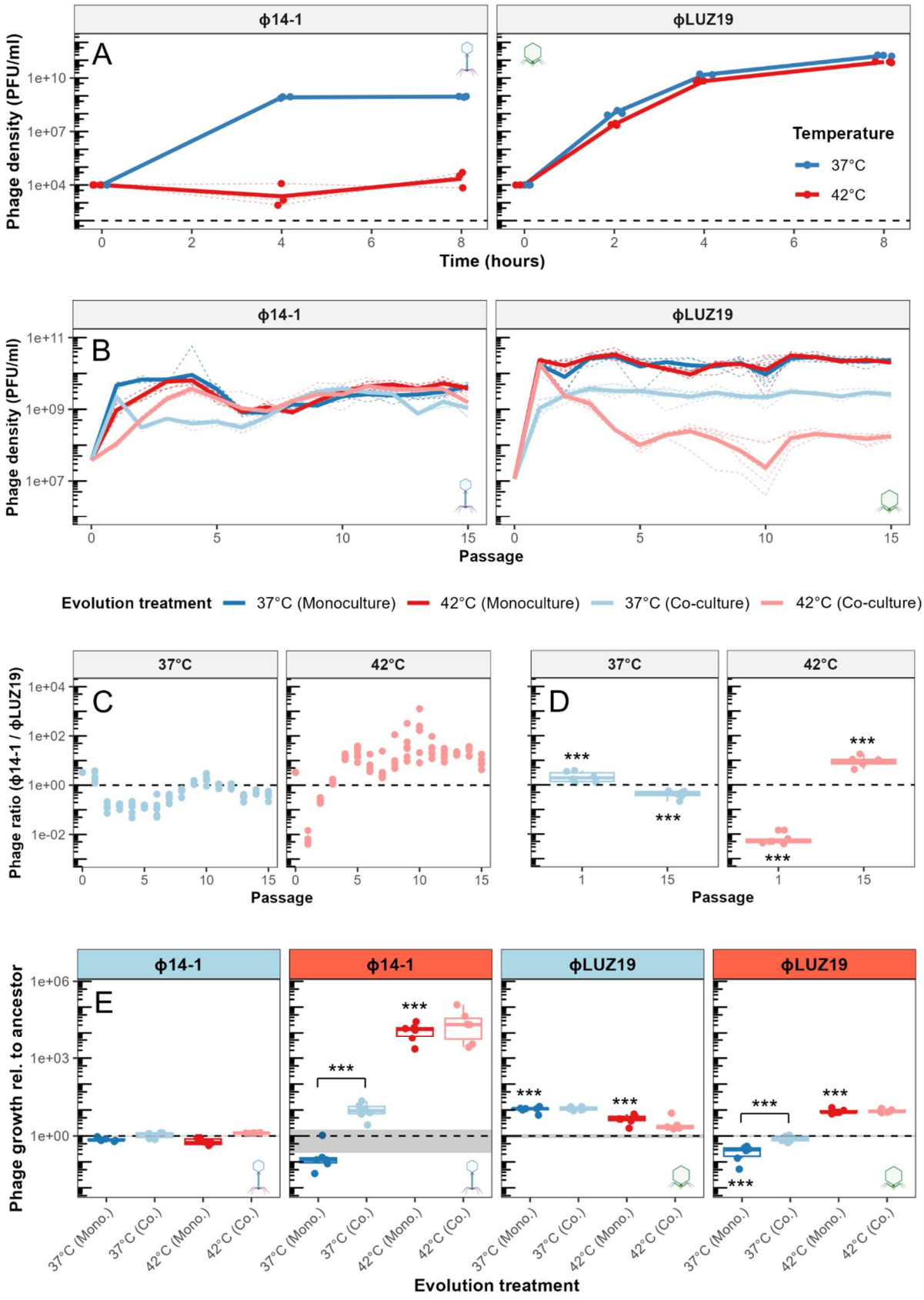
ϕ14-1
ϕLUZ19
A
Phage density (PFU/ml)
1e+10
1e+07
1e+04
Temperature
37°C
42°C
Time (hours)
B
1e+11
1e+09
1e+07
Passage
Evolution treatment
37°C (Monoculture)
42°C (Monoculture)
37°C (Co-culture)
42°C (Co-culture)
C
D
Phage ratio (ϕ14-1 / ϕLUZ19)
1e+04
1e+02
1e+00
1e-02
***
E
Phage growth rel. to ancestor
1e+06
1e+03
1e+00
37°C (Mono.)
37°C (Co.)
42°C (Mono.)
42°C (Co.)
Evolution treatment

Figure 2. Evolutionary rescue alters the competitive hierarchy. A) Growth curves of ancestral phages across temperatures at a starting density of 10^4 PFU/ml. Lines show ancestral phage growth curves at 37°C (deep blue) and 42°C (deep red). Black dashed line marks the limit of detection. **B)** Phage population densities under each evolution treatment across passages. Lines show phage population densities during the first 15 evolutionary passages of phages in monoculture (37°C in deep blue, 42°C in deep red) and in co-culture (37°C in light blue, 42°C in light red). Solid lines show average values of six biological replicates (each shown as dashed line). Values show densities at the end of each passage prior to dilution. **C)** Ratio of φ14-1 to φLUZ19 densities in co-culture treatments across passages. Values show phage ratios at the end of each passage where each dot shows a replicate population. Phage ratio of 1:1 is shown with black dashed line. **D)** φ14-1 to φLUZ19 ratios in co-culture treatments at passage 1 and passage 15. Asterisks show significant differences to a phage ratio of 1:1 (black dashed line) where *** = $p < 0.001$. **E)** Growth rates of end-point evolved phage populations relative to the ancestral population tested in monoculture at 37°C (light blue strip) and 42°C (light red strip). φ14-1 populations were compared after 4h growth and φLUZ19 populations were compared after 2h growth. Evolved phage growth (box) is shown relative to ancestor (black dotted line). Shaded grey region shows ancestor standard errors from three biological replicates, each being an average of three technical replicates. Asterisks above line connectors show significant differences between evolved populations. Asterisks above boxes show significant differences from the ancestor. *** = $p < 0.001$. Co-culture populations were not compared to the ancestor. Otherwise, no asterisk reflects non-significance.

3.4.2 Evolutionary rescue alters the competitive hierarchy

While thermal adaptation occurred in monoculture, we hypothesised that adaptation would be restricted in co-cultures due to evolutionary constraint from inter-phage competition (5,27). Both φ14-1 and φLUZ19 were initially found to have lower population densities in co-culture than in monoculture (Figure 2B). At 37°C, φ14-1 and φLUZ19 had ~10-fold lower densities in co-culture up to passage 6, after which φLUZ19 densities remained suppressed and φ14-1 densities converged with those of the monoculture populations. While φ14-1 was heavily restricted by φLUZ19 in early passages at 42°C, it reached similar densities to monoculture populations by passage 4. In contrast, φLUZ19 co-culture densities were initially high at 42°C but rapidly decreased before stabilising.

We hypothesised that the population decline in φLUZ19 42°C co-culture populations occurred due to a shift in the competitive equilibrium with φ14-1 following evolutionary rescue. We assessed the competition dynamics by tracking the ratio of φ14-1 and φLUZ19 densities across co-culture passages where a ratio > 1 reflects a φ14-1 competitive advantage and vice versa. At 42°C, the ratio of φ14-1 densities relative to φLUZ19 fell in the initial passage but then rapidly increased before stabilising at passage 5 (Figure 2C). The phage ratio conversely remained relatively stable across all passages in the control. By analysing phage ratios at passages 1 and 15, we found that, at 42°C, φ14-1 had a significant competitive disadvantage at passage 1 ($t(19.9) = -27.5$, $p < 0.001$) but a significant advantage by passage 15 ($t(19.9) = 11.7$, $p < 0.001$). φ14-1 competitive advantage showed a small decrease between passage 1 and 15 in the control (Passage 1: $t(19.9) = 3.9$, $p < 0.001$; Passage 15: $t(19.9) = -4.7$, $p < 0.001$).

We further investigated the competitive profile of the rescued phage in time-shifted, direct competition assays at low and high MOI between evolved φ14-1 co-culture populations against a φLUZ19 ancestral population (Figure S5). At low MOI, the restriction of φLUZ19 ancestral growth by φ14-1 was significantly lower in the φ14-1 37°C co-culture population than the φ14-1 ancestor at 42°C ($t(21.6) = -4.4$, $p < 0.01$). At high MOI, φLUZ19 ancestor restriction at 42°C was significantly greater in the φ14-1 42°C co-culture populations than the φ14-1 ancestor

($t(21.6) = 3.9$, $p < 0.01$), but the magnitude of change was relatively small. The φ14-1 competitive advantage in 42°C co-culture populations did not reflect an escalating increase in competitive fitness across evolutionary time.

By restricting phage growth, we hypothesised that the presence of a competitor would constrain phage thermal adaptation. We assessed thermal adaptation by comparing phage thermal phenotypes in monoculture and co-culture evolved populations (Figure 2E). For both phages, we found that growth rates depended on an interaction between evolution treatment (monoculture and co-culture) and assay temperature (φ14-1: $F_{4,39} = 132$, $p < 0.0001$; φLUZ19: $F_{4,39} = 108$, $p < 0.0001$). There was no significant difference in growth rates between monoculture and co-culture evolved populations at their evolved temperatures (37°C - φ14-1: $t(39) = -0.87$, $p = 0.99$; φLUZ19: $t(39) = 0.38$, $p = 1.0$; 42°C - φ14-1: $t(39) = -1.1$, $p = 0.98$; φLUZ19: $t(39) = -0.19$, $p = 1.0$). Surprisingly, phages evolved at 37°C in co-culture showed significantly higher fitness at 42°C than those evolved in monoculture (φ14-1: $t(39) = -9.19$, $p < 0.0001$; φLUZ19: $t(39) = -6.04$, $p < 0.0001$).

3.4.3 Temperature and competition select for mutations in tail proteins and replication machinery

To further understand the genomic causes of adaptation to temperature and competition, we conducted phage population sequencing and determined the identity and frequency of genetic variants (Figure 3). Putative adaptive variants were defined as those with a frequency > 20% and which occurred in genes which acquired mutations in at least two biological replicates across all treatments (Table S2 for summary, Appendix for all mutations).

As φLUZ19 growth is restricted by slow host attachment rates (see Chapter 2), we hypothesised that φLUZ19 mutations would occur in tail proteins responsible for attachment. The most prominent genetic changes in the φLUZ19 evolved populations were a series of high frequency SNPs in two genes encoding a tail protein and tail fiber protein. While the tail

protein mutations were only found in monoculture populations, tail fiber protein mutations were found across all temperature and phage combination treatments suggesting that these reflect adaptation to the host rather than to inter-specific competition or thermal stress. φLUZ19 42°C evolved populations also all contained insertions in an intergenic region between two hypothetical proteins, suggesting that altered regulation of gene expression may also contribute to thermal adaptation in φLUZ19. Other mutations were exclusively found in 37°C evolved populations and included putative bacterial immune system-associated nucleotidyltransferase (64), RNA polymerase, and DNA polymerase mutations. These mutations may contribute to φLUZ19 low temperature adaptation by increasing phage replication within cells.

We also sequenced the φ14-1 evolved populations to confirm that the changes to thermal phenotypes reflect evolutionary rescue rather than a plastic response. φ14-1 rescue at 42°C was linked to a series of high frequency SNPs in a gene encoding the phage tail sheath, a phage component involved in DNA transfer into bacterial cells (65). We also observed parallel deletions and SNPs in the 42°C monoculture and 37°C co-culture populations in a putative DNA ligase (BlastP: 97.47% identity, 95% sequence overlap with Pseudomonas phage PhL_UNISO_PA-DSM_ph0031 DNA ligase protein), a protein that is essential for phage DNA replication and fitness (66,67). These results imply that competition and high temperature co-select for altered DNA replication in φ14-1.

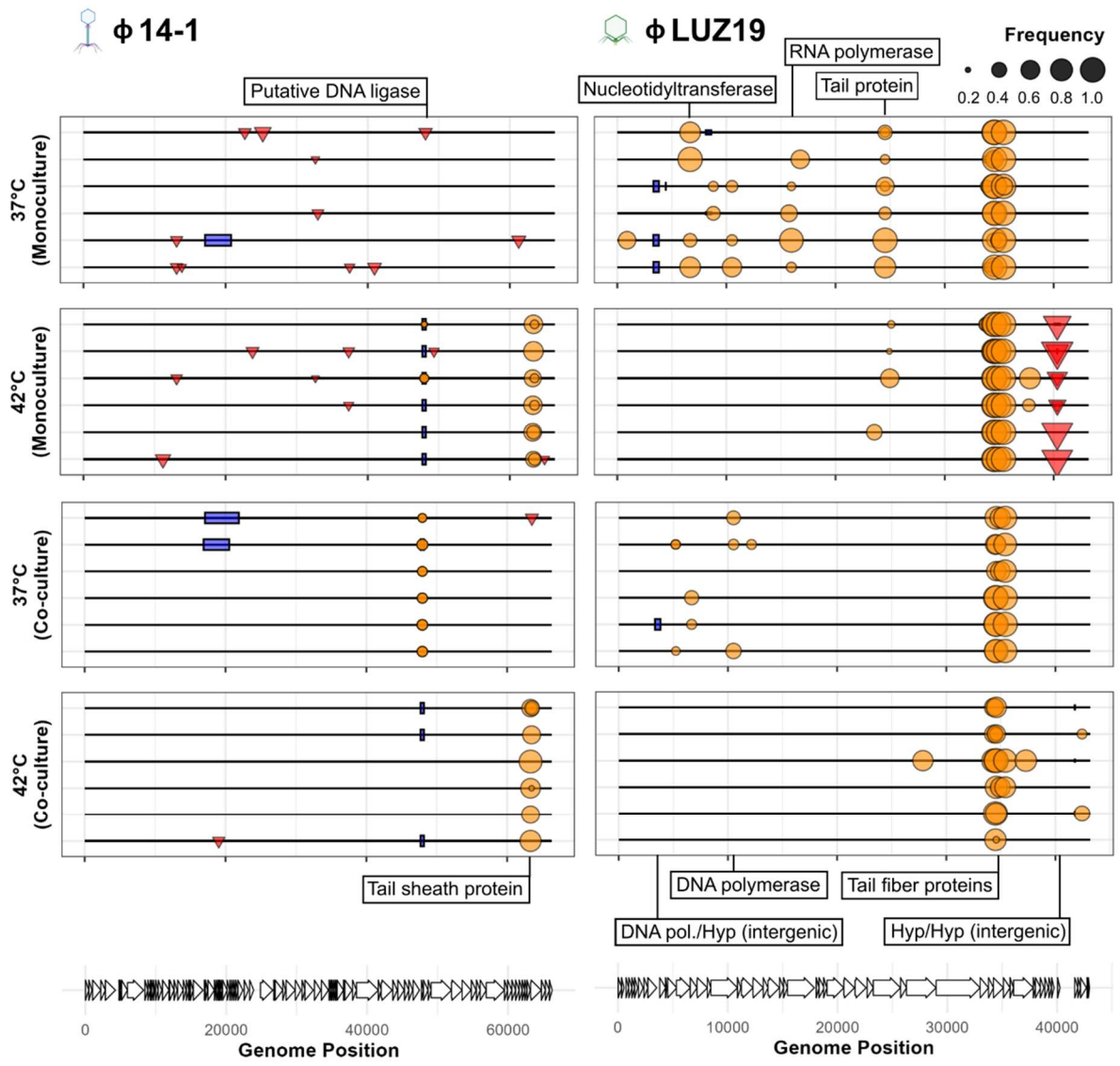

Figure 3. Competition and temperature select for mutations in tail proteins and replication machinery. Mutation plots show genetic variants associated with thermal adaptation and competition in phage populations. Lines represent individual biological replicates. Symbols within plots show variants across the phage genome at >20% prevalence and which were not observed in the ancestral population. Symbols reflect mutation type where circle = SNP, box = deletion, inverted triangle = insertion. Length of deletion bars represent the size of deletion except for the φ14-1 deletion at ~48kb which is a 1bp deletion but given a fixed size for visibility. Labels show annotations for genes which contain mutations in at least three replicate populations in the same evolution treatment, reflecting parallel evolution. All

putative adaptive variants are presented in **Table S2**. Putative DNA ligase in φ14-1 was originally annotated a hypothetical protein but has high homology to Pseudomonas phage PhL_UNISO_PA-DSM_ph0031 DNA ligase protein.

3.4.4 Thermal stress and competition shape phage molecular evolution

Phage populations evolved at high temperatures differed from control populations both in terms of thermal phenotypes and the mutations they acquired. We hypothesised that 37°C and 42°C evolved populations would also diverge at the whole-genome level due to differing evolutionary trajectories. PCoA analysis based on phage Euclidean genetic distances showed that both φ14-1 and φLUZ19 had significant genetic divergence between 37°C and 42°C evolved populations (φ14-1: ANOSIM: $R = 1.0$, $p < 0.01$; φLUZ19: ANOSIM: $R = 0.91$, $p < 0.01$) (Figure 4A). We then hypothesised that evolution rates would be highest in the populations that experienced the greatest change in growth rates. φ14-1 had significantly higher evolution rates at 42°C than at 37°C ($F_{1,10} = 30.3$, $p < 0.001$) (Figure 4B). No significant difference in evolution rates was observed between temperatures for φLUZ19 populations ($F_{1,10} = 1.2$, $p < 0.30$).

As phages showed both phenotypic and genomic divergence based on thermal regime, we hypothesised that genetically similar phage populations may have similar thermal fitness. We assessed the relationship between thermal fitness and genomic change by measuring congruence between neighbour-joining trees constructed based on Euclidean phenotypic and genetic distances (Figure 4C). Highly significant congruence was observed for both phages based on growth rates at 42°C (φ14-1: $M^2_{xy} = 5.8$, $p < 0.01$; φLUZ19: $M^2_{xy} = 15.9$, $p < 0.001$). For 37°C growth, significant congruence was observed for φLUZ19 ($M^2_{xy} = 20.4$, $p < 0.05$) but not for φ14-1 ($M^2_{xy} = 8.1$, $p = 0.18$).

Given the evolutionary constraint of competition, we also hypothesised that co-culture evolved populations would diverge from monoculture evolved populations and have slower evolution

rates. Significant genomic divergence was observed between monoculture and co-culture populations for φ14-1 at 37°C and for φLUZ19 at 42°C (φ14-1: ANOSIM: R = 0.18, p < 0.005; φLUZ19: ANOSIM: R = 0.81, p < 0.005). Divergence was not significant for φ14-1 at 42°C or for φLUZ19 at 37°C (φ14-1: ANOSIM: R = 0.27, p = 0.057; φLUZ19: ANOSIM: R = 0.15, p = 0.07) (Figure S6). φ14-1 populations had similar evolution rates in monoculture and co-culture (37°C: t(20) = -0.972, p = 0.77; 42°C: t(20) = 1.77, p = 0.31). However, φLUZ19 evolved populations had significantly slower evolution rates in co-culture compared to monoculture at both 37°C and 42°C (37°C: t(20) = 3.1, p < 0.05; 42°C: t(20) = 5.3, p < 0.001) (Figure 4D).

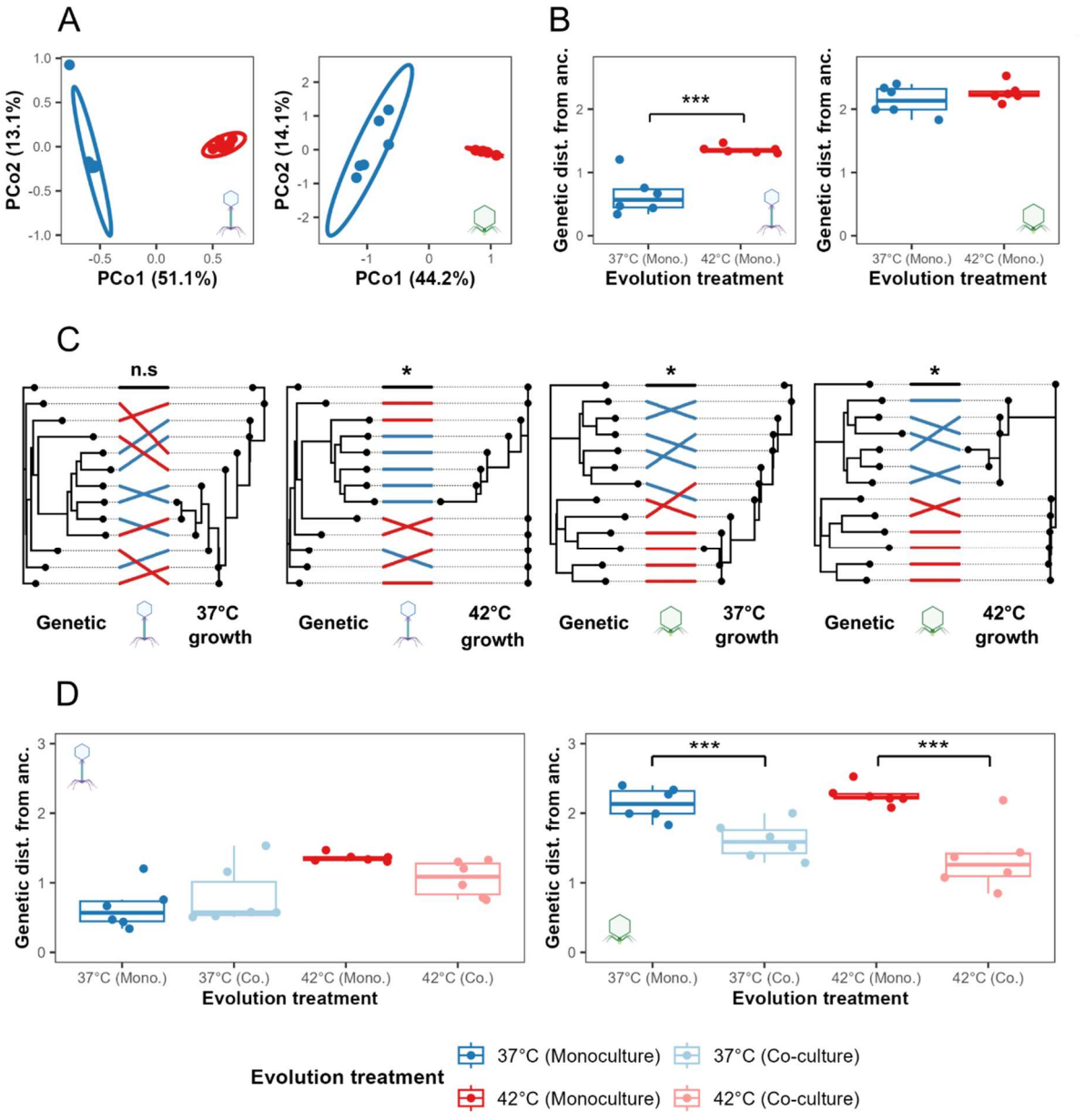

Figure 4. Thermal stress accelerates and competition constrains phage molecular evolution. A) Genomic divergence between evolved monoculture phage populations. PCoA plots show Euclidean genetic distance clustering between 37°C and 42°C evolved phage populations based on mutation position and frequency. **B)** Evolution rates of evolved monoculture phage populations based on the Euclidean genetic distance from ancestor. *** = $p < 0.001$. No asterisk reflects non-significance. **C)** Congruence analysis of neighbour-joining trees constructed based on Euclidean genetic distances (left-hand plots, labelled "Genetic") and Euclidean distances based on phage growth rates at 37°C and 42°C (right-hand plots, labelled "37°C growth" and "42°C growth", respectively). Congruence is shown by the alignment of tips corresponding to individual replicate populations between trees. High congruence is shown by few cross-overs. 37°C monoculture population connections are shown in deep blue, 42°C monoculture populations in deep red, and the ancestral phage in black. Trees are rooted using the ancestral phage. **D)** Evolution rates of evolved monoculture phage populations compared to evolved co-culture populations. Evolution rates are determined based on Euclidean genetic distance from ancestor. *** = $p < 0.001$. No asterisk reflects non-significance.

3.5 Discussion

Environmental stress reduces biodiversity by restricting the growth of sensitive community members and destabilising competitive hierarchies (28). We show that the φ14-1 phage can avoid heat-driven extinction through evolutionary rescue, even in the presence of a thermally tolerant φLUZ19 phage competitor. We further found that competition at permissive temperatures, where both phages grow efficiently, can drive the evolution of elevated φ14-1 thermal tolerance. These findings support previous studies by demonstrating that phages are highly evolvable in response to environmental stress (16,68,69). The results nevertheless contradict findings that competitive interactions constrain environmental adaptation by reducing growth rates and mutational supply (5,27). One potential explanation is that, while

strong competition may constrain evolution, weak or moderate competition may have increased the strength of selection for φ14-1 thermal adaptation (4,28,70). Alternatively, adaptation may have been driven through co-selection by competition and temperature for the same traits. We identified mutations in the same genes in φ14-1 populations evolving under both high temperature selection and at permissive temperatures in the presence of competition. The evolution of stress tolerance in free-living organisms has historically been associated with trade-offs in competitive fitness (71–73). Increased selection or mutualistic pleiotropy could mean that competition in parasite systems leads to trade-ups rather than trade-offs with adaptation to environmental stress.

Evolutionary rescue has largely been thought to maintain biodiversity by preventing taxa from becoming extinct (8). Within communities, however, we found that evolutionary rescue can cause one species to become a superior competitor, thereby promoting the competitive exclusion of others. Evolutionary rescue may thus be insufficient to prevent, and may even facilitate, biodiversity loss under environmental stress. Evolutionary rescue can come at an ecological cost where increased environmental tolerance leads a trade-off with growth rates (74,75). However, ecological de-stabilisation can occur via trade-ups if growth rates increase in the recently adapted population (12,13). Competitive shifts may essentially depend on how rescue affects species absolute fitness. We showed that while the rescued phage at 42°C gained a competitive advantage over its sympatric competitor, rescued phage competitiveness did not escalate across evolutionary time and was not elevated against the ancestral competitor. These findings could be explained by the competitor experiencing a decrease in relative fitness following 42°C adaptation (74,75). Competitive dominance may alternatively be specific to co-evolving competitors. By reducing competitor population densities, evolutionary rescue had the additional impact of constraining competitor evolution rates and restricting the acquisition of putative adaptive mutations. Rescue may therefore cause community instability by both depressing competitor population densities and limiting community adaptability in response to future environmental stress (5).

Despite being suppressed by the newly dominant φ14-1, φLUZ19 competitor phage populations ultimately stabilised at reduced densities. Modern co-existence theory states that co-existence can occur through stabilising mechanisms such as niche differences or through competitors having similar relative fitness (19). Phage co-existence has previously been attributed to variation in host cell susceptibility to infection (20). In our system, φ14-1 and φLUZ19 use different bacterial surface receptors to infect cells (33,76). We propose that heterogeneity in the expression of phage receptors in the bacterial population (77) may have created a niche that enabled φLUZ19 persistence, but which was inaccessible to the rescued φ14-1 population. Alternatively, phage fitness differences may have been resolved through φLUZ19 co-evolution. For example, φLUZ19 acquired tail fiber and tail protein mutations which likely contribute to host attachment rates and within-host competitiveness (78). While the exact cause of co-existence remains unclear, the results highlight that stabilising mechanisms could buffer against total competitive exclusions that arise through evolutionary rescue.

Global biodiversity is decreasing due to environmental stress caused by land use change, pollution, and climate change (15,79,80). This study highlights a process by which evolutionary rescue, a force typically associated with preserving biodiversity, can make the community less resilient over ecological and evolutionary time. That parasites, and specifically viruses, can undergo evolutionary rescue has implications for our understanding of how parasites might evolve in the context of novel and hostile environments, such as following spillover events (81) or in hosts treated for infection (82). A loss of parasite diversity could increase the survival rates of some host species (83); there could be a reduced burden of infection, fewer co-infections, and weaker selection favouring virulence due to less inter-specific competition (84). Given parasites are beneficial for keeping pest or pathogenic hosts (as in this study) at bay (82,85), lower diversity would have negative consequences for animal, plant, and ecosystem health. Ultimately, consideration of the eco-evolutionary dynamics will help us better understand how communities will respond to increasingly frequent environmental stressors in a changing world.

3.6 References

1. Thomas CD, Cameron A, Green RE, Bakkenes M, Beaumont LJ, Collingham YC, et al. Extinction risk from climate change. Nature. 2004 Jan;427(6970):145–8.

2. Bellard C, Bertelsmeier C, Leadley P, Thuiller W, Courchamp F. Impacts of climate change on the future of biodiversity. Ecology Letters. 2012;15(4):365–77.

3. Donhauser J, Niklaus PA, Rousk J, Larose C, Frey B. Temperatures beyond the community optimum promote the dominance of heat-adapted, fast growing and stress resistant bacteria in alpine soils. Soil Biology and Biochemistry. 2020 Sep 1;148:107873.

4. Westley J, García FC, Warfield R, Yvon-Durocher G. The community background alters the evolution of thermal performance. Evolution Letters. 2024 Mar 16;qrae007.

5. de Mazancourt C, Johnson E, Barraclough TG. Biodiversity inhibits species' evolutionary responses to changing environments. Ecol Lett. 2008 Apr;11(4):380–8.

6. Smith KG, Almeida RJ. When are extinctions simply bad luck? Rarefaction as a framework for disentangling selective and stochastic extinctions. Journal of Applied Ecology. 2020;57(1):101–10.

7. Dakos V, Matthews B, Hendry AP, Levine J, Loeuille N, Norberg J, et al. Ecosystem tipping points in an evolving world. Nat Ecol Evol. 2019 Mar;3(3):355–62.

8. Carlson SM, Cunningham CJ, Westley PAH. Evolutionary rescue in a changing world. Trends in Ecology & Evolution. 2014 Sep 1;29(9):521–30.

9. Low-Décarie E, Kolber M, Homme P, Lofano A, Dumbrell A, Gonzalez A, et al. Community rescue in experimental metacommunities. Proceedings of the National Academy of Sciences. 2015 Nov 17;112(46):14307–12.

10. Fugère V, Hébert MP, da Costa NB, Xu CCY, Barrett RDH, Beisner BE, et al. Community rescue in experimental phytoplankton communities facing severe herbicide pollution. Nat Ecol Evol. 2020 Apr;4(4):578–88.

11. O'Connor LMJ, Fugère V, Gonzalez A. Evolutionary Rescue Is Mediated by the History of Selection and Dispersal in Diversifying Metacommunities. Front Ecol Evol. 2020 Dec 9;8.

12. Yacine Y, Allhoff KT, Weinbach A, Loeuille N. Collapse and rescue of evolutionary food webs under global warming. Journal of Animal Ecology. 2021;90(3):710–22.

13. Rodríguez-Verdugo A, Ackermann M. Rapid evolution destabilizes species interactions in a fluctuating environment. The ISME Journal. 2021 Feb 1;15(2):450–60.

14. Åkesson A, Curtsdotter A, Eklöf A, Ebenman B, Norberg J, Barabás G. The importance of species interactions in eco-evolutionary community dynamics under climate change. Nat Commun. 2021 Aug 6;12(1):4759.

15. Carlson CJ, Burgio KR, Dougherty ER, Phillips AJ, Bueno VM, Clements CF, et al. Parasite biodiversity faces extinction and redistribution in a changing climate. Science Advances. 2017 Sep 6;3(9):e1602422.

16. Knies JL, Izem R, Supler KL, Kingsolver JG, Burch CL. The Genetic Basis of Thermal Reaction Norm Evolution in Lab and Natural Phage Populations. PLOS Biology. 2006 Jun 6;4(7):e201.

17. Eggert H, Diddens-de Buhr MF, Kurtz J. A temperature shock can lead to trans-generational immune priming in the Red Flour Beetle, Tribolium castaneum. Ecol Evol. 2015 Mar;5(6):1318–26.

18. Hochberg ME, Holt RD. The Coexistence of Competing Parasites. I. The Role of Cross-Species Infection. The American Naturalist. 1990 Oct;136(4):517–41.

19. Chesson P. Mechanisms of Maintenance of Species Diversity. Annual Review of Ecology, Evolution, and Systematics. 2000 Nov 1;31(Volume 31, 2000):343–66.

20. Pyenson NC, Leeks A, Nweke O, Goldford JE, Schluter J, Turner PE, et al. Diverse phage communities are maintained stably on a clonal bacterial host. Science. 2024 Dec 13;386(6727):1294–300.

21. Poulin R, Salloum PM, Bennett J. Evolution of parasites in the Anthropocene: new pressures, new adaptive directions. Biological Reviews. 2024;99(6):2234–52.

22. Viney ME, Graham AL. Patterns and processes in parasite co-infection. Adv Parasitol. 2013;82:321–69.

23. Vezzulli L, Colwell RR, Pruzzo C. Ocean warming and spread of pathogenic vibrios in the aquatic environment. Microb Ecol. 2013 May;65(4):817–25.

24. Hernandez AD, Poole A, Cattadori IM. Climate changes influence free-living stages of soil-transmitted parasites of European rabbits. Glob Chang Biol. 2013 Apr;19(4):1028–42.

25. Molnár PK, Kutz SJ, Hoar BM, Dobson AP. Metabolic approaches to understanding climate change impacts on seasonal host-macroparasite dynamics. Ecol Lett. 2013 Jan;16(1):9–21.

26. Aleuy OA, Kutz S. Adaptations, life-history traits and ecological mechanisms of parasites to survive extremes and environmental unpredictability in the face of climate change. International Journal for Parasitology: Parasites and Wildlife. 2020 Aug 1;12:308–17.

27. Hall JPJ, Harrison E, Brockhurst MA. Competitive species interactions constrain abiotic adaptation in a bacterial soil community. Evol Lett. 2018 Sep 25;2(6):580–9.

28. Osmond MM, de Mazancourt C. How competition affects evolutionary rescue. Philos Trans R Soc Lond B Biol Sci. 2013 Jan 19;368(1610):20120085.

29. Kashiwagi A, Kadoya T, Kumasaka N, Kumagai T, Tsushima FS, Yomo T. Influence of adaptive mutations, from thermal adaptation experiments, on the infection cycle of RNA bacteriophage Qβ. Arch Virol. 2018 Oct 1;163(10):2655–62.

30. Knies JL, Kingsolver JG, Burch CL. Hotter is better and broader: thermal sensitivity of fitness in a population of bacteriophages. Am Nat. 2009 Apr;173(4):419–30.

31. van Eldijk TJB, Bisschop K, Etienne RS. Uniting Community Ecology and Evolutionary Rescue Theory: Community-Wide Rescue Leads to a Rapid Loss of Rare Species. Front Ecol Evol. 2020 Oct 29;8.

32. Tabare E, Glonti T, Cochez C, Ngassam C, Pirnay JP, Amighi K, et al. A Design of Experiment Approach to Optimize Spray-Dried Powders Containing Pseudomonas aeruginosaPodoviridae and Myoviridae Bacteriophages. Viruses. 2021 Oct;13(10):1926.

33. Chibeu A, Ceyssens PJ, Hertveldt K, Volckaert G, Cornelis P, Matthijs S, et al. The adsorption of Pseudomonas aeruginosa bacteriophage phiKMV is dependent on expression regulation of type IV pili genes. FEMS Microbiol Lett. 2009 Jun;296(2):210–8.

34. Lavigne R, Lecoutere E, Wagemans J, Cenens W, Aertsen A, Schoofs L, et al. A multifaceted study of Pseudomonas aeruginosa shutdown by virulent podovirus LUZ19. mBio. 2013 Mar 19;4(2):e00061-00013.

35. Ceyssens PJ, Miroshnikov K, Mattheus W, Krylov V, Robben J, Noben JP, et al. Comparative analysis of the widespread and conserved PB1-like viruses infecting Pseudomonas aeruginosa. Environmental Microbiology. 2009;11(11):2874–83.

36. Betts A, Gifford DR, MacLean RC, King KC. Parasite diversity drives rapid host dynamics and evolution of resistance in a bacteria-phage system. Evolution. 2016;70(5):969–78.

37. Betts A, Vasse M, Kaltz O, Hochberg ME. Back to the future: evolving bacteriophages to increase their effectiveness against the pathogen Pseudomonas aeruginosa PAO1. Evolutionary Applications. 2013;6(7):1054–63.

38. Betts A, Kaltz O, Hochberg ME. Contrasted coevolutionary dynamics between a bacterial pathogen and its bacteriophages. Proceedings of the National Academy of Sciences. 2014 Jul 29;111(30):11109–14.

39. Betts A, Gray C, Zelek M, MacLean RC, King KC. High parasite diversity accelerates host adaptation and diversification. Science. 2018 May 25;360(6391):907–11.

40. Kropinski AM, Mazzocco A, Waddell TE, Lingohr E, Johnson RP. Enumeration of Bacteriophages by Double Agar Overlay Plaque Assay. In: Clokie MRJ, Kropinski AM, editors. Bacteriophages: Methods and Protocols, Volume 1: Isolation, Characterization, and Interactions. Totowa, NJ: Humana Press; 2009. p. 69–76.

41. Wang J, Wang X, Yang K, Lu C, Fields B, Xu Y, et al. Phage selection drives resistance-virulence trade-offs in Ralstonia solanacearum plant-pathogenic bacterium irrespective of the growth temperature. Evol Lett. 2024 Apr;8(2):253–66.

42. Zhang M, Qian J, Xu X, Ahmed T, Yang Y, Yan C, et al. Resistance of Xanthomonas oryzae pv. oryzae to Lytic Phage X2 by Spontaneous Mutation of Lipopolysaccharide Synthesis-Related Glycosyltransferase. Viruses. 2022 May 18;14(5):1088.

43. Lenski RE, Rose MR, Simpson SC, Tadler SC. Long-Term Experimental Evolution in Escherichia coli. I. Adaptation and Divergence During 2,000 Generations. The American Naturalist. 1991;138(6):1315–41.

44. Langmead B, Salzberg SL. Fast gapped-read alignment with Bowtie 2. Nat Methods. 2012 Apr;9(4):357–9.

45. Li H, Handsaker B, Wysoker A, Fennell T, Ruan J, Homer N, et al. The Sequence Alignment/Map format and SAMtools. Bioinformatics. 2009 Aug 15;25(16):2078–9.

46. Seemann T. Prokka: rapid prokaryotic genome annotation. Bioinformatics. 2014 Jul 15;30(14):2068–9.

47. Deatherage DE, Barrick JE. Identification of mutations in laboratory evolved microbes from next-generation sequencing data using breseq. Methods Mol Biol. 2014;1151:165–88.

48. Wick RR, Howden BP, Stinear TP. Autocycler: long-read consensus assembly for bacterial genomes. bioRxiv; 2025. p. 2025.05.12.653612. Available from: https://www.biorxiv.org/content/10.1101/2025.05.12.653612v1

49. Koren S, Walenz BP, Berlin K, Miller JR, Bergman NH, Phillippy AM. Canu: scalable and accurate long-read assembly via adaptive k-mer weighting and repeat separation. Genome Res. 2017 May;27(5):722–36.

50. Li H. Minimap and miniasm: fast mapping and de novo assembly for noisy long sequences. Bioinformatics. 2016 Jul 15;32(14):2103–10.

51. Bouras G, Sheppard AE, Mallawaarachchi V, Vreugde S. Plassembler: an automated bacterial plasmid assembly tool. Bioinformatics. 2023 Jul 1;39(7):btad409.

52. Vaser R, Šikić M. Time- and memory-efficient genome assembly with Raven. Nat Comput Sci. 2021 May;1(5):332–6.

53. Chen S, Zhou Y, Chen Y, Gu J. fastp: an ultra-fast all-in-one FASTQ preprocessor. Bioinformatics. 2018 Sep 1;34(17):i884–90.

54. Li H, Durbin R. Fast and accurate short read alignment with Burrows–Wheeler transform. Bioinformatics. 2009 Jul 15;25(14):1754–60.

55. Wick RR, Holt KE. Polypolish: Short-read polishing of long-read bacterial genome assemblies. PLOS Computational Biology. 2022 Jan 24;18(1):e1009802.

56. Bouras G, Grigson SR, Papudeshi B, Mallawaarachchi V, Roach MJ. Dnaapler: A tool to reorient circular microbial genomes. Journal of Open Source Software. 2024 Jan 11;9(93):5968.

57. Li H. Minimap2: pairwise alignment for nucleotide sequences. Bioinformatics. 2018 Sep 15;34(18):3094–100.

58. RStudio Team. RStudio: Integrated Development for R. [Internet]. RStudio, PBC, Boston, M; 2020. Available from: http://www.rstudio.com/

59. R Core Team. R: A language and environment for statistical computing. [Internet]. Foundation for Statistical Computing, Vienna, Austria.; 2021. Available from: https://www.R-project.org/

60. Wickham H, Averick M, Bryan J, Chang W, McGowan LD, François R, et al. Welcome to the Tidyverse. Journal of Open Source Software. 2019 Nov 21;4(43):1686.

61. Bates D, Mächler M, Bolker B, Walker S. Fitting Linear Mixed-Effects Models Using lme4. Journal of Statistical Software. 2015 Oct 7;67:1–48.

62. Paradis E, Claude J, Strimmer K. APE: Analyses of Phylogenetics and Evolution in R language. Bioinformatics. 2004 Jan 22;20(2):289–90.

63. Hutchinson MC, Cagua EF, Balbuena JA, Stouffer DB, Poisot T. paco: implementing Procrustean Approach to Cophylogeny in R. Methods in Ecology and Evolution. 2017;8(8):932–40.

64. Ho P, Chen Y, Biswas S, Canfield E, Abdolvahabi A, Feldman DE. Bacteriophage antidefense genes that neutralize TIR and STING immune responses. Cell Reports. 2023 Apr 25;42(4):112305.

65. Aksyuk AA, Leiman PG, Kurochkina LP, Shneider MM, Kostyuchenko VA, Mesyanzhinov VV, et al. The tail sheath structure of bacteriophage T4: a molecular machine for infecting bacteria. EMBO J. 2009 Apr 8;28(7):821–9.

66. Harcombe WR, Springman R, Bull JJ. Compensatory evolution for a gene deletion is not limited to its immediate functional network. BMC Evol Biol. 2009 Dec;9(1):1–11.

67. Rokyta D, Badgett MR, Molineux IJ, Bull JJ. Experimental Genomic Evolution: Extensive Compensation for Loss of DNA Ligase Activity in a Virus. Mol Biol Evol. 2002 Mar 1;19(3):230–8.

68. Holder KK, Bull JJ. Profiles of adaptation in two similar viruses. Genetics. 2001 Dec;159(4):1393–404.

69. Bull JJ, Badgett MR, Wichman HA. Big-Benefit Mutations in a Bacteriophage Inhibited with Heat. Molecular Biology and Evolution. 2000 Jun 1;17(6):942–50.

70. Tseng M, O'Connor MI. Predators modify the evolutionary response of prey to temperature change. Biol Lett. 2015 Dec;11(12):20150798.

71. Phan K, Ferenci T. A design-constraint trade-off underpins the diversity in ecologically important traits in species Escherichia coli. The ISME Journal. 2013 Oct 1;7(10):2034–43.

72. Limberger R, Fussmann GF. Adaptation and competition in deteriorating environments. Proceedings of the Royal Society B: Biological Sciences. 2021 Mar 10;288(1946):20202967.

73. Bristiel P, Gillespie L, Østrem L, Balachowski J, Violle C, Volaire F. Experimental evaluation of the robustness of the growth–stress tolerance trade-off within the perennial grass Dactylis glomerata. Functional Ecology. 2018;32(8):1944–58.

74. Zhou DH, Zhang QG. Loss and recovery of ecological diversity associated with evolutionary rescue in abruptly and gradually deteriorating environments. Evol. 2024 Apr 1;78(4):768–77.

75. Vogwill T, MacLean RC. The genetic basis of the fitness costs of antimicrobial resistance: a meta-analysis approach. Evol Appl. 2015 Mar;8(3):284–95.

76. Garbe J, Wesche A, Bunk B, Kazmierczak M, Selezska K, Rohde C, et al. Characterization of JG024, a pseudomonas aeruginosa PB1-like broad host range phage under simulated infection conditions. BMC Microbiology. 2010 Nov 26;10(1):301.

77. Fuente CADL, Lahoud N, Meyer JR. Cryptic host phenotypic heterogeneity drives diversification of bacteriophage λ. bioRxiv; 2024. p. 2024.08.05.606710. Available from: https://www.biorxiv.org/content/10.1101/2024.08.05.606710v1

78. Burmeister AR, Tzintzun-Tapia E, Roush C, Mangal I, Barahman R, Bjornson RD, et al. Experimental Evolution of the TolC-Receptor Phage U136B Functionally Identifies a Tail Fiber Protein Involved in Adsorption through Strong Parallel Adaptation. Appl Environ Microbiol. 89(6):e00079-23.

79. Jaureguiberry P, Titeux N, Wiemers M, Bowler DE, Coscieme L, Golden AS, et al. The direct drivers of recent global anthropogenic biodiversity loss. Science Advances. 2022 Nov 9;8(45):eabm9982.

80. Wood CL, Welicky RL, Preisser WC, Leslie KL, Mastick N, Greene C, et al. A reconstruction of parasite burden reveals one century of climate-associated parasite decline. Proceedings of the National Academy of Sciences. 2023 Jan 17;120(3):e2211903120.

81. Ellwanger JH, Chies JAB. Zoonotic spillover: Understanding basic aspects for better prevention. Genet Mol Biol. 44(1 Suppl 1):e20200355.

82. Strathdee SA, Hatfull GF, Mutalik VK, Schooley RT. Phage therapy: From biological mechanisms to future directions. Cell. 2023 Jan 5;186(1):17–31.

83. Susi H, Barrès B, Vale PF, Laine AL. Co-infection alters population dynamics of infectious disease. Nat Commun. 2015 Jan 8;6(1):5975.

84. de Roode JC, Pansini R, Cheesman SJ, Helinski MEH, Huijben S, Wargo AR, et al. Virulence and competitive ability in genetically diverse malaria infections. Proceedings of the National Academy of Sciences. 2005 May 24;102(21):7624–8.

85. Bale JS, van Lenteren JC, Bigler F. Biological control and sustainable food production. Philos Trans R Soc Lond B Biol Sci. 2008 Feb 27;363(1492):761–76.

3.7 Supplementary figures

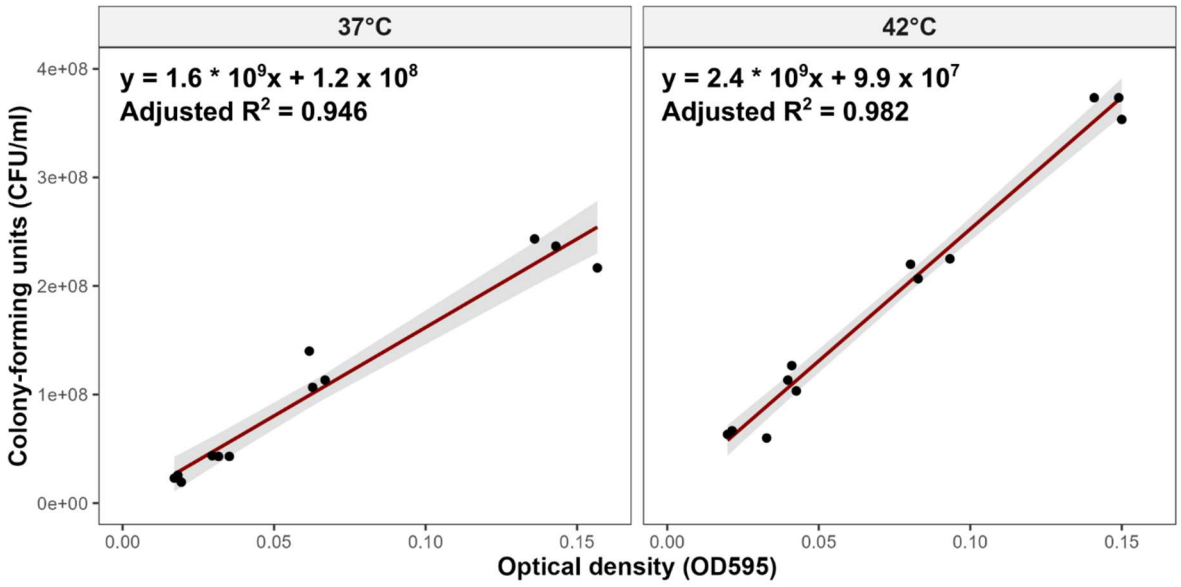

Figure S1. Optical density v colony-forming units standard curve. A regression of optical density and colony-forming units was used to determine the optical density of *P. aeruginosa* PAO1 overnights required to have ~10^8 CFU/ml.

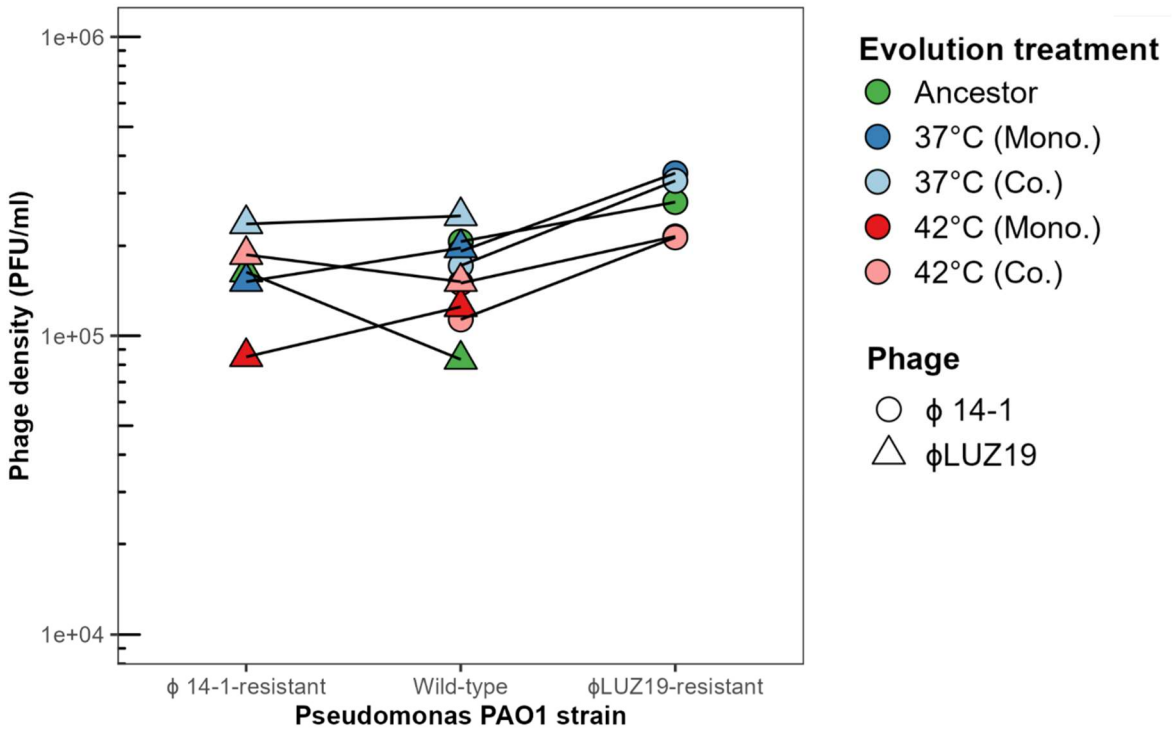

Figure S2. Efficiency of plaque formation is the same for evolved and ancestral phage populations. Plot shows the density of evolved and ancestral phage lysates as measured with plaque assays on the wild-type and resistant PAO1 strains. Lines between points show phage counts on the same stocks on separate hosts.

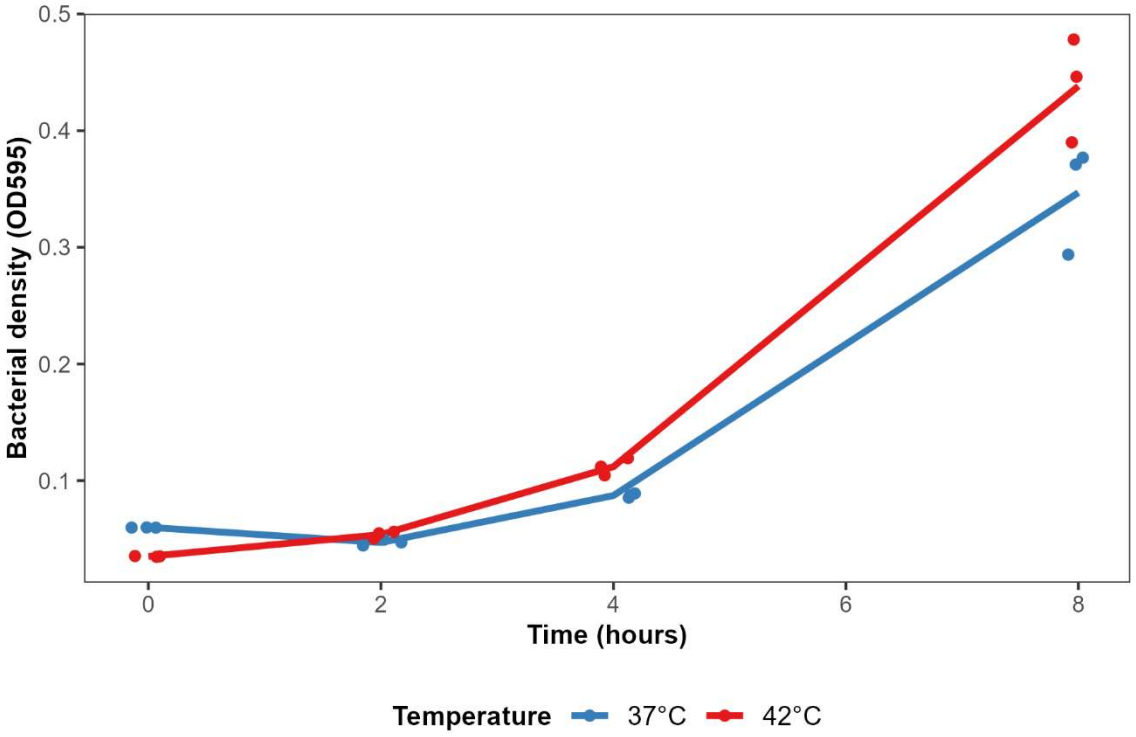

Figure S3. Bacterial growth in absence of phage is similar across temperature. Growth curves of no phage bacterial control. Dots reflect an average of three technical replicates. Bacterial growth was measured three separate times.

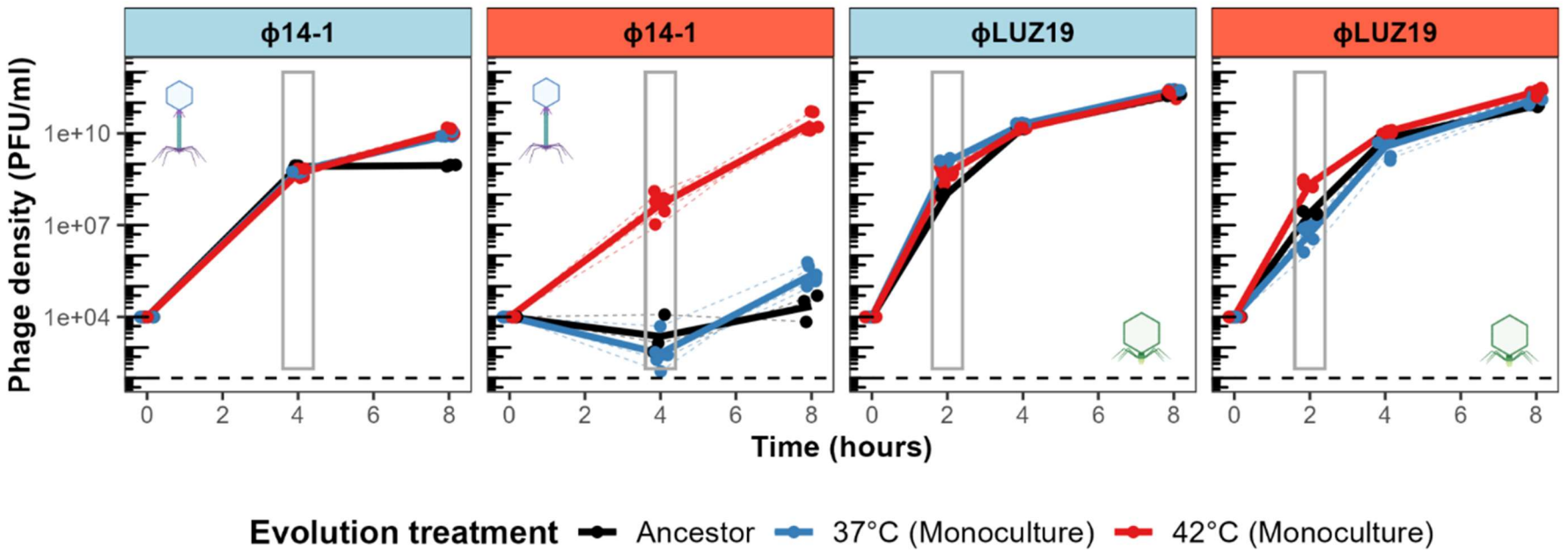

Figure S4. Evolved and ancestral phage growth curves at 37°C and 42°C. Grey box shows time points selected for fitness comparison. Black dashed line shows lower detection limit. Phage growth was assessed at 37°C (light blue strip) and 42°C (light red strip).

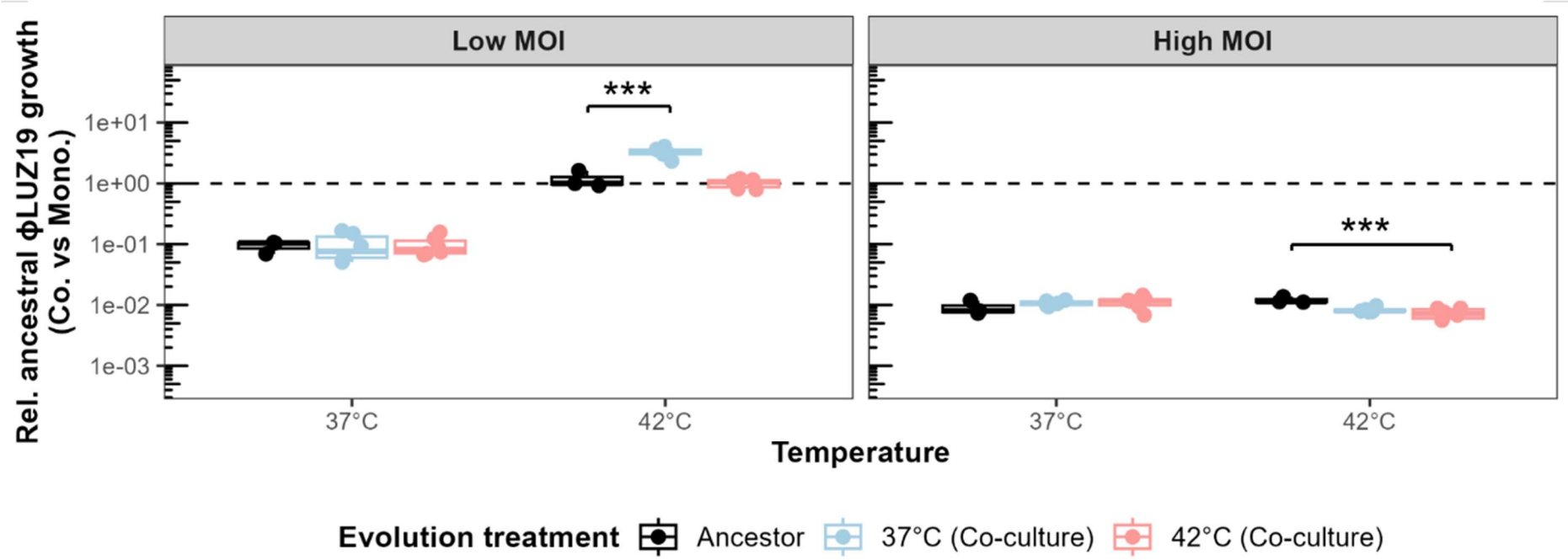

Figure S5. φ14-1 co-culture evolved populations have similar competitiveness to ancestor. Boxplots show the growth of ancestral φLUZ19 at 37°C and 42°C in co-culture with the ancestral and co-culture evolved φ14-1 populations relative to growth in monoculture. φ14-1 ancestral and evolved population competitiveness was determined at both low MOI (MOI = 0.0001) and high MOI (MOI = 5). Values below 1 (dashed black line) indicate φLUZ19 growth is inhibited by the presence of φ14-1 populations. Asterisks show significant differences in growth restriction between φ14-1 evolution treatments. ** = $p < 0.01$.

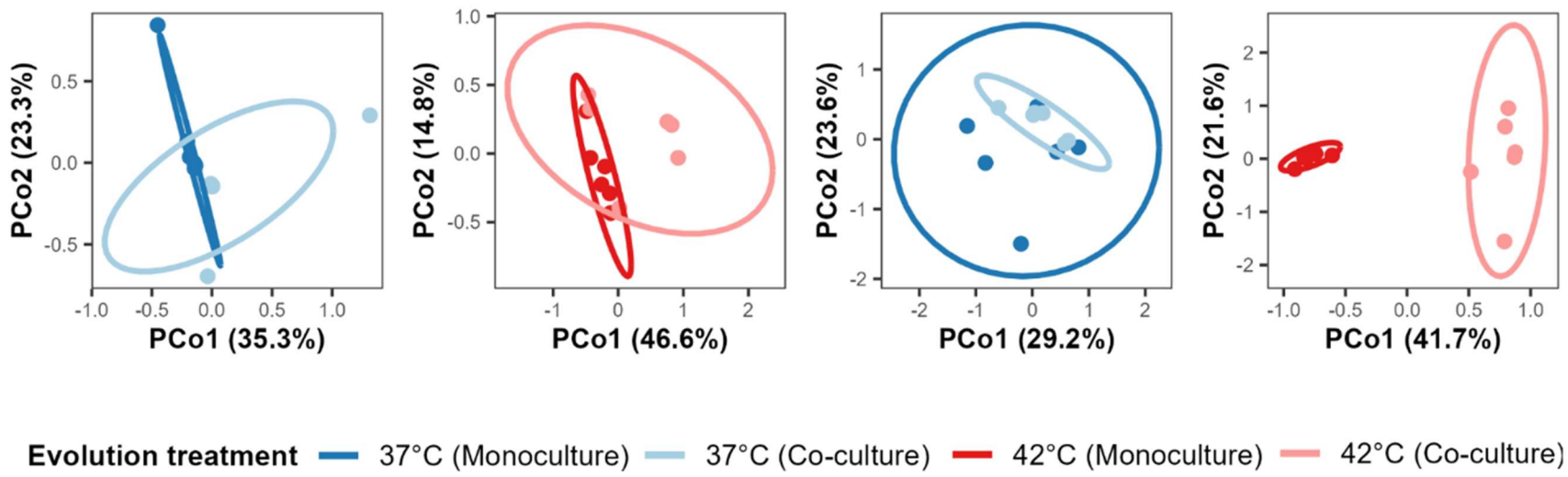

Figure S6. Phages show significant genetic divergence between monoculture and co-culture populations. PCoA plots show Euclidean genetic distance clustering between monoculture (37°C in deep blue, 42°C in deep red) and co-culture (37°C in light blue, 42°C in light red) evolved populations.

3.8 Supplementary tables

Table S1. Phage-resistant PAO1 mutant mutations compared to ancestral assembly

Strain	Mutation type	Position	Gene start	Gene stop	Strand	Gene annotation assembly	NCBI Blastp	Blast identity, query cover
φLUZ19-resistant	SNP	2991269	2991042	2992007	+	hypothetical protein	HEAT repeat domain-containing protein	99.69, 100
φLUZ19-resistant	SNP	3714180	3713964	3714440	+	hypothetical protein	MarR family transcriptional regulator	99.37, 100
φLUZ19-resistant	SNP	3714184	3713964	3714440	+	hypothetical protein	MarR family transcriptional regulator	99.37, 100
φLUZ19-resistant	SNP	4256540	4256531	4256740	-	Major cold shock protein CspA		
φLUZ19-resistant	SNP	4774319	4773168	4774382	-	hypothetical protein	type II secretion system protein GspL	99.5, 100
φLUZ19-resistant	SNP	4774320	4773168	4774382	-	hypothetical protein	type II secretion system protein GspL	99.5, 100
φLUZ19-resistant	SNP	4774321	4773168	4774382	-	hypothetical protein	type II secretion system protein GspL	99.5, 100
φLUZ19-resistant	SNP	4932144	4931195	4932412	-	Arginine biosynthesis bifunctional protein ArgJ		
φLUZ19-resistant	SNP	5186882	5185101	5191565	-	hypothetical protein	two-partner secretion system adhesin CdrA	100,100
φLUZ19-resistant	SNP	5186900	5185101	5191565	-	hypothetical protein	two-partner secretion system adhesin CdrA	100,100
φ14-1-resistant	SNP	2718271	2717669	2719432	+	Thiol:disulfide interchange protein DsbD		
φ14-1-resistant	SNP	2718278	2717669	2719432	+	Thiol:disulfide interchange protein DsbD		
φ14-1-resistant	SNP	2718286	2717669	2719432	+	Thiol:disulfide interchange protein DsbD		
φ14-1-resistant	SNP	2718287	2717669	2719432	+	Thiol:disulfide interchange protein DsbD		

φ14-1-resistant	SNP	2718293	2717669	2719432	+	Thiol:disulfide interchange protein DsbD		
φ14-1-resistant	SNP	2718305	2717669	2719432	+	Thiol:disulfide interchange protein DsbD		
φ14-1-resistant	SNP	2718314	2717669	2719432	+	Thiol:disulfide interchange protein DsbD		
φ14-1-resistant	SNP	2718326	2717669	2719432	+	Thiol:disulfide interchange protein DsbD		
φ14-1-resistant	SNP	2718327	2717669	2719432	+	Thiol:disulfide interchange protein DsbD		
φ14-1-resistant	SNP	2718335	2717669	2719432	+	Thiol:disulfide interchange protein DsbD		
φ14-1-resistant	SNP	2718337	2717669	2719432	+	Thiol:disulfide interchange protein DsbD		
φ14-1-resistant	SNP	2735670	2734627	2736324	+	hypothetical protein	two-partner secretion system transporter TpsB1	99.82, 100
φ14-1-resistant	SNP	2735735	2734627	2736324	+	hypothetical protein	two-partner secretion system transporter TpsB1	99.82, 100
φ14-1-resistant	SNP	2735772	2734627	2736324	+	hypothetical protein	two-partner secretion system transporter TpsB1	99.82, 100
φ14-1-resistant	SNP	2735828	2734627	2736324	+	hypothetical protein	two-partner secretion system transporter TpsB1	99.82, 100
φ14-1-resistant	SNP	2736490	2736437	2753320	+	hypothetical protein	two-partner secretion system transporter TpsB1	99.82, 100
φ14-1-resistant	SNP	2736614	2736437	2753320	+	hypothetical protein	two-partner secretion system transporter TpsB1	99.82, 100
φ14-1-resistant	SNP	2736684	2736437	2753320	+	hypothetical protein	two-partner secretion system transporter TpsB1	99.82, 100
φ14-1-resistant	SNP	2892580	2891980	2894529	-	Protein ClpV1		
φ14-1-resistant	SNP	4256540	4256531	4256740	-	Major cold shock protein CspA		

φ14-1-resistant	SNP	4774319	4773168	4774382	-	hypothetical protein	type II secretion system protein GspL	99.5, 100
φ14-1-resistant	SNP	4774320	4773168	4774382	-	hypothetical protein	type II secretion system protein GspL	99.5, 100
φ14-1-resistant	SNP	4774321	4773168	4774382	-	hypothetical protein	type II secretion system protein GspL	99.5, 100
φ14-1-resistant	SNP	5186882	5185101	5191565	-	hypothetical protein	two-partner secretion system adhesin CdrA	100,100
φ14-1-resistant	SNP	5186900	5185101	5191565	-	hypothetical protein	two-partner secretion system adhesin CdrA	100,100
φ14-1-resistant	SNP	5628878	5628334	5629290	-	hypothetical protein	glycosyltransferase	99.69, 100

Table S2. Putative adaptive phage mutations present at > 20% frequency in more than one replicate

Phage	Mutation type	Position	Mutation	Annotation	Gene	Gene description	37°C monoculture	37°C co-culture	42°C monoculture	42°C co-culture
Φ14-1	INS	13109	+ACCGACCATG	IGINKLAI_00020 → / → IGINKLAI_00021	intergenic (+79/-8)	hypothetical protein/hypothetical protein	2	0	1	0
Φ14-1	INS	32640	+AGGCCA	IGINKLAI_00052 →	coding (121/885 nt)	hypothetical protein	1	0	1	0
Φ14-1	INS	37330	+CCGATAGCGACC	IGINKLAI_00061 →	coding (493/1017 nt)	polynucleotide kinase/ phosphorylase	0	0	2	0
Φ14-1	DEL	47943	Δ1 bp	IGINKLAI_00071 →	coding (235/252 nt)	hypothetical protein (DNA ligase)	0	1	6	3
Φ14-1	SNP	47955	G→T	IGINKLAI_00071 →	E83* (GAA→TAA)‡	hypothetical protein (DNA ligase)	0	6	2	0
Φ14-1	SNP	47957	A→T	IGINKLAI_00071 →	E83D (GAA→GAT)‡	hypothetical protein (DNA ligase)	0	6	2	0
Φ14-1	SNP	47959	A→C	IGINKLAI_00071 →	*84S (TAA→TCA)	hypothetical protein (DNA ligase)	0	6	2	0
Φ14-1	SNP	63226	A→C	IGINKLAI_00089 →	F496V (TTC→GTC)	tail sheath	0	0	2	0
Φ14-1	SNP	63330	C→A	IGINKLAI_00089 →	C461F (TGC→TTC)	tail sheath	0	0	0	1
Φ14-1	SNP	63330	C→T	IGINKLAI_00089 →	C461Y (TGC→TAC)	tail sheath	0	0	4	4
Φ14-1	SNP	63478	T→C	IGINKLAI_00089 →	T412A (ACC→GCC)	tail sheath	0	0	4	3
ΦLUZ19	DEL	3563	Δ1 bp	gp12 → / → JPEJBOGK_00010	intergenic (+33/-237)	DNA polymerase/ hypothetical protein	2	1	0	0
ΦLUZ19	SNP	6673	T→G	gp16 →	L32W (TTG→TGG)	nucleotidyltransferase	4	2	0	0
ΦLUZ19	SNP	8801	T→G	gp19 →	S114R (AGT→AGG)	DNA polymerase	2	0	0	0
ΦLUZ19	SNP	10509	T→C	gp19 →	F684L (TTC→CTC)	DNA polymerase	3	3	0	0

ΦLUZ19	SNP	15953	A→C	gp26 →	D171A (GAT→GCT)	RNA polymerase	3	0	0	0
ΦLUZ19	SNP	24541	G→A	gp34 →	D429N (GAC→AAC)‡	tail protein	2	0	0	0
ΦLUZ19	SNP	24542	A→C	gp34 →	D429A (GAC→GCC)‡	tail protein	2	0	0	0
ΦLUZ19	SNP	24542	A→G	gp34 →	D429G (GAC→GGC)‡	tail protein	4	0	0	0
ΦLUZ19	SNP	33834	T→C	gp39 →	M28T (ATG→ACG)‡	tail fiber protein	2	0	1	0
ΦLUZ19	SNP	34332	A→G	gp40 →	T44A (ACC→GCC)	tail fiber protein	0	0	1	3
ΦLUZ19	SNP	34506	C→A	gp40 →	Q102K (CAG→AAG)‡	tail fiber protein	1	0	6	5
ΦLUZ19	SNP	34507	A→G	gp40 →	Q102R (CAG→CGG)‡	tail fiber protein	5	4	0	1
ΦLUZ19	SNP	34524	C→A	gp40 →	Q108K (CAA→AAA)	tail fiber protein	2	0	0	0
ΦLUZ19	SNP	34560	G→A	gp40 →	D120N (GAT→AAT)	tail fiber protein	0	0	0	2
ΦLUZ19	SNP	34561	A→G	gp40 →	D120G (GAT→GGT)	tail fiber protein	0	2	0	0
ΦLUZ19	SNP	34582	C→A	gp40 →	T127K (ACG→AAG)	tail fiber protein	6	6	6	5
ΦLUZ19	SNP	34951	A→C	gp40 →	Q250P (CAG→CCG)	tail fiber protein	0	0	0	1
ΦLUZ19	SNP	34951	A→G	gp40 →	Q250R (CAG→CGG)	tail fiber protein	1	2	0	0
ΦLUZ19	SNP	34954	T→C	gp40 →	V251A (GTC→GCC)	tail fiber protein	0	0	6	0
ΦLUZ19	SNP	35404	G→A	gp41 →	C98Y (TGT→TAT)	tail fiber protein	6	6	6	2
ΦLUZ19	INS	40324	+CTAGC	JPEJBOGK_00049 → / → JPEJBOGK_00050	intergenic (-55/-1288)	hypothetical protein/hypothetical protein	0	0	3	0

ΦLUZ19	INS	40327	+GCCTT	JPEJBOGK_00049 → / → JPEJBOGK_00050	intergenic (-58/-1285)	hypothetical protein/hypothetical protein	0	0	3	0
ΦLUZ19	SNP	42443	A→G	JPEJBOGK_00052 →	T104A (ACC→GCC)	hypothetical protein	0	0	0	2

‡ = Regarded by Breseq as a significant effect mutation

4

Competition constrains parasite adaptation to thermal heterogeneity

This Chapter is in prep and has been released on BioRvx

4.1 Abstract

Temporal thermal heterogeneity is expected to favour intermediate, generalist phenotypes that can maintain growth across a broad thermal range but have sub-optimal growth at any single temperature. Yet, thermal variation typically occurs in the presence of additional selection pressures which may interact to constrain thermal adaptation. We propagated competing lytic viral parasites (bacteriophages φ14-1 and φLUZ19) of *Pseudomonas aeruginosa* under fluctuating temperatures (37-42°C) in monoculture and in co-culture. Without competition, fluctuating temperatures favoured intermediate thermal phenotypes in the phage φ14-1 and resulted in more variable evolutionary outcomes compared to static conditions. However, co-selection from fluctuating temperatures and competition led to restricted thermal adaptation, slower evolutionary rates, and fewer putative adaptive mutations in the φLUZ19 competitor. Our study highlights the potential for reduced adaptive capacity in interacting communities amidst global climate change.

4.2 Introduction

Thermal heterogeneity plays a key role in shaping species' evolutionary trajectories. Spanning a broad range of timescales, temperatures fluctuate across multi-year periods (ENSO), between seasons, and even on the order of hours through diurnal (24-hour) cycles. Very slow or rapid thermal fluctuation frequencies, with respect to generation times, typically lead to similar adaptation to static environments through selective sweeps by specialist variants [1,2]. Moderate fluctuation frequencies select for thermal generalists which have intermediate phenotypes across temperatures [1–3]. Generalist phenotypes often arise through the acquisition of multiple specialist mutations [4] or single pleiotropic mutations [5]. Thermal heterogeneity can also promote diversifying selection [6–8] leading to the maintenance of thermal specialist sub-populations [7]. The mechanisms of adaptation to thermal heterogeneity depend on the fluctuation frequency relative to generation time [9]; fluctuations that far exceed generation times in fast-replicating species may favour specialists, but in slow-replicating species may instead select for generalists.

Thermal heterogeneity typically occurs in the context of multiple selective pressures. For example, warming can impose selection on species that are simultaneously adapting to other abiotic stressors or to interactions with predators, competitors, or antagonists [10,11]. The presence of multiple selection pressures can constrain evolution rates through combined negative effects on species fitness which reduce population sizes and mutational supply [12,13]. Co-selection can also restrict adaptation through pleiotropic fitness trade-offs; high fitness under one stressor reduces fitness under another [14,15]. Temporal thermal heterogeneity is expected to promote genetic diversification by increasing niche differences [16] and so may offset the diversity-suppressing impacts of co-selection. However, some studies have indicated that co-selection involving temporal heterogeneity can exacerbate evolutionary constraint [17–19]. The ability of species to adapt to thermal heterogeneity amidst other selection pressures plays an important role in the maintenance of global biodiversity and species extinction risk [12,20–22].

Parasites provide an ideal group of organisms to study adaptation to thermal heterogeneity. Parasites are often exposed to diverse environments and stressors across their multi-stage life cycles. They can have both free-living, vector-based, and host-associated life stages [23]. By moving through numerous external environments during and between replicative cycles, parasites experience high temporal thermal heterogeneity ([24], see Introduction, 1.3). During the infection stage, parasites can also induce fevers in hosts, driving thermal changes [25]. Finally, parasites are expected to face increasingly frequent thermal extremes as a result of global climate change [26]. While contending with variable thermal environments, parasites must adapt to host immune responses [27] and competition with co-infecting parasites in the same host population or individual [28]. Within and between-host competition are primary determinants of parasite virulence [29] signifying that interactions between competition and environment-based selection can shape parasite evolution [30].

We predicted that thermal heterogeneity would select for generalist parasite populations, which have intermediate phenotypes, and promote genetic diversity [1]. We also predicted that co-selection with other environmental stressors would constrain parasite adaptation [17]. We passaged two lytic viral parasites (thermal generalist φLUZ19 and specialist φ14-1) under a fluctuating thermal regime (37-42°C) in the absence and presence of a phage competitor. Phages evolved with a static bacterial host, *Pseudomonas aeruginosa*. We compared populations evolved under fluctuating temperatures concurrently with those evolved under a static regime (37°C and 42°C), the latter presented in Chapter 3. We evaluated phage phenotypic adaptation through growth assays at 37°C and 42°C. We also conducted phage population sequencing to identify adaptive mutations and measure evolutionary rates.

4.3 Methods and Materials

4.3.1 Strains, storage, and culture conditions

This study builds on the experimental framework outlined in Chapter 3 using the same bacterial host and bacteriophage strains. *Pseudomonas aeruginosa* PAO1 was used as the non-evolving bacterial host throughout. Two lytic phages, φLUZ19 and φ14-1, were used due to their known thermal response differences: φLUZ19 performs well at both 37°C and 42°C, while φ14-1 is growth-restricted at 42°C (see Chapters 2 and 3). Phage lysates and bacterial stocks were prepared as in Chapters 2 and 3.

4.3.2 Experimental evolution

The experimental evolution design closely followed that of Chapter 3 with additional treatments incorporating fluctuating temperatures. Phages were serially passaged for 15 days under four conditions: monoculture and co-culture, each at either static or fluctuating temperatures (daily shifts between 37°C and 42°C). Each treatment included six independent replicate populations initiated from a single ancestral lysate.

Phages were propagated without shaking with a non-evolving ancestral PAO1 bacterial host. For the initial passage, ancestral phage lysates were diluted to 10^8 PFU/ml and 300µl were added to 2.7ml 10^8 CFU/ml bacterial culture in loose-lid 14ml falcon tubes. Phage co-culture populations were prepared by combining 150µl each of φLUZ19 and φ14-1 10^8 PFU/ml lysates prior to mixing with bacteria. The initial passage phage densities were ~10^7 PFU/ml resulting in a phage/bacteria ratio (multiplicity of infection, MOI) = ~0.1. Following addition of bacterial cultures, tubes were incubated statically at 37°C or 42°C in circulating water baths for 8h. Fluctuating passages started and ended at 37°C.

After incubation, phage populations were harvested by centrifugation (3,095×g, 5 min) to pellet bacteria, followed by sterile filtration through 0.2µm filters. Filtrates were stored at 4°C. In subsequent passages, 300µl of lysate was transferred into fresh PAO1 cultures.

4.3.3 Phage quantification

Phage titres were determined via the double-layer overlay method [31] following the same protocols as in Chapters 2 and 3. Briefly, bacterial lawns were prepared by mixing 10mL of melted LB-top agar with 300μL of a *P. aeruginosa* PAO1 overnight culture. Phage lysates were serially diluted, and 10μL was spotted onto the bacterial lawns. After incubating plates for 6–8 h at 37°C, spots with the highest number of discernible plaques were counted and reported. φLUZ19- or φ14-1-resistant PAO1 strains were used for selective plating enabling separate counting of φLUZ19 and φ14-1 densities in co-cultures. These resistant strains were derived by isolating colonies growing on high titre phage plaques and confirmed via sequencing (see Chapter 3). All monoculture and co-culture samples were quantified using the appropriate resistant strains to ensure consistency.

4.3.4 Phage separation and concentration

To generate high-titre and pure phage lysates for downstream assays and sequencing, we employed selective double-layer overlays with resistant hosts. Briefly, phages and φLUZ19- or φ14-1-resistant PAO1 strains were seeded into top agar plates to allow phage propagation. Phages were extracted from plates by scraping top-agar into 15ml falcon tubes containing 5ml of phage buffer (NaCl (100 mM), $MgSO_4$ (10 mM), $CaCl_2$ (5 mM), Tris-HCl (pH 8) (50 mM), Gelatin (0.01%)). Tubes were mixed overnight after which phages were separated from top agar using sterile-filtration. This process was performed three times to ensure removal of phage competitors from co-culture populations. The purification and extraction protocols were identical to those described in Chapter 3.

4.3.5 Phage growth rate assays

The thermal phenotypes of purified evolved phage populations relative to the ancestor were assessed by measuring phage and bacterial growth across an 8h window under static

incubation at 37°C and 42°C. Phage lysates were diluted to 10^5 PFU/ml and 300uL was mixed with 2.7ml of 10^8 CFU/ml wild-type PAO1 to a final MOI = ~0.0001. φLUZ19 was sampled at 2h, 4h, and 8h; φ14-1 at 4h and 8h due to delayed replication. Phage quantification was performed through sterile-filtration through 0.22μm filter plates (Agilent) followed by centrifugation at 2,230xg for 5 mins before spotting onto resistant PAO1 double-layer overlay plates. Each growth rate assay included a single replicate of each evolved phage population and three replicates of the phage ancestor. Growth rate assays were repeated three times across a two-week period to produce three technical replicates.

4.3.6 Phage population genomics

4.3.6.1 DNA extraction and sequencing

Phage DNA was extracted from purified lysates as described in Chapter 3. Briefly, ancestral and evolved phage lysates were treated with DNase and RNase to remove bacterial DNA and RNA. Phage particles were lysed using lysis (AL) buffer and proteinase K. Cell debris was precipitated using precipitation (N4) buffer and removed. Finally, DNA was precipitated and washed using isopropanol and ethanol. DNA quality was assessed with NanoDrop 2000c (Thermo Scientific) and quantified with Qubit 4 (Thermofisher). Short-read Illumina sequencing was performed by AZENTA/GENEWIZ using their Microbe-EZ pipeline for evolved and ancestral populations. Bacterial genomes (wild-type and phage-resistant strains) were sequenced by MicrobesNG using hybrid (long- and short-read) approaches.

4.3.6.2 Sequence analysis

Phage reads were pre-processed with Trim Galore (v.0.5.0) (https://github.com/FelixKrueger/TrimGalore) and downsampled using bbnorm from the bbmap package (v.39.18) (https://sourceforge.net/projects/bbmap/). Reads were then mapped to de novo ancestral assemblies generated with shovill (v1.1.0) (https://github.com/tseemann/shovill) using Bowtie2 (v.2.3.4.2) [32]. Variants were

identified using breseq (v.0.36.1) [33]. Ancestral assemblies were annotated with prokka (v.1.14.5) [34], guided by the NCBI GenBank file for each phage (φ14-1: NC_011703; φLUZ19: NC_010326).

Wild-type and resistant PAO1 genomes were assembled using Autocycler (v. 0.4.0) [35] and polished via Polypolish (v. 0.6.0) [36]. Final assemblies were re-oriented with Dnaapler (v. 1.2.0) [37] and annotated using prokka (v.1.14.5) [34]. The workflow was deployed using a Dockerised Nextflow pipeline (v. 1.0.2) available at https://doi.org/10.5281/zenodo.15706447. Mutations in resistant PAO1 strains were identified by mapping long reads to the wild-type assembly with minimap2 (v.2.24) [38] and variant calling with medaka (v.2.1) (https://github.com/nanoporetech/medaka). All bioinformatic analyses were conducted with default parameters.

4.3.7 Statistical analyses and visualisation

All statistical analyses and data visualisation were conducted using packages in R (v.4.3.2) and RStudio [39,40]. Data wrangling was performed using "Tidyverse" (v.2.0.0) R packages [41]. Phage growth and evolution rates were compared between evolution treatments using linear mixed effect models with the "lme4" (v.1.1-36) R package [42] where the response variable was phage density (pfu/ml) or genetic distance from ancestor, the explanatory variables were an interaction term between evolution treatment and temperature, and batch was a random effect. Within-group variation in genetic distance from ancestor was analysed using Levene's test. The prevalence of unique compared to shared mutations across evolution treatments was analysed using Fisher's exact test. Phage genetic distance between groups was also compared by constructing neighbour-joining trees based on Euclidean genetic distance using the "ggtree" (v.3.10.1) R package [43]. Data and code used in analyses can be found at https://github.com/SamuelGreenrod/Evol_fluctuating. Fluctuating evolved phage sequence reads are accessible on NCBI (https://www.ncbi.nlm.nih.gov/) under BioProject ID: PRJNA1334331. Static evolved phage sequence reads and bacterial sequence reads from

Chapter 3 are accessible under BioProject IDs: PRJNA1332698 and PRJNA1332799, respectively.

4.4 Results

4.4.1 Fluctuating temperatures select for generalist phenotypes in monoculture

Fluctuating environments can favour generalists with intermediate phenotypes across conditions [1]. Given φ14-1 has previously been shown to grow poorly at 42°C, we hypothesised that φ14-1 populations passaged under fluctuating conditions would rapidly adapt to 42°C but have lower fitness at 37°C and 42°C compared to static evolved populations. In monoculture, φ14-1 densities increased during 37°C passages but decreased in 42°C passages (Figure 1A). As phage lysates were diluted 10-fold in between passages, phage density decreases reflect lower than 10-fold φ14-1 population growth during 42°C passages. φLUZ19 monoculture populations reached and then maintained high densities in all passages. This phage showed low variation in inter-passage densities.

We assessed phage evolution by measuring the growth rates of static and fluctuating evolved populations relative to the ancestral phage through growth assays at 37°C and 42°C (Figure 1B). We found that growth rates of both phages in monoculture depended on the interaction between evolution treatment and assay temperature (φ14-1: $F_{3,29} = 125.8$, $p < 0.001$; φLUZ19: $F_{3,29} = 96.0$, $p < 0.001$). At 42°C, φ14-1 fluctuating populations were found to have an intermediate phenotype between those evolved under static conditions. φ14-1 fluctuating populations had significantly higher growth rates at 42°C than 37°C static populations ($t(29) = -12.4$, $p < 0.001$) but lower growth rates than 42°C static populations ($t(29) = 12.7$, $p < 0.001$). At 37°C, φ14-1 fluctuating populations had no significant difference to static populations possibly due to phage growth being measured after phages had reached carrying capacity (see Chapter 3). For φLUZ19, fluctuating evolved populations had significantly higher

growth at 42°C than 37°C static populations ($t(29) = -19.3$, $p < 0.001$). However, growth was not significantly different to 42°C evolved populations ($t(29) = -1.65$, $p = 0.37$). The opposite findings were observed at 37°C; fluctuating evolved populations had significantly higher growth rates than those evolved at 42°C but similar growth rates to 37°C evolved populations (42°C static: $t(29) = -5.2$, $p < 0.001$; 37°C static: $t(29) = -0.99$, $p = 0.75$).

4.4.2 Co-selection from fluctuating temperatures and competition constrains thermal adaptation

The presence of additional selection pressures is expected to constrain adaptation to fluctuating temperatures by reducing mutational supply and compounding fitness trade-offs [12,18,19]. We hypothesised that phages evolved under co-selection from fluctuating temperatures and competition would have lower growth rates at 37°C and 42°C than those evolved under static temperatures or fluctuating monoculture conditions. While φ14-1 densities fluctuated between passages in monoculture, co-culture densities rapidly increased and then stabilised between passages (Figure 1A). In contrast, φLUZ19 populations were stable in monoculture, but during fluctuations in co-culture, experienced high growth at 37°C and low growth at 42°C.

We then assessed evolved phage growth rates at 37°C and 42°C (Figure 1C). We found a significant interaction between evolution treatment (monoculture and co-culture) and temperature regarding growth rates for both phages (φ14-1: $F_{6,59} = 75.0$, $p < 0.0001$; φLUZ19: $F_{6,59} = 103.5$, $p < 0.0001$). While competition had no impact on the growth rates of static φ14-1 populations (37°C: $t(59) = -0.78$, $p = 0.99$; 42°C: $t(59) = -0.98$, $p = 0.99$), fluctuating co-culture evolved populations had significantly higher growth rates at 42°C compared to populations evolved in monoculture ($t(59) = -6.7$, $p < 0.0001$). No significant difference was observed at 37°C ($t(59) = -1.0$, $p = 0.99$). Similar to φ14-1, there was no impact of competition on static evolved φLUZ19 population growth rates (37°C: $t(59) = -0.42$, $p = 1.0$; 42°C: $t(59) =$

-0.21, p = 1.0). However, φLUZ19 populations evolved with fluctuations and competition had significantly lower growth rates at both 37°C and 42°C compared to monoculture (37°C: t(59) = 10.1, p < 0. 0001; 42°C: t(59) = 4.9, p < 0.001).

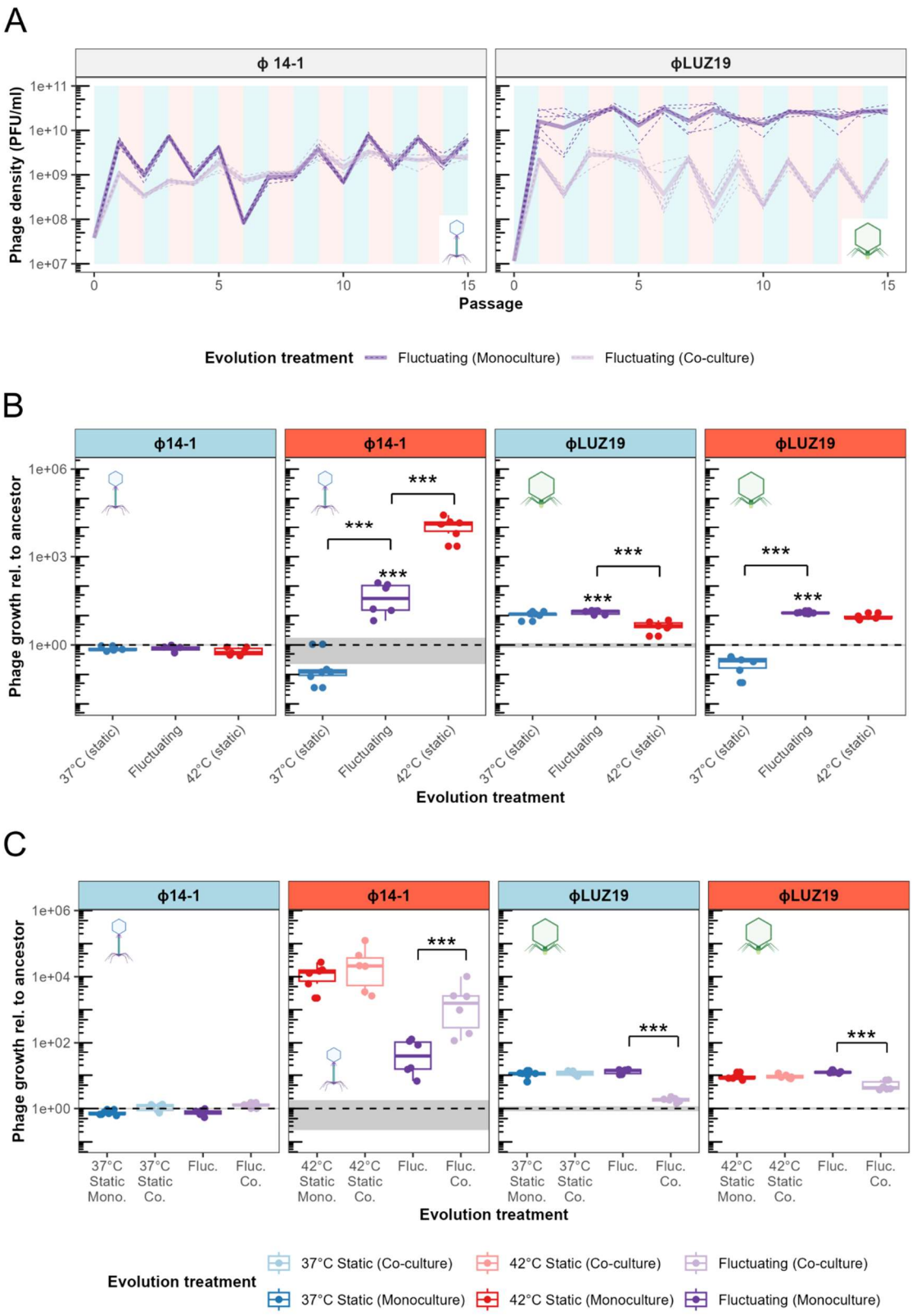

Figure 1. Co-selection in communities constrains adaptation to thermal fluctuations. A) Population dynamics of phages passaged in monoculture and co-culture under fluctuating temperatures. Values show densities at the end of each passage prior to dilution. As phage lysates were diluted 10-fold in between passages, density decreases reflect less than 10-fold population growth during passages. Plot background colour reflects the temperature during that passage where light blue is 37°C and light red is 42°C. Phage icons illustrate the two different phages used in the experiments (φ14-1, myovirus in blue; φLUZ19, autographivirus in green) [44] and are used hereafter to refer to phages in figures. **B)** Fluctuating and static temperature evolved population growth rates relative to the ancestor. Growth rates were measured after 2h for φLUZ19 and 4h for φ14-1. Six biological replicates were assayed, and data points show the average of three technical replicates. Panel strip colour reflects the temperature that growth was tested at where light blue is 37°C and light red is 42°C. Fluctuating populations are presented in purple with 37°C static populations in blue and 42°C static populations in red. Ancestral growth is shown by dashed grey line with standard errors shown as a grey box (n = 3). *** = $p < 0.001$. Absence of asterisk reflects non-significance. Static monoculture temperature data was adapted from Chapter 3. **C)** Growth rates of fluctuating and static temperature monoculture evolved populations compared to co-culture evolved populations. Boxes are coloured by evolution treatment with monoculture in dark (37°C static in blue, 42°C static in red, and fluctuating in purple) and co-culture in light (37°C static in light blue, 42°C static in light red, and fluctuating in light purple). Assay temperature and significance values are presented as in Figure 1B. Six biological replicates were assayed and data points show the average of three technical replicates. Ancestral growth rates and significance signs are presented as in Figure 1B. Static co-culture data was adapted from Chapter 3.

4.4.3 Fluctuating environments favour specialist mutations

Fluctuating temperatures generally select for multiple specialist mutations [4]. We hypothesised that fluctuating evolved populations would show genetic similarities to both high and low temperature static populations. Phage genomic evolution was assessed by constructing neighbour-joining trees of end-point populations based on Euclidean genetic distances (Figure 2A). Genetic distances were calculated based on the presence and frequency of genetic variants (SNPs, indels) that had > 10% frequency. Fluctuating evolved populations did not form a unique clade but instead were found to co-locate with either high or low temperature static populations. φ14-1 fluctuating populations were distributed across the tree and generally did not cluster with static populations. Conversely, φLUZ19 fluctuating populations were primarily found within the 42°C static clade.

We further analysed static and fluctuating population genetic similarities by measuring evolution rates based on Euclidean genetic distance from ancestor (Figure 2B). For φ14-1, fluctuating evolved populations had significantly lower evolution rates than 42°C static populations ($t(15) = -4.1$, $p < 0.01$). However, evolution rates were equal between fluctuating and 37°C static populations ($t(15) = -0.51$, $p = 0.87$). There was no significant difference in evolution rates between φLUZ19 fluctuating populations and either 37°C or 42°C static populations (37°C: $t(15) = -0.46$, $p = 0.89$; 42°C: $t(15) = -0.75$, $p = 0.74$). Notably, φ14-1 fluctuating populations had significantly greater within-group variation in evolution rates compared to 42°C static populations ($t(15) = 2.9$, $p < 0.05$) but not 37°C static populations ($t(15) = -0.70$, $p = 0.77$). φLUZ19 fluctuating populations had no significant difference in within-group variation compared to static populations (37°C: $t(15) = 2.0$, $p = 0.15$; 42°C: $t(15) = -0.10$, $p = 0.99$).

We then determined the prevalence of individual genetic variants (SNPs, indels) that were unique to or shared between evolution treatments (Figure 2C). Only putative adaptive variants with >20% frequency were included. For φ14-1, 2/11 (18%) of 37°C static variants and 5/15 (33%) of 42°C static variants were shared with other evolution treatments compared to 4/9

(44%) variants in fluctuating evolved populations. For φLUZ19, shared variants constituted 8/32 (35%) of 37°C static and 9/20 (45%) of 42°C static variants compared to 12/17 (71%) in fluctuating evolved populations. To assess the overall impact of evolution treatment on the ratio of unique and shared mutations, we pooled mutations from φ14-1 and φLUZ19 observing a significant difference in the prevalence of shared mutations relative to unique mutations between evolution treatments (Fisher's exact test: $p < 0.05$). Significant differences were not observed when analysing phages independently (φ14-1, $p = 0.47$; φLUZ19, $p = 0.08$). φ14-1 fluctuating mutations were primarily shared with 42°C static populations (Figure S1). In contrast, φLUZ19 fluctuating mutations were shared equally with 37°C and 42°C static populations.

Finally, we investigated which mutations drove clustering between fluctuating and static populations (Figure S2; Table S1). While φ14-1 fluctuating and 37°C static populations showed little clustering, two fluctuating populations clustered with the 42°C static clade. These two replicate populations contained parallel deletions in a hypothetical protein with high similarity to a DNA ligase (BlastP: 97.47% identity, 95% sequence overlap with Pseudomonas phage PhL_UNISO_PA-DSM_ph0031 DNA ligase protein), previously identified in all φ14-1 42°C static populations (see Chapter 3). The clustering of 5/6 φLUZ19 fluctuating populations with the 42°C static populations was attributed to parallel insertions in an intergenic region between two hypothetical proteins. This intergenic insertion was also previously identified in all φLUZ19 42°C static populations (see Chapter 3).

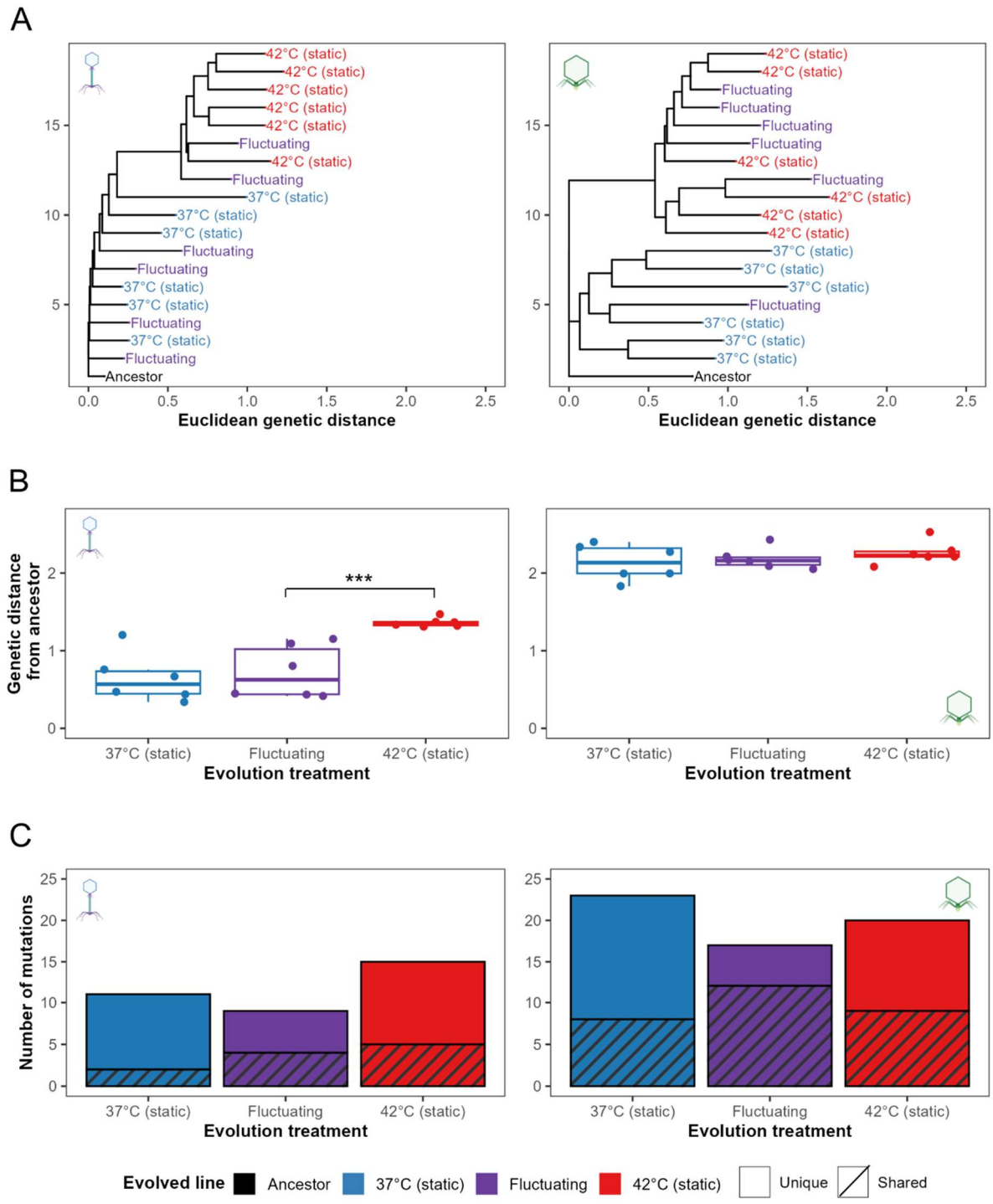

Figure 2. Fluctuating temperatures select for specialist mutations. A) Neighbour-joining trees of evolved and ancestral phage populations constructed using Euclidean genetic distances. Genetic distances were calculated based on the presence and frequency of mutations present at > 10% frequency. Tree is rooted at the ancestor and populations are coloured by evolved treatment. **B)** Phage evolution rates, measured based on Euclidean

genetic distance from the ancestor, for evolved monoculture phage populations. *** = $p < 0.001$. **C)** Stacked bar charts show the number of high frequency (>20% frequency), putative adaptive variants that are unique to or shared between evolution treatments. Bars are coloured by evolution treatment. Unique genes are shown as clear bars and shared genes are shown as striped bars. Static temperature data was adapted from Chapter 3.

4.4.4 Co-selection constrains molecular evolution

By reducing growth rates, co-selection from fluctuating temperatures and competition are expected to reduce evolution rates and restrict the acquisition of adaptive mutations [12]. Due to their elevated growth rates, we hypothesised that φ14-1 fluctuating co-culture populations would have higher evolution rates than monoculture populations. No significant difference in evolution rate was observed for φ14-1 co-culture populations compared to monoculture populations ($F_{1,10} = 4.1$, $p = 0.07$) (Figure 3A). However, non-significance was driven by a single low evolution rate replicate in the co-culture treatment; when the replicate was removed, co-culture populations had significantly greater evolution rates than monoculture ($F_{1,9} = 8.6$, $p < 0.05$). We also found no significant difference in within-group variation in evolution rates between monoculture and co-culture populations ($t(10) = 1.50$, $p = 0.17$), although the difference was also significant once the low evolution rate co-culture replicate was removed ($t(10) = 3.6$, $p < 0.01$).

For φLUZ19, we hypothesised that fluctuating co-culture populations would have lower evolution rates than monoculture populations due to the suppression of φLUZ19 by φ14-1. φLUZ19 fluctuating co-culture populations had significantly lower evolution rates than monoculture populations ($F_{1,10} = 470$, $p < 0.001$). We further hypothesised that φLUZ19 fluctuating co-culture populations, but not φ14-1 populations, would have lower evolution rates than 37°C or 42°C static co-culture populations. Evolution rates were equal between co-culture populations for φ14-1 ($F_{2,15} = 1.2$, $p = 0.3$) (Figure 3B). However, φLUZ19 fluctuating co-culture populations were found to have significantly lower evolution rates than both 37°C

static and 42°C static monoculture populations (37°C: $t(15) = 4.5$, $p < 0.01$; 42°C: $t(30) = 3.0$, $p < 0.05$).

Finally, we assessed the impact of competition on the acquisition of high frequency mutations (> 20% frequency) in fluctuating populations (Figure S3). For φ14-1, while populations no longer acquired singleton mutations, all populations acquired a deletion or SNP in a putative DNA ligase gene. Mutations in this gene are thought to contribute to high temperature adaptation (see Chapter 3) and were also found in the two monoculture populations which clustered with 42°C static populations in Figure 2A. For φLUZ19, while co-culture populations maintained mutations in tail fiber genes, the populations no longer acquired singleton mutations or the intergenic insertion associated with 42°C static populations.

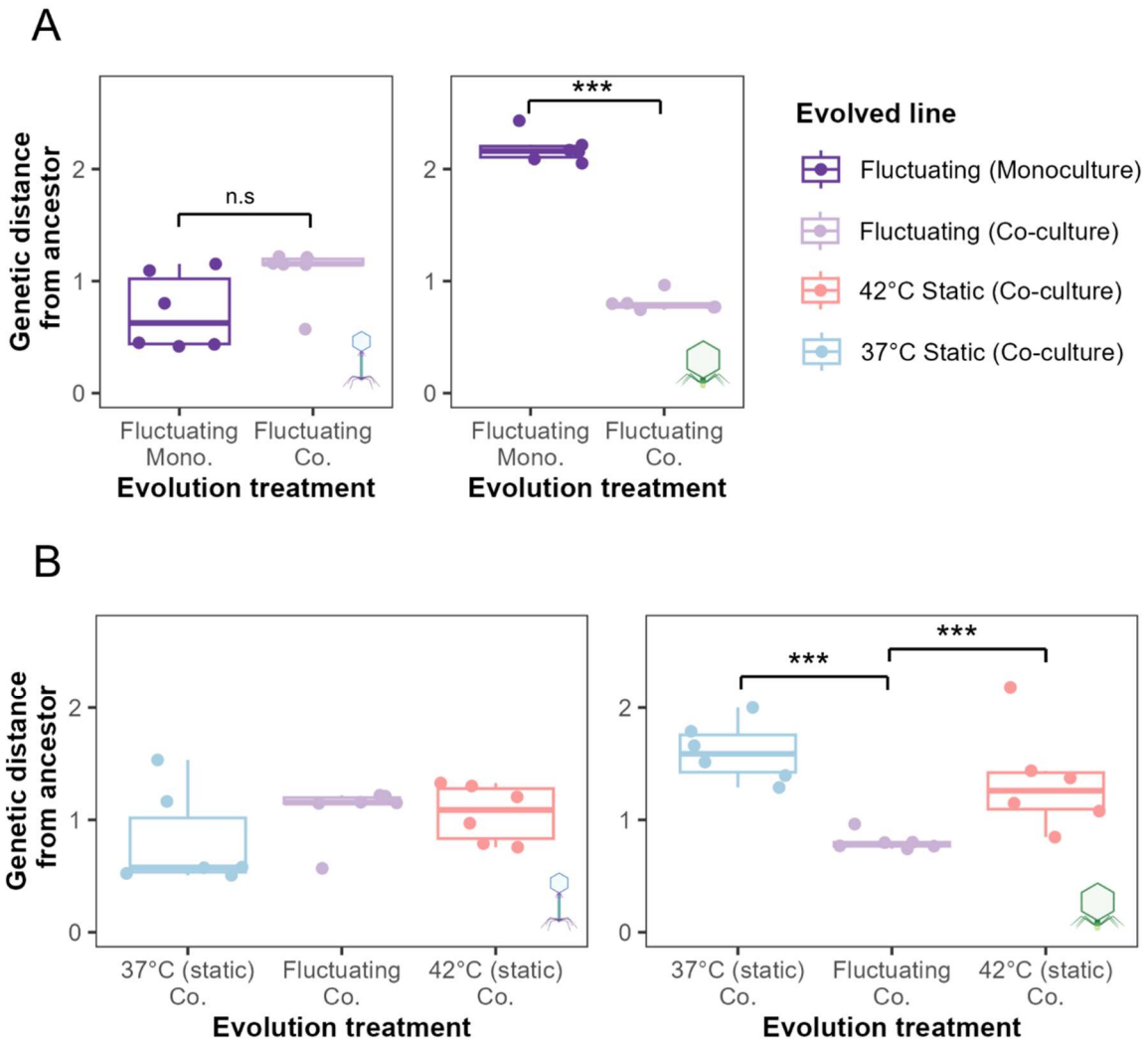

Figure 3. High environmental complexity constrains evolution rates. **A)** Evolution rates, measured based on Euclidean genetic distance from the ancestor, of phage populations evolved under fluctuating temperatures in monoculture (deep purple) and co-culture (light purple). **B)** Evolution rates of 37°C static, fluctuating, and 42°C static co-culture populations. Plot layout is the same as panel A. *** = $p < 0.001$. N.S is used to denote lack of statistical significance. Static temperature data was adapted from Chapter 3.

4.5 Discussion

Under fluctuating selection, both phages were found to rapidly evolve increased growth rates at high temperatures. For phage φ14-1, fluctuating temperatures favoured intermediate thermal phenotypes with lower growth rates at high temperatures compared to phages evolved under static temperatures. The evolution of intermediate growth rates is likely due to weaker selection for adaptation to high temperatures in the fluctuating treatment. Alternatively, adaptation to high temperatures may be constrained during fluctuations due to fitness trade-offs at lower temperatures [45]. For phage φLUZ19, fluctuating temperature populations had the same growth rates as static-evolved populations when measured at their evolved temperature. Given φLUZ19 was shown to exhibit growth rate trade-offs under static selection (see Chapter 3), this finding is indicative of a no-cost generalist strategy [46]. The lack of growth rate costs may reflect an epistatic pleiotropy, whereby the costs of adaptive mutations depend on the genetic background [46]. Costs may also occur in unmeasured traits such as virulence [47] or tolerance to other stresses [15]. These findings highlight that, while fluctuating temperatures select for greater high temperature growth, the exact phenotypic outcomes of fluctuating selection vary between phage taxa.

We found that fluctuating temperatures resulted in more variable evolutionary trajectories; while static evolved populations generally formed clusters, fluctuating populations were genetically similar to both 37°C and 42°C static evolved populations. Further, we found that

parallel mutations acquired under fluctuating selection were the same as those previously identified in static evolved populations (see Chapter 3). These findings could be explained by historical contingency [48] whereby random mutations that are adaptive at low or high temperatures become fixed in a subset of populations [7]. Depending on the timing of mutation appearance, fluctuating populations may then resemble individual static environments. Fluctuating environments have also been shown to select for mutations conferring fitness in the most extreme environment [49]. The clustering of φLUZ19 fluctuating populations with 42°C static populations likely reflects selective sweeps combined with asymmetrical selection where 42°C adaptive variants are fixed more rapidly.

While fluctuating environments can promote genetic diversification, co-selection with other environmental stressors can constrain adaptation [12]. Uiterwaal et al [18] showed that combined fluctuating temperatures and predation restricted adaptation to both selection pressures in *Paramecium caudatum* populations. Similar findings have also been observed in *Daphnia magna* with co-selection from thermal fluctuations and predation/pollutants [19,50]. We found that combined fluctuating temperature- and competition-based selection constrained both thermal adaptation and slowed evolutionary rates in phage φLUZ19. Further, co-selection resulted in greater φLUZ19 evolutionary constraint with fluctuating temperatures than static temperatures. The negative effects of combined environmental stressors are often non-additive and instead exhibit synergies [12]. We have previously shown that selection from high temperatures synergises with competition to constrain φLUZ19 evolution rates (see Chapter 3). The present study extends these findings by showing that the selective synergy between temperature and competition is greater under fluctuating temperatures than static temperatures. One potential explanation for these findings is that fluctuating environments reduce the strength of selection for adaptive mutations [51]. Weaker directional selection combined with suppression by competitors may constrain both the supply and fixation of beneficial mutations leading to particularly low evolution rates.

Anthropogenic activities, including global climate change, mean that species are facing increasingly variable and complex environments [52]. With ongoing global biodiversity loss, species must adapt to tolerate environmental stressors to avoid extinctions. Our findings highlight that while species can rapidly adapt in response to thermal variation, co-selection with other stressors, such as competition, may restrict species adaptive capacity. These results have particular relevance for parasites which must simultaneously adapt to both thermal heterogeneity, community competition in coinfections, and host immune responses. With global parasite biodiversity at risk due to climate change [26], evolutionary constraint caused by co-selection may prevent parasite adaptation to thermal stress and further increase the probability of parasite extinctions. Future studies should consider the evolution-constraining effects of co-selection when assessing species extinction risk in thermally variable environments.

4.6 References

1. Kassen R. The experimental evolution of specialists, generalists, and the maintenance of diversity. Journal of Evolutionary Biology. 2002;15(2):173–90.

2. Sachdeva V, Husain K, Sheng J, Wang S, Murugan A. Tuning environmental timescales to evolve and maintain generalists. Proceedings of the National Academy of Sciences. 2020 Jun 9;117(23):12693–9.

3. Kassen R, Bell G. Experimental evolution in Chlamydomonas. IV. Selection in environments that vary through time at different scales. Heredity. 1998;80(6):732–41.

4. Lambros M, Pechuan-Jorge X, Biro D, Ye K, Bergman A. Emerging Adaptive Strategies Under Temperature Fluctuations in a Laboratory Evolution Experiment of Escherichia Coli. Front Microbiol. 2021 Oct 22;12:724982.

5. Sandberg TE, Lloyd CJ, Palsson BO, Feist AM. Laboratory Evolution to Alternating Substrate Environments Yields Distinct Phenotypic and Genetic Adaptive Strategies. Appl Environ Microbiol. 2017 Jun 16;83(13):e00410-17.

6. Abdul-Rahman F, Tranchina D, Gresham D. Fluctuating Environments Maintain Genetic Diversity through Neutral Fitness Effects and Balancing Selection. Molecular Biology and Evolution. 2021 Oct 1;38(10):4362–75.

7. Harrison E, Laine AL, Hietala M, Brockhurst MA. Rapidly fluctuating environments constrain coevolutionary arms races by impeding selective sweeps. Proc Biol Sci. 2013 Aug 7;280(1764):20130937.

8. Chesson P. Mechanisms of Maintenance of Species Diversity. Annual Review of Ecology, Evolution, and Systematics. 2000 Nov 1;31(Volume 31, 2000):343–66.

9. Gilchrist GW. Specialists and Generalists in Changing Environments. I. Fitness Landscapes of Thermal Sensitivity. The American Naturalist. 1995;146(2):252–70.

10. Gunderson AR, Armstrong EJ, Stillman JH. Multiple Stressors in a Changing World: The Need for an Improved Perspective on Physiological Responses to the Dynamic Marine Environment. Annual Review of Marine Science. 2016 Jan 3;8(Volume 8, 2016):357–78.

11. Hector TE, Hoang KL, Li J, King KC. Symbiosis and host responses to heating. Trends in Ecology & Evolution. 2022 Jul 1;37(7):611–24.

12. Crain CM, Kroeker K, Halpern BS. Interactive and cumulative effects of multiple human stressors in marine systems. Ecology Letters. 2008;11(12):1304–15.

13. Hiltunen T, Cairns J, Frickel J, Jalasvuori M, Laakso J, Kaitala V, et al. Dual-stressor selection alters eco-evolutionary dynamics in experimental communities. Nat Ecol Evol. 2018 Dec;2(12):1974–81.

14. Burmeister AR, Fortier A, Roush C, Lessing AJ, Bender RG, Barahman R, et al. Pleiotropy complicates a trade-off between phage resistance and antibiotic resistance. Proceedings of the National Academy of Sciences. 2020 May 26;117(21):11207–16.

15. Schou MF, Engelbrecht A, Brand Z, Svensson EI, Cloete S, Cornwallis CK. Evolutionary trade-offs between heat and cold tolerance limit responses to fluctuating climates. Science Advances. 2022 May 27;8(21):eabn9580.

16. Yamamichi M, Letten AD, Schreiber SJ. Eco-evolutionary maintenance of diversity in fluctuating environments. Ecol Lett. 2023 Sep;26 Suppl 1:S152–67.

17. Cairns J, Borse F, Mononen T, Hiltunen T, Mustonen V. Strong selective environments determine evolutionary outcome in time-dependent fitness seascapes. Evol Lett. 2022 Jun 1;6(3):266–79.

18. Uiterwaal SF, Lagerstrom IT, Luhring TM, Salsbery ME, DeLong JP. Trade-offs between morphology and thermal niches mediate adaptation in response to competing selective pressures. Ecology and Evolution. 2020;10(3):1368–77.

19. Barbosa M, Pestana J, Soares AMVM. Predation Life History Responses to Increased Temperature Variability. PLoS One. 2014 Sep 24;9(9):e107971.

20. D. Vinebrooke R, L. Cottingham K, Norberg J Marten Scheffer, I. Dodson S, C. Maberly S, Sommer U. Impacts of multiple stressors on biodiversity and ecosystem functioning: the role of species co-tolerance. Oikos. 2004;104(3):451–7.

21. Halpern BS, Walbridge S, Selkoe KA, Kappel CV, Micheli F, D'Agrosa C, et al. A Global Map of Human Impact on Marine Ecosystems. Science. 2008 Feb 15;319(5865):948–52.

22. Bellard C, Bertelsmeier C, Leadley P, Thuiller W, Courchamp F. Impacts of climate change on the future of biodiversity. Ecology Letters. 2012;15(4):365–77.

23. Nguyen PL, Gokhale CS. On multiple infections by parasites with complex life cycles. Oikos. 2025;2025(4):e10493.

24. Silva LM, King KC, Koella JC. Dissecting transmission to understand parasite evolution. PLoS Pathog. 2025 Mar 25;21(3):e1012964.

25. Oakley MS, Gerald N, McCutchan TF, Aravind L, Kumar S. Clinical and molecular aspects of malaria fever. Trends in Parasitology. 2011 Oct 1;27(10):442–9.

26. Carlson CJ, Burgio KR, Dougherty ER, Phillips AJ, Bueno VM, Clements CF, et al. Parasite biodiversity faces extinction and redistribution in a changing climate. Science Advances. 2017 Sep 6;3(9):e1602422.

27. Buckingham LJ, Ashby B. Coevolutionary theory of hosts and parasites. j evol Biol. 2022 Feb 1;35(2):205–24.

28. Pedersen AB, Fenton A. Emphasizing the ecology in parasite community ecology. Trends in Ecology & Evolution. 2007 Mar 1;22(3):133–9.

29. Hasik AZ, King KC, Hawlena H. Interspecific host competition and parasite virulence evolution. Biology Letters. 2023 May 3;19(5):20220553.

30. Limberger R, Fussmann GF. Adaptation and competition in deteriorating environments. Proceedings of the Royal Society B: Biological Sciences. 2021 Mar 10;288(1946):20202967.

31. Kropinski AM, Mazzocco A, Waddell TE, Lingohr E, Johnson RP. Enumeration of Bacteriophages by Double Agar Overlay Plaque Assay. In: Clokie MRJ, Kropinski AM, editors. Bacteriophages: Methods and Protocols, Volume 1: Isolation, Characterization, and Interactions. Totowa, NJ: Humana Press; 2009. p. 69–76.

32. Langmead B, Salzberg SL. Fast gapped-read alignment with Bowtie 2. Nat Methods. 2012 Apr;9(4):357–9.

33. Deatherage DE, Barrick JE. Identification of mutations in laboratory evolved microbes from next-generation sequencing data using breseq. Methods Mol Biol. 2014;1151:165–88.

34. Seemann T. Prokka: rapid prokaryotic genome annotation. Bioinformatics. 2014 Jul 15;30(14):2068–9.

35. Wick RR, Howden BP, Stinear TP. Autocycler: long-read consensus assembly for bacterial genomes. bioRxiv; 2025. p. 2025.05.12.653612. Available from: https://www.biorxiv.org/content/10.1101/2025.05.12.653612v1

36. Wick RR, Holt KE. Polypolish: Short-read polishing of long-read bacterial genome assemblies. PLOS Computational Biology. 2022 Jan 24;18(1):e1009802.

37. Bouras G, Grigson SR, Papudeshi B, Mallawaarachchi V, Roach MJ. Dnaapler: A tool to reorient circular microbial genomes. Journal of Open Source Software. 2024 Jan 11;9(93):5968.

38. Li H. Minimap2: pairwise alignment for nucleotide sequences. Bioinformatics. 2018 Sep 15;34(18):3094–100.

39. RStudio Team. RStudio: Integrated Development for R. [Internet]. RStudio, PBC, Boston, M; 2020. Available from: http://www.rstudio.com/

40. R Core Team. R: A language and environment for statistical computing. [Internet]. Foundation for Statistical Computing, Vienna, Austria.; 2021. Available from: https://www.R-project.org/

41. Wickham H, Averick M, Bryan J, Chang W, McGowan LD, François R, et al. Welcome to the Tidyverse. Journal of Open Source Software. 2019 Nov 21;4(43):1686.

42. Bates D, Mächler M, Bolker B, Walker S. Fitting Linear Mixed-Effects Models Using lme4. Journal of Statistical Software. 2015 Oct 7;67:1–48.

43. Yu G, Smith DK, Zhu H, Guan Y, Lam TTY. ggtree: an r package for visualization and annotation of phylogenetic trees with their covariates and other associated data. Methods in Ecology and Evolution. 2017;8(1):28–36.

44. Tabare E, Glonti T, Cochez C, Ngassam C, Pirnay JP, Amighi K, et al. A Design of Experiment Approach to Optimize Spray-Dried Powders Containing Pseudomonas aeruginosaPodoviridae and Myoviridae Bacteriophages. Viruses. 2021 Oct;13(10):1926.

45. Visher E, Boots M. The problem of mediocre generalists: population genetics and eco-evolutionary perspectives on host breadth evolution in pathogens. Proc Biol Sci. 2020 Aug 26;287(1933):20201230.

46. Remold S. Understanding specialism when the jack of all trades can be the master of all. Proceedings of the Royal Society B: Biological Sciences. 2012 Oct 24;279(1749):4861–9.

47. Ashrafi R, Bruneaux M, Sundberg LR, Pulkkinen K, Valkonen J, Ketola T. Broad thermal tolerance is negatively correlated with virulence in an opportunistic bacterial pathogen. Evolutionary Applications. 2018;11(9):1700–14.

48. Blount ZD, Lenski RE, Losos JB. Contingency and determinism in evolution: Replaying life's tape. Science. 2018 Nov 9;362(6415):eaam5979.

49. Arribas M, Kubota K, Cabanillas L, Lázaro E. Adaptation to Fluctuating Temperatures in an RNA Virus Is Driven by the Most Stringent Selective Pressure. PLOS ONE. 2014 Jun 25;9(6):e100940.

50. Barbosa M, Inocentes N, Soares AMVM, Oliveira M. Synergy effects of fluoxetine and variability in temperature lead to proportionally greater fitness costs in Daphnia: A multigenerational test. Aquatic Toxicology. 2017 Dec 1;193:268–75.

51. Cvijović I, Good BH, Jerison ER, Desai MM. Fate of a mutation in a fluctuating environment. Proc Natl Acad Sci U S A. 2015 Sep 8;112(36):E5021–8.

52. Jaureguiberry P, Titeux N, Wiemers M, Bowler DE, Coscieme L, Golden AS, et al. The direct drivers of recent global anthropogenic biodiversity loss. Science Advances. 2022 Nov 9;8(45):eabm9982.

4.7 Supplementary figures

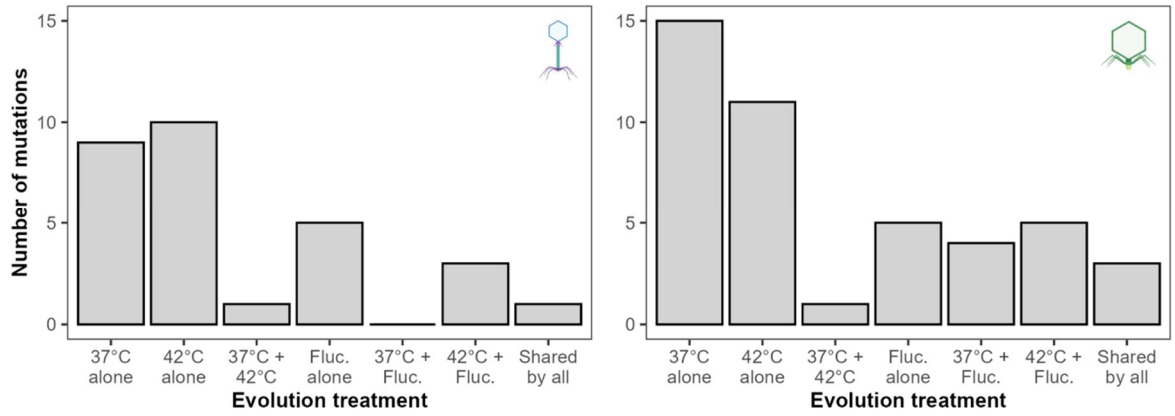

Figure S1. Bar charts show the number of high frequency variants (> 20% frequency) that are unique to or shared between evolution treatments. Variants are shown as either unique to individual evolution treatments, shared between two treatments, or shared by all three. Static temperature data was adapted from Chapter 3.

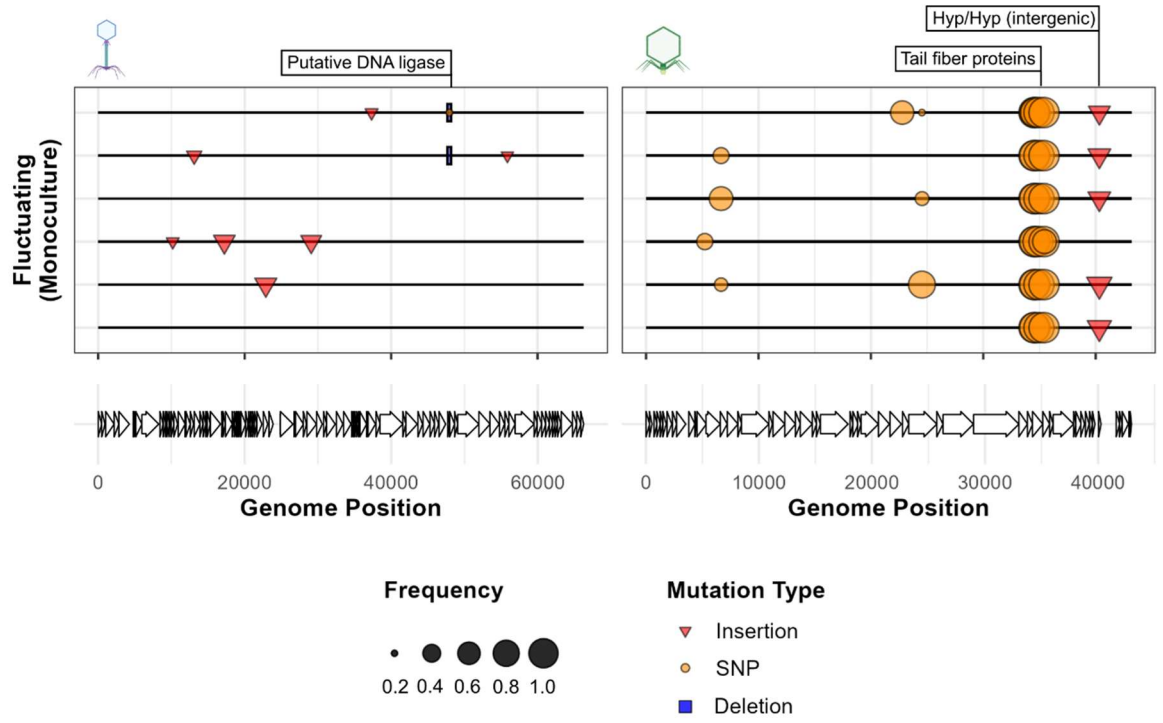

Figure S2. Fluctuating temperatures select for specialist mutations. Mutation plots show genetic variants associated with fluctuating temperatures in monoculture in phage populations. Lines represent individual biological replicates. Symbols within plots show variants across the phage genome at > 20% prevalence and which were not observed in the ancestral population. Length of deletion bars represent the size of deletion except for the φ14-1 deletion at ~48kb which is a 1bp deletion but given a fixed size for visibility. Labels show gene annotations for mutations found in 37°C and 42°C evolved populations (see Chapter 3). Putative DNA ligase in φ14-1 was originally annotated a hypothetical protein but has high homology to Pseudomonas phage PhL_UNISO_PA-DSM_ph0031 DNA ligase protein.

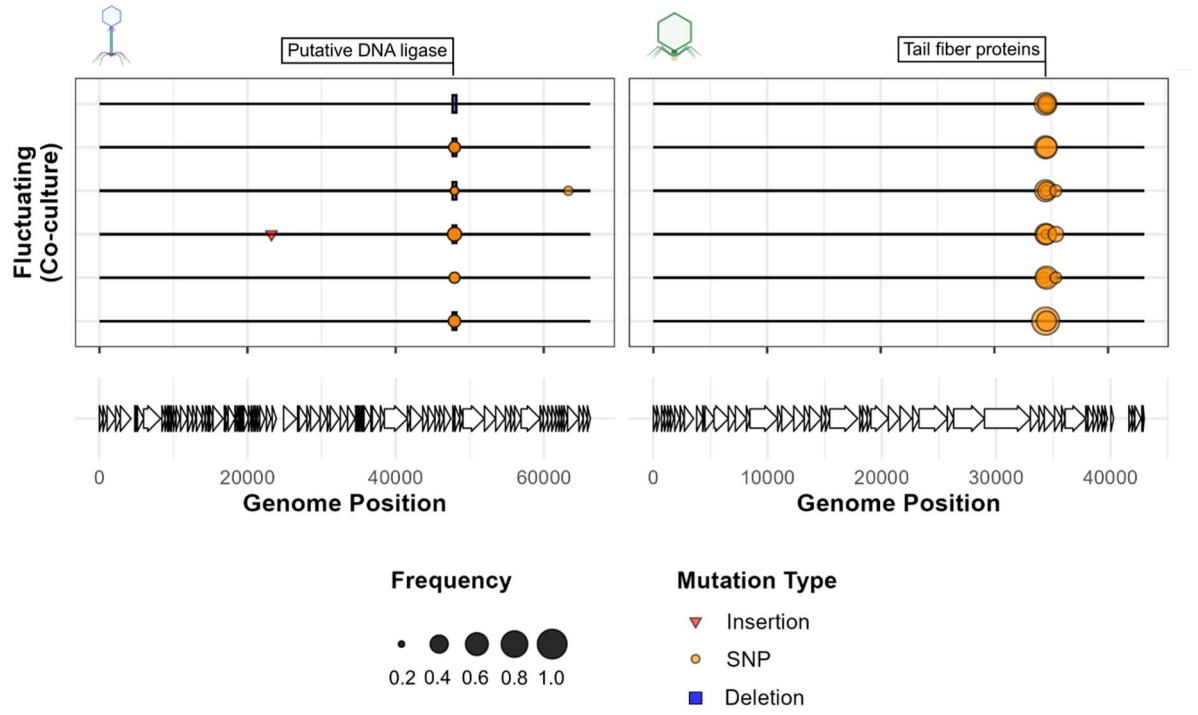

Figure S3. Competition restricts the acquisition of high frequency mutations. Mutation plots show genetic variants associated with fluctuating temperatures in co-culture in phage populations. Lines represent individual biological replicates. Symbols within plots show variants across the phage genome at > 20% prevalence and which were not observed in the ancestral population. Length of deletion bars represent the size of deletion except for the φ14-1 deletion at ~48kb which is a 1bp deletion but given a fixed size for visibility. Labels show gene annotations for mutations found in 37°C and 42°C evolved populations (see Chapter 3). Putative DNA ligase in φ14-1 was originally annotated a hypothetical protein but has high homology to Pseudomonas φPhL_UNISO_PA-DSM_ph0031 DNA ligase protein.

4.8 Supplementary tables

Table S1. Mutations with frequency > 20% in fluctuating evolved phage genomes.

Phage	Competition status	Replicate	Mutation position	Mutation type	Mutation	Frequency	Gene description
Φ14-1	Monoculture	2	22889	INS	+ACCAAAGAG	0.34	hypothetical protein
Φ14-1	Monoculture	3	6005	INS	+TGG	0.23	minor head protein
Φ14-1	Monoculture	3	10177	INS	+CATCGCCAAGAC	0.21	hypothetical protein
Φ14-1	Monoculture	3	17227	INS	+CATGGGCATCAC	0.33	hypothetical protein
Φ14-1	Monoculture	3	24893	INS	+GCCCGGACT	0.32	hypothetical protein
Φ14-1	Monoculture	3	29090	INS	+TACAGCAC	0.32	hypothetical protein
Φ14-1	Monoculture	5	13109	INS	+ACCGACCATG	0.23	hypothetical protein
Φ14-1	Monoculture	5	47943	DEL	Δ1 bp	1	hypothetical protein
Φ14-1	Monoculture	5	55879	INS	+CTTCCGGATGGT	0.21	hypothetical protein
Φ14-1	Monoculture	6	37330	INS	+CCGATAGCGACC	0.21	polynucleotide kinase/phosphorylase
Φ14-1	Monoculture	6	47943	DEL	Δ1 bp	1	hypothetical protein
Φ14-1	Monoculture	6	47959	SNP	A→C	0.2	hypothetical protein
Φ14-1	Co-culture	1	47943	DEL	Δ1 bp	1	hypothetical protein
Φ14-1	Co-culture	1	47955	SNP	G→T	0.24	hypothetical protein
Φ14-1	Co-culture	1	47957	SNP	A→T	0.24	hypothetical protein
Φ14-1	Co-culture	1	47959	SNP	A→C	0.25	hypothetical protein
Φ14-1	Co-culture	2	47955	SNP	G→T	0.23	hypothetical protein
Φ14-1	Co-culture	2	47957	SNP	A→T	0.22	hypothetical protein
Φ14-1	Co-culture	2	47959	SNP	A→C	0.23	hypothetical protein
Φ14-1	Co-culture	3	23234	INS	+CCTAGAACAGC	0.21	hypothetical protein
Φ14-1	Co-culture	3	47943	DEL	Δ1 bp	1	hypothetical protein
Φ14-1	Co-culture	3	47955	SNP	G→T	0.27	hypothetical protein
Φ14-1	Co-culture	3	47957	SNP	A→T	0.27	hypothetical protein

Φ14-1	Co-culture	3	47959	SNP	A→C	0.28	hypothetical protein
Φ14-1	Co-culture	4	47943	DEL	Δ1 bp	1	hypothetical protein
Φ14-1	Co-culture	4	47955	SNP	G→T	0.21	hypothetical protein
Φ14-1	Co-culture	4	47957	SNP	A→T	0.2	hypothetical protein
Φ14-1	Co-culture	4	47959	SNP	A→C	0.21	hypothetical protein
Φ14-1	Co-culture	4	63330	SNP	C→T	0.21	tail sheath
Φ14-1	Co-culture	5	47943	DEL	Δ1 bp	1	hypothetical protein
Φ14-1	Co-culture	5	47955	SNP	G→T	0.23	hypothetical protein
Φ14-1	Co-culture	5	47957	SNP	A→T	0.23	hypothetical protein
Φ14-1	Co-culture	5	47959	SNP	A→C	0.24	hypothetical protein
Φ14-1	Co-culture	6	47943	DEL	Δ1 bp	1	hypothetical protein
ΦLUZ19	Monoculture	1	34506	SNP	C→A	1	tail fiber protein
ΦLUZ19	Monoculture	1	34582	SNP	C→A	1	tail fiber protein
ΦLUZ19	Monoculture	1	34954	SNP	T→C	1	tail fiber protein
ΦLUZ19	Monoculture	1	35404	SNP	G→A	1	tail fiber protein
ΦLUZ19	Monoculture	1	40324	INS	+CTAGC	0.39	hypothetical protein
ΦLUZ19	Monoculture	2	6673	SNP	T→G	0.27	nucleotidyltransferase
ΦLUZ19	Monoculture	2	24541	SNP	G→A	0.79	tail protein
ΦLUZ19	Monoculture	2	34506	SNP	C→A	1	tail fiber protein
ΦLUZ19	Monoculture	2	34582	SNP	C→A	1	tail fiber protein
ΦLUZ19	Monoculture	2	34954	SNP	T→C	1	tail fiber protein
ΦLUZ19	Monoculture	2	35404	SNP	G→A	1	tail fiber protein
ΦLUZ19	Monoculture	2	40324	INS	+CTAGC	0.42	hypothetical protein
ΦLUZ19	Monoculture	3	5227	SNP	C→A	0.33	DNA primase
ΦLUZ19	Monoculture	3	34507	SNP	A→G	1	tail fiber protein
ΦLUZ19	Monoculture	3	34582	SNP	C→A	1	tail fiber protein
ΦLUZ19	Monoculture	3	34866	SNP	G→C	1	tail fiber protein
ΦLUZ19	Monoculture	3	35404	SNP	G→A	1	tail fiber protein
ΦLUZ19	Monoculture	3	35446	SNP	T→A	0.63	tail fiber protein
ΦLUZ19	Monoculture	4	6673	SNP	T→G	0.63	nucleotidyltransferase

ΦLUZ19	Monoculture	4	24553	SNP	A→C	0.28	tail protein
ΦLUZ19	Monoculture	4	34506	SNP	C→A	1	tail fiber protein
ΦLUZ19	Monoculture	4	34582	SNP	C→A	1	tail fiber protein
ΦLUZ19	Monoculture	4	34954	SNP	T→C	1	tail fiber protein
ΦLUZ19	Monoculture	4	35404	SNP	G→A	1	tail fiber protein
ΦLUZ19	Monoculture	4	40322	INS	+GGCTA	0.35	hypothetical protein
ΦLUZ19	Monoculture	5	6673	SNP	T→G	0.33	nucleotidyltransferase
ΦLUZ19	Monoculture	5	34506	SNP	C→A	1	tail fiber protein
ΦLUZ19	Monoculture	5	34582	SNP	C→A	1	tail fiber protein
ΦLUZ19	Monoculture	5	34954	SNP	T→C	1	tail fiber protein
ΦLUZ19	Monoculture	5	35404	SNP	G→A	1	tail fiber protein
ΦLUZ19	Monoculture	5	40324	INS	+CTAGC	0.36	hypothetical protein
ΦLUZ19	Monoculture	6	22788	SNP	C→T	0.61	tail tubular protein A
ΦLUZ19	Monoculture	6	24541	SNP	G→A	0.2	tail protein
ΦLUZ19	Monoculture	6	34332	SNP	A→G	0.67	tail fiber protein
ΦLUZ19	Monoculture	6	34506	SNP	C→A	1	tail fiber protein
ΦLUZ19	Monoculture	6	34582	SNP	C→A	1	tail fiber protein
ΦLUZ19	Monoculture	6	34603	SNP	A→G	0.91	tail fiber protein
ΦLUZ19	Monoculture	6	34954	SNP	T→C	1	tail fiber protein
ΦLUZ19	Monoculture	6	35404	SNP	G→A	1	tail fiber protein
ΦLUZ19	Monoculture	6	40327	INS	+GCCTT	0.34	hypothetical protein
ΦLUZ19	Co-culture	1	34506	SNP	C→A	0.83	tail fiber protein
ΦLUZ19	Co-culture	1	34582	SNP	C→A	0.45	tail fiber protein
ΦLUZ19	Co-culture	2	34332	SNP	A→G	0.23	tail fiber protein
ΦLUZ19	Co-culture	2	34506	SNP	C→A	0.43	tail fiber protein
ΦLUZ19	Co-culture	2	34582	SNP	C→A	0.57	tail fiber protein
ΦLUZ19	Co-culture	2	35404	SNP	G→A	0.23	tail fiber protein
ΦLUZ19	Co-culture	3	34506	SNP	C→A	0.5	tail fiber protein
ΦLUZ19	Co-culture	3	34507	SNP	A→G	0.21	tail fiber protein
ΦLUZ19	Co-culture	3	34582	SNP	C→A	0.45	tail fiber protein

ΦLUZ19	Co-culture	3	35404	SNP	G→A	0.31	tail fiber protein
ΦLUZ19	Co-culture	4	34506	SNP	C→A	0.52	tail fiber protein
ΦLUZ19	Co-culture	4	34560	SNP	G→A	0.23	tail fiber protein
ΦLUZ19	Co-culture	4	34582	SNP	C→A	0.37	tail fiber protein
ΦLUZ19	Co-culture	4	35404	SNP	G→A	0.24	tail fiber protein
ΦLUZ19	Co-culture	5	34506	SNP	C→A	0.57	tail fiber protein
ΦLUZ19	Co-culture	5	34582	SNP	C→A	0.48	tail fiber protein
ΦLUZ19	Co-culture	6	34506	SNP	C→A	0.55	tail fiber protein
ΦLUZ19	Co-culture	6	34560	SNP	G→A	0.29	tail fiber protein
ΦLUZ19	Co-culture	6	34582	SNP	C→A	0.4	tail fiber protein

5

Discussion, conclusions, and future work

This thesis investigates the impact of thermal stress and variability on ecology and evolution in phage communities. In this section, I highlight the main findings of each chapter, followed by a discussion of the wider implications of this body of work.

5.1 Key findings

5.1.1 Chapter 2

- Phages co-infecting the same bacterial hosts vary in their responses to temperature.
- Phage replication under thermal stress depends on the thermal sensitivity of phage life-history traits including attachment to hosts and within-host replication.
- Thermal change can alter phage competition outcomes directly leading to shifts in phage community composition.

5.1.2 Chapter 3

- Phages can avoid thermal extinction through evolutionary rescue.

- Co-selection by thermal stress and competition can facilitate thermal tolerance evolution by targeting the same phage traits.
- Evolutionary rescue can shift the competitive hierarchy and alter community dynamics by promoting the exclusion of phage competitors.
- Population decline in competitors leads to constrained evolution rates.
- Competitive exclusion can be prevented by stabilising mechanisms.

5.1.3 Chapter 4

- Thermal heterogeneity can select for intermediate thermal phenotypes relative to static temperatures but can also lead to no-cost generalist strategies.
- Phages evolved under thermal heterogeneity have less predictable evolutionary outcomes than static temperatures by selecting for both high and low temperature-associated mutations.
- The evolutionary constraint arising from co-selection by temperature and competition is exacerbated under thermal heterogeneity compared to static temperatures.

5.2 General themes and future work

5.2.1 Bacteria-phage interactions

5.2.1.1 Phageomes

Phages often form associations with animals or plants as members of their microbiomes [1,2]. Phage lytic activity is crucial for maintaining microbiome diversity through negative, frequency-dependent selection and nutrient cycling [3,4]. Microbial diversification in turn increases the resilience of microbiomes to environmental perturbations and reduces the impacts of thermal stress [5]. Chapter 2 highlighted that phages vary in their thermal responses such that warming can inactivate some phages and increase the relative fitness of others. Thermal shifts in phageome community dynamics have important implications for

animal and plant health. Thermal upregulation of phages targeting keystone microbiome members is expected to reduce microbiome stability and remove the microbiome's protective effects against pathogens [6,7]. Additionally, thermal inactivation of phages may disrupt the protective effects that phageomes confer against infecting pathogens. For example, Yang et al. [8] showed that plant rhizospheres contain pathogen-targeting phages that can protect plants from infections. However, the same researchers then showed that plant pathogen-targeting phages can be temperature-sensitive [9].

Chapter 3 highlighted that phage thermal inactivation can be avoided via evolutionary rescue. However, both Chapters 3 and 4 showed that evolutionary rescue may disrupt phage community dynamics by promoting the population decline and evolutionary constraint of phage competitors. These findings mean that, while phages may be able to persist in the phageome through rapid adaptation, thermal change may ultimately lead to phageome diversity loss. Phageome diversity loss is expected to weaken phage-induced frequency-dependent selection and reduce genetic diversification in bacterial microbiomes [3]. Diversity loss may also reduce microbiome resilience and adaptability to other environmental stresses by constraining the transfer of fitness-associated genes between bacteria via temperate phage lysogeny [10,11].

5.2.1.2 Phage therapy

Because of their lysis of bacterial cells, lytic phages are increasingly being viewed as a potential supplement or alternative to antibiotics in the treatment of animal and plant bacterial infections [12,13]. In the selection of candidates for phage therapies, efforts are made to ensure phages can operate at host body temperatures. For example, phages used in human therapies are tested for in vitro lytic potential at 37°C (resting human body temperature) [14]. In contrast, phages targeting plant pathogens are tested at lower, more physiologically relevant temperatures [13,15]. The findings from Chapter 2 indicate that phage candidates that perform well at in situ temperatures may be disrupted by thermal upshifts caused by fevers (e.g., in endothermic animals) or heatwaves (e.g., in plants). For example, Chapter 2 directly showed

that thermal increases above 37°C can inactivate phages previously used in human phage therapy treatments (e.g., φ14-1; see [14]).

Thermal inactivation of phage therapies could be overcome using two approaches: phage cocktails, and phage training. Phage cocktails, where multiple phages are applied simultaneously, are a standard practice in phage therapy where they are deployed to target polymicrobial infections or restrict the evolution of phage resistance [16]. Phage cocktails could be designed to be more effective across temperatures by containing phages that have broad thermal tolerance ranges. Alternatively, phages can instead be pre-evolved, or "trained", with their bacterial targets to increase therapy efficacy [17,18]. The findings from Chapter 3 suggest that phage training at or above in situ temperatures could expand phage upper thermal limits, improve the position of phage thermal optima, and increase maximum performance [19].

5.2.2 Thermal change modulates eco-evolutionary dynamics in parasite communities

Parasite thermal biology literature to date has largely focused on interactions between parasites and their hosts [20–23]. Yet, parasite infections rarely occur in isolation but instead occur in the presence of other parasite species through co-infections [24]. Studies which have looked at how thermal change affects parasite communities have assessed parasite ecological and evolutionary responses, separately. On an ecological level, thermal change alters parasite relative fitness with temperatures exceeding upper thermal limits in some species but approaching thermal optima for others [25]. This outcome was highlighted in Chapter 2 and shows that thermal change can lead to shifts in the relative abundance and composition of parasite communities [25]. On an evolutionary level, parasites can rapidly adapt to thermal change by altering the positioning of their thermal optima or extending their upper thermal limits [26,27], the latter occurring through evolutionary rescue [28]. Ecological and

evolutionary responses to temperature are intertwined through eco-evolutionary feedbacks, where ecological change can affect evolution and vice versa [29]. Chapters 3 and 4 aimed to assess the impact of thermal change on parasite eco-evolutionary dynamics.

The first main finding in Chapters 3 and 4 was that inter-specific competition can co-select with thermal stress for elevated thermal tolerance. While many studies have demonstrated co-selection for stress tolerance, these mainly occur between abiotic environmental stressors. For example, the evolution of heavy metal resistance often confers resistance to other heavy metals [30] and environmental contaminants often co-select for antibiotic resistance [31]. Recently, Westley et al. [32] suggested that thermal adaptation can be accelerated by competition in a bacterial community due to stronger selection. Given Chapter 3 linked high temperature and competition-based selection to mutations in a single gene, co-selection in this case instead appears to be driven by selection pressures acting on the same traits. Studies using *Drosophila* sp. showed similar results whereby competition independently selected for thermal tolerance by promoting expression changes in a heat shock protein [33,34]. However, further studies showing abiotic stress and competition-based co-selection were difficult to find. It is possible that co-selection between these factors is restricted to specific systems, such as phages, where traits that are typically restricted by temperature are also essential for competitive fitness (see Introduction – 1.3; Chapter 2). Alternatively, it could reflect a research gap as very few studies have independently assessed the impact of thermal tolerance evolution on competitiveness and vice versa. Further experimental studies using different systems are required to determine whether this phenomenon is more widespread.

The second main finding in Chapters 3 and 4 was that phage evolutionary rescue in response to thermal stress can promote the exclusion and evolutionary constraint of competitors. Previous modelling studies have suggested that evolutionary rescue may accelerate competitive exclusion of rare species, assuming constant competition [35,36]. Chapters 3 and 4 extend these findings experimentally by showing that, once evolutionary rescue has occurred, exclusion can additionally happen to equally abundant community members

through changes in species competitive fitness. This finding adds an important nuance to the diversity loss typically associated with rising temperatures [37–39]. Firstly, evolutionary rescue may accelerate diversity loss if more species are competitively excluded than are rescued. Secondly, even if species avoid exclusion through stabilising mechanisms, their reduced population densities and evolution rates may still accelerate diversity loss by making them less adaptable to future environmental stresses [40] and restricting their ability to co-evolve with competitors [41]. As mentioned previously, it is possible that the shift in competition outcomes following evolutionary rescue is restricted to systems where thermal stress and competition-based selection act on the same traits. Yet, these findings, along with other recent studies [36,42,43], highlight the need to include eco-evolutionary responses when assessing community responses to climate change.

5.2.3 Parasite extinctions and co-existence under climate change

Parasite diversity is projected to decrease with climate change [44]. Collectively, Chapters 2, 3, and 4 all support this projection and highlight that diversity loss can be driven by thermal disruption of both parasite ecology and eco-evolutionary dynamics. Parasite diversity loss has wide-ranging implications for ecosystem stability, food security, and the spread of infectious disease. From a conservation perspective, wildlife disease severity is expected to increase under future climate change due to mismatches in host and parasite thermal performances [21]. The findings in this thesis highlight that while parasite infections may become more severe, the frequency of parasite co-infections may decrease. As a result, parasite infections, when they do occur, may on balance have a smaller impact on host fitness and thus lower rates of host mortality [45]. Host mortality rates may further decrease due to reduced selection for parasite virulence during single infections [46] and increased host upper thermal limits [47]. Reduced parasite diversity with warming may ultimately help host populations withstand the diversity-eroding impacts of climate change [38].

Reduced parasite diversity is expected to be beneficial for human health during infections for the reasons mentioned above. However, human health and wellbeing are further affected by the impact of reduced parasite diversity on crops and livestock. Crops are highly sensitive to parasite infections as they are typically grown in close proximity and, being monocultures, lack the genetic variation required to develop parasite resistance [48]. Plant parasitic nematodes alone are thought to cause losses of ~12.3% in crop yields globally [49], with higher percentages reported in certain areas [50]. Similarly, livestock are frequently infected by parasites with billions of USD in losses reported annually in beef cattle [51] and farmed fish [52]. Low parasite diversity due to rising temperatures may reduce the burden of parasites on crop and livestock yields, leading to a small improvement in food security as crop growing conditions become more difficult and global demand for food increases.

Finally, parasites do not always remain in one location but instead experience novel, stressful environments by moving geographically or moving between species through spillover events [53]. As parasites evolve in response to their new environment, they may either drive resident parasite diversity loss or increase the strength of inter-parasite competition. If a geographical shift or spillover reduces resident parasite community diversity, parasite movement may improve host health outcomes [45]. Alternatively, if parasite competition becomes stronger, selection may increase for virulence leading to worse host outcomes [46]. Understanding how parasite movement alters the resident parasite community requires further theoretical development and within-host experimentation.

5.3 Concluding remarks

With global biodiversity under threat from climate change, understanding how rising temperatures affect the burden of infectious disease is becoming increasingly important. Determining the ecological and evolutionary impacts of thermal change on parasite communities is crucial to predict whether parasite burden will become greater or weaker in

the future, with important implications for host extinction risk. Future focus should be on assessing inter-parasite eco-evolutionary responses to thermal change to better determine the role of community context in the thermal sensitivity of host-parasite systems. The experiments presented in this thesis could help with the development of theoretical frameworks and highlight future experiments to further explore parasite community responses to global climate change.

5.4 References

1. Ashy RA, Jalal RS, Sonbol HS, Alqahtani MD, Sefrji FO, Alshareef SA, et al. Functional annotation of rhizospheric phageome of the wild plant species Moringa oleifera. Frontiers in Microbiology. 2023;14.

2. Manrique P, Bolduc B, Walk ST, van der Oost J, de Vos WM, Young MJ. Healthy human gut phageome. Proceedings of the National Academy of Sciences. 2016 Sep 13;113(37):10400–5.

3. Maslov S, Sneppen K. Population cycles and species diversity in dynamic Kill-the-Winner model of microbial ecosystems. Sci Rep. 2017 Jan 4;7(1):39642.

4. Wilhelm SW, Suttle CA. Viruses and Nutrient Cycles in the Sea: Viruses play critical roles in the structure and function of aquatic food webs. BioScience. 1999 Oct 1;49(10):781–8.

5. Lozupone CA, Stombaugh JI, Gordon JI, Jansson JK, Knight R. Diversity, stability and resilience of the human gut microbiota. Nature. 2012 Sep 13;489(7415):220–30.

6. Amit G, Bashan A. Top-down identification of keystone taxa in the microbiome. Nat Commun. 2023 Jul 4;14(1):3951.

7. Spragge F, Bakkeren E, Jahn MT, B. N. Araujo E, Pearson CF, Wang X, et al. Microbiome diversity protects against pathogens by nutrient blocking. Science. 2023 Dec 15;382(6676):eadj3502.

8. Yang K, Wang X, Hou R, Lu C, Fan Z, Li J, et al. Rhizosphere phage communities drive soil suppressiveness to bacterial wilt disease. Microbiome. 2023 Feb 1;11(1):16.

9. Wang J, Wang X, Yang K, Lu C, Fields B, Xu Y, et al. Phage selection drives resistance-virulence trade-offs in Ralstonia solanacearum plant-pathogenic bacterium irrespective of the growth temperature. Evol Lett. 2024 Apr;8(2):253–66.

10. Wang X, Kim Y, Ma Q, Hong SH, Pokusaeva K, Sturino JM, et al. Cryptic prophages help bacteria cope with adverse environments. Nat Commun. 2010 Dec 21;1(1):147.

11. Touchon M, Moura de Sousa JA, Rocha EP. Embracing the enemy: the diversification of microbial gene repertoires by phage-mediated horizontal gene transfer. Current Opinion in Microbiology. 2017 Aug 1;38:66–73.

12. Pirnay JP, Djebara S, Steurs G, Griselain J, Cochez C, De Soir S, et al. Personalized bacteriophage therapy outcomes for 100 consecutive cases: a multicentre, multinational, retrospective observational study. Nat Microbiol. 2024 Jun;9(6):1434–53.

13. Wang X, Wei Z, Yang K, Wang J, Jousset A, Xu Y, et al. Phage combination therapies for bacterial wilt disease in tomato. Nature Biotechnology. 2019 Dec;37(12):1513–20.

14. Van Nieuwenhuyse B, Van der Linden D, Chatzis O, Lood C, Wagemans J, Lavigne R, et al. Bacteriophage-antibiotic combination therapy against extensively drug-resistant Pseudomonas aeruginosa infection to allow liver transplantation in a toddler. Nat Commun. 2022 Sep 29;13(1):5725.

15. Fujiwara A, Fujisawa M, Hamasaki R, Kawasaki T, Fujie M, Yamada T. Biocontrol of Ralstonia solanacearum by Treatment with Lytic Bacteriophages. Appl Environ Microbiol. 2011 Jun;77(12):4155–62.

16. Abedon ST, Danis-Wlodarczyk KM, Wozniak DJ. Phage Cocktail Development for Bacteriophage Therapy: Toward Improving Spectrum of Activity Breadth and Depth. Pharmaceuticals (Basel). 2021 Oct 3;14(10):1019.

17. Borin JM, Avrani S, Barrick JE, Petrie KL, Meyer JR. Coevolutionary phage training leads to greater bacterial suppression and delays the evolution of phage resistance. Proceedings of the National Academy of Sciences. 2021 Jun 8;118(23):e2104592118.

18. Eskenazi A, Lood C, Wubbolts J, Hites M, Balarjishvili N, Leshkasheli L, et al. Combination of pre-adapted bacteriophage therapy and antibiotics for treatment of fracture-related infection due to pandrug-resistant Klebsiella pneumoniae. Nat Commun. 2022 Jan 18;13(1):302.

19. Knies JL, Kingsolver JG, Burch CL. Hotter is better and broader: thermal sensitivity of fitness in a population of bacteriophages. Am Nat. 2009 Apr;173(4):419–30.

20. Cohen JM, Venesky MD, Sauer EL, Civitello DJ, McMahon TA, Roznik EA, et al. The thermal mismatch hypothesis explains host susceptibility to an emerging infectious disease. Ecology Letters. 2017;20(2):184–93.

21. Cohen JM, Sauer EL, Santiago O, Spencer S, Rohr JR. Divergent impacts of warming weather on wildlife disease risk across climates. Science. 2020 Nov 20;370(6519):eabb1702.

22. Padfield D, Castledine M, Buckling A. Temperature-dependent changes to host–parasite interactions alter the thermal performance of a bacterial host. ISME J. 2020 Feb;14(2):389–98.

23. Gehman ALM, Hall RJ, Byers JE. Host and parasite thermal ecology jointly determine the effect of climate warming on epidemic dynamics. Proceedings of the National Academy of Sciences. 2018 Jan 23;115(4):744–9.

24. Mideo N. Parasite adaptations to within-host competition. Trends in Parasitology. 2009 Jun 1;25(6):261–8.

25. Garcia FC, Warfield R, Yvon-Durocher G. Thermal traits govern the response of microbial community dynamics and ecosystem functioning to warming. Frontiers in Microbiology. 2022;13.

26. Bull JJ, Badgett MR, Wichman HA. Big-Benefit Mutations in a Bacteriophage Inhibited with Heat. Molecular Biology and Evolution. 2000 Jun 1;17(6):942–50.

27. Mazé-Guilmo E, Blanchet S, Rey O, Canto N, Loot G. Local adaptation drives thermal tolerance among parasite populations: a common garden experiment. Proceedings of the Royal Society B: Biological Sciences. 2016 May 11;283(1830):20160587.

28. Toll-Riera M, Olombrada M, Castro-Giner F, Wagner A. A limit on the evolutionary rescue of an Antarctic bacterium from rising temperatures. Science Advances. 2022 Jul 15;8(28):eabk3511.

29. Pelletier F, Garant D, Hendry AP. Eco-evolutionary dynamics. Philos Trans R Soc Lond B Biol Sci. 2009 Jun 12;364(1523):1483–9.

30. Bazzicalupo AL, Kahn PC, Ao E, Campbell J, Otto SP. Evolution of cross-tolerance to metals in yeast. Proceedings of the National Academy of Sciences. 2025 Sep 16;122(37):e2505337122.

31. Murray LM, Hayes A, Snape J, Kasprzyk-Hordern B, Gaze WH, Murray AK. Co-selection for antibiotic resistance by environmental contaminants. npj Antimicrob Resist. 2024 Apr 1;2(1):9.

32. Westley J, García FC, Warfield R, Yvon-Durocher G. The community background alters the evolution of thermal performance. Evolution Letters. 2024 Mar 16;qrae007.

33. Kapila R, Kashyap M, Gulati A, Narasimhan A, Poddar S, Mukhopadhaya A, et al. Evolution of sex-specific heat stress tolerance and larval Hsp70 expression in populations of Drosophila melanogaster adapted to larval crowding. J Evol Biol. 2021 Sep;34(9):1376–85.

34. Sørensen JG, Loeschcke V. Larval crowding in *Drosophila melanogaster* induces Hsp70 expression, and leads to increased adult longevity and adult thermal stress resistance. Journal of Insect Physiology. 2001 Nov 1;47(11):1301–7.

35. van Eldijk TJB, Bisschop K, Etienne RS. Uniting Community Ecology and Evolutionary Rescue Theory: Community-Wide Rescue Leads to a Rapid Loss of Rare Species. Front Ecol Evol. 2020 Oct 29;8.

36. Åkesson A, Curtsdotter A, Eklöf A, Ebenman B, Norberg J, Barabás G. The importance of species interactions in eco-evolutionary community dynamics under climate change. Nat Commun. 2021 Aug 6;12(1):4759.

37. de Mazancourt C, Johnson E, Barraclough TG. Biodiversity inhibits species' evolutionary responses to changing environments. Ecol Lett. 2008 Apr;11(4):380–8.

38. Bellard C, Bertelsmeier C, Leadley P, Thuiller W, Courchamp F. Impacts of climate change on the future of biodiversity. Ecology Letters. 2012;15(4):365–77.

39. Thomas CD, Cameron A, Green RE, Bakkenes M, Beaumont LJ, Collingham YC, et al. Extinction risk from climate change. Nature. 2004 Jan;427(6970):145–8.

40. Hall JPJ, Harrison E, Brockhurst MA. Competitive species interactions constrain abiotic adaptation in a bacterial soil community. Evol Lett. 2018 Sep 25;2(6):580–9.

41. Barber JN, Sezmis AL, Woods LC, Anderson TD, Voss JM, McDonald MJ. The evolution of coexistence from competition in experimental co-cultures of Escherichia coli and Saccharomyces cerevisiae. ISME J. 2021 Mar;15(3):746–61.

42. Faillace CA, Sentis A, Montoya JM. Eco-evolutionary consequences of habitat warming and fragmentation in communities. Biol Rev Camb Philos Soc. 2021 Oct 1;96(5):1933–50.

43. Cotto O, Wessely J, Georges D, Klonner G, Schmid M, Dullinger S, et al. A dynamic eco-evolutionary model predicts slow response of alpine plants to climate warming. Nat Commun. 2017 May 5;8(1):15399.

44. Carlson CJ, Burgio KR, Dougherty ER, Phillips AJ, Bueno VM, Clements CF, et al. Parasite biodiversity faces extinction and redistribution in a changing climate. Science Advances. 2017 Sep 6;3(9):e1602422.

45. Griffiths EC, Pedersen AB, Fenton A, Petchey OL. The nature and consequences of coinfection in humans. J Infect. 2011 Sep;63(3):200–6.

46. de Roode JC, Pansini R, Cheesman SJ, Helinski MEH, Huijben S, Wargo AR, et al. Virulence and competitive ability in genetically diverse malaria infections. Proceedings of the National Academy of Sciences. 2005 May 24;102(21):7624–8.

47. Hector TE, Sgrò CM, Hall MD. Pathogen exposure disrupts an organism's ability to cope with thermal stress. Global Change Biology. 2019;25(11):3893–905.

48. Kaur S, Bedi M, Singh S, Kour N, Bhatti SS, Bhatia A, et al. Chapter Eight - Monoculture of crops: A challenge in attaining food security. In: Sharma A, Kumar M, Sharma P, editors. Advances in Food Security and Sustainability. Elsevier; 2024. p. 197–213.

49. Singh S, Singh B, Singh AP. Nematodes: A Threat to Sustainability of Agriculture. Procedia Environmental Sciences. 2015 Jan 1;29:215–6.

50. Kumar V, Khan MR, Walia RK. Crop Loss Estimations due to Plant-Parasitic Nematodes in Major Crops in India. Natl Acad Sci Lett. 2020 Oct 1;43(5):409–12.

51. Strydom T, Lavan RP, Torres S, Heaney K. The Economic Impact of Parasitism from Nematodes, Trematodes and Ticks on Beef Cattle Production. Animals (Basel). 2023 May 10;13(10):1599.

52. Tavares-Dias M, Martins ML. An overall estimation of losses caused by diseases in the Brazilian fish farms. J Parasit Dis. 2017 Dec 1;41(4):913–8.

53. Poulin R, Salloum PM, Bennett J. Evolution of parasites in the Anthropocene: new pressures, new adaptive directions. Biological Reviews. 2024;99(6):2234–52.

6

Appendix

Phage mutations present at > 20% frequency in static evolved phage populations

Phage	Temp. treatment (°C)	Competition	Rep.	Mut. type	Pos.	Mutation	Freq	Annotation	Gene	Gene description
Φ14-1	37	Monoculture	1	INS	13109	+ACCGACCATG	0.24	intergenic (+79/-8)	IGINKLAI_00020 → / → IGINKLAI_00021	hypothetical protein/ hypothetical protein
Φ14-1	37	Monoculture	1	INS	13838	+CAATGCCGGGAC	0.21	coding (722/780 nt)	IGINKLAI_00021 →	hypothetical protein
Φ14-1	37	Monoculture	1	INS	37459	+CCGAAGACCCGA	0.21	coding (622/1017 nt)	IGINKLAI_00061 →	polynucleotide kinase/ phosphorylase
Φ14-1	37	Monoculture	1	INS	40959	+TGAAGGCCGATC	0.26	coding (2476/3108 nt)	IGINKLAI_00063 →	DNA polymerase
Φ14-1	37	Monoculture	2	INS	13109	+ACCGACCATG	0.23	intergenic (+79/-8)	IGINKLAI_00020 → / → IGINKLAI_00021	hypothetical protein/ hypothetical protein
Φ14-1	37	Monoculture	2	DEL	17115	Δ3664 bp	1	*NA*	[IGINKLAI_00028]–IGINKLAI_00037	[IGINKLAI_00028], IGINKLAI_00029, IGINKLAI_00030, IGINKLAI_00031, IGINKLAI_00032, IGINKLAI_00033, IGINKLAI_00034, IGINKLAI_00035, IGINKLAI_00036, IGINKLAI_00037
Φ14-1	37	Monoculture	2	INS	61258	+AAGAGTTGCAAC	0.26	coding (319/504 nt)	IGINKLAI_00084 ←	tail fiber protein
Φ14-1	37	Monoculture	3	INS	32991	+AGGAAGAGC	0.23	coding (472/885 nt)	IGINKLAI_00052 →	hypothetical protein
Φ14-1	37	Monoculture	5	INS	32640	+AGGCCA	0.2	coding (121/885 nt)	IGINKLAI_00052 →	hypothetical protein

Φ14-1	37	Monoculture	6	INS	22710	+AGGAAGAGGCCTTCC	0.24	coding (163/612 nt)	IGINKLAI_00042 →	hypothetical protein
Φ14-1	37	Monoculture	6	INS	25236	+TGATCAGAACAT	0.31	coding (1373/1749 nt)	IGINKLAI_00044 ←	DNA primase
Φ14-1	37	Monoculture	6	INS	48135	+CAGAAGAACCAGG	0.25	coding (513/663 nt)	IGINKLAI_00072 ←	endolysin
Φ14-1	37	Co-culture	1	SNP	47955	G→T	0.26	E83* (GAA→TAA)‡	IGINKLAI_00071 →	hypothetical protein
Φ14-1	37	Co-culture	1	SNP	47957	A→T	0.25	E83D (GAA→GAT)‡	IGINKLAI_00071 →	hypothetical protein
Φ14-1	37	Co-culture	1	SNP	47959	A→C	0.26	*84S (TAA→TCA)	IGINKLAI_00071 →	hypothetical protein
Φ14-1	37	Co-culture	2	SNP	47955	G→T	0.27	E83* (GAA→TAA)‡	IGINKLAI_00071 →	hypothetical protein
Φ14-1	37	Co-culture	2	SNP	47957	A→T	0.26	E83D (GAA→GAT)‡	IGINKLAI_00071 →	hypothetical protein
Φ14-1	37	Co-culture	2	SNP	47959	A→C	0.26	*84S (TAA→TCA)	IGINKLAI_00071 →	hypothetical protein
Φ14-1	37	Co-culture	3	SNP	47955	G→T	0.26	E83* (GAA→TAA)‡	IGINKLAI_00071 →	hypothetical protein
Φ14-1	37	Co-culture	3	SNP	47957	A→T	0.25	E83D (GAA→GAT)‡	IGINKLAI_00071 →	hypothetical protein
Φ14-1	37	Co-culture	3	SNP	47959	A→C	0.26	*84S (TAA→TCA)	IGINKLAI_00071 →	hypothetical protein
Φ14-1	37	Co-culture	4	SNP	47955	G→T	0.25	E83* (GAA→TAA)‡	IGINKLAI_00071 →	hypothetical protein
Φ14-1	37	Co-culture	4	SNP	47957	A→T	0.24	E83D (GAA→GAT)‡	IGINKLAI_00071 →	hypothetical protein
Φ14-1	37	Co-culture	4	SNP	47959	A→C	0.25	*84S (TAA→TCA)	IGINKLAI_00071 →	hypothetical protein
Φ14-1	37	Co-culture	5	DEL	16883	Δ3635 bp	1	*NA*	IGINKLAI_00027–IGINKLAI_00036	IGINKLAI_00027, IGINKLAI_00028, IGINKLAI_00029, IGINKLAI_00030, IGINKLAI_00031, IGINKLAI_00032, I

										GINKLAI_00033, IGINKLAI_00034, IGINKLAI_00035, IGINKLAI_00036
Φ14-1	37	Co-culture	5	DEL	47943	Δ1 bp	1	coding (235/252 nt)	IGINKLAI_00071 →	hypothetical protein
Φ14-1	37	Co-culture	5	SNP	47955	G→T	0.27	E83* (GAA→TAA)‡	IGINKLAI_00071 →	hypothetical protein
Φ14-1	37	Co-culture	5	SNP	47957	A→T	0.27	E83D (GAA→GAT)‡	IGINKLAI_00071 →	hypothetical protein
Φ14-1	37	Co-culture	5	SNP	47959	A→C	0.27	*84S (TAA→TCA)	IGINKLAI_00071 →	hypothetical protein
Φ14-1	37	Co-culture	6	DEL	17082	Δ4803 bp	1	*NA*	[IGINKLAI_00028]–[IGINKLAI_00041]	[IGINKLAI_00028], IGINKLAI_00029, IGINKLAI_00030, IGINKLAI_00031, IGINKLAI_00032, IGINKLAI_00033, IGINKLAI_00034, IGINKLAI_00035, IGINKLAI_00036, IGINKLAI_00037, IGINKLAI_00038, IGINKLAI_00039, IGINKLAI_00040, [IGINKLAI_00041]
Φ14-1	37	Co-culture	6	SNP	47955	G→T	0.23	E83* (GAA→TAA)‡	IGINKLAI_00071 →	hypothetical protein
Φ14-1	37	Co-culture	6	SNP	47957	A→T	0.22	E83D (GAA→GAT)‡	IGINKLAI_00071 →	hypothetical protein
Φ14-1	37	Co-culture	6	SNP	47959	A→C	0.23	*84S (TAA→TCA)	IGINKLAI_00071 →	hypothetical protein
Φ14-1	37	Co-culture	6	INS	63520	+CAGGAACAGGTC	0.25	coding (1192/1515 nt)	IGINKLAI_00089 ←	tail sheath
Φ14-1	42	Monoculture	1	INS	11190	+TACAAAGAG	0.29	coding (237/933 nt)	IGINKLAI_00017 →	hypothetical protein
Φ14-1	42	Monoculture	1	DEL	47943	Δ1 bp	1	coding (235/252 nt)	IGINKLAI_00071 →	hypothetical protein

Φ14-1	42	Monoculture	1	SNP	63330	C→T	0.44	C461Y (TGC→TAC)	IGINKLAI_00089 ←	tail sheath
Φ14-1	42	Monoculture	1	SNP	63478	T→C	0.31	T412A (ACC→GCC)	IGINKLAI_00089 ←	tail sheath
Φ14-1	42	Monoculture	1	INS	64892	+TGATCTGGAG	0.21	coding (417/582 nt)	IGINKLAI_00090 ←	tail completion or Neck1 protein
Φ14-1	42	Monoculture	2	DEL	47943	Δ1 bp	1	coding (235/252 nt)	IGINKLAI_00071 →	hypothetical protein
Φ14-1	42	Monoculture	2	SNP	63226	A→C	0.54	F496V (TTC→GTC)	IGINKLAI_00089 ←	tail sheath
Φ14-1	42	Monoculture	2	SNP	63330	C→T	0.35	C461Y (TGC→TAC)	IGINKLAI_00089 ←	tail sheath
Φ14-1	42	Monoculture	3	INS	37330	+CCGATAGCGACC	0.21	coding (493/1017 nt)	IGINKLAI_00061 →	polynucleotide kinase/ phosphorylase
Φ14-1	42	Monoculture	3	DEL	47943	Δ1 bp	1	coding (235/252 nt)	IGINKLAI_00071 →	hypothetical protein
Φ14-1	42	Monoculture	3	SNP	63258	G→T	0.58	T485K (ACG→AAG)	IGINKLAI_00089 ←	tail sheath
Φ14-1	42	Monoculture	3	SNP	63478	T→C	0.24	T412A (ACC→GCC)	IGINKLAI_00089 ←	tail sheath
Φ14-1	42	Monoculture	4	INS	13109	+ACCGACCATG	0.23	intergenic (+79/-8)	IGINKLAI_00020 → / → IGINKLAI_00021	hypothetical protein/ hypothetical protein
Φ14-1	42	Monoculture	4	INS	32640	+AGGCCA	0.2	coding (121/885 nt)	IGINKLAI_00052 →	hypothetical protein
Φ14-1	42	Monoculture	4	DEL	47943	Δ1 bp	1	coding (235/252 nt)	IGINKLAI_00071 →	hypothetical protein
Φ14-1	42	Monoculture	4	SNP	47955	G→T	0.23	E83* (GAA→TAA)‡	IGINKLAI_00071 →	hypothetical protein
Φ14-1	42	Monoculture	4	SNP	47957	A→T	0.23	E83D (GAA→GAT)‡	IGINKLAI_00071 →	hypothetical protein
Φ14-1	42	Monoculture	4	SNP	47959	A→C	0.23	*84S (TAA→TCA)	IGINKLAI_00071 →	hypothetical protein
Φ14-1	42	Monoculture	4	SNP	63226	A→C	0.5	F496V (TTC→GTC)	IGINKLAI_00089 ←	tail sheath

Φ14-1	42	Monoculture	4	SNP	63478	T→C	0.23	T412A (ACC→GCC)	IGINKLAI_00089 ←	tail sheath
Φ14-1	42	Monoculture	5	INS	23791	+CAGGTCGATGTA	0.24	coding (106/570 nt)	IGINKLAI_00043 ←	hypothetical protein
Φ14-1	42	Monoculture	5	INS	37330	+CCGATAGCGACC	0.23	coding (493/1017 nt)	IGINKLAI_00061 →	polynucleotide kinase/ phosphorylase
Φ14-1	42	Monoculture	5	DEL	47943	Δ1 bp	1	coding (235/252 nt)	IGINKLAI_00071 →	hypothetical protein
Φ14-1	42	Monoculture	5	INS	49333	+TGTAGTTGT	0.22	coding (2633/2889 nt)	IGINKLAI_00074 ←	tail protein
Φ14-1	42	Monoculture	5	SNP	63330	C→T	0.65	C461Y (TGC→TAC)	IGINKLAI_00089 ←	tail sheath
Φ14-1	42	Monoculture	6	DEL	47943	Δ1 bp	1	coding (235/252 nt)	IGINKLAI_00071 →	hypothetical protein
Φ14-1	42	Monoculture	6	SNP	47955	G→T	0.2	E83* (GAA→TAA)‡	IGINKLAI_00071 →	hypothetical protein
Φ14-1	42	Monoculture	6	SNP	47957	A→T	0.2	E83D (GAA→GAT)‡	IGINKLAI_00071 →	hypothetical protein
Φ14-1	42	Monoculture	6	SNP	47959	A→C	0.2	*84S (TAA→TCA)	IGINKLAI_00071 →	hypothetical protein
Φ14-1	42	Monoculture	6	SNP	63330	C→T	0.59	C461Y (TGC→TAC)	IGINKLAI_00089 ←	tail sheath
Φ14-1	42	Monoculture	6	SNP	63478	T→C	0.23	T412A (ACC→GCC)	IGINKLAI_00089 ←	tail sheath
Φ14-1	42	Co-culture	1	INS	19039	+CAAGCAAGACCTGTA	0.24	coding (5/216 nt)	IGINKLAI_00033 →	hypothetical protein
Φ14-1	42	Co-culture	1	DEL	47943	Δ1 bp	1	coding (235/252 nt)	IGINKLAI_00071 →	hypothetical protein
Φ14-1	42	Co-culture	1	SNP	63330	C→T	0.75	C461Y (TGC→TAC)	IGINKLAI_00089 ←	tail sheath
Φ14-1	42	Co-culture	2	SNP	63330	C→T	0.56	C461Y (TGC→TAC)	IGINKLAI_00089 ←	tail sheath
Φ14-1	42	Co-culture	3	SNP	63330	C→T	0.67	C461Y (TGC→TAC)	IGINKLAI_00089 ←	tail sheath

Φ14-1	42	Co-culture	3	SNP	63478	T→C	0.2	T412A (ACC→GCC)	IGINKLAI_00089 ←	tail sheath
Φ14-1	42	Co-culture	4	SNP	63330	C→T	0.89	C461Y (TGC→TAC)	IGINKLAI_00089 ←	tail sheath
Φ14-1	42	Co-culture	5	DEL	47943	Δ1 bp	1	coding (235/252 nt)	IGINKLAI_00071 →	hypothetical protein
Φ14-1	42	Co-culture	5	SNP	63478	T→C	0.57	T412A (ACC→GCC)	IGINKLAI_00089 ←	tail sheath
Φ14-1	42	Co-culture	6	DEL	47943	Δ1 bp	1	coding (235/252 nt)	IGINKLAI_00071 →	hypothetical protein
Φ14-1	42	Co-culture	6	SNP	63330	C→A	0.54	C461F (TGC→TTC)	IGINKLAI_00089 ←	tail sheath
Φ14-1	42	Co-culture	6	SNP	63478	T→C	0.3	T412A (ACC→GCC)	IGINKLAI_00089 ←	tail sheath
Φ14-1	42	Co-culture	6	SNP	63531	T→C	0.4	D394G (GAC→GGC)	IGINKLAI_00089 ←	tail sheath
ΦLUZ19	37	Monoculture	1	DEL	3563	Δ1 bp	1	intergenic (+33/-237)	gp12 → / → JPEJBOGK_00010	DNA polymerase/ hypothetical protein
ΦLUZ19	37	Monoculture	1	SNP	6673	T→G	0.72	L32W (TTG→TGG)	gp16 →	nucleotidyltransferase
ΦLUZ19	37	Monoculture	1	SNP	10509	T→C	0.64	F684L (TTC→CTC)	gp19 →	DNA polymerase
ΦLUZ19	37	Monoculture	1	SNP	15953	A→C	0.25	D171A (GAT→GCT)	gp26 →	RNA polymerase
ΦLUZ19	37	Monoculture	1	SNP	24542	A→G	0.78	D429G (GAC→GGC)‡	gp34 →	tail protein
ΦLUZ19	37	Monoculture	1	SNP	33975	T→A	0.24	L75Q (CTG→CAG)	gp39 →	tail fiber protein
ΦLUZ19	37	Monoculture	1	SNP	34506	C→A	0.34	Q102K (CAG→AAG)‡	gp40 →	tail fiber protein
ΦLUZ19	37	Monoculture	1	SNP	34507	A→G	0.59	Q102R (CAG→CGG)‡	gp40 →	tail fiber protein
ΦLUZ19	37	Monoculture	1	SNP	34582	C→A	1	T127K (ACG→AAG)	gp40 →	tail fiber protein
ΦLUZ19	37	Monoculture	1	SNP	35404	G→A	1	C98Y (TGT→TAT)	gp41 →	tail fiber protein
ΦLUZ19	37	Monoculture	2	SNP	892	G→A	0.53	R57H (CGC→CAC)	JPEJBOGK_00003 →	hypothetical protein
ΦLUZ19	37	Monoculture	2	DEL	3549	Δ1 bp	1	intergenic (+19/-251)	gp12 → / → JPEJBOGK_00010	DNA polymerase/ hypothetical protein
ΦLUZ19	37	Monoculture	2	SNP	6673	T→G	0.35	L32W (TTG→TGG)	gp16 →	nucleotidyltransferase
ΦLUZ19	37	Monoculture	2	SNP	10509	T→C	0.27	F684L (TTC→CTC)	gp19 →	DNA polymerase

ΦLUZ19	37	Monoculture	2	SNP	15953	A→C	0.95	D171A (GAT→GCT)	gp26 →	RNA polymerase
ΦLUZ19	37	Monoculture	2	SNP	24542	A→G	1	D429G (GAC→GGC)	gp34 →	tail protein
ΦLUZ19	37	Monoculture	2	SNP	34507	A→G	0.38	Q102R (CAG→CGG)	gp40 →	tail fiber protein
ΦLUZ19	37	Monoculture	2	SNP	34582	C→A	1	T127K (ACG→AAG)	gp40 →	tail fiber protein
ΦLUZ19	37	Monoculture	2	SNP	34951	A→G	0.44	Q250R (CAG→CGG)	gp40 →	tail fiber protein
ΦLUZ19	37	Monoculture	2	SNP	35404	G→A	1	C98Y (TGT→TAT)	gp41 →	tail fiber protein
ΦLUZ19	37	Monoculture	3	SNP	8801	T→G	0.36	S114R (AGT→AGG)	gp19 →	DNA polymerase
ΦLUZ19	37	Monoculture	3	SNP	15734	A→G	0.49	Y98C (TAC→TGC)	gp26 →	RNA polymerase
ΦLUZ19	37	Monoculture	3	SNP	24542	A→C	0.32	D429A (GAC→GCC)‡	gp34 →	tail protein
ΦLUZ19	37	Monoculture	3	SNP	34507	A→G	0.87	Q102R (CAG→CGG)	gp40 →	tail fiber protein
ΦLUZ19	37	Monoculture	3	SNP	34582	C→A	1	T127K (ACG→AAG)	gp40 →	tail fiber protein
ΦLUZ19	37	Monoculture	3	SNP	35404	G→A	1	C98Y (TGT→TAT)	gp41 →	tail fiber protein
ΦLUZ19	37	Monoculture	4	DEL	3563	Δ1 bp	1	intergenic (+33/-237)	gp12 → / → JPEJBOGK_00010	DNA polymerase/ hypothetical protein
ΦLUZ19	37	Monoculture	4	DEL	4444	Δ13 bp	0.65	coding (113-125/129 nt)	JPEJBOGK_00011 →	hypothetical protein
ΦLUZ19	37	Monoculture	4	SNP	8801	T→G	0.25	S114R (AGT→AGG)	gp19 →	DNA polymerase
ΦLUZ19	37	Monoculture	4	SNP	10509	T→C	0.29	F684L (TTC→CTC)	gp19 →	DNA polymerase
ΦLUZ19	37	Monoculture	4	SNP	15953	A→C	0.23	D171A (GAT→GCT)	gp26 →	RNA polymerase
ΦLUZ19	37	Monoculture	4	SNP	24541	G→A	0.24	D429N (GAC→AAC)‡	gp34 →	tail protein
ΦLUZ19	37	Monoculture	4	SNP	24542	A→G	0.58	D429G (GAC→GGC)‡	gp34 →	tail protein
ΦLUZ19	37	Monoculture	4	SNP	33834	T→C	0.31	M28T (ATG→ACG)	gp39 →	tail fiber protein
ΦLUZ19	37	Monoculture	4	SNP	34507	A→G	1	Q102R (CAG→CGG)	gp40 →	tail fiber protein
ΦLUZ19	37	Monoculture	4	SNP	34582	C→A	1	T127K (ACG→AAG)	gp40 →	tail fiber protein
ΦLUZ19	37	Monoculture	4	SNP	35404	G→A	1	C98Y (TGT→TAT)	gp41 →	tail fiber protein
ΦLUZ19	37	Monoculture	4	SNP	35446	T→A	0.53	F112Y (TTC→TAC)	gp41 →	tail fiber protein
ΦLUZ19	37	Monoculture	5	SNP	6673	T→G	1	L32W (TTG→TGG)	gp16 →	nucleotidyltransferase
ΦLUZ19	37	Monoculture	5	SNP	16769	C→A	0.59	S443Y (TCC→TAC)	gp26 →	RNA polymerase
ΦLUZ19	37	Monoculture	5	SNP	24542	A→G	0.24	D429G (GAC→GGC)	gp34 →	tail protein
ΦLUZ19	37	Monoculture	5	SNP	33834	T→C	0.21	M28T (ATG→ACG)	gp39 →	tail fiber protein

ΦLUZ19	37	Monoculture	5	SNP	34507	A→G	0.4	Q102R (CAG→CGG)	gp40 →	tail fiber protein
ΦLUZ19	37	Monoculture	5	SNP	34524	C→A	0.56	Q108K (CAA→AAA)	gp40 →	tail fiber protein
ΦLUZ19	37	Monoculture	5	SNP	34582	C→A	1	T127K (ACG→AAG)	gp40 →	tail fiber protein
ΦLUZ19	37	Monoculture	5	SNP	35404	G→A	1	C98Y (TGT→TAT)	gp41 →	tail fiber protein
ΦLUZ19	37	Monoculture	6	SNP	6673	T→G	0.72	L32W (TTG→TGG)	gp16 →	nucleotidyltransferase
ΦLUZ19	37	Monoculture	6	DEL	8360	Δ1 bp	0.4	coding (218/321 nt)	JPEJBOGK_00016 →	hypothetical protein
ΦLUZ19	37	Monoculture	6	SNP	24541	G→A	0.25	D429N (GAC→AAC)‡	gp34 →	tail protein
ΦLUZ19	37	Monoculture	6	SNP	24542	A→C	0.38	D429A (GAC→GCC)‡	gp34 →	tail protein
ΦLUZ19	37	Monoculture	6	SNP	34524	C→A	1	Q108K (CAA→AAA)	gp40 →	tail fiber protein
ΦLUZ19	37	Monoculture	6	SNP	34582	C→A	1	T127K (ACG→AAG)	gp40 →	tail fiber protein
ΦLUZ19	37	Monoculture	6	SNP	35404	G→A	1	C98Y (TGT→TAT)	gp41 →	tail fiber protein
ΦLUZ19	37	Co-culture	1	SNP	5227	C→A	0.23	L234I (CTC→ATC)	gp14 →	DNA primase
ΦLUZ19	37	Co-culture	1	SNP	10509	T→C	0.44	F684L (TTC→CTC)	gp19 →	DNA polymerase
ΦLUZ19	37	Co-culture	1	SNP	34507	A→G	0.84	Q102R (CAG→CGG)	gp40 →	tail fiber protein
ΦLUZ19	37	Co-culture	1	SNP	34582	C→A	0.95	T127K (ACG→AAG)	gp40 →	tail fiber protein
ΦLUZ19	37	Co-culture	1	SNP	35404	G→A	0.93	C98Y (TGT→TAT)	gp41 →	tail fiber protein
ΦLUZ19	37	Co-culture	2	DEL	3563	Δ1 bp	1	intergenic (+33/-237)	gp12 → / → JPEJBOGK_00010	DNA polymerase/ hypothetical protein
ΦLUZ19	37	Co-culture	2	SNP	6673	T→G	0.25	L32W (TTG→TGG)	gp16 →	nucleotidyltransferase
ΦLUZ19	37	Co-culture	2	SNP	34507	A→G	0.94	Q102R (CAG→CGG)	gp40 →	tail fiber protein
ΦLUZ19	37	Co-culture	2	SNP	34582	C→A	1	T127K (ACG→AAG)	gp40 →	tail fiber protein
ΦLUZ19	37	Co-culture	2	SNP	35404	G→A	1	C98Y (TGT→TAT)	gp41 →	tail fiber protein
ΦLUZ19	37	Co-culture	3	SNP	6673	T→G	0.38	L32W (TTG→TGG)	gp16 →	nucleotidyltransferase
ΦLUZ19	37	Co-culture	3	SNP	34507	A→G	1	Q102R (CAG→CGG)	gp40 →	tail fiber protein
ΦLUZ19	37	Co-culture	3	SNP	34582	C→A	1	T127K (ACG→AAG)	gp40 →	tail fiber protein
ΦLUZ19	37	Co-culture	3	SNP	35404	G→A	1	C98Y (TGT→TAT)	gp41 →	tail fiber protein
ΦLUZ19	37	Co-culture	4	SNP	34561	A→G	0.31	D120G (GAT→GGT)	gp40 →	tail fiber protein
ΦLUZ19	37	Co-culture	4	SNP	34582	C→A	0.65	T127K (ACG→AAG)	gp40 →	tail fiber protein
ΦLUZ19	37	Co-culture	4	SNP	34951	A→G	0.66	Q250R (CAG→CGG)	gp40 →	tail fiber protein

ΦLUZ19	37	Co-culture	4	SNP	35404	G→A	0.86	C98Y (TGT→TAT)	gp41 →	tail fiber protein
ΦLUZ19	37	Co-culture	5	SNP	5206	A→G	0.24	S227G (AGT→GGT)‡	gp14 →	DNA primase
ΦLUZ19	37	Co-culture	5	SNP	5208	T→A	0.24	S227R (AGT→AGA)‡	gp14 →	DNA primase
ΦLUZ19	37	Co-culture	5	SNP	10509	T→C	0.27	F684L (TTC→CTC)	gp19 →	DNA polymerase
ΦLUZ19	37	Co-culture	5	SNP	12162	T→C	0.25	V306A (GTG→GCG)	JPEJBOGK_00019 →	hypothetical protein
ΦLUZ19	37	Co-culture	5	SNP	34507	A→G	0.69	Q102R (CAG→CGG)	gp40 →	tail fiber protein
ΦLUZ19	37	Co-culture	5	SNP	34561	A→G	0.28	D120G (GAT→GGT)	gp40 →	tail fiber protein
ΦLUZ19	37	Co-culture	5	SNP	34582	C→A	0.64	T127K (ACG→AAG)	gp40 →	tail fiber protein
ΦLUZ19	37	Co-culture	5	SNP	35404	G→A	0.88	C98Y (TGT→TAT)	gp41 →	tail fiber protein
ΦLUZ19	37	Co-culture	6	SNP	10509	T→C	0.37	F684L (TTC→CTC)	gp19 →	DNA polymerase
ΦLUZ19	37	Co-culture	6	SNP	34582	C→A	0.88	T127K (ACG→AAG)	gp40 →	tail fiber protein
ΦLUZ19	37	Co-culture	6	SNP	34951	A→G	0.72	Q250R (CAG→CGG)	gp40 →	tail fiber protein
ΦLUZ19	37	Co-culture	6	SNP	35404	G→A	0.91	C98Y (TGT→TAT)	gp41 →	tail fiber protein
ΦLUZ19	42	Monoculture	1	SNP	34506	C→A	1	Q102K (CAG→AAG)	gp40 →	tail fiber protein
ΦLUZ19	42	Monoculture	1	SNP	34582	C→A	1	T127K (ACG→AAG)	gp40 →	tail fiber protein
ΦLUZ19	42	Monoculture	1	SNP	34954	T→C	1	V251A (GTC→GCC)	gp40 →	tail fiber protein
ΦLUZ19	42	Monoculture	1	SNP	35404	G→A	1	C98Y (TGT→TAT)	gp41 →	tail fiber protein
ΦLUZ19	42	Monoculture	1	INS	40324	+CTAGC	0.87	intergenic (-55/-1288)	JPEJBOGK_00049 ← / → JPEJBOGK_00050	hypothetical protein/ hypothetical protein
ΦLUZ19	42	Monoculture	2	SNP	23558	A→G	0.43	Q101R (CAG→CGG)	gp34 →	tail protein
ΦLUZ19	42	Monoculture	2	SNP	34506	C→A	1	Q102K (CAG→AAG)	gp40 →	tail fiber protein
ΦLUZ19	42	Monoculture	2	SNP	34582	C→A	1	T127K (ACG→AAG)	gp40 →	tail fiber protein
ΦLUZ19	42	Monoculture	2	SNP	34954	T→C	1	V251A (GTC→GCC)	gp40 →	tail fiber protein
ΦLUZ19	42	Monoculture	2	SNP	35404	G→A	1	C98Y (TGT→TAT)	gp41 →	tail fiber protein
ΦLUZ19	42	Monoculture	2	INS	40327	+GCCTT	0.89	intergenic (-58/-1285)	JPEJBOGK_00049 ← / → JPEJBOGK_00050	hypothetical protein/ hypothetical protein
ΦLUZ19	42	Monoculture	3	SNP	34506	C→A	1	Q102K (CAG→AAG)	gp40 →	tail fiber protein
ΦLUZ19	42	Monoculture	3	SNP	34582	C→A	1	T127K (ACG→AAG)	gp40 →	tail fiber protein
ΦLUZ19	42	Monoculture	3	SNP	34954	T→C	1	V251A (GTC→GCC)	gp40 →	tail fiber protein

ΦLUZ19	42	Monoculture	3	SNP	35404	G→A	1	C98Y (TGT→TAT)	gp41 →	tail fiber protein
ΦLUZ19	42	Monoculture	3	SNP	37724	G→A	0.32	A565T (GCT→ACT)	gp43 →	terminase large subunit
ΦLUZ19	42	Monoculture	3	INS	40330	+T	0.23	intergenic (-61/-1282)	JPEJBOGK_00049 ← / → JPEJBOGK_00050	hypothetical protein/ hypothetical protein
ΦLUZ19	42	Monoculture	3	INS	40332	(GCCTT)1→2	0.33	intergenic (-63/-1280)	JPEJBOGK_00049 ← / → JPEJBOGK_00050	hypothetical protein/ hypothetical protein
ΦLUZ19	42	Monoculture	4	SNP	24974	A→T	0.59	Q573L (CAG→CTG)	gp34 →	tail protein
ΦLUZ19	42	Monoculture	4	SNP	34506	C→A	1	Q102K (CAG→AAG)	gp40 →	tail fiber protein
ΦLUZ19	42	Monoculture	4	SNP	34582	C→A	1	T127K (ACG→AAG)	gp40 →	tail fiber protein
ΦLUZ19	42	Monoculture	4	SNP	34954	T→C	1	V251A (GTC→GCC)	gp40 →	tail fiber protein
ΦLUZ19	42	Monoculture	4	SNP	35404	G→A	1	C98Y (TGT→TAT)	gp41 →	tail fiber protein
ΦLUZ19	42	Monoculture	4	SNP	37828	A→G	0.75	R599R (CGA→CGG)	gp43 →	terminase large subunit
ΦLUZ19	42	Monoculture	4	INS	40324	+CTAGC	0.25	intergenic (-55/-1288)	JPEJBOGK_00049 ← / → JPEJBOGK_00050	hypothetical protein/ hypothetical protein
ΦLUZ19	42	Monoculture	4	INS	40327	+GCCTT	0.41	intergenic (-58/-1285)	JPEJBOGK_00049 ← / → JPEJBOGK_00050	hypothetical protein/ hypothetical protein
ΦLUZ19	42	Monoculture	5	SNP	24934	A→G	0.2	S560G (AGC→GGC)	gp34 →	tail protein
ΦLUZ19	42	Monoculture	5	SNP	34332	A→G	0.38	T44A (ACC→GCC)	gp40 →	tail fiber protein
ΦLUZ19	42	Monoculture	5	SNP	34506	C→A	1	Q102K (CAG→AAG)	gp40 →	tail fiber protein
ΦLUZ19	42	Monoculture	5	SNP	34582	C→A	1	T127K (ACG→AAG)	gp40 →	tail fiber protein
ΦLUZ19	42	Monoculture	5	SNP	34603	A→G	0.9	D134G (GAT→GGT)	gp40 →	tail fiber protein
ΦLUZ19	42	Monoculture	5	SNP	34954	T→C	1	V251A (GTC→GCC)	gp40 →	tail fiber protein
ΦLUZ19	42	Monoculture	5	SNP	35404	G→A	1	C98Y (TGT→TAT)	gp41 →	tail fiber protein
ΦLUZ19	42	Monoculture	5	DEL	40316	Δ8 bp	0.4	intergenic (-47/-1289)	JPEJBOGK_00049 ← / → JPEJBOGK_00050	hypothetical protein/ hypothetical protein
ΦLUZ19	42	Monoculture	5	INS	40321	+TGGCT	0.49	intergenic (-52/-1291)	JPEJBOGK_00049 ← / → JPEJBOGK_00050	hypothetical protein/ hypothetical protein

ΦLUZ19	42	Monoculture	5	INS	40327	+GCCTT	0.92	intergenic (-58/-1285)	JPEJBOGK_00049 ← / → JPEJBOGK_00050	hypothetical protein/ hypothetical protein
ΦLUZ19	42	Monoculture	6	SNP	25105	C→T	0.21	H617Y (CAC→TAC)	gp34 →	tail protein
ΦLUZ19	42	Monoculture	6	SNP	33765	T→C	0.36	I5T (ATC→ACC)	gp39 →	tail fiber protein
ΦLUZ19	42	Monoculture	6	SNP	33834	T→C	0.36	M28T (ATG→ACG)‡	gp39 →	tail fiber protein
ΦLUZ19	42	Monoculture	6	SNP	34506	C→A	1	Q102K (CAG→AAG)	gp40 →	tail fiber protein
ΦLUZ19	42	Monoculture	6	SNP	34582	C→A	1	T127K (ACG→AAG)	gp40 →	tail fiber protein
ΦLUZ19	42	Monoculture	6	SNP	34954	T→C	1	V251A (GTC→GCC)	gp40 →	tail fiber protein
ΦLUZ19	42	Monoculture	6	SNP	35404	G→A	1	C98Y (TGT→TAT)	gp41 →	tail fiber protein
ΦLUZ19	42	Monoculture	6	INS	40324	+CTAGC	0.71	intergenic (-55/-1288)	JPEJBOGK_00049 ← / → JPEJBOGK_00050	hypothetical protein/ hypothetical protein
ΦLUZ19	42	Co-culture	1	SNP	34506	C→A	0.8	Q102K (CAG→AAG)	gp40 →	tail fiber protein
ΦLUZ19	42	Co-culture	1	SNP	34582	C→A	0.2	T127K (ACG→AAG)	gp40 →	tail fiber protein
ΦLUZ19	42	Co-culture	2	SNP	34506	C→A	1	Q102K (CAG→AAG)	gp40 →	tail fiber protein
ΦLUZ19	42	Co-culture	2	SNP	34560	G→A	0.79	D120N (GAT→AAT)	gp40 →	tail fiber protein
ΦLUZ19	42	Co-culture	2	DEL	41781	Δ6 bp	0.37	coding (170-175/285 nt)	JPEJBOGK_00050 →	hypothetical protein
ΦLUZ19	42	Co-culture	2	SNP	42443	A→G	0.45	T104A (ACC→GCC)	JPEJBOGK_00052 →	hypothetical protein
ΦLUZ19	42	Co-culture	3	SNP	34506	C→A	0.22	Q102K (CAG→AAG)	gp40 →	tail fiber protein
ΦLUZ19	42	Co-culture	3	SNP	34582	C→A	0.85	T127K (ACG→AAG)	gp40 →	tail fiber protein
ΦLUZ19	42	Co-culture	3	SNP	34951	A→C	0.68	Q250P (CAG→CCG)	gp40 →	tail fiber protein
ΦLUZ19	42	Co-culture	3	SNP	35404	G→A	0.75	C98Y (TGT→TAT)	gp41 →	tail fiber protein
ΦLUZ19	42	Co-culture	4	SNP	27861	A→G	0.71	K527R (AAG→AGG)	gp36 →	internal virion lysozyme motif protein
ΦLUZ19	42	Co-culture	4	SNP	34332	A→G	0.95	T44A (ACC→GCC)	gp40 →	tail fiber protein
ΦLUZ19	42	Co-culture	4	SNP	34507	A→G	0.91	Q102R (CAG→CGG)‡	gp40 →	tail fiber protein
ΦLUZ19	42	Co-culture	4	SNP	34582	C→A	1	T127K (ACG→AAG)	gp40 →	tail fiber protein
ΦLUZ19	42	Co-culture	4	SNP	35404	G→A	0.92	C98Y (TGT→TAT)	gp41 →	tail fiber protein
ΦLUZ19	42	Co-culture	4	SNP	37294	G→T	0.79	A421A (GCG→GCT)	gp43 →	terminase large subunit

ΦLUZ19	42	Co-culture	5	SNP	34332	A→G	0.56	T44A (ACC→GCC)	gp40 →	tail fiber protein
ΦLUZ19	42	Co-culture	5	SNP	34506	C→A	0.45	Q102K (CAG→AAG)	gp40 →	tail fiber protein
ΦLUZ19	42	Co-culture	5	SNP	34560	G→A	0.34	D120N (GAT→AAT)	gp40 →	tail fiber protein
ΦLUZ19	42	Co-culture	5	SNP	34582	C→A	0.59	T127K (ACG→AAG)	gp40 →	tail fiber protein
ΦLUZ19	42	Co-culture	5	SNP	42443	A→G	0.25	T104A (ACC→GCC)	JPEJBOGK_00052 →	hypothetical protein
ΦLUZ19	42	Co-culture	6	SNP	34332	A→G	0.58	T44A (ACC→GCC)	gp40 →	tail fiber protein
ΦLUZ19	42	Co-culture	6	SNP	34506	C→A	0.51	Q102K (CAG→AAG)	gp40 →	tail fiber protein
ΦLUZ19	42	Co-culture	6	SNP	34582	C→A	0.72	T127K (ACG→AAG)	gp40 →	tail fiber protein
ΦLUZ19	42	Co-culture	6	DEL	41768	Δ28 bp	0.4	coding (157-184/285 nt)	JPEJBOGK_00050 →	hypothetical protein